7-20-2011

The role of amyloid-beta assembly state in monocyte maturation and smooth muscle cell degeneration

Nikkilina Renee Crouse
University of Missouri-St. Louis, ncrouse@charter.net

Follow this and additional works at: https://irl.umsl.edu/dissertation

Part of the Chemistry Commons

THE ROLE OF AMYLOID-BETA ASSEMBLY STATE IN MONOCYTE

MATURATION AND SMOOTH MUSCLE CELL DEGENERATION

by

NIKKILINA RENEE CROUSE
M.S., Biochemistry, University of Missouri - St. Louis, 2006
B.A., Chemistry, Carthage College, 2004

A DISSERTATION

Submitted to the Graduate School of the

UNIVERSITY OF MISSOURI - ST. LOUIS
In partial fulfillment of the Requirements for the Degree

DOCTOR OF PHILOSOPHY

in

CHEMISTRY
with an emphasis in Biochemistry

May, 2009

Advisory Committee

Michael R. Nichols, PhD
Chairperson

Chung Wong, PhD

Valerian D'Souza, PhD

Wendy Olivas, PhD

I would like to dedicate this thesis to my husband, Bob. You are my best friend, and my partner in everything. I could never have done this without your love and support. The faith that you have had in me and my dreams leave me in grateful awe. I can never repay the debt that I owe to you, but I will do my best to make you proud.

ACKNOWLEDGMENTS

through this process. Your love and prayers have always helped to guide my life. Without you I could never have made it this far in my career or become the person I am today.

TABLE OF CONTENTS

LIST OF TABLES

LIST OF FIGURES

LIST OF ABBREVIATIONS

AAO- Average Age of Onset

Aβ - Amyloid β

AC - Adenylate Cyclase

AD - Alzheimer's Disease

ADDLs - Amyloid β Derived Diffusible Ligands

AFM - Atomic Force Microscopy

APP - Amyloid Precursor Protein

BBB - Blood Brain Barrier

BSA - Bovine Serum Albumin

CAA - Cerebral Amyloid Angiopathy

cAMP - Cyclic Adenosine Monophosphate

cdk5 - Cyclin Dependent Protein Kinase - 5

CHO- Chinese Hamster Ovary cells

CNS - Central Nervous System

CSF - Cerebrospinal Fluid

dbcAMP - Dibutyryl Cyclic Adenosine Monophosphate

DC - Dendritic Cell

DMSO - Dimethyl Sulfoxide

ECGS - Endothelial Cell Growth Supplement

ELISA - Enzyme Linked Immunosorbent Assay

EOAD - Early Onset Alzheimer's Disease

FAD - Familial Alzheimer's Disease

FBS - Fetal Bovine Serum

FPRL1 - Formyl Peptide Receptor-like 1

Fn - Fibronectin

Fsk - Forskolin

GFP - Green Fluorescent Protein

GSK-3 - Glycogen Synthase Kinase - 3

HA-VSMC - Human Aortic Vascular Smooth Muscle Cells

HBMVEC - Human Brain Microvascular Endothelial Cells

HEK293 - Human Embryonic Kidney cells

HFIP - Hexafluoroisopropanol

HRP - Horseradish Peroxidase

IBMX - Isobutylmethylxanthine

IL - Interleukin

LPS - Lipopolysaccharide

LTP - Long Term Potentiation

MAP - Microtubule Associate Protein

MTT - 3-(4,5-dimethylthiazol-2-yl)-2,5-diphenyltetrazolium bromide

NFT - Neurofibrillary Tangles

Pam$_3$CSK$_4$ - Tripalmitoyl cysteinyl seryl tetralysine

PBMC - Peripheral Blood Monocytes

PBS - Phosphate Buffered Saline

PDE - Phosphodiesterase

PDPK - Proline-directed Protein Kinase

PDTC - Pyrrolidinecarbodithiolate

PHF - Paired Helical Filaments

PMA - 12-myristate 13-acetate

PMS - Phenazine methosulfate

RAGE - Receptor for Advance Glycation End Products

SMC - Smooth Muscle Cell

TES - 2-[Tris(hydroxymethyl)methylamino]-1-ethane sulfonic acid

TLR - Toll-like Receptor

TNFα - Tumor Necrosis Factor α

TRAIL - TNF-Related Apoptosis-Inducing Ligand

WRW$_4$ - Trp-Arg-Trp-Trp-Trp-TrpCO-NH$_2$

WT - Wild Type

XTT - 2,3-Bis(2-methoxy-4-nitro-5-sulfophenyl)-2H-tetrazolium-5-carboxanilide

ABSTRACT

Crouse, Nikkilina R. Ph.D, University of Missouri-St. Louis, May 2009. THE ROLE OF AMYLOID-BETA ASSEMBLY STATE IN MONOCYTE MATURATION AND SMOOTH MUSCLE CELL DEGERATION. Major Professor: Michael R. Nichols.

Alzheimer's Disease (AD) is a progressive, neurodegenerative disorder which is ranked as one of the leading causes of death among Americans. AD is characterized by the presence of intracellular neurofibrillary tangles comprised of hyperphosphorylated tau protein, and extracellular plaques made of amyloid β (Aβ). Together these two pathologies lead to severe memory impairment in afflicted patients, but research has implicated the presence of the Aβ deposits as likely causes for AD progression. Aβ is produced through the proteolytic cleavage of the integral membrane amyloid precursor protein (APP) which occurs through the action of β- and γ-secretases which produce 39-43 amino acid Aβ peptides. In AD, the Aβ plaques are comprised of mostly 40 or 42 amino acid Aβ (Aβ(1-40) and Aβ(1-42) respectively). There is some evidence that in response to the presence of Aβ in the brain, monocytic cells circulating in the blood are recruited across the blood brain barrier and transformed into brain macrophages, also known as microglia. Here we investigate the ability of Aβ to transform cultured THP-1 monocytes into macrophage-like cells as a model of the *in vivo* process. Our results indicate that an early-formed Aβ oligomer which is formed when Aβ(1-42) is aggregated in water has

the ability to potently transform the non-adherent monocytes into adherent cells with many properties consistent with macrophages. Our data also shows that Aβ(1-40) is unable to form a species with a similar activity. We have determined that the transforming activity of Aβ(1-42) occurs through the formyl peptide receptor-like 1 (FPRL1) receptor, but not through TLR2, TLR4 or an NF-κB dependent mechanism. Here we also study the involvement of cAMP in a model system of cerebral amyloid angiopathy (CAA), a condition in which Aβ deposits within the walls of cerebral vessels leading to hemorrhagic activity. CAA is reported to occur in many cases of AD, but especially in many early onset AD cases associated with Aβ mutations. We studied the ability of cAMP to rescue human aortic vascular smooth muscle cells (HA-VSMC) from Aβ induced toxicity. We found that in our experiments treatment with some cAMP elevating compounds can subtly protect the cells from Aβ. Overall we show that Aβ is a peptide which has a wide variety of activities that are dependent upon the peptide's assembly state.

PUBLICATION

available at www.sciencedirect.com

ScienceDirect

www.elsevier.com/locate/brainres

BRAIN RESEARCH

ELSEVIER

Research Report

Oligomeric amyloid-β(1–42) induces THP-1 human monocyte adhesion and maturation

Nikkilina R. Crouse, Deepa Ajit, Maria L.D. Udan, Michael R. Nichols*

Department of Chemistry and Biochemistry and Center for Nanoscience, University of Missouri-St. Louis, One University Boulevard, St. Louis, MO 63121, USA

ARTICLE INFO

ABSTRACT

Amyloid-β (Aβ) is a naturally occurring 40- or 42-residue peptide fragment with a primary role in Alzheimer's disease (AD). Aggregated Aβ accumulates as both dense core plaques and diffuse deposits in the brains of AD patients. Aβ plaques are surrounded by activated microglia, some of which are believed to be derived from peripheral blood monocytes that have infiltrated the central nervous system and differentiated into phagocytes in response to Aβ. We have modeled this process using THP-1 human monocytes and found Aβ(1–42) to be as effective as phorbol myristate acetate at differentiating THP-1 monocytes based on cell adhesion, fibronectin binding, CD11b cell-surface expression, and morphological changes. Cell adhesion studies and atomic force microscopy imaging revealed an inverse correlation between Aβ(1–42)-induced monocyte maturation and aggregation progression. Freshly reconstituted Aβ(1–42) solutions were the most effective, yet continued aggregation reduced, and eventually abolished, the ability to induce monocyte adhesion. Aβ(1–40), lower aggregation concentrations of Aβ(1–42), and an aggregation-restricted Aβ(1–42) L34P mutant had little effect on monocyte adhesion under the same conditions as Aβ(1–42). These findings implicated an oligomeric, but not monomeric or fibrillar, Aβ(1–42) aggregation species in the monocyte maturation process. The rapidly-formed Aβ(1–42) oligomers were distinct from Aβ-derived diffusible ligands which did not elicit significant THP-1 monocyte adhesion. These data demonstrate that a specific oligomeric Aβ(1–42) aggregation species can potently initiate the THP-1 monocyte maturation process.

© 2008 Elsevier B.V. All rights reserved.

1. Introduction

A newly published and telling statistic reports that while deaths from heart disease, breast cancer, prostate cancer, and stroke have declined from 2000 to 2005, deaths from Alzheimer's disease (AD) have increased by 45% during the same time period (Maslow, 2008). Accordingly, basic research focused on the neurodegenerative mechanisms in AD is needed for therapeutic advances to be made. A principal pathological characteristic of AD is the presence of senile plaques in the brains of affected patients (Selkoe, 2001). The plaques are primarily composed of fibrillar amyloid-β protein (Aβ) assembled by non-covalent polymerization of Aβ monomers which originate from enzymatic cleavage of amyloid precursor protein (Selkoe, 2004a,b). Significant localized inflammation has been observed in the AD brain as evidenced

---

by clusters of dystrophic neurites (Selkoe, 1998), activated microglial cells (McGeer et al., 1987), and proinflammatory cytokines (Dickson et al., 1993) within close proximity of the extracellular parenchymal plaques.

Data in mouse models indicate that a population of the parenchymal microglial cells may originate from infiltrating myeloid cells of the hematopoietic system (Eglitis and Mezey, 1997). In fact, the presence of Aβ appears to encourage monocyte/macrophage infiltration to sites of accumulation (El Khoury et al., 2007; Simard et al., 2006; Wegiel et al., 2004). Furthermore, Aβ has been shown to modulate monocyte chemotaxis (Giri et al., 2000; Le et al., 2001), adhesion (Yan et al., 1996), and differentiation into macrophages (Fiala et al., 1998). Although the irradiation bone marrow chimeric methodologies used in some of the infiltration studies have limitations (reviewed in Carson et al., 2007), these data suggest that parenchymal Aβ accumulation might induce monocyte migration across the blood-brain barrier and differentiation into phagocytic microglial cells.

The aggregation state of Aβ plays an important role in its ability to interact with cells and stimulate a response. In vitro aggregation studies have identified a continuum of species in the assembly of monomeric Aβ into a fibrillar form. These Aβ species vary in their size, length, solubility, and morphology (Harper et al., 1997, 1999; Stine et al., 2003; Walsh et al., 1997, 1999). Monomeric, oligomeric, protofibrillar, fibrillar, and amorphous species possess distinct toxic and biological activities and potencies (Dahlgren et al., 2002; Deshpande et al., 2006; Lorenzo and Yankner, 1994; Pike et al., 1991; Walsh et al., 2002). Significant Aβ polymorphism is also observed in vivo most conspicuously in the form of neuritic plaques and diffuse deposits (Selkoe, 2004a,b). Microglial cells appear to exhibit selectivity for particular Aβ species in that they are typically observed in an activated state clustered around the dense core plaques as opposed to the diffuse Aβ deposits in both humans (Selkoe, 2004a,b) and in transgenic AD mouse models (Meyer-

Luehmann et al., 2008). It is not fully understood what Aβ aggregation state or receptor mechanisms drive monocyte/microglia recruitment, monocyte differentiation, and microglial activation. We have previously reported that Aβ(1–42) rapidly and effectively transforms THP-1 monocytes into adherent cells (Udan et al., 2008). Here we further explore the ability of Aβ to induce monocyte maturation and the dependence of this process on Aβ aggregation state.

2. Results

2.1. Aβ(1–42) effectively induces THP-1 monocyte adhesion and maturation

Human THP-1 monocytes are a well established model system for studying monocyte differentiation (Auwerx, 1991). A prominent marker of THP-1 differentiation and macrophage formation is the development of an adherent cell phenotype (Ding et al., 2007). Numerous studies have used THP-1 adhesion as a measure of monocyte differentiation in response to compounds such as lipopolysaccharide (LPS) (Hmama et al., 1999), 1α,25-dihydroxycholecalciferol (Vitamin D3) (Schwende et al., 1996), and 4α-phorbol 12-myristate 13-acetate (PMA) (Tsuchiya et al., 1982). PMA is widely used as a monocyte differentiating agent (Park et al., 2007) and it was used in these in vitro studies to compare and contrast its effects with those of Aβ. Our studies showed that Aβ(1–42) induced adhesion of THP-1 monocytes as effectively as PMA following a 6 h exposure (Fig. 1A). Adhesion was determined by direct counting of attached cells as described in the Experimental procedures and produced values of 42±4% (SE) and 43±4% adhesion for Aβ(1–42) and PMA respectively. Controls for Aβ (water) and PMA (0.0005% DMSO) induced 5±1% and 6±1% adhesion respectively. Induction of THP-1 monocyte adhesion was also dependent on the final peptide concentration that was used
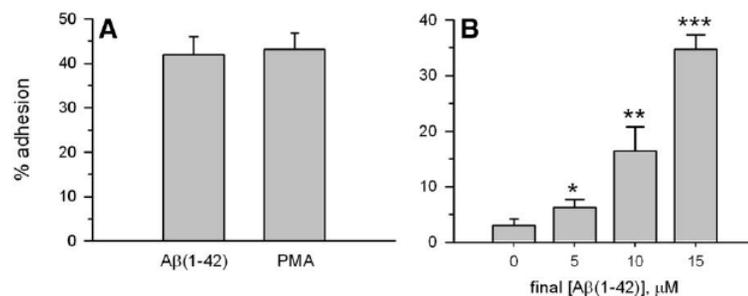
Fig. 1 – Effect of Aβ(1–42) and PMA on THP-1 monocyte adhesion. THP-1 monocytes were treated with 10 ng/ml PMA or 15 μM Aβ(1–42) from a freshly reconstituted 100 μM water solution. Panel A. Cells were incubated for 6 h and % adhesion determined by direct cell counting as described in the Experimental procedures. % adhesion is the number of adherent cells divided by the total cells plated. Water (Aβ) and 0.0005% DMSO (PMA) controls induced 5±1% and 6±1% adhesion respectively. Panel B. Aβ(1–42) was reconstituted in sterile water (100 μM) and immediately added to prepared THP-1 monocytes in different volumes to produce the final concentrations shown in Panel B. All treatments had the same cell number and volume of sterile water. Following a 6 h incubation at 37 °C, cell adhesion was determined as described in Panel A. Standard error bars (SE) were calculated from $n=17$ trials for PMA and $n=22$ trials for Aβ(1–42) (Panel A) and $n=7$ trials in Panel B. Statistical differences in Panel B from water-induced adhesion (0 μM Aβ) are denoted with asterisks at the following significance levels (*$p<0.05$, **$p<0.01$, ***$p<0.005$).

to treat the cells. Freshly reconstituted Aβ(1–42) (100 μM) was added to THP-1 monocytes at different volumes to produce different final concentrations. The ability to induce cell adhesion was dose-dependent with the highest adhesion at 15 μM Aβ(1–42) (Fig. 1B). In this set of experiments, 15 μM freshly reconstituted Aβ(1–42) induced 35±3% adhesion, while 10 μM and 5 μM induced 16±4% and 6±1% adhesion respectively. Higher concentrations were not tested. Aβ concentrations are based on monomeric peptide and may not reflect the actual concentrations of the bioactive species which could be much lower.

Fibronectin (Fn), a multifunctional adhesion protein and major component in the extracellular matrix, serves as an attachment substrate for integrin receptors expressed by multiple cell types (Ruoslahti and Pierschbacher, 1987). Fn has been shown to stabilize lipopolysaccharide-induced THP-1 cell adhesion (Kounalakis and Corbett, 2006). THP-1 cell adhesion induced by Aβ(1–42) or PMA was enhanced nearly two-fold in both cases by pre-coating the cell culture plate with 5 μg Fn (Fig. 2A). Untreated THP-1 monocytes did not bind to Fn above control levels (5% adhesion). The enhanced adhesion to Fn by Aβ-stimulated THP-1 monocytes suggested a phenotypic change in the cells. A recognized marker of

monocyte maturation and differentiation to macrophages is expression of cell-surface CD11b, a subunit of the β2 integrin receptor (Hickstein et al., 1992). Schwende et al. previously demonstrated that while THP-1 monocytes express low levels of CD11b, PMA treatment induced monocyte adhesion and significant increases in cell-surface expression of CD11b (Schwende et al., 1996). In the present study, using an enzyme-linked colorimetric immunoassay, it was found that addition of Aβ(1–42) to THP-1 monocytes increased CD11b cell-surface expression to greater levels than that induced by PMA after 6 h and 24 h of treatment. CD11b expression induced by Aβ(1–42) occurred in the absence (data not shown) and presence of Fn (Fig. 2B). The relative absorbance values from each well, which reflected CD11b immunodetection, were normalized by the number of adherent cells for each condition. Microscope images of the Aβ(1–42)-treated cells showed a marked change in morphology from spherical suspension cells (Fig. 2B, inset) to flattened and elongated adherent cells (Fig. 2C). Processes were noted extending from the cell body. The change in THP-1 cell morphology along with cell-surface CD11b expression confirmed that monocyte adhesion induced by Aβ(1–42) was reflective of monocyte maturation and differentiation.
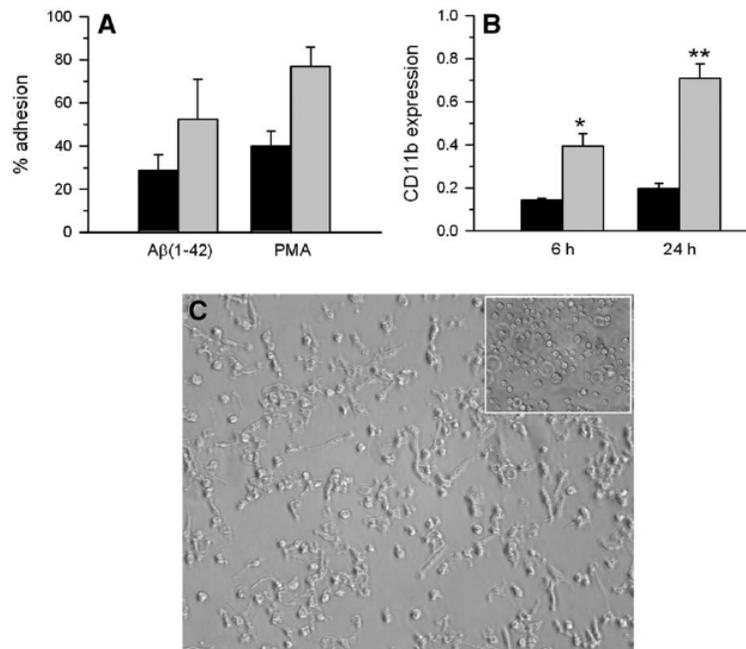
Fig. 2 – Aβ(1–42) induces differentiation of monocytes into macrophages. Freshly reconstituted Aβ(1–42) in sterile water (100 μM solution, 15 μM final concentration) and 10 ng/ml PMA were added to THP-1 monocytes as in Fig. 1. Panel A. Monocyte adhesion was determined in uncoated wells (black bars) and wells precoated with 5 μg Fibronectin (Fn) (gray bars). SE bars are for $n=2$ trials. Panel B. THP-1 monocytes were treated as in Panel A in Fn-coated wells and the resulting adherent cells were analyzed for cell-surface CD11b expression at 6 and 24 h as described in the Experimental procedures. Normalized CD11b expression is represented as absorbance/10^5 adherent cells for PMA (black bars) and Aβ(1–42) (gray bars). SE bars are for $n=5$ trials. Statistical differences between PMA- and Aβ(1–42)-induced CD11b expression in Panel B are denoted with asterisks at the following significance levels (*$p<0.01$ and **$p<0.0025$). Panel C. Representative microscope images from suspension THP-1 monocytes (inset) and adherent THP-1 cells following 24 h Aβ(1–42) treatment.

2.2. Freshly solubilized Aβ(1–42) induces monocyte maturation more effectively than aggregated Aβ(1–42)

Experiments in Figs. 1 and 2 were conducted using Aβ(1–42) immediately following reconstitution in sterile water. In an effort to understand how Aβ aggregation state influences its ability to differentiate monocytes, we incubated Aβ(1–42) for longer periods and evaluated the cellular effect using THP-1 monocyte adhesion as a maturation marker. Aβ(1–42) was reconstituted in sterile water, incubated at 4 °C, and periodically, aliquots of the solution were applied to the cells. As Aβ(1–42) aggregation progressed, the ability to induce monocyte adhesion

diminished and ultimately was lost (Fig. 3A). The most effective induction of adhesion by Aβ(1–42) occurred immediately after reconstitution, continued during the first 48 h of Aβ(1–42) aggregation, and then rapidly decreased at later time points. By 216 h of aggregation, the Aβ lost all ability to transform the cells compared to that induced by treatment with a water control. We have previously observed and described that Aβ(1–42), when incubated in these conditions, begins to form fibrillar structures by 48 h (Udan et al., 2008), which increase in number and length with continued incubation. This progression is also shown in Fig. 3B–E with representative AFM images of Aβ(1–42) aggregation at particular time points. Short rod-like structures
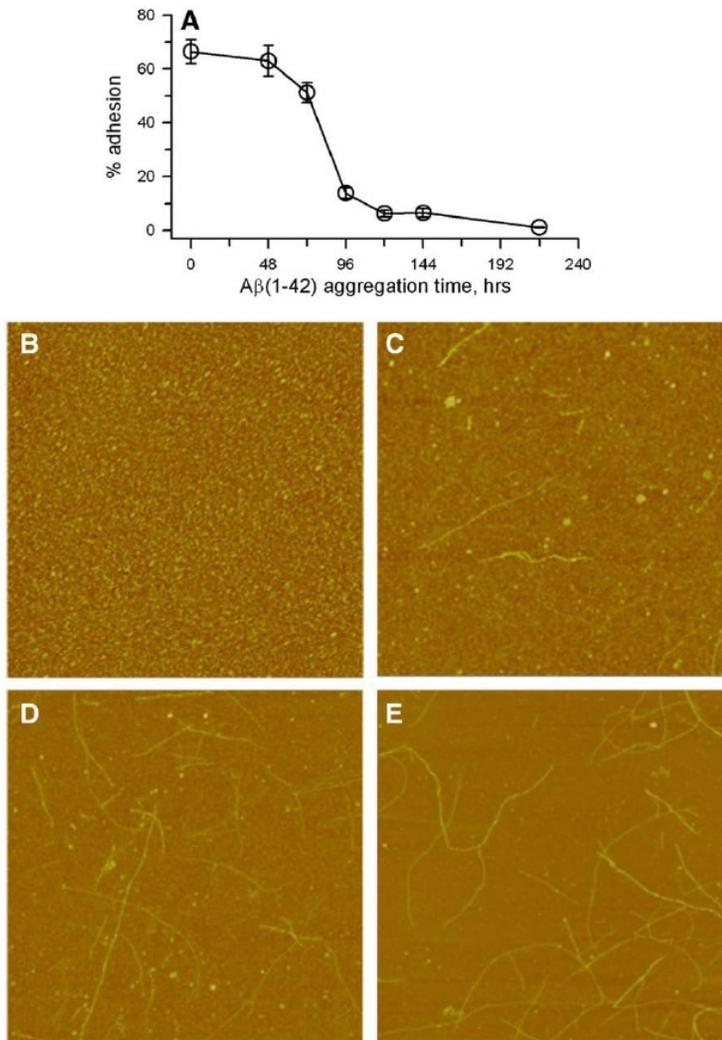
Fig. 3 – Effect of Aβ(1–42) aggregation state on induced monocyte adhesion. Panel A. Lyophilized Aβ(1–42) was reconstituted in sterile water (100 μM) and incubated at 4 °C. At given times, cells were treated with 15 μM Aβ(1–42) for 6 h and adhesion was measured and presented as described in Fig. 1 legend and the Experimental procedures. Error bars represent SE for n trials of 19 (0 h), 17 (48 h), 4 (72 h), 5 (96 h), 7 (120 h), 3 (144 h), and 7 (216 h). Panels B–E. AFM images (5 μm×5 μm, height mode) from a representative Aβ(1–42) aggregation reaction conducted in the same conditions as in Panel A at 0 (B), 48 (C), 96 (D), and 216 (E) h. Aβ(1–42) was diluted to 1 μM in water for application to the mica disc.

with heights averaging 4–5 nm began to appear which lengthened and multiplied over time. Average heights diameters increased only slightly by 216 h to 5–6 nm although the overall height dispersity was larger with more fibrils over 6 nm that at earlier times. This may reflect some intertwining and lateral association of single fibrils. Of particular note was the significant decrease in diffuse Aβ(1–42) over time (Figs 3B–E). The diffuse material is <1 nm in height, visible upon Aβ(1–42) reconstitution and disappears as aggregation and fiber formation progresses. The decline in monocyte adhesion-inducing ability by Aβ as aggregation progressed (Fig. 3A) indicated that fibrillar aggregates were not the most effective Aβ species at inducing THP-1 macrophage formation. During these studies, batch-to-batch variations were found with respect to the magnitude of cell adhesion induced by freshly reconstituted Aβ(1–42). Furthermore, some Aβ(1–42) batches began losing monocyte maturation activity more rapidly than 48 h. Despite these variations, the trend shown in Fig. 3 was consistently observed.

2.3. Modulation of Aβ(1–42) aggregation conditions alters the ability to induce monocyte maturation

The data in Fig. 3 suggested that increased Aβ(1–42) aggregation decreased the peptide's ability to induce monocyte maturation. In order to strengthen this result, solution conditions were modulated to alter the rate at which aggregation occurred immediately after reconstitution of the peptide. Aβ assembly occurs via a nucleation-dependent polymerization process (Jarrett and Lansbury, 1993). The nucleation step is characterized by a lag time which can be significantly shortened with increased peptide concentration. Rapid polymerization and fibril formation ensues. Based on this information, a more concentrated Aβ(1–42) solution (1 mM) was prepared and compared to the same 100 μM Aβ(1–42) solution used in the previous figures. Different volumes were applied to THP-1 monocytes in order to maintain equal Aβ final concentrations of 15 μM. The more-concentrated 1 mM Aβ(1–42) solution showed a decreased ability to induce monocyte adhesion (Fig. 4A) and accelerated aggregation after reconstitution (Figs. 4B, C) compared to 100 μM Aβ(1–42) (Figs. 4A, 3B). Microscopy analysis of the 1 mM Aβ(1–42) solution revealed formation of fibers with heights of 2–3 nm immediately after reconstitution by AFM (Fig. 4B) and widths of 6–10 nm by EM (Fig. 4C). Incubation of the 1 mM Aβ(1–42) solution for 24 h at 4 °C produced an overwhelming number of long, thicker (4–5 nm height) fibers (Fig. 4D) and a sharp drop in monocyte adhesion-inducing activity to near control cell adhesion levels (data not shown).
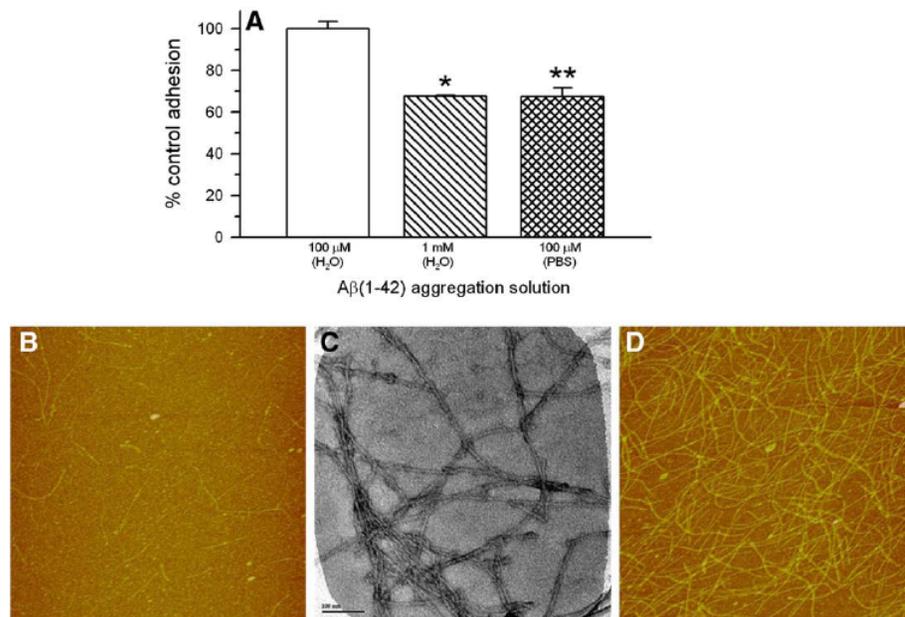
Fig. 4 – Solution conditions modulate Aβ(1–42) aggregation and the ability to induce monocyte adhesion. Aβ(1–42) was reconstituted in sterile water at 100 μM and 1 mM or in PBS at 100 μM and immediately added to THP-1 cells for 6 h at a final concentration of 15 μM. Monocyte adhesion was measured as in Fig. 1 and presented as % control adhesion with the control assigned to the 100 μM Aβ(1–42)/H2O sample. SE bars represent $n = 5$ trials for 100 μM Aβ(1–42) in water or PBS and $n = 3$ trials for 1 mM Aβ(1–42) in water. Statistical differences between adhesion values for the 100 μM Aβ(1–42)/water control and the 1 mM Aβ(1–42)/water and 100 μM Aβ(1–42)/PBS samples are denoted with asterisks at the following significance levels (*$p < 0.005$ and **$p < 0.0025$). Panels B–D. Samples from the above Aβ(1–42) solutions were diluted for imaging to 1 μM for AFM and 10 μM for EM and analyzed as described in the Experimental procedures. Presented images are of freshly reconstituted 1 mM Aβ(1–42) in sterile water (Panel B, AFM, Panel C, EM) and after 24 h incubation at 4 °C (Panel D, AFM). AFM images (5 μm × 5 μm) are presented in height mode. The scale bar for the EM image is 100 nm.

Although immediate cell treatment after Aβ(1–42) reconstitution at higher concentration (1 mM) produced a modest effect (Fig. 4A, 67% of activity induced by 100 μM) it indicated that accelerated aggregation within approximately 15 min began to deplete the Aβ species inducing monocyte maturation.

Microelectrode measurements of unbuffered water Aβ(1–42) solutions had a pH of 3.6, thus it was of interest to see how reconstitution of Aβ(1–42) in phosphate-buffered saline (PBS) would affect monocyte maturation. The pH of a 100 μM Aβ(1–42) in PBS solution was measured at 7.1 and this increase in pH and ionic strength decreased the ability of freshly reconstituted Aβ(1–42) to induce monocyte adhesion by 33% (Fig. 4A). Control treatments with PBS were not significantly different from water. No fibrillar species were observed in the 100 μM Aβ(1–42)/PBS solution at 0 h by AFM or EM (data not shown) and further incubation of this solution at 4 °C for 24 h did not produce a subsequent active species. Although dramatic cellular activity differences were not observed after initial reconstitution of Aβ(1–42) in buffered saline compared to lower pH, hypotonic conditions, monocyte adhesion-inducing activity dropped much more quickly in the Aβ(1–42)/PBS solution compared to Aβ(1–42) in water by 24 h (data not shown). The cumulative findings indicated that continued Aβ(1–42) aggregation was inversely correlated with THP-1 monocyte maturation and implicated either a monomeric or oligomeric Aβ species in the process. Furthermore, solution conditions were able to modulate Aβ(1–42) aggregation and its ability to induce monocyte maturation.

2.4. Aβ(1–40) under similar conditions does not induce monocyte maturation

The shorter Aβ(1–40) peptide remains in a monomeric state longer than Aβ(1–42) under similar conditions (Walsh et al., 1997) and also oligomerizes through a distinct pathway from that of Aβ(1–42) (Bitan et al., 2003). To further test our theory that either monomer or early oligomer forms of Aβ are responsible for inducing monocyte maturation, we examined the age-dependent activity of Aβ(1–40) reconstituted in sterile water and incubated at three temperatures. A dramatic difference was observed between Aβ(1–42) and Aβ(1–40) immediately after reconstitution (Fig. 5). The longer peptide induced 55% monocyte adhesion while the shorter peptide had no effect implying that monomeric Aβ(1–40) is not the active species. Furthermore, continued aging of Aβ(1–40), even at higher temperatures, did not significantly induce THP-1 adhesion. Separate incubations of Aβ(1–40) indicated that after 216 h some fibrils were formed at all three temperatures based on AFM images (data not shown). The results suggested that adhesion-inducing activity was mediated by some form of Aβ(1–42) that was not produced on the Aβ(1–40) aggregation pathway (Fig. 5).

2.5. Oligomeric, not monomeric, Aβ(1–42) induces monocyte maturation

Two possible interpretations emanated from the results in Fig. 5. One, that the two additional residues on Aβ(1–42) were
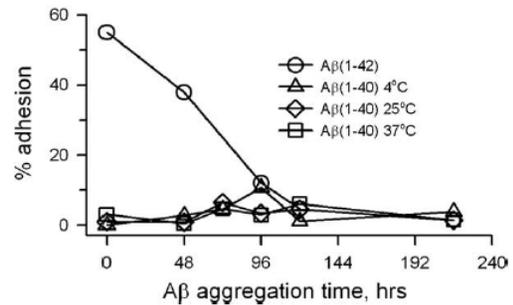
Fig. 5 – Comparison of Aβ(1–40) and Aβ(1–42) for induction of monocyte adhesion. Aβ(1–40) and Aβ(1–42) were reconstituted in sterile water (100 μM) and incubated at varying temperatures. At the above times, cells were treated for 6 h with either Aβ(1–42) incubated at 4 °C (circle) or Aβ(1–40) incubated at 4 °C (triangle), 25 °C (diamond), or 37 °C (square). % adhesion was determined and presented as in Fig. 1. Aβ(1–40) data is the average of n=3 trials for 4 °C and n=2 trials for 25 °C and 37 °C over two experiments. SE bars were not included for clarity but none exceeded 5% of the data points. Aβ(1–42) was used as a positive control in one of the two experiments.

critical for monomer-induced monocyte adhesion or two, that only Aβ(1–42) can form the oligomeric species responsible for this activity. To probe this question, the Aβ(1–42) oligomerization rate was modulated to alter the monomer:oligomer ratio in the solution and gain further information as to the identity of the species of Aβ which induces THP-1 monocyte adhesion. It was reasoned that a lower Aβ(1–42) concentration would slow the aggregation process and maintain a higher monomer:oligomer ratio. By the same token, higher Aβ(1–42) concentrations would decrease this ratio. Two freshly reconstituted Aβ(1–42) preparations (100 μM and 50 μM) were prepared and immediately applied to the THP-1 monocytes while maintaining the same final Aβ(1–42) treatment concentration. As in Fig. 3, the final Aβ(1–42) concentrations for cell incubation were maintained at 15 μM, but cells treated from the freshly reconstituted 100 μM Aβ(1–42) solution induced 58±4% adhesion while the samples treated from the 50 μM Aβ(1–42) solution induced only 16±4% adhesion (Fig. 6). 24 h of additional incubation of the Aβ(1–42) solutions at 4 °C reduced the activity of both aggregation reactions to 41±5 and 12±3 % adhesion for the 100 μM and 50 μM Aβ(1–42) respectively. Further declines in Aβ(1–42) activity were observed after 48 h of aggregation (data not shown). AFM images of the freshly reconstituted solutions were similar and no distinct morphological species could be delineated between the two preparations (data not shown), yet at 48 h of aggregation it was evident that the 100 μM Aβ(1–42) aggregation had progressed more rapidly (data not shown). Longer and more numerous fibers were observed in the 100 μM solution compared to 50 μM.

A mutational approach was also used to ascertain the active Aβ(1–42) species. Proline mutants have been studied previously for their effect on Aβ aggregation kinetics and thermodynamics (Williams et al., 2004). One of these, Aβ(1–42) L34P, was tested for
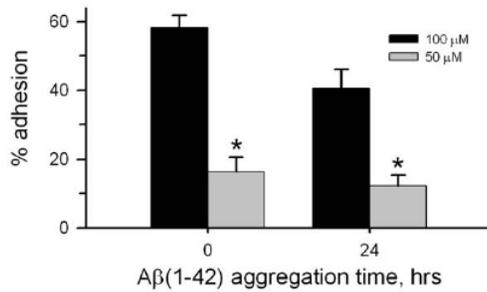
Fig. 6 – Decreased Aβ(1–42) concentration at reconstitution significantly lowers Aβ(1–42)-induced monocyte adhesion. Aβ(1–42) was reconstituted in sterile water at 4 °C at either 100 μM (black bars) or 50 μM (grey bars). At the above times, monocytes were treated with a final concentration of 15 μM from each solution and adhesion was determined and presented as in Fig. 1. SE bars are for $n=3$ (0 h) and $n=2$ (24 h) trials. Water-induced adhesion controls (2.8±0.4%) were subtracted from final % adhesion presented. Statistically significant differences between 100 μM and 50 μM solutions were noted at 0 ($^*p<0.0005$) and 24 ($^*p<0.005$) h of aggregation.

its ability to induce monocyte adhesion. The leucine to proline change at residue 34 slows Aβ aggregation and destabilizes fibrils (Williams et al., 2004) thereby enabling the peptide to remain in a monomeric state longer. Fig. 7 demonstrates that Aβ(1–42) L34P prepared under the same conditions as Aβ(1–42) (100 μM, 4 °C) did not induce monocyte adhesion after reconstitution in sterile water even though the cells were responsive to PMA in those experiments (diamonds). Further incubation of Aβ(1–42) L34P at 4 °C to 216 h did not result in cell adhesion (Fig. 7). AFM images of freshly reconstituted Aβ(1–42) L34P (data not shown) were similar to wild-type Aβ(1–42) (Fig. 3B) and did not change even after incubation for 168 h at 4 °C. The Aβ(1–42) L34P lacked any fibrillar structures at later time points (data not shown) in contrast to wild-type Aβ(1–42) (Figs. 3D, E). These observations indicated that Aβ(1–42) L34P was restricted in its ability to aggregate and the combined data suggested that a rapidly-forming oligomeric Aβ(1–42) species was responsible for inducing THP-1 monocyte adhesion rather than the monomeric Aβ(1–42).

2.6. ADDLs are not effective inducers of monocyte adhesion

A previously reported and well-characterized oligomeric Aβ(1–42) species termed Aβ-derived diffusible ligands (ADDLs) has been shown to possess multiple biological activities including cell-surface binding, neurotoxicity, and inhibition of long-term potentiation in hippocampal neurons (Hepler et al., 2006; Lambert et al., 1998), Having established that an oligomeric Aβ(1–42) species is responsible for THP-1 monocyte maturation, ADDLs were prepared as described in the Experimental procedures and tested for the same activity. The last step in the ADDLs preparation involves centrifugation and supernatant collection. In this experiment both ADDLs and the pre-centrifugation solution were tested.

Aβ(1–42) ADDLs and the total aggregation mixture induced 6±3% and 7±2% adhesion respectively. The adhesion induced by ADDLs was above that of a medium control (1.4±0.3%) but with a low statistical significance ($p>0.05$). For comparison, PMA-treated samples in this experiment showed 46±4% adhesion (Fig. 8). Since the ADDLs preparation requires a 24 h incubation at 4 °C, the effectiveness of the total aggregation mixture and the ADDLs in Fig. 8 can be compared to the 24 h 100 μM Aβ(1–42) aggregation sample in Fig. 6 which induced 41% monocyte adhesion. An AFM image (Fig. 8 inset) of the ADDLs prepared in this study showed similar morphological features to those reported earlier (Dahlgren et al., 2002) with primarily small oligomeric structures. Height analysis of the image produced a range from 1–6 nm (mean=3.0±1.3 nm SD) for 90% of the $n=212$ measurements. The cellular results suggested that Aβ(1–42) oligomers formed under the conditions described in this report differ from ADDLs and were better at inducing monocyte maturation.

3. Discussion

Cell adhesion, increased cell-surface expression of CD11b, and morphological changes are markers of monocyte maturation and differentiation (Ding et al., 2007; Hickstein et al., 1992). The transformation of monocytes into macrophages may play a significant role in neurodegenerative diseases such as AD. In this report, we have shown that the longer, 42-residue form of Aβ is a rapid inducer of THP-1 monocyte maturation. The data further demonstrate that monomeric and fibrillar Aβ(1–42) are not the active aggregation state, but rather implicates an oligomeric species as the initiator of this process. Aβ(1–42) is the primary component of the dense core plaques (Gravina et al., 1995) as well as the diffuse deposits (Selkoe, 2004a,b) found in AD brains. Less is known about the assembly state of
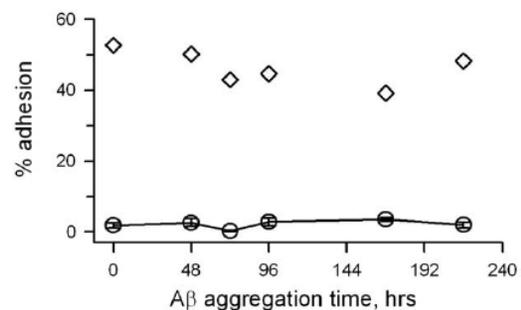
Fig. 7 – A C-terminal proline mutation in Aβ(1–42) blocks monocyte adhesion-inducing ability. Aβ(1–42) L34P was reconstituted in sterile water (100 μM) and incubated at 4 °C. At 0, 48, 72, 96, 168 and 216 h of aggregation, cells were treated with 15 μM of Aβ(1–42) L34P for 6 h and % adhesion was determined as described in Fig. 1. Aβ(1–42) L34P data points (circles) are the average ±SE from two experiments ($n=5$ trials total). A 10 ng/ml PMA control treatment and adhesion measurement (diamonds) was done at each time point.
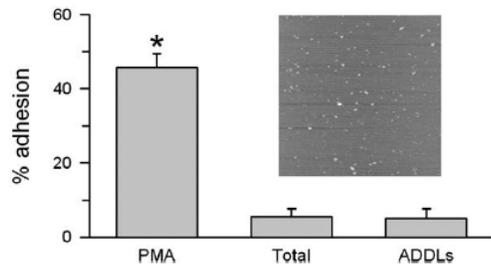
Fig. 8 – Effect of ADDLs on monocyte adhesion. ADDLs were prepared as described in the Experimental procedures. Cells were treated with either the total aggregation mixture prior to centrifugation (Total) or ADDLs at a final concentration of 15 µM Aβ(1–42). A 10 ng/ml PMA control was also included. Adhesion is presented as described in Fig. 1 legend and is the average ± SE for $n=2$ trials for PMA and $n=4$ trials for Total and ADDLs over two separate experiments. Treatment with a Hams F12/2% DMSO medium control induced 1.4±0.3% adhesion. The level of PMA-induced adhesion was similar to the result in Fig. 1 and the cumulative PMA data was significantly different ($^*p<0.0005$) from DMSO-induced adhesion (Fig. 1 legend). Statistical differences were noted for the Total and ADDLs but only to a significance level of $p<0.1$. Inset. A representative AFM image of the ADDLs preparation (1 µM) used to treat THP-1 monocytes. The image was obtained as described in the Experimental procedures and is 5 µm × 5 µm in dimension.

diffuse Aβ compared to the fibril-containing plaques. In fact, the overall parenchymal Aβ accumulation has been characterized as a continuum of structures some of which may represent fibrillar precursors (Selkoe, 2004a,b).

Several studies have reported that infiltration of peripheral blood cells of the monocyte/macrophage lineage occurs in response to Aβ accumulation. Rivest and colleagues demonstrated a significant influx of blood-derived microglia to Aβ neuritic plaques in a transgenic AD mouse model and these newly infiltrated phagocytes were much more effective at eliminating plaques compared to the resident microglia (Simard et al., 2006). The bone-marrow irradiation techniques used in the Rivest study may have some limitations by potentially inducing a non-specific influx of blood-derived macrophages (discussed in Carson et al., 2007). However, the finding was supported by a report from Luster and colleagues who used a unique immunoreactivity profile to identify microglial cells that were of peripheral blood origin. They observed significant increases in the blood-derived microglia in the brains of APP transgenic mice compared to non-transgenic mice (El Khoury et al., 2007). Furthermore, deletion of the Ccr2 chemokine receptor impaired monocyte infiltration and accelerated AD progression. The implication from these findings is that a population of the brain microglial cells clustering around Aβ plaques is derived from infiltrating blood monocytes.

The point (i.e. cellular location) at which infiltrating monocytic cells differentiate into phagocytic microglia is not clear but the data presented in this report suggests that early oligomeric Aβ(1–42) aggregates may have a role in transforming monocytes

in vivo. Aβ differentiation of human peripheral monocytes has been reported previously (Fiala et al., 1998) and we have extended those studies by determining what form of Aβ triggers the monocyte maturation process. Fig. 3 showed that freshly reconstituted Aβ(1–42) produced the optimal species for inducing monocyte adhesion. Later-stage fibrillar Aβ(1–42) aggregation species did not have this ability. Furthermore, Fig. 5 established that Aβ(1–40), in the same conditions as Aβ(1–42), was inactive. This finding is not altogether surprising since Bitan et al. (2003) reported distinct oligomerization pathways for Aβ(1–42) and Aβ(1–40). The strongest data implicating an oligomeric species rather than monomer is provided in Fig. 6 wherein Aβ(1–42) aggregation concentrations were adjusted to shift the equilibrium towards monomer and away from oligomer formation. Final cell treatment concentrations were kept the same. The lower Aβ(1–42) concentration, which would favor the monomeric form, was much less able to induce monocyte maturation. In support of these experiments was the inability of a mutant Aβ(1–42) L34P peptide to induce monocyte adhesion (Fig. 7). The proline point mutation slows Aβ aggregation kinetics (Williams et al., 2004) resulting in a large monomer:oligomer ratio particularly at early stages of Aβ incubation.

The relative inability of ADDLs to induce THP-1 monocyte adhesion in Fig. 8 was somewhat surprising although the list of distinct soluble Aβ aggregation species is expanding to include protofibrils (Walsh et al., 1997), oligomers (Kayed et al., 2003), ADDLs (Lambert et al., 1998), Aβ*56 (Lesne et al., 2006), and other less-defined species. Significant differences in biological activity have already been observed between different soluble species. Busciglio and colleagues reported that Aβ oligomers were more toxic to human cortical neurons and decreased mitochondrial membrane potential to a greater extent than ADDLs (Deshpande et al., 2006). Both Aβ oligomers and ADDLs (Lambert et al., 1998) were shown to be more potent than fibrillar Aβ based on results from in vitro cell assays. It is difficult to determine if size or conformation dictates differences in biological activity and potency between soluble Aβ aggregates. Hepler et al. found that ADDLs eluted in the void volume of a Superdex 75 column and absolute molecular weight measurements by multi-angle light scattering revealed a larger mass (150,000 to 1,000,000 Da) for ADDLs than originally thought (Hepler et al., 2006). It is possible that the oligomeric Aβ(1–42) species described in this report is formed earlier in the aggregation pathway than ADDLs although further research will be needed to identify structural aspects that are important for inducing monocyte maturation.

The previous finding that oligomeric Aβ(1–42) has potent monocyte chemotactic activity (Giri et al., 2000; Le et al., 2001) and the results in our current study suggest that oligomeric Aβ may influence peripheral monocyte infiltration and differentiation in vivo. El Khoury et al. (2007) demonstrated that microglial accumulation begins before formation of senile plaques and suggested that Aβ oligomers may be capable of inducing the recruitment of mononuclear phagocytes from blood. Microglial activation by Aβ may be a distinct process from that of monocyte recruitment and differentiation and be provoked by fibrillar forms of the peptide. In fact, several receptors have been identified on microglia and monocytes that recognize fibrillar Aβ and mediate proinflammatory responses typical of activated microglia (Bamberger et al., 2003; Fassbender et al., 2004; Udan

et al., 2008). Although our studies have yet to fully characterize the Aβ species that induces monocyte maturation, a careful correlation of aggregation progression and cellular activity, modulation of aggregation kinetics, and the use of a mutant Aβ peptide strongly implicated oligomeric Aβ(1–42) in the process. Our findings underscore the complex interplay of Aβ aggregation state and immune cell response and may provide clues into early inflammatory processes in AD.

4. Experimental procedures

4.1. Cell culture

THP-1 cells were obtained from American Type Culture Collection (ATCC, Manassas, VA) and maintained in RPMI-1640 culture medium (HyClone, Logan, UT) containing 2 mM L-glutamine, 25 mM HEPES, 1.5 g/L sodium bicarbonate, 10% fetal bovine serum (HyClone), 50 U/ml penicillin, 50 μg/ml streptomycin (HyClone), and 50 μM β-mercaptoethanol at 37 °C in 5% CO_2. For cellular assays, THP-1 cells were centrifuged and resuspended in reduced FBS (2%) growth medium. Cell concentrations were adjusted to 7×10^5 cells/ml and 0.204 ml (approximately 140,000 cells) was added to individual wells of a 48-well sterile culture plate.

4.2. Preparation of Aβ peptides

All Aβ(1–42) and Aβ(1–40) peptides (rPeptide, Bogarth, GA) used in these studies were dissolved in 100% hexafluoroiso-propanol (HFIP) (Sigma, St. Louis, MO) for 1 h, aliquotted into sterile microcentrifuge tubes, dried in a vacuum centrifuge, and stored at −20 °C. Prior to cell treatment the lyophilized peptides were resuspended in sterile water or phosphate-buffered saline (PBS) to 50 μM, 100 μM or 1 mM peptide concentration and incubated at 4 °C, 25 °C or 37 °C. Aβ(1–42) L34P was obtained as a gift from Ron Wetzel, (University of Pittsburgh) and treated in the same manner as commercially obtained Aβ peptides. THP-1 monocytes were exposed to a final Aβ concentration of 15 μM based on monomer units unless stated otherwise in the figure legend. Aβ-derived diffusible ligands (ADDLs) were prepared as described previously (Stine et al., 2003). Briefly, 0.25 mg of lyophilized Aβ(1–42) was resuspended to a concentration of 5 mM in dimethyl sulfoxide (DMSO) (Sigma) and then diluted to 100 μM in ice cold Ham's F12 medium with phenol red (Hyclone). The sample was incubated at 4 °C for 24 h, centrifuged for 10 min at 14,000 ×g, and supernatant (ADDLs) collected for further use.

4.3. Cell adhesion assay

THP-1 cell adhesion was induced by direct addition of 10 ng/ml phorbol 12-myristate 13-acetate (PMA) (Sigma) or 15 μM Aβ peptides to THP-1 monocytes prepared in reduced FBS growth medium unless otherwise noted. Vehicle controls were 0.0005% DMSO and sterile water for PMA and Aβ respectively. THP-1 monocytes were prepared immediately prior to each experiment. Following incubation at 37 °C for 6 h, the non-adherent cells were removed and the adherent cells were washed with PBS (Hyclone). The adherent cells were then removed with 0.25% trypsin-EDTA (HyClone), and counted under a microscope using a hemocytometer. Percent adhesion was determined by the adherent cell number divided by the plated cell number. Surface coating of 48-well cell culture plates with human fibronectin (Fn) (Sigma) was done by addition of 0.1 ml per well of 50 μg/ml Fn in sterile PBS and incubation for 1 h at 25 °C. The plate was covered and stored at 4 °C until needed for an experiment. Statistical analysis was done using a Student t-test to determine the confidence limit at which measurements were statistically different. p values were obtained and are presented in the figure legends.

4.4. Cell surface CD11b expression

THP-1 cells were treated with effectors for either 6 or 24 h to induce adhesion. Following treatment, medium was removed by aspiration and the adherent cells were washed with PBS containing 0.05% Tween 20. Detection of CD11b was done using an enzyme-linked colorimetric immunoassay at 25 °C with PBS/Tween washes in between each step. Cells were fixed with 0.25 ml of 3.7% formaldehyde for 15 min and blocked for 1 h with PBS containing 1% BSA. 0.2 ml of mouse anti-human CD11b antibody (1:500 dilution in PBS containing 1% dry milk) were added to each well, incubated 3 h, followed by incubation with 0.2 ml anti-mouse IgG conjugated to horseradish pero-xidase (1:500 dilution in PBS/1% BSA) for 1 h. 0.25 ml HRP substrate was added for 20 min and stopped with 0.125 ml 1 M H_2SO_4. The acid-treated solution was transferred to a 96-well plate and the absorbance was read for each well at 450 nm minus background absorbance at 540. Absorbance readings were normalized by dividing by the number of adherent cells ($\times 10^5$) for each condition.

4.5. Atomic force microscopy (AFM)

AFM imaging of Aβ was conducted as described previously (Udan et al., 2008). Briefly, Aβ aggregation solutions were diluted to 1 μM in water and applied (50 μl) to freshly cleaved grade V1 mica discs (Ted Pella, Inc., Redding, CA). Samples were allowed to adsorb for 15 min, washed twice with water, air dried, and stored in a container with desiccant. Images were obtained with a Nanoscope III multimode atomic force microscope (Digital Instruments, Santa Barbara, CA) in TappingMode™. Height analysis was performed using Nano-scope III software on flattened height mode images.

4.6. Transmission electron microscopy

Aβ aggregation solutions were diluted to 20 μM in water and 10 μl was applied to a 200-mesh formvar-coated copper grid (Ted Pella, Inc.). Samples were allowed to adsorb for 10 min at 25 °C, followed by removal of excess sample solution with blotting paper. Grids were washed three times by placing sample side down on a droplet of water. Heavy metal staining of the samples was done in a similar manner by incubation on a droplet of 2% uranyl acetate (Electron Microscopy Sciences, Hatfield, PA) for 5 min, followed by removal of excess solution and air drying. Affixed samples were visualized with a JEOL JEM-2000 FX transmission electron microscope operated at 200 keV.

Acknowledgments

REFERENCES

Auwerx, J., 1991. The human leukemia cell line, THP-1: a multifacetted model for the study of monocyte-macrophage differentiation. Experientia 47, 22–31.

Bamberger, M.E., Harris, M.E., McDonald, D.R., Husemann, J., Landreth, G.E., 2003. A cell surface receptor complex for fibrillar β-amyloid mediates microglial activation. J. Neurosci. 23, 2665–2674.

Bitan, G., Kirkitadze, M.D., Lomakin, A., Vollers, S.S., Benedek, G.B., Teplow, D.B., 2003. Amyloid β-protein (Aβ) assembly: Aβ40 and Aβ42 oligomerize through distinct pathways. Proc. Natl. Acad. Sci. U. S. A. 100, 330–335.

Carson, M.J., Bilousova, T.V., Puntambekar, S.S., Melchior, B., Doose, J.M., Ethell, I.M., 2007. A rose by any other name? The potential consequences of microglial heterogeneity during CNS health and disease. Neurotherapeutics 4, 571–579.

Dahlgren, K.N., Manelli, A.M., Stine Jr., W.B., Baker, L.K., Krafft, G.A., LaDu, M.J., 2002. Oligomeric and fibrillar species of amyloid-β peptides differentially affect neuronal viability. J. Biol. Chem. 277, 32046–32053.

Deshpande, A., Mina, E., Glabe, C., Busciglio, J., 2006. Different conformations of amyloid β induce neurotoxicity by distinct mechanisms in human cortical neurons. J. Neurosci. 26, 6011–6018.

Dickson, D.W., Lee, S.C., Mattiace, L.A., Yen, S.H.C., Brosnan, C., 1993. Microglia and cytokines in neurological disease, with special reference to AIDS and Alzheimer disease. Glia 7, 75–83.

Ding, Q., Jin, T., Wang, Z., Chen, Y., 2007. Catalase potentiates retinoic acid-induced THP-1 monocyte differentiation into macrophage through inhibition of peroxisome proliferator-activated receptor γ. J. Leukoc. Biol. 81, 1568–1576.

Eglitis, M.A., Mezey, E., 1997. Hematopoietic cells differentiate into both microglia and macroglia in the brains of adult mice. Proc. Natl. Acad. Sci. U. S. A. 94, 4080–4085.

El Khoury, J., Toft, M., Hickman, S.E., Means, T.K., Terada, K., Geula, C., Luster, A.D., 2007. Ccr2 deficiency impairs microglial accumulation and accelerates progression of Alzheimer-like disease. Nat. Med. 13, 432–438.

Fassbender, K., Walter, S., Kuhl, S., Landmann, R., Ishii, K., Bertsch, T., Stalder, A.K., Muehlhauser, F., Liu, Y., Ulmer, A.J., Rivest, S., Lentschat, A., Gulbins, E., Jucker, M., Staufenbiel, M., Brechtel, K., Walter, J., Multhaup, G., Penke, B., Adachi, Y., Hartmann, T., Beyreuther, K., 2004. The LPS receptor (CD14) links innate immunity with Alzheimer's disease. FASEB J. 18, 203–205.

Fiala, M., Zhang, L., Gan, X., Sherry, B., Taub, D., Graves, M.C., Hama, S., Way, D., Weinand, M., Witte, M., Lorton, D., Kuo, Y.M., Roher, A.E., 1998. Amyloid-β induces chemokine secretion and monocyte migration across a human blood-brain barrier model. Mol. Med. 4, 480–489.

Giri, R., Shen, Y.M., Stins, M., Yan, S.D., Schmidt, A.M., Stern, D., Kim, K.S., Zlokovic, B., Kalra, V.K., 2000. β-Amyloid-induced migration of monocytes across human brain endothelial cells involves RAGE and PECAM-1. Am. J. Physiol. Cell Physiol. 279, C1772–C1781.

Gravina, S.A., Ho, L., Eckman, C.B., Long, K.E., Otvos Jr., L., Younkin, L.H., Suzuki, N., Younkin, S.G., 1995. Amyloid β protein (Aβ) in Alzheimer's disease brain. Biochemical and immunocytochemical analysis with antibodies specific for forms ending at Aβ40 or Aβ42(43). J. Biol. Chem. 270, 7013–7016.

Harper, J.D., Wong, S.S., Lieber, C.M., Lansbury Jr., P.T., 1997. Observation of metastable Aβ amyloid protofibrils by atomic force microscopy. Chem. Biol. 4, 119–125.

Harper, J.D., Wong, S.S., Lieber, C.M., Lansbury Jr., P.T., 1999. Assembly of Aβ amyloid peptides: an in vitro model for a possible early event in Alzheimer's disease. Biochemistry 38, 8972–8980.

Hepler, R.W., Grimm, K.M., Nahas, D.D., Breese, R., Dodson, E.C., Acton, P., Keller, P.M., Yeager, M., Wang, H., Shughrue, P., Kinney, G., Joyce, J.G., 2006. Solution state characterization of amyloid β-derived diffusible ligands. Biochemistry 45, 15157–15167.

Hickstein, D.D., Baker, D.M., Gollahon, K.A., Back, A.L., 1992. Identification of the promoter of the myelomonocytic leukocyte integrin CD11b. Proc. Natl. Acad. Sci. U. S. A. 89, 2105–2109.

Hmama, Z., Knutson, K.L., Herrera-Velit, P., Nandan, D., Reiner, N.E., 1999. Monocyte adherence induced by lipopolysaccharide involves CD14, LFA-1, and cytohesin-1. Regulation by Rho and phosphatidylinositol 3-kinase. J. Biol. Chem. 274, 1050–1057.

Jarrett, J.T., Lansbury Jr., P.T., 1993. Seeding "one-dimensional crystallization" of amyloid: a pathogenic mechanism in Alzheimer's disease and scrapie? Cell 73, 1055–1058.

Kayed, R., Head, E., Thompson, J.L., McIntire, T.M., Milton, S.C., Cotman, C.W., Glabe, C.G., 2003. Common structure of soluble amyloid oligomers implies common mechanism of pathogenesis. Science 300, 486–489.

Kounalakis, N.S., Corbett, S.A., 2006. Lipopolysaccharide transiently activates THP-1 cell adhesion. J. Surg. Res. 135, 137–143.

Lambert, M.P., Barlow, A.K., Chromy, B.A., Edwards, C., Freed, R., Liosatos, M., Morgan, T.E., Rozovsky, I., Trommer, B., Viola, K.L., Wals, P., Zhang, C., Finch, C.E., Drafft, G.A., Klein, W.L., 1998. Diffusible, nonfibrillar ligands derived from Aβ1–42 are potent central nervous system neurotoxins. Proc. Natl. Acad. Sci. U. S. A. 95, 6448–6453.

Le, Y., Gong, W., Tiffany, H.L., Tumanov, A., Nedospasov, S., Shen, W., Dunlop, N.M., Gao, J.L., Murphy, P.M., Oppenheim, J.J., Wang, J.M., 2001. Amyloid β42 activates a G-protein-coupled chemoattractant receptor, FPR-like 1. J. Neurosci. 21, RC123.

Lesne, S., Koh, M.T., Kotilinek, L., Kayed, R., Glabe, C.G., Yang, A., Gallagher, M., Ashe, K.H., 2006. A specific amyloid-β protein assembly in the brain impairs memory. Nature 440, 352–357.

Lorenzo, A., Yankner, B.A., 1994. β-amyloid neurotoxicity requires fibril formation and is inhibited by Congo red. Proc. Natl. Acad. Sci. U. S. A. 91, 12243–12247.

Maslow, K., 2008. 2008 Alzheimer's disease facts and figures. Alzheimer's Dement. 4, 110–133.

McGeer, P.L., Itagaki, S., Tago, H., McGeer, E.G., 1987. Reactive microglia in patients with senile dementia of the Alzheimer type are positive for the histocompatibility glycoprotein HLA-DR. Neurosci. Lett. 79, 195–200.

Meyer-Luehmann, M., Spires-Jones, T.L., Prada, C., Garcia-Alloza, M., de Calignon, A., Rozkalne, A., Koenigsknecht-Talboo, J., Holtzman, D.M., Bacskai, B.J., Hyman, B.T., 2008. Rapid appearance and local toxicity of amyloid-β plaques in a mouse model of Alzheimer's disease. Nature 451, 720–724.

Park, E.K., Jung, H.S., Yang, H.I., Yoo, M.C., Kim, C., Kim, K.S., 2007. Optimized THP-1 differentiation is required for the detection of responses to weak stimuli. Inflamm. Res. 56, 45–50.

Pike, C.J., Walencewicz, A.J., Glabe, C.G., Cotman, C.W., 1991. In vitro aging of β-amyloid protein causes peptide aggregation and neurotoxicity. Brain Res. 563, 311–314.

Ruoslahti, E., Pierschbacher, M.D., 1987. New perspectives in cell adhesion: RGD and integrins. Science 238, 491–497.

Schwende, H., Fitzke, E., Ambs, P., Dieter, P., 1996. Differences in the state of differentiation of THP-1 cells induced by phorbol ester and 1,25-dihydroxyvitamin D_3. J. Leukoc. Biol. 59, 555–561.

Selkoe, D.J., 1998. The cell biology of β-amyloid precursor protein and presenilin in Alzheimer's disease. Trends Cell Biol. 8, 447–453.

Selkoe, D.J., 2001. Alzheimer's disease: genes, proteins, and therapy. Physiol. Rev. 81, 741–766.

Selkoe, D.J., 2004a. Alzheimer disease: mechanistic understanding predicts novel therapies. Ann. Intern. Med. 140, 627–638.

Selkoe, D.J., 2004b. Cell biology of protein misfolding: the examples of Alzheimer's and Parkinson's diseases. Nat. Cell Biol. 6, 1054–1061.

Simard, A.R., Soulet, D., Gowing, G., Julien, J.P., Rivest, S., 2006. Bone marrow-derived microglia play a critical role in restricting senile plaque formation in Alzheimer's disease. Neuron 49, 489–502.

Stine, W.B.J., Dahlgren, K.N., Krafft, G.A., LaDu, M.J., 2003. In vitro characterization of conditions for amyloid-β peptide oligomerization and fibrillogenesis. J. Biol. Chem. 278, 11612–11622.

Tsuchiya, S., Kobayashi, Y., Goto, Y., Okumura, H., Nakae, S., Konno, T., Tada, K., 1982. Induction of maturation in cultured human monocytic leukemia cells by a phorbol diester. Cancer Res. 42, 1530–1536.

Udan, M.L., Ajit, D., Crouse, N.R., Nichols, M.R., 2008. Toll-like receptors 2 and 4 mediate Aβ(1–42) activation of the innate immune response in a human monocytic cell line. J. Neurochem. 104, 524–533.

Walsh, D.M., Lomakin, A., Benedek, G.B., Condron, M.M., Teplow, D.B., 1997. Amyloid β-protein fibrillogenesis: detection of a protofibrillar intermediate. J. Biol. Chem. 272, 22364–22372.

Walsh, D.M., Hartley, D.M., Kusumoto, Y., Fezoui, Y., Condron, M.M., Lomakin, A., Benedek, G.B., Selkoe, D.J., Teplow, D.B., 1999. Amyloid β-protein fibrillogenesis: structure and biological activity of protofibrillar intermediates. J. Biol. Chem. 274, 25945–25952.

Walsh, D.M., Klyubin, I., Fadeeva, J.V., Cullen, W.K., Anwyl, R., Wolfe, M.S., Rowan, M.J., Selkoe, D.J., 2002. Naturally secreted oligomers of amyloid β protein potently inhibit hippocampal long-term potentiation in vivo. Nature 416, 535–539.

Wegiel, J., Imaki, H., Wang, K.C., Rubenstein, R., 2004. Cells of monocyte/microglial lineage are involved in both microvessel amyloidosis and fibrillar plaque formation in APPsw tg mice. Brain Res. 1022, 19–29.

Williams, A.D., Portelius, E., Kheterpal, I., Guo, J.T., Cook, K.D., Xu, Y., Wetzel, R., 2004. Mapping Aβ amyloid fibril secondary structure using scanning proline mutagenesis. J. Mol. Biol. 335, 833–842.

Yan, S.D., Chen, X., Fu, J., Chen, M., Zhu, H., Roher, A., Slattery, T., Zhao, L., Nagashima, M., Morser, J., Migheli, A., Nawroth, P., Stern, D., Schmidt, A.M., 1996. RAGE and amyloid-β peptide neurotoxicity in Alzheimer's disease. Nature 382, 685–691.

1 INTRODUCTION

1.1 Alzheimer's Disease

Alzheimer's Disease (AD) is a progressive, neurodegenerative disorder that affects the memory of afflicted patients. First described in 1906 by Alois Alzheimer, AD has become the most common form of dementia experienced by aging people (St George-Hyslop, 2000). In the 20th century, the average life expectancy increased from 49 to 76 years, which is believed to be a contributing factor to the increased numbers of AD patients (Selkoe, 2001a). In fact, AD currently ranks as the 5th leading cause of death among Americans over age 65 and the 7th leading cause of death for all Americans (Maslow, 2008).

Most cases of AD exhibit two classical brain lesions (Walsh and Selkoe, 2004), amyloid β (Aβ) plaques (Teplow, 1998; Selkoe, 2001b) and neurofibrillary tangles (Mandelkow and Mandelkow, 1998) (NFTs), both of which were first noted in the brain of the original AD patient Alzheimer studied (Selkoe, 2001b). Although these pathological hallmarks of AD are present in most sufferers, tau tangles can occur in other neurodegenerative diseases in the absence of Aβ plaques (Selkoe, 2001b). Also, some cases of AD have been classified as "tangle poor" (Selkoe, 2001b) due to the presence of Aβ plaques but very few NFTs (Terry et al., 1987).

Aside from Aβ plaques and NFTs, other common hallmarks of AD include the presence of dystrophic neurites and an increase in brain atrophy (Mori et al., 1997). Inflammation in the brain is also commonly found in patients with AD (McGeer et al., 1987).

1.2 Neurofibrillary Tangles (NFTs)

The protein tau is a microtubule associated protein (MAP) typically found in axons. MAPs serve as stabilization agents for neuronal microtubules that allow the microtubules to perform their designated roles in intracellular transport, the establishment of cellular polarity as well as the development of other cellular processes (Mandelkow and Mandelkow, 1998). Tau also promotes the assembly of the microtubules and is regulated by it's level of phosphorylation (Iqbal et al., 2005). When tau is phosphorylated with 2-3 moles of phosphate per mole of tau, it is optimized for peak function (Kopke et al., 1993).

In AD, tau becomes hyperphosporylated (Mandelkow et al., 1995; Trojanowski and Lee, 1995; Delacourte and Buee, 1997) which leads to disruptions in intracellular transport and ultimately axonal death (Mandelkow and Mandelkow, 1998). It has been seen that tau becomes abnormally glycosylated before it is hyperphosphorylated (Wang et al., 1996a; Liu et al., 2002b) leading to the theory that the glycosylation actually promotes the hyperphosphorylation (Liu et al., 2002a; Liu et al., 2002b).

Tau can undergo abnormal phosphorylation at more than 30 different sites in AD, most of which are either serine or threonine residues followed by a proline residue sug-

gesting that proline-directed protein kinases (PDPK) may participate in the phosphoryla-tion of tau residues. Tau is known to be a substrate for several protein kinases, including glycogen synthase kinase-3 (GSK-3), cyclin dependent protein kinase-5 (cdk5), ERK 1/2, protein kinase A, calcium and calmodulin-dependent protein kinase-II and stress-activated protein kinases (Pei et al., 2003). Of the known kinases that phosphorylate tau, GSK-3, cdk5 and ERK 1/2 are PDPKs (Iqbal et al., 2005). When tau becomes phos-phorylated at Serine 214 or Serine 262, it dissociates from and leads to the disassembly of the microtubule (Alonso et al., 1994; Alonso et al., 1996; Alonso et al., 1997; Man-delkow and Mandelkow, 1998).

When the phosphorylation level of tau reaches 4-6 moles of phosphate per mole of tau, the hyperphosphorylated tau gains the ability to sequester normal tau. Alonso et al. showed that there is a high affinity between normal and hyperphosphorylated tau that was unable to be saturated with higher concentrations of the normal tau. They speculate that the hyperphosphorylated tau serves as a nucleation center for the normal tau allow-ing the normal protein to aggregate into the tau tangles. This process leads to further microtubule disassembly and eventually more axonal death, possibly through a competi-tion between hyperphosphorylated tau and tubulin for the normal tau (Alonso et al., 1994; Alonso et al., 1996; Alonso et al., 1997; Alonso Adel et al., 2004).

If tau is phosphorylated at a level equal to 10 or more moles of phosphate per mole of tau, the protein begins to aggregate and it loses the ability to sequester normal tau (Alonso Adel et al., 2004). The additional phosphorylation is believed to neutralize a large, negatively charged area within a basic domain of tau (Ruben et al., 1991) that has been shown to self-assemble *in vitro* (von Bergen et al., 2000). The aggregates can have

the structure of paired helical filaments (PHF), twisted ribbons or straight filaments (Ruben et al., 1993). The PHF are reported to range in size from 10-20 nm wide and contain crossover repeats of about 80 nm (Schweers et al., 1995). It has been proposed that in order to stop the sequestering of normal tau and the disassembly of microtubules, neurons promote PHF formation by increasing the phosphorylation of tau (Iqbal et al., 2005). The PHF and straight filaments eventually combine to make the NFTs seen in AD brains.

Aside from an increase in hyperphosphorylated tau, an increase in the overall level of tau is found in AD patients (Vigo-Pelfrey et al., 1995). In fact, it was shown that AD brains contain 4-8 times more total tau than age-matched non-demented brains (von Bergen et al., 2000). Once hyperphosphorylated, tau resists the proteolytic activity of calcium activated neutral protease (Wang et al., 1995; Wang et al., 1996b). Also, in AD the p70 S6 kinase is activated, which upregulates the translation of tau (An et al., 2003), accounting for an increase in normal tau and contributing to the levels of hyperphos-phorylated tau seen in AD.

Although certainly an integral portion of AD pathology, it is not entirely clear whether or not tau is actually the causative factor of AD. Because "tangle poor" AD cases can occur (Terry et al., 1987; Selkoe, 2001b), it is likely that the hyperphosphory-lation of tau is actually an event that occurs once the AD process has begun. Some re-search has suggested that the presence of Aβ may play a role in the induction of the tau hyperphosphorylation process (Busciglio et al., 1995), and Dickson suggests that Aβ interactions with cells may lead to the activation of apoptosis and, eventually caspases, which in turn leads to the proteolysis of tau (Dickson, 2004). Taken together, the studies

suggest that Aβ is actually the more causative factor in AD and leads to the tau pathology.

1.3 Amyloid β (Aβ)

The Aβ peptide is a 39-43 residue protein (Citron et al., 1994) that is cleaved from a larger, 770 residue integral membrane protein known as the amyloid precursor protein (APP). The cleavage of APP can occur via an amyloidogenic or a non-amyloidogic pathway.

In non-amyloidogenic APP cleavage, α-secretase cleaves APP in the middle of the Aβ sequence between APP residues 687 and 688, which correspond to Aβ positions 16 and 17. This cleavage pathway results in the production of two protein fragments that are non-pathogenic (Weidemann et al., 1989; Esch et al., 1990; Sisodia et al., 1990). However in AD, Aβ is produced through the cleaving action of β- and γ-secretases (Selkoe, 2001c; Hardy and Selkoe, 2002) (Fig. 1.1) (Bateman et al., 2006). β-secretase cleaves the N-terminal end of Aβ between APP residues 671 and 672. γ-secretase provides the C-terminal cleavage of Aβ near the APP residue 713 (Selkoe, 2001b). Depending on the actual location of the γ-secretase cleavage of APP, the Aβ peptide is most commonly either 40- or 42-residues long (Aβ(1-40) and Aβ(1-42) respectively) and can be found as a component of the central nervous system (CNS) (Seubert et al., 1992; Busciglio et al., 1993). It has also been shown that in cases of AD where β-secretase cleavage is increased, there is a corresponding increase in the amount of Aβ present (Citron et al., 1992; Cai et al., 1993; Citron et al., 1994).

Aβ(1-40) - DAEFRHDSGYEVHHQKLVFFAEDVGSNKGAIIGLMVGGVV
Aβ(1-42) - DAEFRHDSGYEVHHQKLVFFAEDVGSNKGAIIGLMVGGVVIA
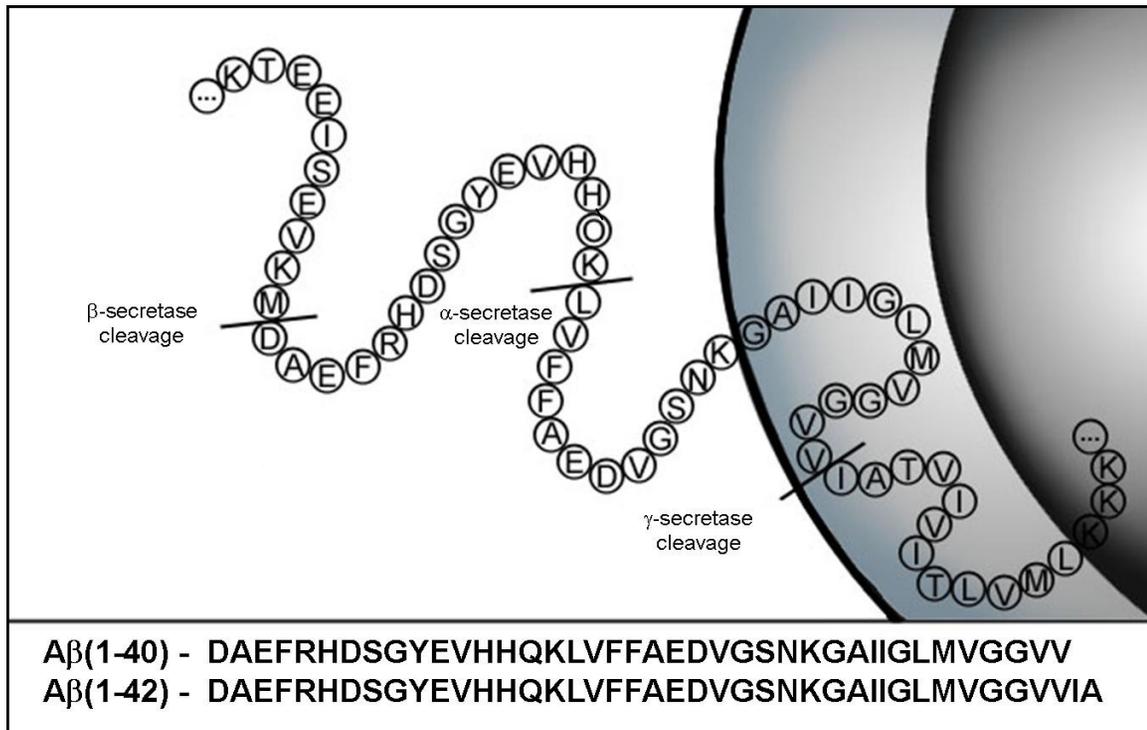
Fig. 1.1 Amyloid Precursor Protein is proteolytically cleaved to produce the Aβ peptides. The Amyloid Precursor Protein (APP) is an integral membrane protein that is cleaved by β-secretase in the lumen to produce the N-terminus of the Aβ peptides. Cleavage by γ-secretase produces the C-terminal end of the Aβ peptides. Varying lengths of Aβ are produced, depending on the location of the γ-secretase cleavage. Figure modified from Bateman et al., 2006.

Determining the role of Aβ in AD has been difficult to study due to the location of Aβ plaques within the human brain, which has limited *in vivo* work to post-mortem studies. To help further the *in vivo* work, mouse models have been developed to mimic AD pathology. A common mouse line, TG2576, is a close model for human AD in that the mice develop Aβ plaques, dystrophic neurites and inflammation within the brain (Hsiao et al., 1996; Irizarry et al., 1997; Benzing et al., 1999) despite their lack of tau tangles (Irizarry et al., 1997).

Animal studies have suggested a correlation between increased Aβ loads and increased levels of neuronal disfuntion (Games et al., 1995; Hsiao et al., 1996; Masliah et al., 1996). When Tg2576 mice were subjected to a Morris water maze test, $2 - 6$ month old mice had a similar escape latency to non-transgenic litter mates, but 9 month old transgenic mice were significantly slower at escaping. Following the testing, the escape platform was removed and the mice were allowed to swim for 60 second while the researchers measured the amount of time the mice spent in the quadrant where the platform was. They again saw the young transgenic mice perform similarly to non-transgenic mice while the older Tg2576 mice performed significantly more poorly. The transgenic mice were shown to express about 5 times more APP in the brain than non-transgenic mice suggesting the relationship between Aβ and neuronal disfunction (Hsiao et al., 1996).

The correlation was later found to be consistent with human studies. A comparison of brain slices from 23 AD patients and 10 non-pathologic patients was undertaken to determine if there was a relationship between the pre-mortem mental function and the post-mortem physiology. The samples were removed from the brains with formic acid

and the levels of Aβ(1-42) and Aβ(1-40) were analyzed with an enzyme-linked immu-

nosorbent assay (ELISA). Patients exhibiting increased AD characteristics were found

to have higher loads of insoluble Aβ in post-mortem brain slices than age-matched, non-

AD brains. There was an average of a 330-fold increase in Aβ(1-42) and a 1050-fold

increase in Aβ(1-40) found in the AD brains compared to non-AD brains. It was also

determined that of the Aβ found in the brains, a significantly higher portion was insolu-

ble in the AD brains versus the non-AD brains (Wang et al., 1999).

Despite the difficulties found in studying AD *in vivo*, the *in vitro* work has

yielded much insight in the subject. Researchers have shown that once cleaved from the

APP, Aβ begins to aggregate through a nucleation-dependent polymerization (Jarrett

and Lansbury, 1993; Lomakin et al., 1996) (Fig. 1.2a). The aggregation begins with the

formation of a nucleus from monomer units, which is the rate limiting step of the proc-

ess. Once formed, the nucleus structure is then further polymerized, which leads to an

intermediate aggregation species commonly referred to as a protofibril, which itself un-

dergoes further aggregation to form large Aβ fibrils (Walsh et al., 1997) (Fig. 1.2b). As

seen in figure 1.2, there is a lag time associated with the formation of the nucleus struc-

ture. However, if the aggregation mixture is seeded with pre-formed aggregates, the lag

time disappears and both aggregations end with the attainment of an equilibrium state

(Walsh et al., 1997).

Recent research has found that a variety of aggregation intermediates exist be-

tween the monomer and fibril stages of the polymerization model (Harper et al., 1997a;

Walsh et al., 1997; Harper et al., 1999; Walsh et al., 1999; Stine et al., 2003). These Aβ

aggregates are the primary component of the neuritic plaques found in AD brains, but

A

B

Monomers → Nucleus → Protofibril → Fibrils
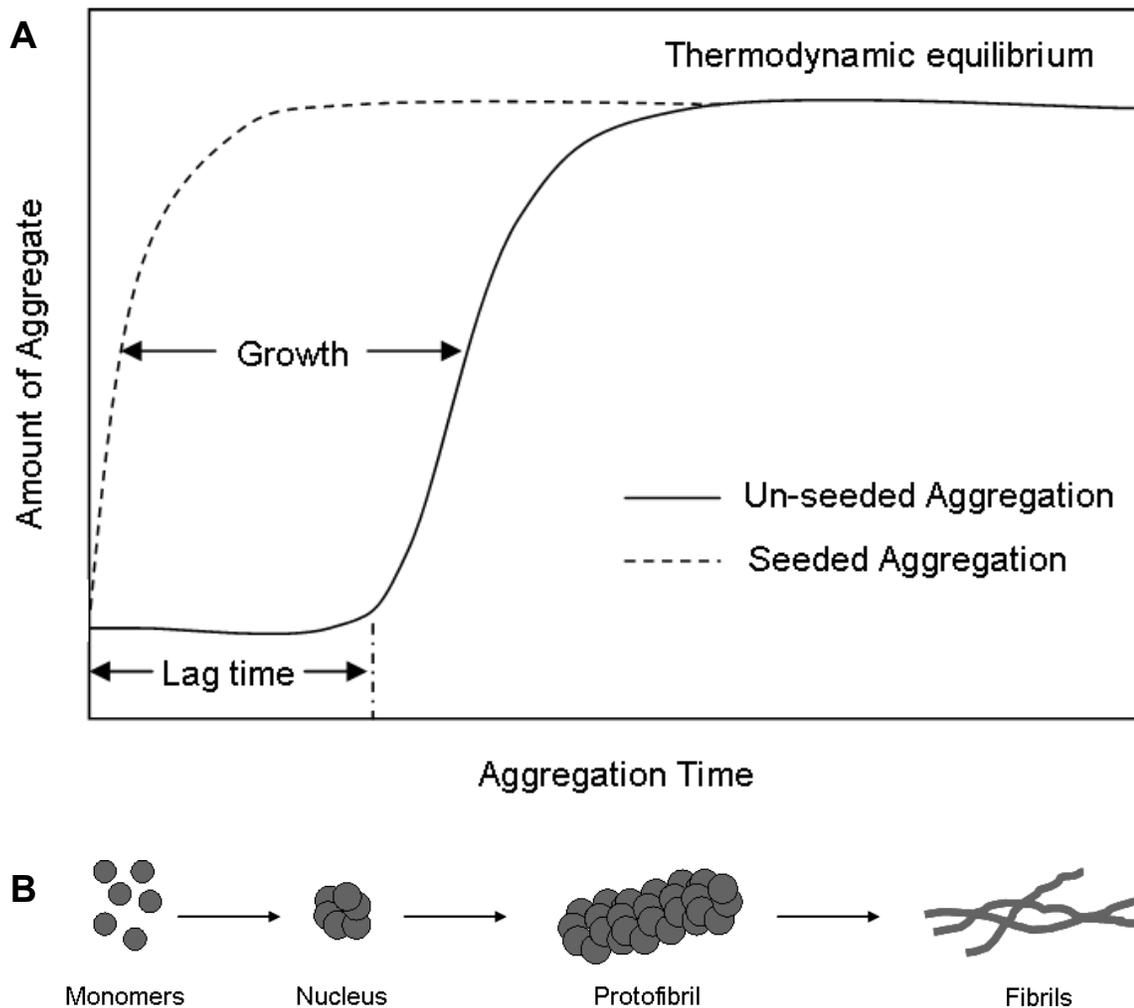
Fig. 1.2 Aβ aggregates through a nucleation dependent polymerization mechanism.
A) The formation of the Aβ nucleus structure causes a lag time in the aggregation kinetics (solid line) followed by much faster formation of later aggregate species. If the aggregation mixture is seeded with pre-formed intermediates at the beginning (dashed line) the lag time disappears and the aggregation precedes to late stage aggregates quickly. Figure modified from Jarrett and Lansbury, 1993. B) The Aβ aggregation process begins with monomer assembly into a nucleus which seeds the formation of protofibrils and eventually fibers (fibrils). Figure modified from Walsh et al., 1997.

there is a degree of polymorphism seen within the plaques (Selkoe, 2004). The terms protofibril and oligomer are vague and can refer to many different aggregate structures and assembly states.

Extensive solid state NMR studies on aggregated Aβ have shown that the protein adopts a primarily β-sheet secondary structure (Balbach et al., 2002; Bu et al., 2007). These studies have been supplemented with x-ray diffraction results, which suggest a cross-β structure wherein the side chains line up perpendicular and the interchain hydrogen bonding patterns line up parallel to the long axis of the fibril (Inouye et al., 1993; Malinchik et al., 1998; Serpell et al., 2000).

Studies of aggregated Aβ have also indicated that Aβ(1-42), the most prevalent form of Aβ found in the senile plaques of AD patients (Gravina et al., 1995), has a higher propensity for aggregation than the Aβ(1-40) form (Iwatsubo et al., 1994; Suzuki et al., 1994; Harper et al., 1997b) and is thus considered to be the more toxic species of Aβ. In fact, many early studies of Aβ(1-42) aggregates suggested that it was the highly aggregated fibrillar assembly that was responsible for the toxicity seen in cells (Pike et al., 1991; Roher et al., 1991; Pike et al., 1993).

However, more recent research has suggested an intermediate aggregate species as the most toxic. When rat brains were treated with solutions containing Aβ monomers and soluble oligomers a significant decrease in long term potentiation (LTP), a measure of synaptic plasticity, was found. If the Aβ solutions were immunodepleted before treating the rats, there was no decrease in LTP (Walsh et al., 2002). Westerman et al. found that in Tg2576 mice, older mice with high Aβ plaque loads did not exhibit significant cognitive dysfunction compared to non-transgenic mice (Westerman et al., 2002). Fur-

ther support for soluble Aβ species being the most toxic is supported by studies with a mouse model expressing APP without the development of plaques. The APP mice performed worse than non-APP expressing mice in Morris water maze tests and dry arena tests suggesting an impairment of neuronal function. The lack of plaque development in the mouse brains suggests that a soluble Aβ species is responsible for differences in performance in the different mouse lines tested (Koistinaho et al., 2001).

There has been some difficulty in determining the exact identity of the toxic intermediate species because of its soluble nature. The research labs of Teplow (Walsh et al., 1997) and Lansbury (Harper et al., 1997b) both reported the presence of an aggregation intermediate that they named protofibrils. These species showed molecular weights >100,000 kDa with diameters up to 8 nm and lengths <200 nm (Walsh et al., 1997; Harper et al., 1999; Nybo et al., 1999; Walsh et al., 1999; Blackley et al., 2000). Despite the evidence of the protofibril assembly, other aggregate intermediates have been found to be toxic as well. Aβ-derived diffusible ligands (ADDLs) are soluble, globlular assemblies that range in size from 4-6 nm in diameter and 17-42 kDa in mass (Lambert et al., 1998), and have been found to be toxic during *in vitro* studies (Oda et al., 1995; Lambert et al., 1998).

Other Aβ aggregation intermediates have been found and included in the class of soluble oligomers. Protofibrils of 2.7 to 4.2 nm in length have been previously described (Hartley et al., 1999). Kayed et al. described an oligomer-specific antibody that recognizes oligomeric conformations of various amyloidogenic peptides. The smallest assembly recognized with the antibody measured ~40 kDa, which corresponds to an Aβ octamer (Kayed et al., 2003). A study involving Tg2576 mice found that the decline in

memory function found in the middle aged mice correlated to the presence of a soluble Aβ intermediate. The species measured 56 kDa and was named Aβ*56. When Aβ*56 was administered to young mice with no cognitive defects, the mice developed memory impairments (Lesne et al., 2006).

Interestingly, the Aβ aggregation pathway can be altered by changing the aggregation environment. Studies by Harper et al. show that as the concentration of the aggregation solution is increased, the rate of Aβ aggregation also increases. They also found that when the pre-formed protofibrils are diluted, they disassembled into shorter protofibrils of about half their original length. Aggregations at higher temperatures were found to have faster rates of assembly than lower temperature systems. Protofibril elongation was also increased by higher ionic strength solutions. Variations in pH were also found to affect the aggregation process (Harper et al., 1999).

1.4 Familial AD Mutations

The collective research indicates that although tau is involved in the overall AD pathology, Aβ is most likely the causative factor for much of the neurodegeneration seen in AD. Adding to this viewpoint is the existence of familial forms of AD (FADs). Although the majority of AD cases are classified as sporadic and occur as a normal part of the aging process, a smaller group fall under the umbrella of FADs and often present with earlier average age of onset (AAO) of pathology than sporadic cases, which is also referred to as early onset AD (EOAD). Many times FAD cases come to light through the appearance of early onset AD within multiple generations of a family.

Mutation	Name	Phenotype	AAO	Reference
Lys 670 Asn Met 671 Leu	Swedish	AD	52	Mullan et al. 1992a; Mullan et al. 1992b; Haass et al. 1995; Mann et al. 1996; Scheuner et al. 1996;
His 677 Arg		AD	55	Janssen et al. 2003
Asp 678 Asn		AD with occasional aggression	60	Wakutani et al. 2004
Ala 692 Gly	Flemish	Large, dense core plaques and CAA	40 - 60	Wisniewski et al. 1991; Hendriks et al. 1992; Clements et al. 1993; Haass et al. 1994; Cras et al. 1998; De Jonghe et al. 1998; Kumar-Singh et al. 2000a; Roks et al. 2000; Walsh et al. 2001; Kumar-Singh et al. 2002b
Glu 693 Gly	Arctic	AD	58	Kamino et al. 1992; Nilsberth et al. 2001; Lashuel et al. 2003; Pavio et al. 2004; Whalen et al. 2005
Glu 693 Gln	Dutch	HCHWA-D (repeated strokes)	50	Van Broeckhoven et al. 1990; Soto et al. 1995; Mann et al. 1996; De Jonghe et al. 1998; Kumar-Singh et al. 2002a Baumketner et al. 2008
Glu 693 Lys	Italian	Cerebral hemorrhages		Murakami et al. 2003
Asp 694 Asn	Iowa	AD or cerebral hemorrhage	60	Grabowski et al. 2001; Van Nostrand et al. 2001
Ala 713 Thr		AD	59	Carter et al. 1992
Ala 713 Val		Schizophrenia		Jones et al. 1992
Thr 714 Ile	Austrian	AD with high plaque loads	35 - 45	Kumar-Singh et al. 2000b
Thr 714 Ala	Iranian	AD	52	Pasalar et al. 2002; Zekanowski et al. 2003
Val 715 Met	French	AD	52	Ancolio et al. 1999; De Jonghe et al. 2001
Val 715 Ala	German	AD	47	De Jonghe et al. 2001; Cruts et al. 2003;
Ile 716 Val	Florida	AD	53	Eckman et al. 1997
Ile 716 Thr		AD	55	Terreni et al. 2002
Val 717 Phe	Indiana	AD	47	Murrell et al. 1991
Val 717 Gly		AD	55	Chartier-Harlin et al. 1991
Val 717 Ile	London	AD	55	Goate et al. 1991; De Jonghe et al. 1998; De Jonghe et al. 2001
Val 717 Leu		AD	38	Murrell et al. 2000; De Jonghe et al 2001
Leu 723 Pro	Australian	AD	56	Kwok et al. 2000; De Jonghe et al. 2001

Table 1.1 Mutations identified within the APP sequence.
Early-onset of AD symptoms can often be found within multiple generations of a single family. Genetic analysis of these patients have brought about the identification of several APP mutations that contribute varying pathologies to the AD models. Highlighted mutations occur within the Aβ(1-42) sequence of APP.

Once presented to the medical community, researchers attempt to elucidate the causes behind the unusual symptoms presented by FAD sufferers. Currently, many cases of FAD have been linked to mutations within the APP protein sequence (Table 1.1). Most of the mutations occur outside of the Aβ(1-42) sequence, which is located from residue 672 – 713 within the APP protein.

Mutations within similar locations of the APP sequence share overall pathological manifestations. For example, several mutations have been identified from residues 714-723 of APP, just C-terminal to the Aβ sequence. These mutations are associated with early AAO and an increase in the ratio of Aβ(1-42):Aβ(1-40) produced during APP cleavage, likely due to their proximity to the γ-secretase cleavage site. On the N-terminal end of the Aβ sequence only one pathogenic mutation has been identified. Mutations within the Aβ sequence are often associated with cerebral amyloid angiopathy (CAA), which will be described in depth later, and often result in cerebral hemorrhages. The following sections are detailed discussions of the various forms of FAD.

1.4.1 APP Mutations C-terminal to the Aβ Sequence

Many of the mutations within the APP sequence occur C-terminal to the Aβ(1-42) sequence, near the γ-secretase cleavage site between residues 713 and 714. These mutations share some pathogenic features, possibly due to their proximity to the γ-secretase site.

Two mutations, the Austrian (Kumar-Singh et al., 2000b) and the Iranian (Pasalar et al., 2002), have been reported to occur at APP position 714 and involve the

conversion of the threonine residue to an isoleucine or an alanine, respectively. Both mutations lead to early appearance of AD symptoms, with the Iranian mutation having an AAO in the mid fifties while the Austrian leads to an AAO of about 35 years (Kumar -Singh et al., 2000b; Pasalar et al., 2002)

The first patient (proband) identified with the Austrian mutation was, along with her family, studied intensively. Blood plasma samples were tested from the proband, a relative lacking in the mutation and several age-matched, unrelated control subjects. The plasma was analyzed for Aβ content, and it was determined that the proband contained a 2.5-fold higher Aβ(1-42):Aβ(1-40) ratio than the other test subjects. Later postmortem studies of the proband showed pathological manifestations that included Aβ plaques and NFTs in the brain. Of interest was the exceptionally large plaque load comprised of dif-fuse plaques that contained very little, if any, Aβ(1-40), which correlated with the earlier plasma analyses. Some of the Aβ found in the diffuse plaques was determined to be truncated at the N-terminus, but Aβ located in the vessel walls or as the dense cores of plaques were full length (Kumar-Singh et al., 2000b).

The *in vivo* results were complemented with an *in vitro* study in which the T714I mutation was transfected into human embryonic kidney cells (HEK293). The research-ers found that here too, the ratio of Aβ(1-42):Aβ(1-40) was higher than in HEK293 cells transfected with wild type (WT) APP. Further analysis showed that the change in ratio was directly related to an increase in the level of Aβ(1-42) and a decrease in Aβ(1-40) (Kumar-Singh et al., 2000b).

The Iranian mutation was originally reported to be found in nine people within three generations of an Iranian family (Pasalar et al., 2002), but was later found to occur

in a patient living in Poland (Zekanowski et al., 2003). It is suspected that their may be some familial ties between the two instances. To date, no pathological information is available relating to the T714A mutation.

One position later, at 715, two more mutations in APP have been noted. The French mutation (V715M) has an AAO of about 52 with a duration of approximately 14 years. Transfection of the mutation into HEK293 cells revealed a decrease in overall Aβ production when compared to WT transfected cells. Both transfections produced similar amounts of Aβ(1-42), but the V715M transfection led to a decrease in Aβ(1-40) production (Ancolio et al., 1999). This result was confirmed in a study in which the mutation was transfected into primary mouse neurons, which resulted in a 30% decrease in Aβ(1-40) production (De Jonghe et al., 2001). Therefore, the ratio of Aβ(1-42):Aβ(1-40) was again higher in the presence of the French mutation (Ancolio et al., 1999).

The other 715 APP mutation is the German mutation of V715A. The clinical AAO is 52 years. The mutation was transfected into HEK293 cells and the levels of Aβ were determined. The ratio of Aβ(1-42):Aβ(1-40) was about 4 times higher than WT APP transfected cells (Cruts et al., 2003). The V715A mutation was also transfected into mouse primary neurons, resulting in a nearly 50% decrease in the production of Aβ(1-40) and a 50% increase in the production of Aβ(1-42) (De Jonghe et al., 2001).

Two mutations are reported at APP position 716, but the mutation I716T is very poorly represented in the literature (Terreni et al., 2002) despite appearing in databases detailing APP mutations (http://www.molgen.ua.ac.be/ADMutations). The Florida mutation (I716V) has an AAO of 53 years. In an analysis of Aβ levels in the blood plasma of patients with the mutation there was an increase in the Aβ(1-42) levels compared to

patients not expressing the mutation. When the mutation was transfected into HEK293 cells, an increase was seen in the Aβ(1-42):Aβ(1-40) ratio due to an increase in Aβ(1-42) levels. The ratio increase was also seen when the I716V mutation was transfected into Chinese hamster ovary (CHO) cells, but in this instance both the Aβ(1-42) and Aβ (1-40) levels increased compared to WT APP transfection controls (Eckman et al., 1997).

There are currently four separate mutations reported to the 717 position of APP. Two of the mutations, V717G and V717I (London mutation) each have AAO of 55 years (Chartier-Harlin et al., 1991; Goate et al., 1991). Both lead to typical manifestations of AD. The London mutant has been shown to decrease the production of Aβ(1-40) 2-fold while increasing the Aβ(1-42):Aβ(1-40) ratio 3-fold following transfection into CHO and HEK293 cells (De Jonghe et al., 1998). An increase in the Aβ(1-42):Aβ(1-40) ratio was also seen when the V717I APP mutant was transfected into primary mouse cortical neurons (De Jonghe et al., 2001).

Another APP 717 mutation, the Indiana mutation (V717F), has been reported to have an AAO of 47 years. AD associated with the Indiana mutation typically has a duration of 7 years. Post-mortem studies of affected patients revealed typical AD pathology with very little Aβ deposition in the vessels and no sign of cerebral hemorrhage (Murrell et al., 1991).

The fourth mutation at the 717 position of APP is also the one with the earliest AAO, 38. The V717L change in APP leads to a duration of about 10 years (Murrell et al., 2000). As with the London mutation, when the V717L mutant was transfected into primary mouse cortical neurons, an increase in the Aβ(1-42):Aβ(1-40) ratio was seen

(De Jonghe et al., 2001).

The final C-terminal APP mutation that has been reported is the Australian mutation, L723P. The mean AAO is 56 years for the Australian form of FAD. When APP containing the Australian mutation was transfected into CHO cells, the amount of Aβ(1-42) produced was increased nearly two-fold when compared to WT APP transfections. It was also found that the presence of the L723P mutation was inducing apoptotic cell death in the CHO cells (Kwok et al., 2000).

Collectively, mutations in the C-terminal region of APP appear to increase the Aβ(1-42):Aβ(1-40) ratio. In studies in which six of the C-terminal APP mutations were individually transfected into primary mouse neurons, they all showed an increase in the ratio of Aβ(1-42):Aβ(1-40). The authors were also able to find an inverse correlation between the ratio and the AAO. As the ratio of Aβ(1-42):Aβ(1-40) increased, the AAO decreased with V717I having the lowest ratio and the highest AAO, and T714I having the highest ratio and the lowest AAO of the mutations studied (De Jonghe et al., 2001).

The current theory is that due to the proximity of these particular mutations to the γ-secretase cleavage site they are more likely to affect the cleavage of Aβ. The research suggests that whether it be from an increase in the production of Aβ(1-42) or a decrease in the production of Aβ(1-40), a higher ratio of Aβ(1-42):Aβ(1-40) leads to a more pathogenic form of AD.

1.4.2 APP Mutations N-terminal to the Aβ Sequence

Only one pathogenic mutation has been reported in APP N-terminal to the Aβ

sequence. The Swedish double mutation of K670N/M671L is located directly before the Aβ sequence. The β-secretase cleavage site is located between residues 671 and 672 of APP. The Swedish mutation leads to AD with an AAO from 45 – 61 years with a median AAO of 55 and a duration of about seven years (Mullan et al., 1992a; Mullan et al., 1992b).

Analysis of brain slices from patients with the Swedish mutation showed high levels of overall Aβ, but very little accumulation of Aβ(1-40) in the brain. They also revealed the presence of parenchymal vessel deposition of Aβ(1-40) consistent with CAA (discussed later) (Mann et al., 1996). A study of Aβ(1-42) levels in blood plasma found that patients with the Swedish mutation who were not exhibiting AD symptoms had levels of Aβ(1-42) similar to patients with the Swedish mutation who were symptomatic (57 ± 3 pM and 67 ± 10 pM, respectively). Also, both groups had more Aβ(1-42) than controls, 28 ± 2 pM, and sporadic AD patients, 27 ± 3 pM (Scheuner et al., 1996).

The increases in Aβ content related to the Swedish mutation are likely due to a variation in β-secretase cleavage possibly related to the location of the mutations. Haass et al. made some headway in understanding the effect that the Swedish mutation has on β-secretase cleavage. The researchers transfected mutant and WT APP into HEK cells. When they collapsed the Golgi network with inhibitory compounds, the production of Aβ was decreased in the cells transfected with the Swedish APP, but not in the cells with WT APP. Antibody staining revealed that the Aβ from the mutant APP was localized in vesicles between the Golgi apparatus and the cell surface. The authors concluded that while WT APP is cleaved by β-secretase in endosomes during APP recycling, β-secretase cleaves Swedish APP in secretory vesicles that are en route to the cell surface

(Haass et al., 1995).

1.4.3 APP Mutations within the Aβ sequence

In addition to APP mutations that occur outside of the N- and C-terminal ends, some mutations have been reported to occur within the Aβ(1-42) sequence. When Janssen and colleagues undertook a mutational analysis of 31 families with suspected FAD, they discovered the H677R mutation. Although it hasn't been studied in depth, this mutation has an AAO of 55 years (Janssen et al., 2003).

Another little studied mutation was found in a family of Japanese origin. The D678N mutation has an AAO of 60 years and presents with a traditional AD pathology with no vascularization. Of interest was that this particular mutation appears to lead to periodic increased aggression (Wakutani et al., 2004).

One of the more well-studied Aβ mutations is the Flemish mutation, A692G (APP numbering) or A21G (Aβ numbering). The AAO for this mutation can range from 40 – 60 and has been associated with cerebral hemorrhage. Some patients with the Flemish mutation exhibited no symptoms of dementia but did present with strokes (Hendriks et al., 1992; Roks et al., 2000). Postmortem evaluations have revealed that the Flemish mutation leads to high levels of NFTs and large senile plaques that contain some of the largest cores found across the AD spectrum. The plaques were high in Aβ(1-40) content and the cores were centered on the vasculature (Kumar-Singh et al., 2002b). One study showed the cores of the senile plaques were up to 30μM in diameter (Cras et al., 1998). The location of the deposits is likely the reason that this particular

mutation leads to strokes.

Extensive studies have been performed to further understand the behavior of the Flemish Aβ mutant. Several research groups have analyzed the aggregation behavior of Aβ A21G and found that the peptide aggregates more slowly than WT Aβ. However, the mutant fibrilization pathway is skewed towards the production of larger, more stable aggregate structures (Wisniewski et al., 1991; Clements et al., 1993; Walsh et al., 2001). Creation of transgenic mouse models expressing Flemish APP have revealed that the human APP mutant is expressed in the brains of the mice and highly toxic, but in the mice there was very little Aβ deposition found and no tau pathology. The mutant mice showed an increase in mortality rates compared to WT mice, but the deaths of the mice were preceded by no warnings. The transgenic mice were also more likely to have seizures and aggressive tendencies (Kumar-Singh et al., 2000a).

When the Flemish APP variant was transfected into CHO and HEK293 cells, the researchers found an increase in both Aβ(1-42) and Aβ(1-40) and no change in the ratio between them (Haass et al., 1994; De Jonghe et al., 1998). The researchers suggest that the increase in Aβ production may be due to an interaction between the mutation and α-secretase, which cleaves between residues 16 and 17 of Aβ, and leading to an increase in β-secretase cleavage (De Jonghe et al., 1998).

Several mutations have been reported at the 693 APP position (position 22 in Aβ). The Arctic mutation, E693G or E22G, has an AAO of 58. Postmortem studies of afflicted patients revealed the presence of neuritic plaques, NFTs and moderate to severe amyloid deposition in the vasculature (Kamino et al., 1992). Evaluations of the plasma from patients with the Arctic mutation showed they had decreased levels of both Aβ(1-

42) and Aβ(1-40) compared to non-expressing family members. However, when the mutation was transfected into HEK293 cells, only Aβ(1-42) levels decreased (Nilsberth et al., 2001).

When Aβ(1-40) E22G was added to primary mouse neurons in culture, degeneration was seen after 24 hours while WT Aβ(1-40) required 96 hours. Also, the mutant Aβ was able to lead to almost complete degeneration of axons and dendrites over a 20 hour exposure. Primary human neurons responded in a similar manner to the mouse neurons suggesting a high level of toxicity from the Arctic mutation (Whalen et al., 2005).

A series of *in vitro* aggregation studies with the Aβ(1-42) and Aβ(1-40) E22G mutants showed that the mutants aggregate faster than WT Aβ(1-40) with Aβ(1-42) E22G aggregating the fastest (Lashuel et al., 2003). Interestingly, the mutant aggregation pathway is unique from that of the WT peptide in that the mutant forms very stable protofibril structures. When the Aβ(1-40) E22G was allowed to aggregate, the ratio of protofibrils:monomer decreased by about half after 4.5 hours, but then remained stable over the next 23 hours suggesting an equilibrium within the system (Paivio et al., 2004).

Another well-studied mutation at position 693 is the Dutch mutation (E693Q). Also known as hereditary cerebral hemorrhage with amyloidosis of the Dutch type (HCHWA-D), the Dutch mutation leads to severe Aβ deposition in the vasculature accompanied by senile plaques in the parenchyma but no NFTs. The mutation leads to repeated strokes that can begin in the mid-30s, but the AD associated symptoms have an AAO of 50 years (Van Broeckhoven et al., 1990). Patients expressing this mutation have been found to have Aβ(1-40) located only in the vascular deposits and only Aβ(1-

42) in the parenchymal plaques (Mann et al., 1996).

When the E693Q mutant APP was transfected into HEK293 and CHO cells, there was a decrease in the expression of Aβ(1-42) and Aβ(1-40) but no change in the ratio between them (De Jonghe et al., 1998). When SH-SY5Y cells, cultured human neurons, were treated with Aβ(1-42) E22Q the cells showed no degeneration after two hours, but a high degree after 24 hours. The cells also showed an increase in phosphorylation of tau (Kumar-Singh et al., 2002a).

A study using molecular dynamic simulations suggested that the Dutch Aβ mutant has an increase in β-sheet structure in the 17 − 21 region, which is usually unstructured. The researchers hypothesized that this structuring may make it easier for the Aβ units to add on to aggregates and lead to an increase in fibrilization (Baumketner et al., 2008) as previously seen (Soto et al., 1995).

The final mutation at position 693 is the Italian mutation (E693K). The presence of this mutation leads to significant cerebral hemorrhages. When PC12 neuronal cells were treated with either Aβ(1-42) or Aβ(1-40) E22K or the WT versions of the peptides, both mutants were more toxic to the cells than their WT analogues. Aβ(1-42) E22K was more toxic than Aβ(1-40) E22K. Analysis of the aggregation rates for both mutants revealed that both Aβ(1-42) and Aβ(1-40) aggregate faster than their WT analogues (Murakami et al., 2003).

Position 694 has one known mutation, D694N (Iowa mutation). The presence of the Iowa mutation has an AAO of 60 years and leads to cerebral amyloid deposits and NFTs but sparse senile plaques. There is also a decrease in the Aβ(1-42):Aβ(1-40) ratio in the plaques (Grabowski et al., 2001).

When the Iowa APP mutant was transfected into human H4 neuroglioma cells, analysis of the APP processing revealed no difference in the amount of Aβ produced compared to WT APP, but there was an increase in the amount of Aβ(1-40) produced. The *in vitro* aggregation of Aβ(1-40) D23N was much faster than that of WT Aβ(1-40) (Van Nostrand et al., 2001). It is possible that the loss of the charged asparagine residue may alter the aggregation properties of the Aβ leading to a faster aggregation.

There have been two other mutations reported at the 42 position of Aβ(1-42). The first, A42T was found in only one patient with no family history of AD. The patient had an AAO of 59 (Carter et al., 1992). Due to the lack of family history or other patients expressing the A42T mutation, it may not be pathogenic. The second mutation at Aβ 42 is A42V, the Iranian mutation. It was found within a single Iranian family in which a few people expressed AD symptoms, but several people in the kindred presented with Schizophrenia (Jones et al., 1992). It is possible that this mutation may also be non-pathogenic to AD.

1.5 Cerebral Amyloid Angiopathy (CAA)

As previously mentioned, some FAD mutations lead to the presence of CAA. In fact, more than 80% of all AD patients develop CAA (Joachim et al., 1988; Vinters et al., 1996; Jellinger, 2002; Attems et al., 2008), and the presence of the CAA phenomenon has been shown to increase cognitive defects in AD patients (Pfeifer et al., 2002). The most severe cases of CAA have been found in patients expressing the Flemish, Iowa or Dutch APP mutations (Revesz et al., 2003).

The primary component of CAA is the deposition of Aβ into the cerebral blood vessels, particularly smaller vessels like the leptomeningeal and cortical arteries, the arterioles and capillaries. The deposition leads to changes within the vasculature (Pezzini and Padovani, 2008). Initially, the Aβ deposits in the outer membranes of the vessels leaving the layer of smooth muscle cells (SMCs) unharmed. As CAA progresses, the Aβ deposits move into the SMC layer and surrounds the SMCs leading to their degeneration. In severe cases of CAA a "double barrel" deposition is seen in the vessels (Fig. 1.3) as Aβ deposits itself into two distinct layers. These cases also have fibrinoid necrosis and microannurisms and, eventually, the vessels rupture leading to hemorrhages or infarctions (Vinters and Gilbert, 1983; Mandybur, 1986; Vinters, 1987; Vonsattel et al., 1991; Greenberg and Vonsattel, 1997; Thal et al., 2008).

1.6 Immune response to AD

1.6.1 The Human Immune System

The human body is a complex system that is able to defend itself from various foreign invaders like bacteria, fungi or protozoa as well as in cases of localized trauma (Serbina et al., 2008). In response to the presence of pathogens, the human immune system activates monocytic cells that are in normal circulation in the blood stream (Volkman and Gowans, 1965b, 1965a; Gordon and Taylor, 2005). The activation process, also known as differentiation, transforms the monocytes into either macrophages or dendritic cells in an effort to first contain the pathogen and later develop antibodies

Normal   **1 = mild**   **2 = moderate**   **3 = severe**

Media with Smooth Muscle Cells

Aventitia

Ab deposits at the basement membrane

Ab deposits in the media & degeration of smooth muscle cells

Double barreling, hemorrhage, fibrinoid necrosis

Ab deposits   Fibrinoid necrosis   Erythrocyte   Siderophage
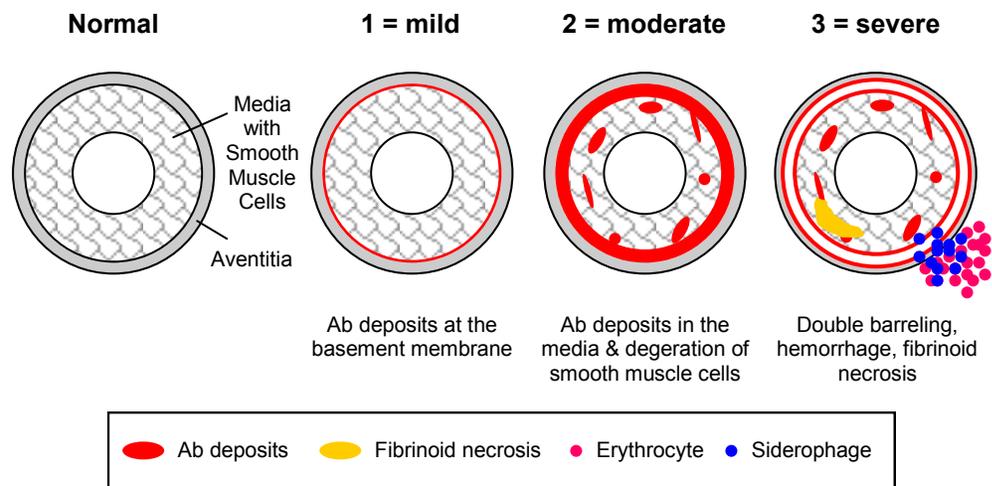
Fig. 1.3 A model of the CAA development pathology found in AD
CAA, as found in AD, begins in the arteries and veins with no deposition as in the Normal case. As the disease progresses to mild CAA, the Aβ begins to deposit in the membrane of the vessels. Moderate CAA cases display further deposition in the SMC layer leading to the degeneration of the SMCs. The final stage of CAA, classified as severe, involves the breakdown of the vessel walls which leads to the appearance of double-barreled Ab deposition and a high degree of SMC degeneration. Areas of fibrinoid necrosis often appear and lead to hemorrhaging in the vessels. Figure modified from Thal et al., 2008).

against the foreign invader (Volkman and Gowans, 1965b, 1965a; Gordon and Taylor, 2005) (Fig. 1.4).

Monocytes are produced from pluripotent bone marrow stem cells and normally circulate in the blood. These cells are a subset of white blood cells and make up 5-10% of the circulating white blood cell population. Under normal circumstances the monocytes circulate for a few days before entering tissues and transforming into macrophages as a way to maintain homeostasis within the tissues (Volkman and Gowans, 1965b, 1965a; Gordon and Taylor, 2005; Seta and Kuwana, 2007; Serbina et al., 2008). However, if pro-inflammatory, metabolic or immune stimuli are sensed in the periphery, monocytes are recruited to the area and differentiated in one of two ways (Van Furth et al., 1973; Reya et al., 2001).

The first pathway is the formation of macrophages, members of the innate immune response. Macrophages are known to have roles in maintaining the homeostasis of the body through the removal of old cells and the repairing of tissues following a proinflammatory response (Gordon, 1998). However, macrophages are primarily thought of as antigen presenting cells (Hoebe et al., 2004) with phagocytic (Schwende et al., 1996) and microbicidal (Mackaness, 1964; Benoit et al., 2008) capabilities. It is also believed that the bone marrow derived macrophages have the ability to enter the CNS through the blood brain barrier (BBB) when needed (de Groot et al., 1992; Lawson et al., 1992). The purpose of this differentiation pathway is to immediately attempt to sequester and destroy as much of the foreign pathogen as possible to prevent further damage to the body.

The second pathway available for monocyte differentiation is the formation of dendritic cells (DCs) as part of the adaptive immune response. A vital part of the body's

Monocyte

Innate Immune
Pathway

Adaptive Immune
Pathway

Macrophage

Dendricyte
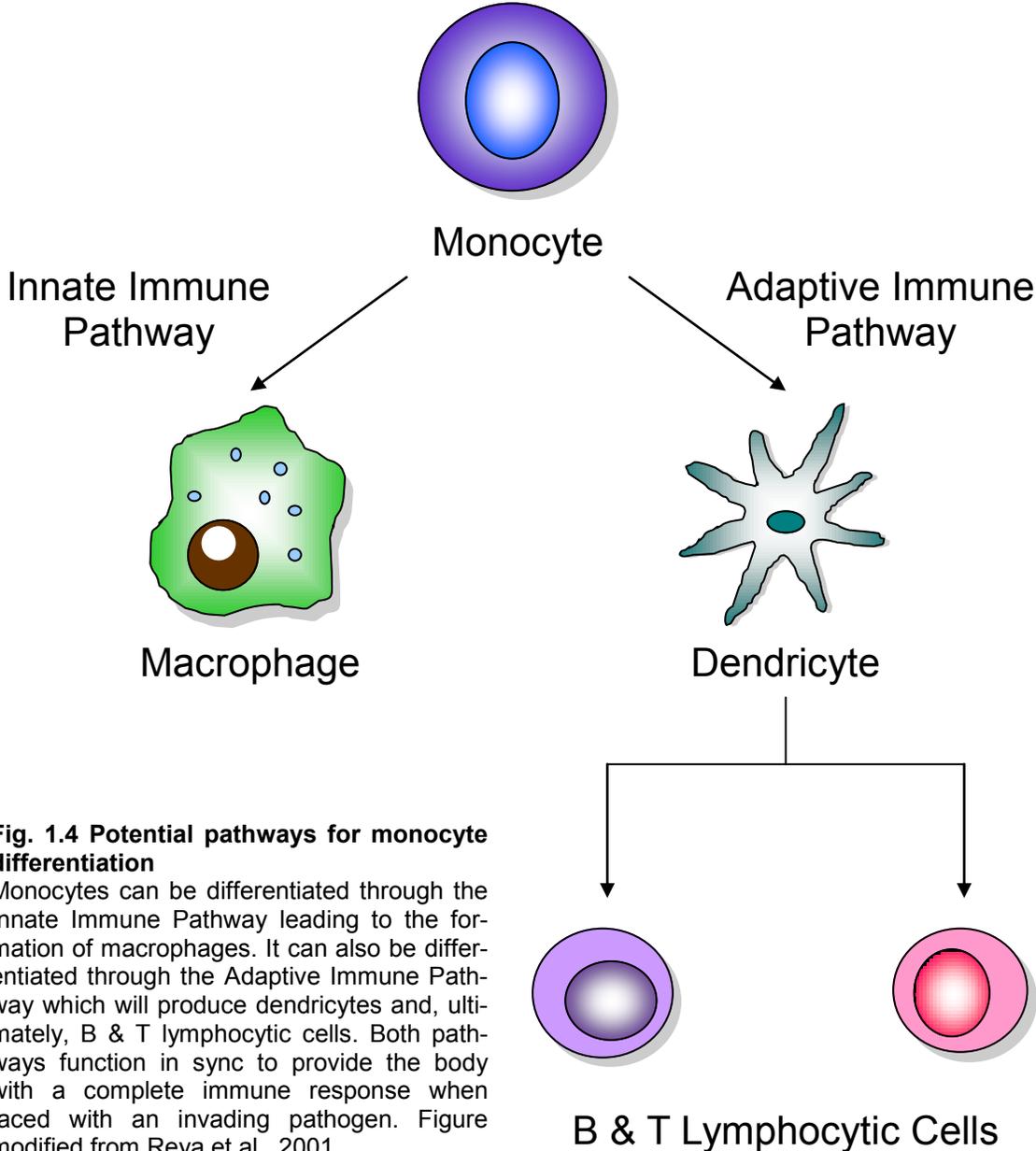
Fig. 1.4 Potential pathways for monocyte differentiation
Monocytes can be differentiated through the Innate Immune Pathway leading to the formation of macrophages. It can also be differentiated through the Adaptive Immune Pathway which will produce dendricytes and, ultimately, B & T lymphocytic cells. Both pathways function in sync to provide the body with a complete immune response when faced with an invading pathogen. Figure modified from Reya et al., 2001.

B & T Lymphocytic Cells

overall protection mechanism is the formation of antibodies against various pathogens to help provide long term immunity. This process is accomplished through the use of B and T lymphocytes, which are both derived from DCs. The B lymphocytes possess the "memory" of native antigens, which prevents the body from attacking itself. The T lymphocytes, however, are members of a complex system of recognition and antibody production that require fragments of pathogens be presented to them by the antigen presenting DCs. This pathway ultimately leads to the production of antibodies to pathogens that have previously attacked the body, which allows for a quicker response if exposure occurs at a later time (Banchereau and Steinman, 1998).

1.6.2 Microglial Activation

Microglia have often been referred to as the macrophages of the brain (Davoust et al., 2008) because they behave as phagocytes in response to local insult (Heneka and O'Banion, 2007). A normal brain contains a uniform population in the white and grey matter (McGeer et al., 1987) known as resident microglia that are able to undergo some degree of proliferation under normal conditions (Davoust et al., 2008).

In the absence of any insult or injury to the brain, microglia have a wide variety of functions. They can induce neuronal apoptosis (Marin-Teva et al., 2004), control synaptogenesis (Roumier et al., 2004), regulate synaptic transmissions (Coull et al., 2005), and synthesize neurotrophic factors (Elkabes et al., 1996). Microglia posses a ramified morphology (Davoust et al., 2008), which is utilized to monitor the condition of the brain. The branches protruding from the cellular body are in constant motion, which al-

lows microglia to survey the entire extracellular space of the parenchyma every few hours (Nimmerjahn et al., 2005; Raivich, 2005; Davoust et al., 2008).

If, during the process of surveying the brain, microglia sense an invading pathogen, an injury or another form of insult, they undergo an activation process that allows them to attempt to control the problem. Upon activation, microglial phagocytosis is functional (Bauer et al., 1994), and they are able to secrete proinflammatory cytokines like interleukin (IL) 1, IL-6 and tumor necrosis factor α (TNFα) (Banati et al., 1993). Activated microglia can also undergo an upregulation of some cell surface receptors like HLA-DR (McGeer et al., 1987), CD11b, Iba-1 and F4/80 in a manner similar to other macrophage cell lines (Davoust et al., 2008) leading to the conclusion that microglia are the first line of defense for the CNS (Kreutzberg, 1996).

Recently a series of mouse studies have added complexity to the microglial activation model. Mice were irradiated to kill all of their bone marrow, which was then replaced with green fluorescent protein (GFP)-labeled bone marrow. Close monitoring of the CNS following an induced brain injury showed an increase in perivascular macrophages and microglia expressing GFP (Eglitis and Mezey, 1997; Priller et al., 2001; Asheuer et al., 2004; Simard and Rivest, 2004). These studies lead to the notion that the microglial activation process may also involve the recruitment of cells from outside the CNS, specifically monocytic cells from the bone marrow. It is believed that bone marrow derived cells can be recruited from the periphery, cross the BBB and then differentiate into microglia (Davoust et al., 2008).

Simard and Rives further extended their studies into an AD model system. When they created the bone marrow chimeric mice they used mice expressing APP. The re-

searchers found that the Aβ deposits in the brain were surrounded by GFP$^+$ microglia. They next made chimera from normal mice and three months later injected them with either Aβ(1-31), Aβ(1-40), Aβ(1-42) or Aβ(1-57). Upon sacrificing the mice up to a week later, the researchers found Aβ plaques surrounded by GFP$^+$ microglia in the mice treated with Aβ(1-40) or Aβ(1-42) but not in the mice treated with the 31 or 57 residue peptides, suggesting these forms of Aβ can recruit cells from outside the CNS (Simard et al., 2006).

There is still some debate within the immunological community as to the importance of the aforementioned studies. It has been suggested that the process of irradiating the mice could, itself, damage the BBB and lead to the infiltration of external cells (Ajami et al., 2007; Carson et al., 2007; Mildner et al., 2007). In one study, two mice were joined together at the circulatory system (parabiosis) and allowed to establish joint circulation. One mouse partner expressed GFP tagged bone marrow and the other did not. The mice were then subjected to facial motoneuron axotomy to induce a microglial response in the brain without damaging the BBB. When the brains of the mice were analyzed, both contained activated microglia but no GFP (Ajami et al., 2007). A separate study used the bone marrow irradiation technique mentioned above, with the slight variation of protecting the heads of the mice from the radiation. This slight change in protocol resulted in no GFP in the brain (Mildner et al., 2007). Together, these studies suggest the labeled monocytic cells could not cross the BBB and enter the CNS because the barrier remained intact.

Chemotaxis, or the movement of cells in response to environmental stimuli, is an important component of the recruitment model. A study involving an *in vitro* model of

chemotaxis across the BBB suggested that Aβ can induce recruitment of monocytes across the barrier. A migration chamber was constructed with a barrier in the middle comprised of human cerebral endothelial cells to serve as the BBB and migration of monocytes from the upper chamber to the lower chamber were monitored. In all of the tests, 5×10^5 monocytes were placed in the upper chamber and allowed to incubate for 24 hours before the number of cells in the lower chamber were counted. When only medium was placed in the lower chamber, approximately 700 cells migrated from the upper chamber. If the lower chamber contained 2×10^4 monocytes, an additional 3000 cells migrated from the upper chamber. However, if the lower chamber contained Aβ in medium or a mixture of Aβ and monocytes, cell migration from the upper chamber increased significantly to 20,000 and 63,000 cells, respectively (Fiala et al., 1998).

Previous work has also indicated that Aβ treated PC12 cells and murine cerebral endothelial cells exhibit an increase in oxidative stress markers attributed to the interaction of Aβ with the receptor for advanced glycation end products (RAGE). Human AD brain homogenates also show an increase in RAGE expression (Yan et al., 1996). Further studies have indicated a role for RAGE in the possible recruitment of monocytes into the CNS. When THP-1 monocytes, a cultured monocytic cell line, were incubated with a monolayer of primary human brain microvascular endothelial cells (HBMVEC) the monocytes were able to adhere to the HBMVEC in a manner that was dependent upon the expression of RAGE. An experiment was performed to determine if RAGE was involved in the movement of monocytes across the HBMVEC layer. When an anti-RAGE antibody was used on the monolayer, a significant decrease in the migration of the monocytes in response to Aβ was noted (Giri et al., 2000).

Another receptor has also been identified to aid in Aβ induced migration and activation of monocytes. The formyl peptide receptor-like 1 (FPRL1) was found to be expressed on CD11b-positive microglial cells surrounding Aβ lesions in AD brains. Aβ was found to induce high levels of chemotaxis and Ca^{2+} influx through FPRL1. Also of interest was the finding that freshly reconstituted Aβ was better able to induce monocyte migration than more highly aggregated Aβ solutions (Le et al., 2001).

Aside from the debate about monocyte recruitment, it is also difficult to distinguish between resident and recruited microglia, partially due to the complexity and low yields obtained when attempting to harvest the primary cells. However, there is some evidence that suggests the CD45 receptor is highly expressed in recruited microglia, unlike resident microglia that have a very low expression.

Interestingly, studies of AD brains revealed that senile plaques are comprised of dystrophic neuritis, astrocytes and activated microglia (McGeer et al., 1987; Spires and Hyman, 2004; Mott and Hulette, 2005; Maragakis and Rothstein, 2006; Heneka and O'Banion, 2007). In a mouse model of AD, a 2-5 fold increase in microglia was seen in the area of Aβ plaques, and the plaques were found to be surrounded by activated, CD11b-positive microglia (Khoury and Luster, 2008). Despite being present in the vicinity of plaques, the role of microglia in AD brains is far from understood.

1.7 Cytokine and chemokine expression in AD

Cyclic AMP (cAMP) is a second messenger that is very highly regulated (Gilman, 1995). It is known to activate protein kinase A, which will, in turn, phosphory-

late tertiary messengers (Kelley et al., 2008). cAMP can also act at a transmitter through binding with cyclic nucleotide gated channels (Matulef and Zagotta, 2003). Production of cAMP is regulated through the conversion of ATP in the presence of Mg^{2+}, a reaction catalyzed by adenylate cyclase (AC) (Table 1.2). The only mechanism for cAMP degradation is through the class of molecules known as phosphodiesterases (PDE), which are used to help maintain homeostasis (Kelley et al., 2008).

Studies involving inflammation have shown that increasing levels of cAMP through the use of PDE inhibitors or AC activators can attenuate the levels of the cytokine TNFα in monocytic cells (Kunkel et al., 1988; Schade and Schudt, 1993; Sinha et al., 1995). Dibutyryl cAMP (dbcAMP), PDE inhibitors and AC activators were also shown to decrease LPS-induced TNFα levels in macrophages (Spengler et al., 1989) and microglia (Facchinetti et al., 2003). It is thought that cAMP may serve as a gatekeeper for inflammation (Jin and Conti, 2002), which may have implications in AD research due to its demonstrated ability to decrease the inflammatory marker TNFα.

Levels of TNFα have been studied in many different models of AD pathology, including *in vivo*. It has been seen that AD patients have higher levels of TNFα in the brain microvessels (Grammas and Ovase, 2001) and cerebral spinal fluid (CSF) than people who do not have AD (Tarkowski et al., 2003). TNFα is also found with microglia surrounding Aβ lesions in humans (McGeer et al., 1987) as well as transgenic mouse models of AD that have high expression of APP (Benzing et al., 1999).

Studies have shown that SMCs produce cytokines after exposure to Aβ (Suo et al., 1998), and AD patients express higher levels of TNFα in brain microvessels than non-demented individuals (Grammas and Ovase, 2001). Experiments on meningeal ves-

Phosphodiesterase Inhibitors	
IBMX	General PDE inhibitor
Milrinone	PDE3 inhibitor
Ro 20-1724	PDE4 inhibitor
Rolipram	PDE4 inhibitor
Zardaverine	PDE3, PDE4 inhibitor
Adenylate Cyclase Activator	
Forskolin	Adenylate cyclase binding molecule
Protein Kinase A Effectors	
R_p-cAMPS	Inhibitor
S_p-cAMPS	Activator
KT5720	Inhibitor
H89	Inhibitor

Table 1.2 Many compounds modulate the cAMP pathway
Selection of agents to modulate the cAMP signal depend on which specific parts of the pathway need altered. IBMX is a general PDE inhibitor and works on the general class of PDEs. Forskolin is the only compound regularly used to activate adenylate cyclase.

sels from AD patients revealed an increase in cAMP staining compared to non-demented patients. Most notably, the cAMP was found to co-localize with the Aβ deposits within the vessels (Martinez et al., 2001). When taken together with an *in vitro* model showing that the presence of TNFα in human myometrium (uterine SMCs) stimulates AC (Gogarten et al., 2003), an interesting picture begins to immerge. The interplay between Aβ induced production of TNFα and the upregulation of cAMP may be a protection mechanism in AD patients.

Other markers of inflammation have been found to participate in the overall AD pathology. Aβ has been shown to increase the production of IL-1β, IL-6 and TNFα in cultured microglia and astrocytes (Gitter et al., 1995; Chong, 1997). IL-6 has also been identified as a component of early senile plaques in AD brains (Luterman et al., 2000; Mehlhorn et al., 2000), and has been found to be secreted by peripheral blood monocytes more in AD patients than non-demented individuals (Ravaglia et al., 2007). IL-1β has been found at increased levels in the CSF of AD affected individuals (Cacabelos et al., 1991; Blum-Degen et al., 1995). Interestingly, IL-6 stimulates the cdk5 kinase system and IL-1β activates MAPK-p38, both of which increase tau phosphorylation (Rojo et al., 2008).

TNF-related apoptosis-inducing ligand (TRAIL) is an integral membrane protein and a member of the TNF family of cytokines (Rojo et al., 2008). It has been found in neuronal cultures treated with Aβ (Cantarella et al., 2003), as well as specifically expressed in AD brains, but not healthy brains. The immunoreactivity of TRAIL was localized near Aβ plaques (Uberti et al., 2004).

Chemokines have also been implicated in AD. A series of chemokine receptors,

CCR1, CCR3, CCR5, CXCR3 and CXCR4, have all been identified in AD brain slices (Xia and Hyman, 1999; Halks-Miller et al., 2003). Microglia from AD brains express increased levels of IL-8 and MIP3α mRNA (Rempel et al., 2001) while high levels of IL-8 and MCP-1 were found in the CSF of AD patients (Galimberti et al., 2006b). MCP-1 is implicated in the recruitment of cells to sites of inflammation. In fact, astrocytes have been shown to migrate towards Aβ deposits due to the presence of MCP-1 (Galimberti et al., 2006a). Once there the astrocytes attempt to clear the Aβ (Rojo et al., 2008) suggesting a potentially protective role for some chemokines.

Overall, the research has shown that AD is a very complicated disorder with many contributing factors. It is of great importance for researchers to elucidate as many pieces of the puzzle as possible. In doing so the chances are increased that one day a cure or prevention will be developed for those suffering with this disease.

1.8 BIBLIOGRAPHY

Ajami B, Bennett JL, Krieger C, Tetzlaff W, Rossi FM (2007) Local self-renewal can sustain CNS microglia maintenance and function throughout adult life. Nat Neurosci 10:1538-1543.

Alonso AC, Grundke-Iqbal I, Iqbal K (1996) Alzheimer's disease hyperphosphorylated tau sequesters normal tau into tangles of filaments and disassembles microtubules. Nat Med 2:783-787.

Alonso AC, Zaidi T, Grundke-Iqbal I, Iqbal K (1994) Role of abnormally phosphorylated tau in the breakdown of microtubules in Alzheimer disease. Proc Natl Acad Sci U S A 91:5562-5566.

Alonso AD, Grundke-Iqbal I, Barra HS, Iqbal K (1997) Abnormal phosphorylation of tau and the mechanism of Alzheimer neurofibrillary degeneration: sequestration of microtubule-associated proteins 1 and 2 and the disassembly of microtubules by the abnormal tau. Proc Natl Acad Sci U S A 94:298-303.

Alonso Adel C, Mederlyova A, Novak M, Grundke-Iqbal I, Iqbal K (2004) Promotion of hyperphosphorylation by frontotemporal dementia tau mutations. J Biol Chem 279:34873-34881.

An WL, Cowburn RF, Li L, Braak H, Alafuzoff I, Iqbal K, Iqbal IG, Winblad B, Pei JJ (2003) Up-regulation of phosphorylated/activated p70 S6 kinase and its relationship to neurofibrillary pathology in Alzheimer's disease. Am J Pathol 163:591-607.

Ancolio K, Dumanchin C, Barelli H, Warter JM, Brice A, Campion D, Frebourg T, Checler F (1999) Unusual phenotypic alteration of beta amyloid precursor protein (betaAPP) maturation by a new Val-715 --> Met betaAPP-770 mutation responsible for probable early-onset Alzheimer's disease. Proc Natl Acad Sci U S A 96:4119-4124.

Asheuer M, Pflumio F, Benhamida S, Dubart-Kupperschmitt A, Fouquet F, Imai Y, Aubourg P, Cartier N (2004) Human CD34+ cells differentiate into microglia and express recombinant therapeutic protein. Proc Natl Acad Sci U S A 101:3557-3562.

Attems J, Lauda F, Jellinger KA (2008) Unexpectedly low prevalence of intracerebral hemorrhages in sporadic cerebral amyloid angiopathy: an autopsy study. J Neurol 255:70-76.

Balbach JJ, Petkova AT, Oyler NA, Antzutkin ON, Gordon DJ, Meredith SC, Tycko R (2002) Supramolecular structure in full-length Alzheimer's beta-amyloid fibrils: evidence for a parallel beta-sheet organization from solid-state nuclear magnetic resonance. Biophys J 83:1205-1216.

Banati RB, Gehrmann J, Schubert P, Kreutzberg GW (1993) Cytotoxicity of microglia. Glia 7:111-118.

Banchereau J, Steinman RM (1998) Dendritic cells and the control of immunity. Nature 392:245-252.

Bateman RJ, Munsell LY, Morris JC, Swarm R, Yarasheski KE, Holtzman DM (2006) Human amyloid-beta synthesis and clearance rates as measured in cerebrospinal fluid in vivo. Nat Med 12:856-861.

Bauer J, Sminia T, Wouterlood FG, Dijkstra CD (1994) Phagocytic activity of macrophages and microglial cells during the course of acute and chronic relapsing experimental autoimmune encephalomyelitis. J Neurosci Res 38:365-375.

Baumketner A, Krone MG, Shea JE (2008) Role of the familial Dutch mutation E22Q in the folding and aggregation of the 15-28 fragment of the Alzheimer amyloid-beta protein. Proc Natl Acad Sci U S A 105:6027-6032.

Benoit M, Desnues B, Mege JL (2008) Macrophage polarization in bacterial infections. J Immunol 181:3733-3739.

Benzing WC, Wujek JR, Ward EK, Shaffer D, Ashe KH, Younkin SG, Brunden KR (1999) Evidence for glial-mediated inflammation in aged APP(SW) transgenic mice. Neurobiol Aging 20:581-589.

Blackley HK, Sanders GH, Davies MC, Roberts CJ, Tendler SJ, Wilkinson MJ (2000) In-situ atomic force microscopy study of beta-amyloid fibrillization. J Mol Biol 298:833-840.

Blum-Degen D, Muller T, Kuhn W, Gerlach M, Przuntek H, Riederer P (1995) Interleukin-1 beta and interleukin-6 are elevated in the cerebrospinal fluid of Alzheimer's and de novo Parkinson's disease patients. Neurosci Lett 202:17-20.

Bu Z, Shi Y, Callaway DJ, Tycko R (2007) Molecular alignment within beta-sheets in Abeta(14-23) fibrils: solid-state NMR experiments and theoretical predictions. Biophys J 92:594-602.

Busciglio J, Gabuzda DH, Matsudaira P, Yankner BA (1993) Generation of beta-amyloid in the secretory pathway in neuronal and nonneuronal cells. Proc Natl Acad Sci U S A 90:2092-2096.

Busciglio J, Lorenzo A, Yeh J, Yankner BA (1995) beta-amyloid fibrils induce tau phosphorylation and loss of microtubule binding. Neuron 14:879-888.

Cacabelos R, Franco-Maside A, Alvarez XA (1991) Interleukin-1 in Alzheimer's disease and multi-infarct dementia: neuropsychological correlations. Methods Find Exp Clin Pharmacol 13:703-708.

Cai XD, Golde TE, Younkin SG (1993) Release of excess amyloid beta protein from a mutant amyloid beta protein precursor. Science 259:514-516.

Cantarella G, Uberti D, Carsana T, Lombardo G, Bernardini R, Memo M (2003) Neutralization of TRAIL death pathway protects human neuronal cell line from beta-amyloid toxicity. Cell Death Differ 10:134-141.

Carson MJ, Bilousova TV, Puntambekar SS, Melchior B, Doose JM, Ethell IM (2007) A rose by any other name? The potential consequences of microglial heterogeneity during CNS health and disease. Neurotherapeutics 4:571-579.

Carter DA, Desmarais E, Bellis M, Campion D, Clerget-Darpoux F, Brice A, Agid Y, Jaillard-Serradt A, Mallet J (1992) More missense in amyloid gene. Nat Genet 2:255-256.

Chartier-Harlin MC, Crawford F, Houlden H, Warren A, Hughes D, Fidani L, Goate A, Rossor M, Roques P, Hardy J, et al. (1991) Early-onset Alzheimer's disease caused by mutations at codon 717 of the beta-amyloid precursor protein gene. Nature 353:844-846.

Chong Y (1997) Effect of a carboxy-terminal fragment of the Alzheimer's amyloid precursor protein on expression of proinflammatory cytokines in rat glial cells. Life Sci 61:2323-2333.

Citron M, Oltersdorf T, Haass C, McConlogue L, Hung AY, Seubert P, Vigo-Pelfrey C, Lieberburg I, Selkoe DJ (1992) Mutation of the beta-amyloid precursor protein in familial Alzheimer's disease increases beta-protein production. Nature 360:672-674.

Citron M, Vigo-Pelfrey C, Teplow DB, Miller C, Schenk D, Johnston J, Winblad B, Venizelos N, Lannfelt L, Selkoe DJ (1994) Excessive production of amyloid beta-protein by peripheral cells of symptomatic and presymptomatic patients carrying the Swedish familial Alzheimer disease mutation. Proc Natl Acad Sci U S A 91:11993-11997.

Clements A, Walsh DM, Williams CH, Allsop D (1993) Effects of the mutations Glu22 to Gln and Ala21 to Gly on the aggregation of a synthetic fragment of the Alzheimer's amyloid beta/A4 peptide. Neurosci Lett 161:17-20.

Coull JA, Beggs S, Boudreau D, Boivin D, Tsuda M, Inoue K, Gravel C, Salter MW, De Koninck Y (2005) BDNF from microglia causes the shift in neuronal anion gradient underlying neuropathic pain. Nature 438:1017-1021.

Cras P, van Harskamp F, Hendriks L, Ceuterick C, van Duijn CM, Stefanko SZ, Hofman A, Kros JM, Van Broeckhoven C, Martin JJ (1998) Presenile Alzheimer dementia characterized by amyloid angiopathy and large amyloid core type senile plaques in the APP 692Ala-->Gly mutation. Acta Neuropathol 96:253-260.

Cruts M, Dermaut B, Rademakers R, Van den Broeck M, Stogbauer F, Van Broeckhoven C (2003) Novel APP mutation V715A associated with presenile Alzheimer's disease in a German family. J Neurol 250:1374-1375.

Davoust N, Vuaillat C, Androdias G, Nataf S (2008) From bone marrow to microglia: barriers and avenues. Trends Immunol 29:227-234.

de Groot CJ, Huppes W, Sminia T, Kraal G, Dijkstra CD (1992) Determination of the origin and nature of brain macrophages and microglial cells in mouse central nervous system, using non-radioactive in situ hybridization and immunoperoxidase techniques. Glia 6:301-309.

De Jonghe C, Zehr C, Yager D, Prada CM, Younkin S, Hendriks L, Van Broeckhoven C, Eckman CB (1998) Flemish and Dutch mutations in amyloid beta precursor protein have different effects on amyloid beta secretion. Neurobiol Dis 5:281-286.

De Jonghe C, Esselens C, Kumar-Singh S, Craessaerts K, Serneels S, Checler F, Annaert W, Van Broeckhoven C, De Strooper B (2001) Pathogenic APP mutations near the gamma-secretase cleavage site differentially affect Abeta secretion and APP C-terminal fragment stability. Hum Mol Genet 10:1665-1671.

Delacourte A, Buee L (1997) Normal and pathological Tau proteins as factors for microtubule assembly. Int Rev Cytol 171:167-224.

Dickson DW (2004) Apoptotic mechanisms in Alzheimer neurofibrillary degeneration: cause or effect? J Clin Invest 114:23-27.

Eckman CB, Mehta ND, Crook R, Perez-tur J, Prihar G, Pfeiffer E, Graff-Radford N, Hinder P, Yager D, Zenk B, Refolo LM, Prada CM, Younkin SG, Hutton M, Hardy J (1997) A new pathogenic mutation in the APP gene (I716V) increases the relative proportion of A beta 42(43). Hum Mol Genet 6:2087-2089.

Eglitis MA, Mezey E (1997) Hematopoietic cells differentiate into both microglia and macroglia in the brains of adult mice. Proc Natl Acad Sci U S A 94:4080-4085.

Elkabes S, DiCicco-Bloom EM, Black IB (1996) Brain microglia/macrophages express neurotrophins that selectively regulate microglial proliferation and function. J Neurosci 16:2508-2521.

Esch FS, Keim PS, Beattie EC, Blacher RW, Culwell AR, Oltersdorf T, McClure D, Ward PJ (1990) Cleavage of amyloid beta peptide during constitutive processing of its precursor. Science 248:1122-1124.

Facchinetti F, Del Giudice E, Furegato S, Passarotto M, Leon A (2003) Cannabinoids ablate release of TNFalpha in rat microglial cells stimulated with lypopolysaccharide. Glia 41:161-168.

Fiala M, Zhang L, Gan X, Sherry B, Taub D, Graves MC, Hama S, Way D, Weinand M, Witte M, Lorton D, Kuo YM, Roher AE (1998) Amyloid-beta induces chemokine secretion and monocyte migration across a human blood--brain barrier model. Mol Med 4:480-489.

Galimberti D, Schoonenboom N, Scheltens P, Fenoglio C, Bouwman F, Venturelli E, Guidi I, Blankenstein MA, Bresolin N, Scarpini E (2006a) Intrathecal chemokine synthesis in mild cognitive impairment and Alzheimer disease. Arch Neurol 63:538-543.

Galimberti D, Fenoglio C, Lovati C, Venturelli E, Guidi I, Corra B, Scalabrini D, Clerici F, Mariani C, Bresolin N, Scarpini E (2006b) Serum MCP-1 levels are increased in mild cognitive impairment and mild Alzheimer's disease. Neurobiol Aging 27:1763-1768.

Games D, Adams D, Alessandrini R, Barbour R, Berthelette P, Blackwell C, Carr T, Clemens J, Donaldson T, Gillespie F, et al. (1995) Alzheimer-type neuropathology in transgenic mice overexpressing V717F beta-amyloid precursor protein. Nature 373:523-527.

Gilman AG (1995) Nobel Lecture. G proteins and regulation of adenylyl cyclase. Biosci Rep 15:65-97.

Giri R, Shen Y, Stins M, Du Yan S, Schmidt AM, Stern D, Kim KS, Zlokovic B, Kalra VK (2000) beta-amyloid-induced migration of monocytes across human brain endothelial cells involves RAGE and PECAM-1. Am J Physiol Cell Physiol 279:C1772-1781.

Gitter BD, Cox LM, Rydel RE, May PC (1995) Amyloid beta peptide potentiates cytokine secretion by interleukin-1 beta-activated human astrocytoma cells. Proc

Natl Acad Sci U S A 92:10738-10741.

Goate A, Chartier-Harlin MC, Mullan M, Brown J, Crawford F, Fidani L, Giuffra L, Haynes A, Irving N, James L, et al. (1991) Segregation of a missense mutation in the amyloid precursor protein gene with familial Alzheimer's disease. Nature 349:704-706.

Gogarten W, Lindeman KS, Hirshman CA, Emala CW (2003) Tumor necrosis factor alpha stimulates adenylyl cyclase activity in human myometrial cells. Biol Reprod 68:751-757.

Gordon S (1998) The role of the macrophage in immune regulation. Res Immunol 149:685-688.

Gordon S, Taylor PR (2005) Monocyte and macrophage heterogeneity. Nat Rev Immunol 5:953-964.

Grabowski TJ, Cho HS, Vonsattel JP, Rebeck GW, Greenberg SM (2001) Novel amyloid precursor protein mutation in an Iowa family with dementia and severe cerebral amyloid angiopathy. Ann Neurol 49:697-705.

Grammas P, Ovase R (2001) Inflammatory factors are elevated in brain microvessels in Alzheimer's disease. Neurobiol Aging 22:837-842.

Gravina SA, Ho L, Eckman CB, Long KE, Otvos L, Jr., Younkin LH, Suzuki N, Younkin SG (1995) Amyloid beta protein (A beta) in Alzheimer's disease brain. Biochemical and immunocytochemical analysis with antibodies specific for forms ending at A beta 40 or A beta 42(43). J Biol Chem 270:7013-7016.

Greenberg SM, Vonsattel JP (1997) Diagnosis of cerebral amyloid angiopathy. Sensitivity and specificity of cortical biopsy. Stroke 28:1418-1422.

Haass C, Hung AY, Selkoe DJ, Teplow DB (1994) Mutations associated with a locus for familial Alzheimer's disease result in alternative processing of amyloid beta-protein precursor. J Biol Chem 269:17741-17748.

Haass C, Lemere CA, Capell A, Citron M, Seubert P, Schenk D, Lannfelt L, Selkoe DJ (1995) The Swedish mutation causes early-onset Alzheimer's disease by beta-secretase cleavage within the secretory pathway. Nat Med 1:1291-1296.

Halks-Miller M, Schroeder ML, Haroutunian V, Moenning U, Rossi M, Achim C, Purohit D, Mahmoudi M, Horuk R (2003) CCR1 is an early and specific marker of Alzheimer's disease. Ann Neurol 54:638-646.

Hardy J, Selkoe DJ (2002) The amyloid hypothesis of Alzheimer's disease: progress and

problems on the road to therapeutics. Science 297:353-356.

Harper JD, Lieber CM, Lansbury PT, Jr. (1997a) Atomic force microscopic imaging of seeded fibril formation and fibril branching by the Alzheimer's disease amyloid-beta protein. Chem Biol 4:951-959.

Harper JD, Wong SS, Lieber CM, Lansbury PT (1997b) Observation of metastable Abeta amyloid protofibrils by atomic force microscopy. Chem Biol 4:119-125.

Harper JD, Wong SS, Lieber CM, Lansbury PT, Jr. (1999) Assembly of A beta amyloid protofibrils: an in vitro model for a possible early event in Alzheimer's disease. Biochemistry 38:8972-8980.

Hartley DM, Walsh DM, Ye CP, Diehl T, Vasquez S, Vassilev PM, Teplow DB, Selkoe DJ (1999) Protofibrillar intermediates of amyloid beta-protein induce acute electrophysiological changes and progressive neurotoxicity in cortical neurons. J Neurosci 19:8876-8884.

Hendriks L, van Duijn CM, Cras P, Cruts M, Van Hul W, van Harskamp F, Warren A, McInnis MG, Antonarakis SE, Martin JJ, et al. (1992) Presenile dementia and cerebral haemorrhage linked to a mutation at codon 692 of the beta-amyloid precursor protein gene. Nat Genet 1:218-221.

Heneka MT, O'Banion MK (2007) Inflammatory processes in Alzheimer's disease. J Neuroimmunol 184:69-91.

Hoebe K, Janssen E, Beutler B (2004) The interface between innate and adaptive immunity. Nat Immunol 5:971-974.

Hsiao K, Chapman P, Nilsen S, Eckman C, Harigaya Y, Younkin S, Yang F, Cole G (1996) Correlative memory deficits, Abeta elevation, and amyloid plaques in transgenic mice. Science 274:99-102.

Inouye H, Fraser PE, Kirschner DA (1993) Structure of beta-crystallite assemblies formed by Alzheimer beta-amyloid protein analogues: analysis by x-ray diffraction. Biophys J 64:502-519.

Iqbal K, Alonso Adel C, Chen S, Chohan MO, El-Akkad E, Gong CX, Khatoon S, Li B, Liu F, Rahman A, Tanimukai H, Grundke-Iqbal I (2005) Tau pathology in Alzheimer disease and other tauopathies. Biochim Biophys Acta 1739:198-210.

Irizarry MC, McNamara M, Fedorchak K, Hsiao K, Hyman BT (1997) APPSw transgenic mice develop age-related A beta deposits and neuropil abnormalities, but no neuronal loss in CA1. J Neuropathol Exp Neurol 56:965-973.

Iwatsubo T, Odaka A, Suzuki N, Mizusawa H, Nukina N, Ihara Y (1994) Visualization of A beta 42(43) and A beta 40 in senile plaques with end-specific A beta mono-clonals: evidence that an initially deposited species is A beta 42(43). Neuron 13:45-53.

Janssen JC, Beck JA, Campbell TA, Dickinson A, Fox NC, Harvey RJ, Houlden H, Rossor MN, Collinge J (2003) Early onset familial Alzheimer's disease: Mutation frequency in 31 families. Neurology 60:235-239.

Jarrett JT, Lansbury PT, Jr. (1993) Seeding "one-dimensional crystallization" of amy-loid: a pathogenic mechanism in Alzheimer's disease and scrapie? Cell 73:1055-1058.

Jellinger KA (2002) Alzheimer disease and cerebrovascular pathology: an update. J Neural Transm 109:813-836.

Jin SL, Conti M (2002) Induction of the cyclic nucleotide phosphodiesterase PDE4B is essential for LPS-activated TNF-alpha responses. Proc Natl Acad Sci U S A 99:7628-7633.

Joachim CL, Morris JH, Selkoe DJ (1988) Clinically diagnosed Alzheimer's disease: autopsy results in 150 cases. Ann Neurol 24:50-56.

Jones CT, Morris S, Yates CM, Moffoot A, Sharpe C, Brock DJ, St Clair D (1992) Mutation in codon 713 of the beta amyloid precursor protein gene presenting with schizophrenia. Nat Genet 1:306-309.

Kamino K, Orr HT, Payami H, Wijsman EM, Alonso ME, Pulst SM, Anderson L, O'Dahl S, Nemens E, White JA, et al. (1992) Linkage and mutational analysis of familial Alzheimer disease kindreds for the APP gene region. Am J Hum Genet 51:998-1014.

Kayed R, Head E, Thompson JL, McIntire TM, Milton SC, Cotman CW, Glabe CG (2003) Common structure of soluble amyloid oligomers implies common mechanism of pathogenesis. Science 300:486-489.

Kelley DJ, Bhattacharyya A, Lahvis GP, Yin JC, Malter J, Davidson RJ (2008) The cy-clic AMP phenotype of fragile X and autism. Neurosci Biobehav Rev 32:1533-1543.

Khoury JE, Luster AD (2008) Mechanisms of microglia accumulation in Alzheimer's disease: therapeutic implications. Trends Pharmacol Sci.

Koistinaho M, Ort M, Cimadevilla JM, Vondrous R, Cordell B, Koistinaho J, Bures J, Higgins LS (2001) Specific spatial learning deficits become severe with age in

beta -amyloid precursor protein transgenic mice that harbor diffuse beta -
amyloid deposits but do not form plaques. Proc Natl Acad Sci U S A 98:14675-
14680.

Kopke E, Tung YC, Shaikh S, Alonso AC, Iqbal K, Grundke-Iqbal I (1993) Microtubule
-associated protein tau. Abnormal phosphorylation of a non-paired helical fila-
ment pool in Alzheimer disease. J Biol Chem 268:24374-24384.

Kreutzberg GW (1996) Microglia: a sensor for pathological events in the CNS. Trends
Neurosci 19:312-318.

Kumar-Singh S, Julliams A, Nuydens R, Ceuterick C, Labeur C, Serneels S, Vennekens
K, Van Osta P, Geerts H, De Strooper B, Van Broeckhoven C (2002a) In vitro
studies of Flemish, Dutch, and wild-type beta-amyloid provide evidence for two-
staged neurotoxicity. Neurobiol Dis 11:330-340.

Kumar-Singh S, Dewachter I, Moechars D, Lubke U, De Jonghe C, Ceuterick C, Che-
cler F, Naidu A, Cordell B, Cras P, Van Broeckhoven C, Van Leuven F (2000a)
Behavioral disturbances without amyloid deposits in mice overexpressing human
amyloid precursor protein with Flemish (A692G) or Dutch (E693Q) mutation.
Neurobiol Dis 7:9-22.

Kumar-Singh S, De Jonghe C, Cruts M, Kleinert R, Wang R, Mercken M, De Strooper
B, Vanderstichele H, Lofgren A, Vanderhoeven I, Backhovens H, Vanmechelen
E, Kroisel PM, Van Broeckhoven C (2000b) Nonfibrillar diffuse amyloid depo-
sition due to a gamma(42)-secretase site mutation points to an essential role for
N-truncated A beta(42) in Alzheimer's disease. Hum Mol Genet 9:2589-2598.

Kumar-Singh S, Cras P, Wang R, Kros JM, van Swieten J, Lubke U, Ceuterick C, Sern-
eels S, Vennekens K, Timmermans JP, Van Marck E, Martin JJ, van Duijn CM,
Van Broeckhoven C (2002b) Dense-core senile plaques in the Flemish variant of
Alzheimer's disease are vasocentric. Am J Pathol 161:507-520.

Kunkel SL, Spengler M, May MA, Spengler R, Larrick J, Remick D (1988) Pros-
taglandin E2 regulates macrophage-derived tumor necrosis factor gene expres-
sion. J Biol Chem 263:5380-5384.

Kwok JB, Li QX, Hallupp M, Whyte S, Ames D, Beyreuther K, Masters CL, Schofield
PR (2000) Novel Leu723Pro amyloid precursor protein mutation increases amy-
loid beta42(43) peptide levels and induces apoptosis. Ann Neurol 47:249-253.

Lambert MP, Barlow AK, Chromy BA, Edwards C, Freed R, Liosatos M, Morgan TE,
Rozovsky I, Trommer B, Viola KL, Wals P, Zhang C, Finch CE, Krafft GA,
Klein WL (1998) Diffusible, nonfibrillar ligands derived from Abeta1-42 are
potent central nervous system neurotoxins. Proc Natl Acad Sci U S A 95:6448-
6453.

Lashuel HA, Hartley DM, Petre BM, Wall JS, Simon MN, Walz T, Lansbury PT, Jr. (2003) Mixtures of wild-type and a pathogenic (E22G) form of Abeta40 in vitro accumulate protofibrils, including amyloid pores. J Mol Biol 332:795-808.

Lawson LJ, Perry VH, Gordon S (1992) Turnover of resident microglia in the normal adult mouse brain. Neuroscience 48:405-415.

Le Y, Gong W, Tiffany HL, Tumanov A, Nedospasov S, Shen W, Dunlop NM, Gao JL, Murphy PM, Oppenheim JJ, Wang JM (2001) Amyloid (beta)42 activates a G-protein-coupled chemoattractant receptor, FPR-like-1. J Neurosci 21:RC123.

Lesne S, Koh MT, Kotilinek L, Kayed R, Glabe CG, Yang A, Gallagher M, Ashe KH (2006) A specific amyloid-beta protein assembly in the brain impairs memory. Nature 440:352-357.

Liu F, Iqbal K, Grundke-Iqbal I, Gong CX (2002a) Involvement of aberrant glycosylation in phosphorylation of tau by cdk5 and GSK-3beta. FEBS Lett 530:209-214.

Liu F, Zaidi T, Iqbal K, Grundke-Iqbal I, Gong CX (2002b) Aberrant glycosylation modulates phosphorylation of tau by protein kinase A and dephosphorylation of tau by protein phosphatase 2A and 5. Neuroscience 115:829-837.

Lomakin A, Chung DS, Benedek GB, Kirschner DA, Teplow DB (1996) On the nucleation and growth of amyloid beta-protein fibrils: detection of nuclei and quantitation of rate constants. Proc Natl Acad Sci U S A 93:1125-1129.

Luterman JD, Haroutunian V, Yemul S, Ho L, Purohit D, Aisen PS, Mohs R, Pasinetti GM (2000) Cytokine gene expression as a function of the clinical progression of Alzheimer disease dementia. Arch Neurol 57:1153-1160.

Mackaness GB (1964) The Immunological Basis Of Acquired Cellular Resistance. J Exp Med 120:105-120.

Malinchik SB, Inouye H, Szumowski KE, Kirschner DA (1998) Structural analysis of Alzheimer's beta(1-40) amyloid: protofilament assembly of tubular fibrils. Biophys J 74:537-545.

Mandelkow EM, Mandelkow E (1998) Tau in Alzheimer's disease. Trends Cell Biol 8:425-427.

Mandelkow EM, Biernat J, Drewes G, Gustke N, Trinczek B, Mandelkow E (1995) Tau domains, phosphorylation, and interactions with microtubules. Neurobiol Aging 16:355-362; discussion 362-353.

Mandybur TI (1986) Cerebral amyloid angiopathy: the vascular pathology and compli-

cations. J Neuropathol Exp Neurol 45:79-90.

Mann DM, Iwatsubo T, Ihara Y, Cairns NJ, Lantos PL, Bogdanovic N, Lannfelt L, Winblad B, Maat-Schieman ML, Rossor MN (1996) Predominant deposition of amyloid-beta 42(43) in plaques in cases of Alzheimer's disease and hereditary cerebral hemorrhage associated with mutations in the amyloid precursor protein gene. Am J Pathol 148:1257-1266.

Maragakis NJ, Rothstein JD (2006) Mechanisms of Disease: astrocytes in neurodegenerative disease. Nat Clin Pract Neurol 2:679-689.

Marin-Teva JL, Dusart I, Colin C, Gervais A, van Rooijen N, Mallat M (2004) Microglia promote the death of developing Purkinje cells. Neuron 41:535-547.

Martinez M, Hernandez AI, Hernanz A (2001) Increased cAMP immunostaining in cerebral vessels in Alzheimer's disease. Brain Res 922:148-152.

Masliah E, Sisk A, Mallory M, Mucke L, Schenk D, Games D (1996) Comparison of neurodegenerative pathology in transgenic mice overexpressing V717F beta-amyloid precursor protein and Alzheimer's disease. J Neurosci 16:5795-5811.

Maslow K (2008) 2008 Alzheimer's disease facts and figures. Alzheimers Dement 4:110-133.

Matulef K, Zagotta WN (2003) Cyclic nucleotide-gated ion channels. Annu Rev Cell Dev Biol 19:23-44.

McGeer PL, Itagaki S, Tago H, McGeer EG (1987) Reactive microglia in patients with senile dementia of the Alzheimer type are positive for the histocompatibility glycoprotein HLA-DR. Neurosci Lett 79:195-200.

Mehlhorn G, Hollborn M, Schliebs R (2000) Induction of cytokines in glial cells surrounding cortical beta-amyloid plaques in transgenic Tg2576 mice with Alzheimer pathology. Int J Dev Neurosci 18:423-431.

Mildner A, Schmidt H, Nitsche M, Merkler D, Hanisch UK, Mack M, Heikenwalder M, Bruck W, Priller J, Prinz M (2007) Microglia in the adult brain arise from Ly-6ChiCCR2+ monocytes only under defined host conditions. Nat Neurosci 10:1544-1553.

Mori E, Hirono N, Yamashita H, Imamura T, Ikejiri Y, Ikeda M, Kitagaki H, Shimomura T, Yoneda Y (1997) Premorbid brain size as a determinant of reserve capacity against intellectual decline in Alzheimer's disease. Am J Psychiatry 154:18-24.

Mott RT, Hulette CM (2005) Neuropathology of Alzheimer's disease. Neuroimaging Clin N Am 15:755-765, ix.

Mullan M, Crawford F, Axelman K, Houlden H, Lilius L, Winblad B, Lannfelt L (1992a) A pathogenic mutation for probable Alzheimer's disease in the APP gene at the N-terminus of beta-amyloid. Nat Genet 1:345-347.

Mullan M, Houlden H, Windelspecht M, Fidani L, Lombardi C, Diaz P, Rossor M, Crook R, Hardy J, Duff K, et al. (1992b) A locus for familial early-onset Alzheimer's disease on the long arm of chromosome 14, proximal to the alpha 1-antichymotrypsin gene. Nat Genet 2:340-342.

Murakami K, Irie K, Morimoto A, Ohigashi H, Shindo M, Nagao M, Shimizu T, Shirasawa T (2003) Neurotoxicity and physicochemical properties of Abeta mutant peptides from cerebral amyloid angiopathy: implication for the pathogenesis of cerebral amyloid angiopathy and Alzheimer's disease. J Biol Chem 278:46179-46187.

Murrell J, Farlow M, Ghetti B, Benson MD (1991) A mutation in the amyloid precursor protein associated with hereditary Alzheimer's disease. Science 254:97-99.

Murrell JR, Hake AM, Quaid KA, Farlow MR, Ghetti B (2000) Early-onset Alzheimer disease caused by a new mutation (V717L) in the amyloid precursor protein gene. Arch Neurol 57:885-887.

Nilsberth C, Westlind-Danielsson A, Eckman CB, Condron MM, Axelman K, Forsell C, Stenh C, Luthman J, Teplow DB, Younkin SG, Naslund J, Lannfelt L (2001) The 'Arctic' APP mutation (E693G) causes Alzheimer's disease by enhanced Abeta protofibril formation. Nat Neurosci 4:887-893.

Nimmerjahn A, Kirchhoff F, Helmchen F (2005) Resting microglial cells are highly dynamic surveillants of brain parenchyma in vivo. Science 308:1314-1318.

Nybo M, Svehag SE, Holm Nielsen E (1999) An ultrastructural study of amyloid intermediates in A beta1-42 fibrillogenesis. Scand J Immunol 49:219-223.

Oda T, Wals P, Osterburg HH, Johnson SA, Pasinetti GM, Morgan TE, Rozovsky I, Stine WB, Snyder SW, Holzman TF, et al. (1995) Clusterin (apoJ) alters the aggregation of amyloid beta-peptide (A beta 1-42) and forms slowly sedimenting A beta complexes that cause oxidative stress. Exp Neurol 136:22-31.

Paivio A, Jarvet J, Graslund A, Lannfelt L, Westlind-Danielsson A (2004) Unique physicochemical profile of beta-amyloid peptide variant Abeta1-40E22G protofibrils: conceivable neuropathogen in arctic mutant carriers. J Mol Biol 339:145-159.

Pasalar P, Najmabadi H, Noorian AR, Moghimi B, Jannati A, Soltanzadeh A, Krefft T, Crook R, Hardy J (2002) An Iranian family with Alzheimer's disease caused by a novel APP mutation (Thr714Ala). Neurology 58:1574-1575.

Pei JJ, Gong CX, An WL, Winblad B, Cowburn RF, Grundke-Iqbal I, Iqbal K (2003) Okadaic-acid-induced inhibition of protein phosphatase 2A produces activation of mitogen-activated protein kinases ERK1/2, MEK1/2, and p70 S6, similar to that in Alzheimer's disease. Am J Pathol 163:845-858.

Pezzini A, Padovani A (2008) Cerebral amyloid angiopathy-related hemorrhages. Neurol Sci 29 Suppl 2:S260-263.

Pfeifer LA, White LR, Ross GW, Petrovitch H, Launer LJ (2002) Cerebral amyloid angiopathy and cognitive function: the HAAS autopsy study. Neurology 58:1629-1634.

Pike CJ, Walencewicz AJ, Glabe CG, Cotman CW (1991) In vitro aging of beta-amyloid protein causes peptide aggregation and neurotoxicity. Brain Res 563:311-314.

Pike CJ, Burdick D, Walencewicz AJ, Glabe CG, Cotman CW (1993) Neurodegeneration induced by beta-amyloid peptides in vitro: the role of peptide assembly state. J Neurosci 13:1676-1687.

Priller J, Flugel A, Wehner T, Boentert M, Haas CA, Prinz M, Fernandez-Klett F, Prass K, Bechmann I, de Boer BA, Frotscher M, Kreutzberg GW, Persons DA, Dirnagl U (2001) Targeting gene-modified hematopoietic cells to the central nervous system: use of green fluorescent protein uncovers microglial engraftment. Nat Med 7:1356-1361.

Raivich G (2005) Like cops on the beat: the active role of resting microglia. Trends Neurosci 28:571-573.

Ravaglia G, Forti P, Maioli F, Chiappelli M, Montesi F, Tumini E, Mariani E, Licastro F, Patterson C (2007) Blood inflammatory markers and risk of dementia: The Conselice Study of Brain Aging. Neurobiol Aging 28:1810-1820.

Rempel H, Kusdra L, Pulliam L (2001) Interleukin-1beta up-regulates expression of neurofilament light in human neuronal cells. J Neurochem 78:640-645.

Revesz T, Ghiso J, Lashley T, Plant G, Rostagno A, Frangione B, Holton JL (2003) Cerebral amyloid angiopathies: a pathologic, biochemical, and genetic view. J Neuropathol Exp Neurol 62:885-898.

Reya T, Morrison SJ, Clarke MF, Weissman IL (2001) Stem cells, cancer, and cancer stem cells. Nature 414:105-111.

Roher AE, Ball MJ, Bhave SV, Wakade AR (1991) Beta-amyloid from Alzheimer disease brains inhibits sprouting and survival of sympathetic neurons. Biochem Biophys Res Commun 174:572-579.

Rojo LE, Fernandez JA, Maccioni AA, Jimenez JM, Maccioni RB (2008) Neuroinflammation: implications for the pathogenesis and molecular diagnosis of Alzheimer's disease. Arch Med Res 39:1-16.

Roks G, Van Harskamp F, De Koning I, Cruts M, De Jonghe C, Kumar-Singh S, Tibben A, Tanghe H, Niermeijer MF, Hofman A, Van Swieten JC, Van Broeckhoven C, Van Duijn CM (2000) Presentation of amyloidosis in carriers of the codon 692 mutation in the amyloid precursor protein gene (APP692). Brain 123 (Pt 10):2130-2140.

Roumier A, Bechade C, Poncer JC, Smalla KH, Tomasello E, Vivier E, Gundelfinger ED, Triller A, Bessis A (2004) Impaired synaptic function in the microglial KARAP/DAP12-deficient mouse. J Neurosci 24:11421-11428.

Ruben GC, Iqbal K, Wisniewski HM, Johnson JE, Jr., Grundke-Iqbal I (1993) Alzheimer neurofibrillary tangles contain 2.1 nm filaments structurally identical to the microtubule-associated protein tau: a high-resolution transmission electron microscope study of tangles and senile plaque core amyloid. Brain Res 602:164-179.

Ruben GC, Iqbal K, Grundke-Iqbal I, Wisniewski HM, Ciardelli TL, Johnson JE, Jr. (1991) The microtubule-associated protein tau forms a triple-stranded left-hand helical polymer. J Biol Chem 266:22019-22027.

Schade FU, Schudt C (1993) The specific type III and IV phosphodiesterase inhibitor zardaverine suppresses formation of tumor necrosis factor by macrophages. Eur J Pharmacol 230:9-14.

Scheuner D, Eckman C, Jensen M, Song X, Citron M, Suzuki N, Bird TD, Hardy J, Hutton M, Kukull W, Larson E, Levy-Lahad E, Viitanen M, Peskind E, Poorkaj P, Schellenberg G, Tanzi R, Wasco W, Lannfelt L, Selkoe D, Younkin S (1996) Secreted amyloid beta-protein similar to that in the senile plaques of Alzheimer's disease is increased in vivo by the presenilin 1 and 2 and APP mutations linked to familial Alzheimer's disease. Nat Med 2:864-870.

Schweers O, Mandelkow EM, Biernat J, Mandelkow E (1995) Oxidation of cysteine-322 in the repeat domain of microtubule-associated protein tau controls the in vitro assembly of paired helical filaments. Proc Natl Acad Sci U S A 92:8463-8467.

Schwende H, Fitzke E, Ambs P, Dieter P (1996) Differences in the state of differentia-

tion of THP-1 cells induced by phorbol ester and 1,25-dihydroxyvitamin D3. J Leukoc Biol 59:555-561.

Selkoe DJ (2001a) Alzheimer's disease results from the cerebral accumulation and cytotoxicity of amyloid beta-protein. J Alzheimers Dis 3:75-80.

Selkoe DJ (2001b) Alzheimer's disease: genes, proteins, and therapy. Physiol Rev 81:741-766.

Selkoe DJ (2001c) Presenilin, Notch, and the genesis and treatment of Alzheimer's disease. Proc Natl Acad Sci U S A 98:11039-11041.

Selkoe DJ (2004) Cell biology of protein misfolding: the examples of Alzheimer's and Parkinson's diseases. Nat Cell Biol 6:1054-1061.

Serbina NV, Jia T, Hohl TM, Pamer EG (2008) Monocyte-mediated defense against microbial pathogens. Annu Rev Immunol 26:421-452.

Serpell LC, Blake CC, Fraser PE (2000) Molecular structure of a fibrillar Alzheimer's A beta fragment. Biochemistry 39:13269-13275.

Seta N, Kuwana M (2007) Human circulating monocytes as multipotential progenitors. Keio J Med 56:41-47.

Seubert P, Vigo-Pelfrey C, Esch F, Lee M, Dovey H, Davis D, Sinha S, Schlossmacher M, Whaley J, Swindlehurst C, et al. (1992) Isolation and quantification of soluble Alzheimer's beta-peptide from biological fluids. Nature 359:325-327.

Simard AR, Rivest S (2004) Bone marrow stem cells have the ability to populate the entire central nervous system into fully differentiated parenchymal microglia. Faseb J 18:998-1000.

Simard AR, Soulet D, Gowing G, Julien JP, Rivest S (2006) Bone marrow-derived microglia play a critical role in restricting senile plaque formation in Alzheimer's disease. Neuron 49:489-502.

Sinha B, Semmler J, Eisenhut T, Eigler A, Endres S (1995) Enhanced tumor necrosis factor suppression and cyclic adenosine monophosphate accumulation by combination of phosphodiesterase inhibitors and prostanoids. Eur J Immunol 25:147-153.

Sisodia SS, Koo EH, Beyreuther K, Unterbeck A, Price DL (1990) Evidence that beta-amyloid protein in Alzheimer's disease is not derived by normal processing. Science 248:492-495.

Soto C, Castano EM, Frangione B, Inestrosa NC (1995) The alpha-helical to beta-strand transition in the amino-terminal fragment of the amyloid beta-peptide modulates amyloid formation. J Biol Chem 270:3063-3067.

Spengler RN, Spengler ML, Lincoln P, Remick DG, Strieter RM, Kunkel SL (1989) Dynamics of dibutyryl cyclic AMP- and prostaglandin E2-mediated suppression of lipopolysaccharide-induced tumor necrosis factor alpha gene expression. Infect Immun 57:2837-2841.

Spires TL, Hyman BT (2004) Neuronal structure is altered by amyloid plaques. Rev Neurosci 15:267-278.

St George-Hyslop PH (2000) Piecing together Alzheimer's. Sci Am 283:76-83.

Stine WB, Jr., Dahlgren KN, Krafft GA, LaDu MJ (2003) In vitro characterization of conditions for amyloid-beta peptide oligomerization and fibrillogenesis. J Biol Chem 278:11612-11622.

Suo Z, Tan J, Placzek A, Crawford F, Fang C, Mullan M (1998) Alzheimer's beta-amyloid peptides induce inflammatory cascade in human vascular cells: the roles of cytokines and CD40. Brain Res 807:110-117.

Suzuki N, Cheung TT, Cai XD, Odaka A, Otvos L, Jr., Eckman C, Golde TE, Younkin SG (1994) An increased percentage of long amyloid beta protein secreted by familial amyloid beta protein precursor (beta APP717) mutants. Science 264:1336-1340.

Tarkowski E, Andreasen N, Tarkowski A, Blennow K (2003) Intrathecal inflammation precedes development of Alzheimer's disease. J Neurol Neurosurg Psychiatry 74:1200-1205.

Teplow DB (1998) Structural and kinetic features of amyloid beta-protein fibrillogenesis. Amyloid 5:121-142.

Terreni L, Fogliarino S, Franceschi, Forloni G (2002) Novel pathogenic mutation in an Italian patient with familial Alzheimer's disease detected in APP gene. Neurobiology of Aging 23:1.

Terry RD, Hansen LA, DeTeresa R, Davies P, Tobias H, Katzman R (1987) Senile dementia of the Alzheimer type without neocortical neurofibrillary tangles. J Neuropathol Exp Neurol 46:262-268.

Thal DR, Griffin WS, de Vos RA, Ghebremedhin E (2008) Cerebral amyloid angiopathy and its relationship to Alzheimer's disease. Acta Neuropathol 115:599-609.

Trojanowski JQ, Lee VM (1995) Phosphorylation of paired helical filament tau in Alzheimer's disease neurofibrillary lesions: focusing on phosphatases. Faseb J 9:1570-1576.

Uberti D, Cantarella G, Facchetti F, Cafici A, Grasso G, Bernardini R, Memo M (2004) TRAIL is expressed in the brain cells of Alzheimer's disease patients. Neuroreport 15:579-581.

Van Broeckhoven C, Haan J, Bakker E, Hardy JA, Van Hul W, Wehnert A, Vegter-Van der Vlis M, Roos RA (1990) Amyloid beta protein precursor gene and hereditary cerebral hemorrhage with amyloidosis (Dutch). Science 248:1120-1122.

Van Furth R, Diesselhoff-den Dulk MC, Mattie H (1973) Quantitative study on the production and kinetics of mononuclear phagocytes during an acute inflammatory reaction. J Exp Med 138:1314-1330.

Van Nostrand WE, Melchor JP, Cho HS, Greenberg SM, Rebeck GW (2001) Pathogenic effects of D23N Iowa mutant amyloid beta -protein. J Biol Chem 276:32860-32866.

Vigo-Pelfrey C, Seubert P, Barbour R, Blomquist C, Lee M, Lee D, Coria F, Chang L, Miller B, Lieberburg I, et al. (1995) Elevation of microtubule-associated protein tau in the cerebrospinal fluid of patients with Alzheimer's disease. Neurology 45:788-793.

Vinters HV (1987) Cerebral amyloid angiopathy. A critical review. Stroke 18:311-324.

Vinters HV, Gilbert JJ (1983) Cerebral amyloid angiopathy: incidence and complications in the aging brain. II. The distribution of amyloid vascular changes. Stroke 14:924-928.

Vinters HV, Wang ZZ, Secor DL (1996) Brain parenchymal and microvascular amyloid in Alzheimer's disease. Brain Pathol 6:179-195.

Volkman A, Gowans JL (1965a) The Production Of Macrophages In The Rat. Br J Exp Pathol 46:50-61.

Volkman A, Gowans JL (1965b) The Origin Of Macrophages From Bone Marrow In The Rat. Br J Exp Pathol 46:62-70.

von Bergen M, Friedhoff P, Biernat J, Heberle J, Mandelkow EM, Mandelkow E (2000) Assembly of tau protein into Alzheimer paired helical filaments depends on a local sequence motif ((306)VQIVYK(311)) forming beta structure. Proc Natl Acad Sci U S A 97:5129-5134.

Vonsattel JP, Myers RH, Hedley-Whyte ET, Ropper AH, Bird ED, Richardson EP, Jr. (1991) Cerebral amyloid angiopathy without and with cerebral hemorrhages: a comparative histological study. Ann Neurol 30:637-649.

Wakutani Y, Watanabe K, Adachi Y, Wada-Isoe K, Urakami K, Ninomiya H, Saido TC, Hashimoto T, Iwatsubo T, Nakashima K (2004) Novel amyloid precursor protein gene missense mutation (D678N) in probable familial Alzheimer's disease. J Neurol Neurosurg Psychiatry 75:1039-1042.

Walsh DM, Selkoe DJ (2004) Deciphering the molecular basis of memory failure in Alzheimer's disease. Neuron 44:181-193.

Walsh DM, Lomakin A, Benedek GB, Condron MM, Teplow DB (1997) Amyloid beta-protein fibrillogenesis. Detection of a protofibrillar intermediate. J Biol Chem 272:22364-22372.

Walsh DM, Hartley DM, Condron MM, Selkoe DJ, Teplow DB (2001) In vitro studies of amyloid beta-protein fibril assembly and toxicity provide clues to the aetiology of Flemish variant (Ala692-->Gly) Alzheimer's disease. Biochem J 355:869-877.

Walsh DM, Klyubin I, Fadeeva JV, Cullen WK, Anwyl R, Wolfe MS, Rowan MJ, Selkoe DJ (2002) Naturally secreted oligomers of amyloid beta protein potently inhibit hippocampal long-term potentiation in vivo. Nature 416:535-539.

Walsh DM, Hartley DM, Kusumoto Y, Fezoui Y, Condron MM, Lomakin A, Benedek GB, Selkoe DJ, Teplow DB (1999) Amyloid beta-protein fibrillogenesis. Structure and biological activity of protofibrillar intermediates. J Biol Chem 274:25945-25952.

Wang J, Dickson DW, Trojanowski JQ, Lee VM (1999) The levels of soluble versus insoluble brain Abeta distinguish Alzheimer's disease from normal and pathologic aging. Exp Neurol 158:328-337.

Wang JZ, Grundke-Iqbal I, Iqbal K (1996a) Glycosylation of microtubule-associated protein tau: an abnormal posttranslational modification in Alzheimer's disease. Nat Med 2:871-875.

Wang JZ, Grundke-Iqbal I, Iqbal K (1996b) Restoration of biological activity of Alzheimer abnormally phosphorylated tau by dephosphorylation with protein phosphatase-2A, -2B and -1. Brain Res Mol Brain Res 38:200-208.

Wang JZ, Gong CX, Zaidi T, Grundke-Iqbal I, Iqbal K (1995) Dephosphorylation of Alzheimer paired helical filaments by protein phosphatase-2A and -2B. J Biol Chem 270:4854-4860.

Weidemann A, Konig G, Bunke D, Fischer P, Salbaum JM, Masters CL, Beyreuther K (1989) Identification, biogenesis, and localization of precursors of Alzheimer's disease A4 amyloid protein. Cell 57:115-126.

Westerman MA, Cooper-Blacketer D, Mariash A, Kotilinek L, Kawarabayashi T, Younkin LH, Carlson GA, Younkin SG, Ashe KH (2002) The relationship between Abeta and memory in the Tg2576 mouse model of Alzheimer's disease. J Neurosci 22:1858-1867.

Whalen BM, Selkoe DJ, Hartley DM (2005) Small non-fibrillar assemblies of amyloid beta-protein bearing the Arctic mutation induce rapid neuritic degeneration. Neurobiol Dis 20:254-266.

Wisniewski T, Ghiso J, Frangione B (1991) Peptides homologous to the amyloid protein of Alzheimer's disease containing a glutamine for glutamic acid substitution have accelerated amyloid fibril formation. Biochem Biophys Res Commun 179:1247-1254.

Xia MQ, Hyman BT (1999) Chemokines/chemokine receptors in the central nervous system and Alzheimer's disease. J Neurovirol 5:32-41.

Yan SD, Chen X, Fu J, Chen M, Zhu H, Roher A, Slattery T, Zhao L, Nagashima M, Morser J, Migheli A, Nawroth P, Stern D, Schmidt AM (1996) RAGE and amyloid-beta peptide neurotoxicity in Alzheimer's disease. Nature 382:685-691.

Zekanowski C, Styczynska M, Peplonska B, Gabryelewicz T, Religa D, Ilkowski J, Kijanowska-Haladyna B, Kotapka-Minc S, Mikkelsen S, Pfeffer A, Barczak A, Luczywek E, Wasiak B, Chodakowska-Zebrowska M, Gustaw K, Laczkowski J, Sobow T, Kuznicki J, Barcikowska M (2003) Mutations in presenilin 1, presenilin 2 and amyloid precursor protein genes in patients with early-onset Alzheimer's disease in Poland. Exp Neurol 184:991-996.

2 METHODS

2.1 Cell Culture

2.1.1 THP-1 Monocytes

THP-1 monocytes were purchased from ATCC (Manassas, VA). Cells were stored in 1 ml aliquots in liquid nitrogen until needed for culture. Cells were cultured in growth medium, which is RPMI 1640 containing 2mM L-glutamine and 1.5 g/L sodium bicarbonate (Hyclone, Logan, UT), supplemented with 10% Fetal Bovine Serum (FBS, Hyclone), 50 U/ml penicillin, 50 μg/ml streptomycin (Hyclone) and 50 μM β-mercapto-ethanol (Fisher, Pittsburg, PA) at 37°C with 5% CO_2. During culturing, cells were diluted 1:1 in fresh growth medium on Monday and Wednesday. On Friday cells were centrifuged at 0.5 x g for 10 minutes. Pellet was resuspended in growth medium for a final cell dilution of 3:7. For experiments, cells were removed from culture flask and centrifuged at 0.5 x g for 10 minutes. The pellet was resuspended in assay medium (same as growth but containing only 2% FBS) so that the resulting cell concentration was near 7×10^5 cells/ml as counted on a hemocytometer.

THP-1 cells are a cultured human peripheral blood monocytes derived from a leukemia patient (Tsuchiya et al., 1980). The cells are non-adherent with a rounded mor-

phology. THP-1 cells have previously been used as a model of cell differentiation (Tsuchiya et al., 1982; Auwerx, 1991).

2.1.2 Human Aortic Vascular Smooth Muscle Cells

Human Aortic Vascular Smooth Muscle Cells (HA-VSMC) were purchased from ATCC. Cells were stored in 1 ml aliquots in liquid nitrogen until needed for culture. Cells were cultured in growth medium, which is Ham's F12K containing 2 mM L-glutamine and 1.5 g/L sodium bicarbonate (Hyclone) and supplemented with 10mM Hepes (Fisher), 10 mM 2-[Tris(hydroxymethyl)methylamino]-1-ethanesulfonic acid (TES, Acros, Morris Plains, NJ), 0.05 mg/ml ascorbic acid (Fisher), 0.03 mg/ml endothelial cell growth supplement (ECGS, BD Biosciences, San Jose, CA), 0.1 mg/ml insulin (Fisher), 0.01 mg/ml transferrin (Fisher), 10 ng/ml selenium (Fisher) and 10% FBS at 37°C with 5% CO_2. During culturing, the old growth medium was removed from the flask and replaced with fresh growth medium on Monday, Wednesday and Friday. Once cells achieved confluence on the bottom of the flask they were passaged as follows. Cells were removed from the flask by exposure to 1 ml of 0.25% trypsin-EDTA (Hyclone) for seven minutes. Trypsin activity was stopped with 4 ml of growth medium and the combined 5 ml containing the cells was collected. The cells were spun at 0.5 x g for 10 minutes. The pellet was resuspended in 10 ml of fresh growth medium and 5 ml was added to a fresh flask containing 5 ml of fresh growth medium. For experiments, cells were removed from the flask and centrifuged as previously described. The pellet was then resuspended to 1 x 10^5 cells/ml in growth medium. Cells were plated into a

sterile 48-well plate and incubated 48 hours to allow for cell adherence before further experimentation was performed. Once adherence was achieved, growth medium was removed from wells and replaced with assay medium which is Ham's F12K containing 2mM L-glutamine and 1.5 g/L sodium bicarbonate (Hyclone) supplemented with 10 mM Hepes, 10 mM TES and 0.05 mg/ml ascorbic acid.

2.1.3 PC12 Cells

PC12 cells were purchased from ATCC. Cells were stored in 1 ml aliquots in liquid nitrogen until needed for culture. Cells were cultured in RPMI 1640 containing 2 mM L-glutamine and 1.5 g/L sodium bicarbonate supplemented with 5% FBS, 10% heat-inactivated horse serum, 50 U/ml penicillin and 50 μg/ml streptomycin at 37°C with 5% CO_2. During culturing, 10 ml of cells were seeded into a T-75 culture flask at a concentration of 1 x 10^5 cells/ml. Growth medium was replaced every two days until cells were either confluent or needed for an experiment. Upon achieving confluence, 2 ml of cells were removed from the flask by agitation and then seeded in a new flask and diluted to 10 ml total volume with growth medium. For experiments, cells were removed from flask and centrifuged at 0.5 x g. The pellet was resuspended in growth medium to 3 x 10^5 cells/ml and plated into wells of a sterile 48-well culture plate. The plate was incubated at 37°C for 72 hours to allow the cells to adhere before further experimentation was conducted.

2.2 Preparation of Aβ peptides

2.2.1 General Aβ preparation

Aβ(1-40) and Aβ(1-42) were purchased from rPeptide (Bogarth, GA) as a lyophilized powder. Peptides were reconstituted in 100% hexafluoroisopropanol (HFIP, Sigma, St. Louis, MO) and incubated at room temperature for 1 hour to dissociate any pre-formed aggregates (Wood et al., 1996; Zagorski et al., 1999). Following incubation, the peptides were aliquotted into sterile microcentrifuge tubes and dried in a vacuum centrifuge before being stored at -20°C. Before using in the cells, peptides were resuspended to 50 μM, 100 μM or 1 mM in sterile water. Reconstituted peptides were stored at 4°C, 25°C or 37°C as indicated in the experiments. Aβ(1-42) L34P was received as a gift from Ron Wetzel (University of Pittsburgh). It was treated in the same way as the commercially available Aβ samples as described above.

2.2.2 Aβ-derived diffusible ligands

Aβ-derived diffusible ligands (ADDLs) were prepared from lyophilized Aβ(1-42) as previously described (Stine et al., 2003). One vial containing 0.25 mg of peptide was resuspended to 5 mM with 11 μL of dimethyl sulfoxide (DMSO, Sigma) and then diluted to 100 μM with 543 μL of ice cold Ham's F12 medium with phenol red (Hyclone). The diluted peptide was incubated for 24 hours at 4°C before being centrifuged for 10 minutes at 14,000 x g. The supernatant, which contained the ADDLs, was collected and used for experiments.

2.3 Cell Adherence Assays

2.3.1 Direct Counting

THP-1 cells were centrifuged and resuspended in assay medium as described above and then 204 μL was plated into wells of a sterile 48-well tissue culture plate. To the wells, ultrapure bacterial LPS (*Escherichia coli* K12), synthetic bacterial lipoprotein tripalmitoyl cysteinyl seryl tetralysine (Pam$_3$CSK$_4$) (InvivoGen, San Diego, CA), phorbol 12-myristate 13-acetate (PMA, Sigma), or Aβ were used to induce adherence in the cells. Cells were exposed to the effectors at 37°C at the concentrations and incubation times indicated in the experiments. After the incubation time, the medium, which contained non-adherent cells, was collected off the wells. The wells were washed with 200 μL of phosphate buffered saline (PBS, Hyclone) and the wash was collected. Cells that remained adherent were treated with 100 μL of trypsin and incubated at 37°C for 7 minutes. Trypsin activity was stopped with the addition of 400 μL of THP-1 growth medium and the adherent cells were collected. Cells in the medium, wash and adherent populations were counted under a microscope on a standard hemocytometer and corrected to total cells present. The percent adherence was determined by dividing the number of adherent cells by the total number of cells plated at the beginning of the experiment (Crouse et al., 2009). Using only the adherent cell counts in the final percent adherence calculation did not significantly alter the results of the experiments (Fig. 2.1).

2.3.2 Calcein Fluorescence
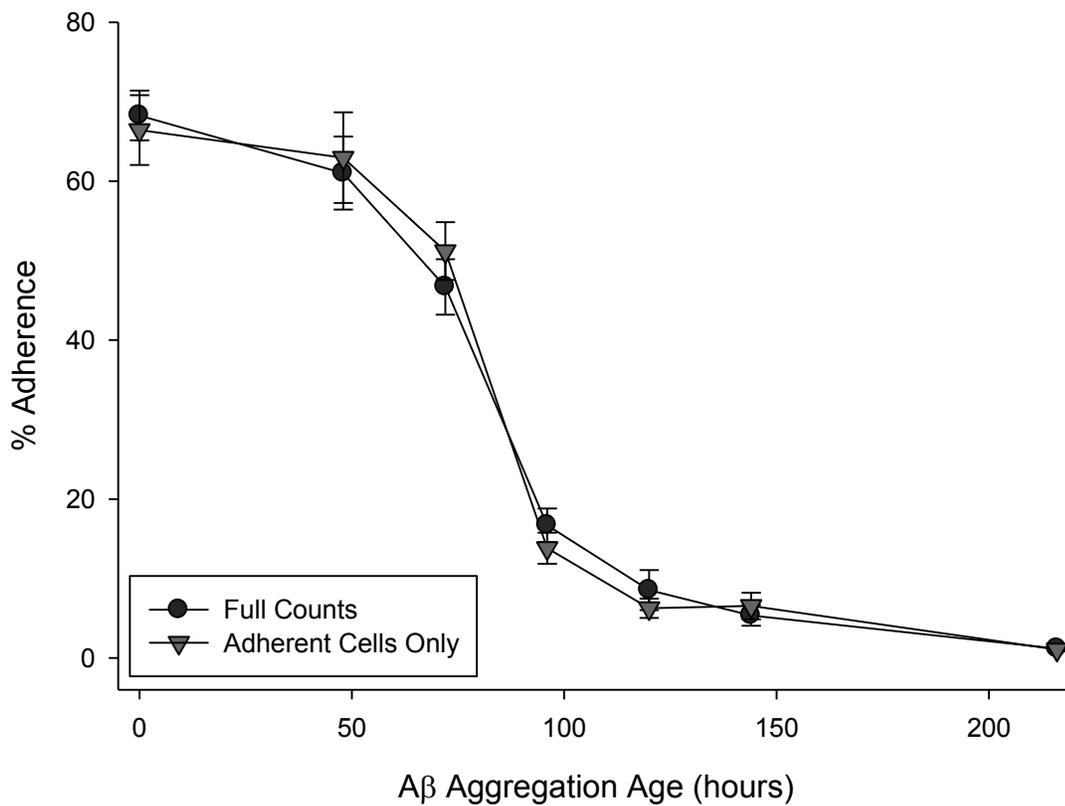
Fig. 2.1 Counting adherent cells only does not significantly modify the results.
THP-1 cells were treated with 15 μM Aβ(1-42) for 6 hours. Following the incubation, non-adherent and adherent cells were collected and counted as described in the Methods. Percent adherence was determined using the adherent cells as a percentage of all of the counted cells (circles) or as a percentage of the plated cells (inverted triangles). Error bars are standard error for n = 19 (0 hours), 17 (48 hours), 4 (72 hours), 5 (96 hours), 7 (120 hours), 3 (144 hours) and 7 (216 hours).
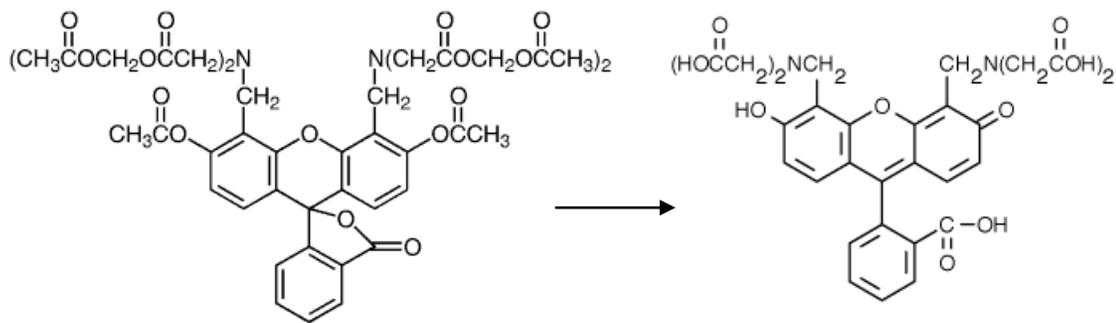
Fig. 2.2 Esterase activity in live cells converts calcein AM to fluorescent calcein
The methyl ester groups are cleaved off of calcein AM by esterase activity in living cells to produce calcein which undergoes >500-fold fluorescence increase.

Calcein AM is a non-fluorescent compound which can be taken up by living cells. Once internalized, esterase activity cleaves the methyl ester groups from the calcein rendering the compound fluorescent at 504 nm excitation and 523 nm emission (Fig. 2.2) (Papadopoulos et al., 1994).

For six hour adherence assays, THP-1 cells were incubated with 10 μM calcein AM for 30 minutes at 37ºC prior to preparation in assay medium. The cells were plated and treated with 10 ng/ml PMA as described above. At the end of the incubation, the medium was removed and the adherent cells in the well were washed with PBS and the fluorescence was read on the Perkin Elmer Victor using the fluorescein filter.

For 24 hour adherence experiments, the cells were prepared in assay medium and treated with PMA as described above and incubated for 24 hours. At the end of the treatment, the medium was removed and the adherent cells were washed with PBS. The adherent cells were incubated with 10 μM calcein AM for 30 minutes at 37ºC. The fluorescence was read on the Perkin Elmer Victor using the fluorescein filter.

2.4 Inhibitor Studies

2.4.1 FPRL1 and NF-κB Pathways

THP-1 cells were prepared in assay medium as described above and plated into a 48-well plate. Cells were pretreated for 15 minutes with 30 μM of FPRL1 antagonist

Trp-Arg-Trp-Trp-Trp-TrpCO-NH$_2$ (WRW$_4$) peptide(Bae et al., 2004) (Tocris, Ellisville, MO) or 1 hour with ammonium pyrrolidinecarbodithiolate (PDTC, Sigma) before the addition of 10 ng/ml PMA or 15 μM Aβ(1-42). The samples were incubated for 6 hours at 37°C before being analyzed for adherence as described above.

2.4.2 Toll-like receptors

THP-1 cells were added to a 48-well cell culture plate and pre-treated with 10 μg/ml TLR antibodies or IgG isotype control for 1 h at 37°C in 5% CO$_2$. Antibodies and isotype controls used were functional grade anti-human TLR2 (clone T2.5) or TLR4 (clone HTA125) antibodies, mouse IgG1κ isotype controls from eBioscience (San Diego, CA, USA. Following the 1 h incubation, Aβ(1–42) was applied in the continuing presence of neutralizing antibodies and the cells were further incubated for 6 h in the same conditions. TNFα from cell supernatants was determined as described below.

2.5 Determination of TNFα Levels

A sandwich enzyme linked immunosorbent assay (ELISA) was performed to measure the levels of secreted TNFα as previously described (Udan et al., 2007). Wells of a 96-well plate were coated with 100 μL of 4 μg/ml monoclonal anti-human TNFα/ TNFSF1A capture antibody (R&D Systems, Minneapolis, MN) and incubated at room temperature overnight. Following the incubation period, the wells were washed three times with PBS containing 0.05% Tween 20 and then blocked for 1 hour at room tem-

perature with 300 µL of PBS containing 1% BSA, 5% sucrose and 0.05% NaN_3. After washing three times as described, 50 µL of 20 mM Tris containing 150 mM NaCl, 0.1% BSA and 0.05% Tween 20 was added to wells followed by 50 µL of TNFα standards or cellular samples. The plate was incubated at room temperature for 2 hours after which it was washed three times as before. Next, 100 µL of biotinylated polyclonal anti-human TNFα/TNFSF1A detection antibody (R&D Systems) in 20 mM Tris with 150 mM NaCl and 0.1% BSA was added for two hours at room temperature. Following the incubation, the wells were washed three times. The wells were treated with 100 µL of streptavidin-horseradish peroxidase (R&D Systems) diluted 200 times in PBS with 1% BSA for 20 minutes at room temperature. The wells were washed three times followed by the addition of 100 µL of a 1:1 mixture of 3,3',5,5'-tetramethylbenzidine and hydrogen peroxide (KPL, Gaithersburg, MD) for 30 minutes. The enzymatic reaction was stopped with the addition of 50 µL of 1 M H_2SO_4. The optical density of each sample was analyzed using a SpectraMax 340 absorbance plate reader at 450 nm with a reference reading at 540 nm. The concentration of TNFα in each sample was calculated from the TNFα standard curve which ranged from 15 – 2000 pg/ml.

2.6 Characterization of adherent cells

2.6.1 Cell Proliferation

THP-1 cells were prepared in assay medium as described above. Cells were plated into wells of a sterile 48-well plate with three wells for each condition. Cells were

treated with either 10 ng/ml PMA or 15 μM freshly prepared Aβ(1-42) (final concentrations) and incubated for 6, 24 or 48 hours at 37°C. After the incubation time, the medium was collected off the wells and the wells were washed with 200 μL of PBS. The wash was also collected. Cells that remained adherent were treated with 100 μL of trypsin and incubated at 37°C for 7 minutes. The trypsin activity was stopped with the addition of 400 μL of THP-1 growth medium and the adherent cells were collected. The collected populations were each centrifuged for 5 minutes at 2000 RPM. The pellets were each resuspended in 500 μL of PBS. A 100 μL aliquot was removed from each of the samples and placed in a fresh microcentrifuge tube containing 100 μL of 0.4% trypan blue (Hyclone). The samples were incubated at room temperature for 3 minutes before the living and dead cells in each sample were counted under a microscope using a hemocytometer. The trypan blue exclusion assay was provided by Hyclone from a previously published method (Freshney, 1994).

2.6.2 Fibronectin (Fn) Coating

Fn (Sigma) was reconstituted in sterile water to 1 mg/ml. It was stored at -20°C in 50μL aliquots. For coating, one aliquot was removed and diluted to 50 μg/ml in sterile PBS. Each well of a sterile 48-well plate to be coated was treated with 100μL of 50 μg/ml Fn (5 μg/well final concentration) and allowed to incubate at room temperature for one hour. The plate was covered and stored at 4°C until needed for an experiment, typically overnight but not longer than two weeks (Seo et al., 2006; Crouse et al., 2009). Prior to the addition of cells, any excess Fn solution was aspirated from the wells.

2.6.3 Cell surface CD11b expression

Analysis of the CD11b expression on the cell surface was modified from a previously published method to measure the cell surface expression of tagged mutant peptides (Conner et al., 2006). CD11b was analyzed as we have previously described (Crouse et al., 2009). THP-1 cells were prepared in assay medium and treated with effectors to induce adherence in wells pre-coated with Fn. Cells were incubated for 6 or 24 hours at 37°C. Following the incubation, the medium was removed by aspiration and the wells were washed one time with 400μL of PBS containing 0.05% Tween 20. The cells were fixed with 250μL of 3.7% formaldehyde for 15 minutes. The wells were washed three times as described and then blocked for one hour at room temperature with 300μL of PBS containing 1% BSA. The wells were washed once. The cells were treated with 200μL of 0.5 mg/ml mouse-raised anti-CD11b antibody diluted 500-fold in PBS containing 1% dry milk and incubated at room temperature for three hours. The wells were washed three times. The cells were treated with 200μL of anti-mouse IgG HRP conjugate diluted 500-fold in PBS containing 1% BSA and incubated at room temperature for one hour. The wells were washed three times. The cells were treated with 250μL of absorbent HRP substrate for 20 minutes at room temperature. The substrate activity was stopped with the addition of 125μL of 1M H_2SO_4. The colored solution was transferred to the wells of a clear 96-well plate before the absorbance was read at 450 nm with the background at 540 nm subtracted out.

2.6.4 XTT Assay

A 1 mg/ml stock solution of 2,3-Bis(2-methoxy-4-nitro-5- sulfophenyl)-2H-tetrazolium-5-carboxanilide (XTT) (Sigma) was prepared in RPMI 1640 without phenol red (Hyclone) supplemented with 2 mM L-glutamine and stored at -20°C. For non-adherent cells, stock solution of XTT was thawed and mixed with 5 mM phenazine methosulfate (PMS, Acros) for a final PMS concentration of 24.9 µM. Samples of 220 µL of cells in XTT assay medium (RPMI 1640 without phenol red supplemented with 2 mM L-glutamine and 2% FBS) were treated with 110 µL of 1 mg/ml XTT/ 24.9 µM PMS and incubated for up to 4 hours at 37°C. For adherent cells, medium was removed and replaced with 0.33 mg/ml XTT/ 8.3 µM PMS in XTT assay medium and incubated for up to 4 hours at 37°C. For indirect measurement of cell adherence, 220 µL of treatment medium containing non-adherent cells was moved from the treatment well to a fresh well. The cells were treated with 110 µL of 1 mg/ml XTT/ 24.9 µM PMS and incubated for up to 4 hours at 37°C. In all cases, XTT reduction was analyzed by absorbance of the solution at 467nm.

The XTT assay is used to measure cellular metabolism. A colorless tetrazolium salt is reduced into an orange soluble fomazan product through the action of mitochondrial succinoxidase and cytochrome p450 as well as favoprotein oxidases (Fig 2.3) (Scudiero et al., 1988; Roehm et al., 1991; Kuhn et al., 2003). The XTT salt has been shown to be reduced more effectively in the presence of PMS (Scudiero et al., 1988). Many researchers in the AD field use a similar 3-(4,5-dimethylthiazol-2-yl)-2,5-diphenyltetrazolium bromide (MTT) assay which forms purple formazan crystals upon
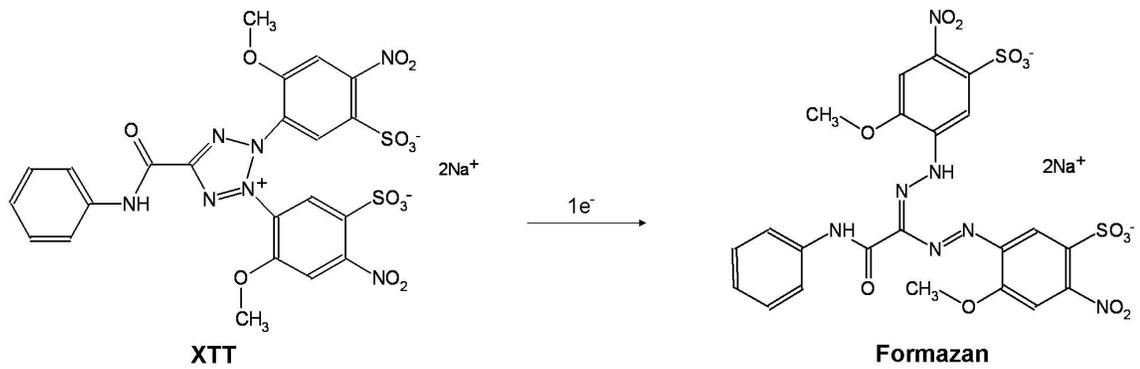
Fig. 2.3 Colorless XTT tetrazolium salt is reduced to soluble, orange formazan
Colorless XTT solution is reduced by one electron. Reduction leads to cleavage of the XTT ring system into the colored formazan structure.

reduction. However, a study comparing the effectiveness of the XTT, MTT and other viability assays showed that use of the MTT assay can suggest more toxicity than actually exists during studies involving Aβ (Wogulis et al., 2005), leading us to utilize the XTT assay for our experiments.

2.7 cAMP studies

2.7.1 Cell treatment with cAMP modulators

THP-1 cells were centrifuged and resuspended in assay medium as described above. The cells were counted and 290 μL plated into individual wells of a sterile 48-well cell culture plate. The plated cells were treated with 10 ng/ml LPS, 1.67% DMSO (control) or different volumes of isobutylmethylxanthine (IBMX, Sigma) and forskolin (Fsk, Sigma) to achieve the final concentrations noted in the experiments. The cells were incubated for up to 6 hours at 37°C. The cells were removed from the well and treated with cAMP lysis buffer (Perkin Elmer) at a lysis buffer to cell ratio of 1:10 for 15 minutes at room temperature. The samples were then stored at -20°C until analyzed.

HA-VSMC were prepared and plated for experiments 48 hours prior to treatment as described above. Following the incubation time, the medium was removed and replaced with 180 μL of fresh HA-VSMC assay medium and 10 ng/ml LPS (final), 15 μM Aβ (final), 1.67% DMSO (control, final) or different volumes IBMX and Fsk to achieve the final concentrations noted in the experiments. When treating the cells, IBMX and Fsk were added first to allow the cells to begin producing cAMP immediately. The cells

were incubated for 48 hours at 37°C with the effectors before medium was removed and XTT analysis was performed.

2.7.2 Determination of cAMP Levels

The levels of cAMP in cells were measured using the competition based DEL-FIA assay kit (Perkin Elmer, Waltham, MA). The DELFIA assay involves the competition of cAMP from the test sample and a cAMP-Europium tracer complex for an anti-cAMP antibody adsorbed to a 96-well plate. After binding to the antibody, the Europium is dissociated from the cAMP and forms chelates with molecules in the Enhancement solution. The time-resolved fluorescence of the Europium is read and compared to a standard curve (Fig. 2.4). All reagents for the assay were included in the DELFIA kit.

The anti-cAMP antibody solution was diluted 100-fold in 20 mM Tris containing 150 mM NaCl, 0.1% BSA and 0.05% Tween 20 and 50 μL was plated into wells of a yellow 96-well plate pre-coated with capture antibody (from kit). The plate was incubated at room temperature for 30 minutes with gentle shaking. The cAMP standard was diluted in cAMP Buffer for Standards and serial dilutions were performed for the standard curve. The Eu tracer was diluted 100-fold in sterile water. To each well of the plate 100 μL of Eu tracer and 50 μL of either cAMP standard or cellular sample were added. The plate was incubated at room temperature for 4 hours with gentle shaking. The plate was washed 3 times with cAMP Wash Buffer. To each well 200 μL of Enhancement Solution was added and the plate was incubated at room temperature for 45 minutes with gentle shaking. The time-resolved fluorescence was read with the Perkin Elmer
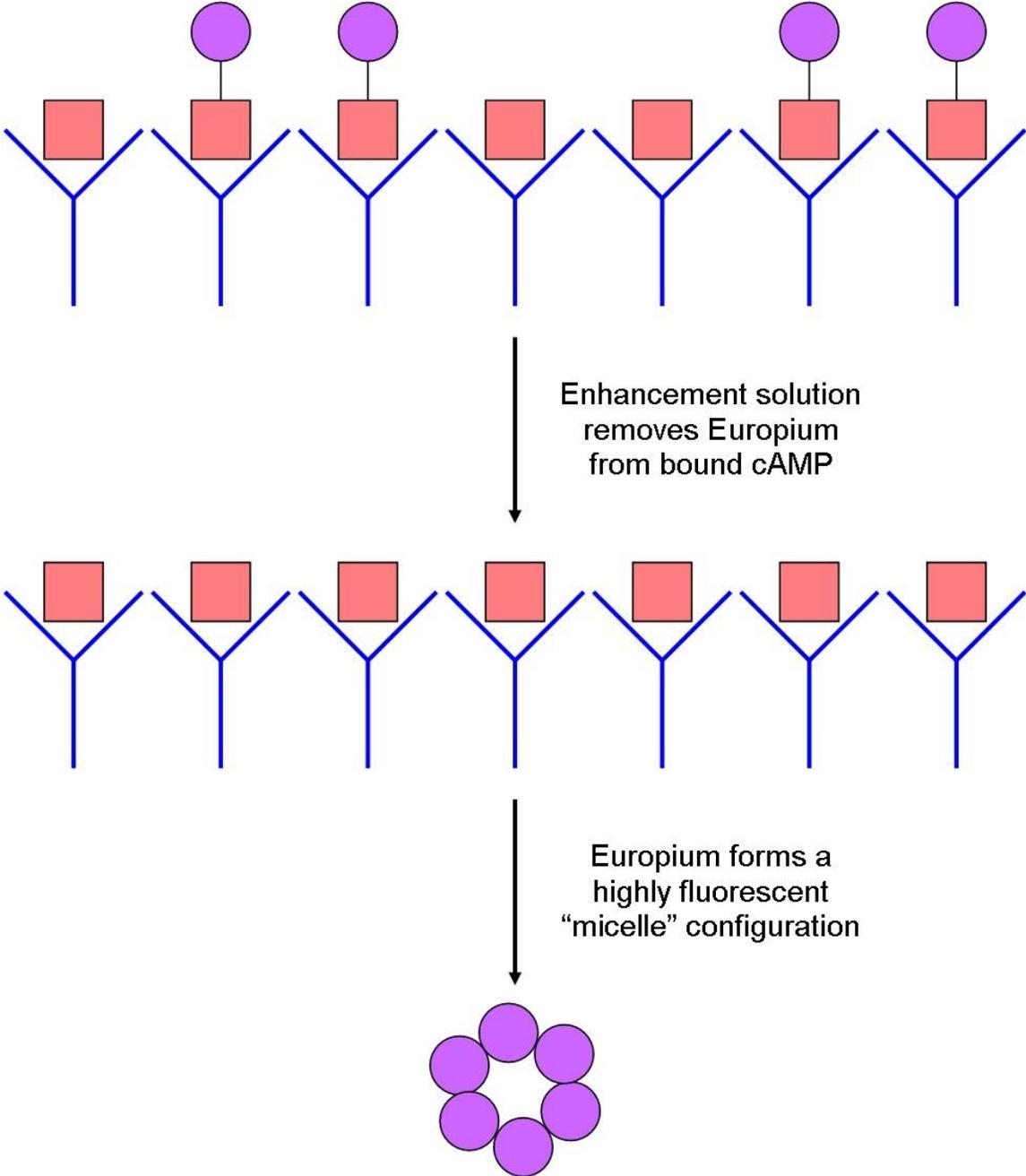
Fig. 2.4 Measurement of cAMP via DELFIA competition assay
Levels of cAMP were determined as described in the Methods. The cAMP produced by the cells (squares) competes with the cAMP-Europium tracer (squares-circles) for the cAMP binding site on the antibody. Once bound, the Europium is cleaved from the bound cAMP and forms a mi-celle-like structure which provides an enhancement in time-resolved fluorescence.

Victor (Perkin Elmer) using the Europium Time Resolved Fluorescence protocol. The concentration of cAMP in each sample was calculated from the cAMP standard curve which ranged from 28.125 – 1800 pmol/ml.

2.7.3 Preparation of cAMP-HRP conjugate

A cAMP-HRP conjugate was prepared using a previously published method (Lombardi and Schooley, 2004). 15 mg of 1-[3-(dimethylamino)propyl]-3-ethylcarbodiimide methiodide (Sigma Aldrich) was added to 1 ml of 5 mg/ml HRP (Sigma Aldrich) buffered in 0.1 M 2-(N-morpholino)-ethane sulfonic acid (Sigma Aldrich) and 0.1 M Tris at pH 5.0. The solution was incubated for 2 hours at room temperature with shaking. The solution was dialyzed overnight twice at 4°C against 1800 ml of PBS at pH 7.4. The solution was removed from dialysis and treated with 1 mg of 2'-O-monosuccinyladenosine 3':5'-cyclic monophosphate sodium salt (Sigma Aldrich), 3.1 mg of N-hydroxysulfosuccinimide (Molecular Probes) and 14 mg of 1-[3-(dimethylamino)propyl]-3-ethylcarbodiimide methiodide. The solution was stored at 4° C overnight with gentle shaking. The solution was dialyzed overnight twice at 4°C against 1800 ml of PBS at pH 7.4. Conjugate was removed from dialysis and stored in a foil-covered tube at 4°C due to light sensitivity.

2.7.4 UMSL cAMP assay modified from Perkin Elmer DELFIA protocol

A white Greiner fluorescence plate (Greiner, Monroe, NC) was coated with 200

μL of 10 μg/ml goat-raised anti-rabbit IgG (Sigma) overnight at room temperature. The plate was washed 3 times with PBS containing 0.05% Tween 20 and then blocked for 1 hour at room temperature with 300 μL of PBS containing 1% BSA, 5% sucrose and 0.05% NaN_3. The plate was washed as described. Anti-cAMP antibody (Nichols and Morimoto, 1999) (Purdue University) was diluted 4000-fold in 20 mM Tris containing 150 mM NaCl, 0.1% BSA and 0.05% Tween 20 and then 50 μL of the diluted serum was plated into the wells of the plate for 45 minutes at room temperature with gentle shaking. Eu tracer (Perkin Elmer) was diluted 100-fold in sterile water and the cAMP standard (Sigma) was diluted to desired concentrations in 20 mM Tris containing 150 mM NaCl, 0.1% BSA and 0.05% Tween 20. To the wells 100 μL of diluted tracer and 50 μL of diluted cAMP standard was added. The plate was incubated at room temperature for 4 hours with gentle shaking followed by a wash as described. Each well was treated with 200 μL of Enhancement Solution (Perkin Elmer) and incubated at room temperature with gentle shaking for 45 minutes. The time-resolved fluorescence was read with the Perkin Elmer Victor using the Europium Time Resolved Fluorescence protocol. The concentration of cAMP in each sample was calculated from the cAMP standard curve which ranged from 28.125 – 1800 pmol/ml.

2.8 Atomic Force Microscopy (AFM)

At designated times during the peptide aggregation, samples were removed from the aggregation population and diluted to 1 μM in water. A 50 μL portion of the diluted sample was immediately applied to freshly cleaved grade V1 mica discs (Ted Pella Inc.,

Redding, CA). Samples were adsorbed onto the discs for 15 minutes before being washed twice with water and left to air dry. Prepared discs were stored in a container with desiccant until imaging. AFM images were obtained using a Nanoscope III multi-mode atomic force microscope (Digital Instruments, Santa Barbara, CA) in Tapping-Mode™. Height analysis was performed using the Nanoscope III software on height mode images that had been flattened.

2.9 BIBLIOGRAPHY

Auwerx J (1991) The human leukemia cell line, THP-1: a multifacetted model for the study of monocyte-macrophage differentiation. Experientia 47:22-31.

Bae YS, Lee HY, Jo EJ, Kim JI, Kang HK, Ye RD, Kwak JY, Ryu SH (2004) Identification of peptides that antagonize formyl peptide receptor-like 1-mediated signaling. J Immunol 173:607-614.

Conner AC, Simms J, Conner MT, Wootten DL, Wheatley M, Poyner DR (2006) Diverse functional motifs within the three intracellular loops of the CGRP1 receptor. Biochemistry 45:12976-12985.

Crouse NR, Ajit D, Udan ML, Nichols MR (2009) Oligomeric amyloid-beta(1-42) induces THP-1 human monocyte adhesion and maturation. Brain Res 1254:109-119.

Freshney RI (1994) Culture of Animal Cells: A Manual of Basic Technique, 3rd Edition. New York, USA: Wiley-Liss.

Kuhn DM, Balkis M, Chandra J, Mukherjee PK, Ghannoum MA (2003) Uses and limitations of the XTT assay in studies of Candida growth and metabolism. J Clin Microbiol 41:506-508.

Lombardi VC, Schooley DA (2004) A method for selective conjugation of an analyte to enzymes without unwanted enzyme-enzyme cross-linking. Anal Biochem 331:40-45.

Nichols MR, Morimoto BH (1999) Tyrosine kinase-independent inhibition of cyclic-AMP phosphodiesterase by genistein and tyrphostin 51. Arch Biochem Biophys 366:224-230.

Papadopoulos NG, Dedoussis GV, Spanakos G, Gritzapis AD, Baxevanis CN, Papamichail M (1994) An improved fluorescence assay for the determination of lymphocyte-mediated cytotoxicity using flow cytometry. J Immunol Methods 177:101-111.

Roehm NW, Rodgers GH, Hatfield SM, Glasebrook AL (1991) An improved colorimet-

ric assay for cell proliferation and viability utilizing the tetrazolium salt XTT. J Immunol Methods 142:257-265.

Scudiero DA, Shoemaker RH, Paull KD, Monks A, Tierney S, Nofziger TH, Currens MJ, Seniff D, Boyd MR (1988) Evaluation of a soluble tetrazolium/formazan assay for cell growth and drug sensitivity in culture using human and other tumor cell lines. Cancer Res 48:4827-4833.

Seo GS, Lee SH, Choi SC, Choi EY, Oh HM, Choi EJ, Park DS, Kim SW, Kim TH, Nah YH, Kim S, Kim SH, You SH, Jun CD (2006) Iron chelator induces THP-1 cell differentiation potentially by modulating intracellular glutathione levels. Free Radic Biol Med 40:1502-1512.

Stine WB, Jr., Dahlgren KN, Krafft GA, LaDu MJ (2003) In vitro characterization of conditions for amyloid-beta peptide oligomerization and fibrillogenesis. J Biol Chem 278:11612-11622.

Tsuchiya S, Yamabe M, Yamaguchi Y, Kobayashi Y, Konno T, Tada K (1980) Establishment and characterization of a human acute monocytic leukemia cell line (THP-1). Int J Cancer 26:171-176.

Tsuchiya S, Kobayashi Y, Goto Y, Okumura H, Nakae S, Konno T, Tada K (1982) Induction of maturation in cultured human monocytic leukemia cells by a phorbol diester. Cancer Res 42:1530-1536.

Udan ML, Ajit D, Crouse NR, Nichols MR (2007) Toll-like receptors 2 and 4 mediate Abeta(1-42) activation of the innate immune response in a human monocytic cell line. J Neurochem.

Wogulis M, Wright S, Cunningham D, Chilcote T, Powell K, Rydel RE (2005) Nucleation-dependent polymerization is an essential component of amyloid-mediated neuronal cell death. J Neurosci 25:1071-1080.

Wood SJ, Maleeff B, Hart T, Wetzel R (1996) Physical, morphological and functional differences between ph 5.8 and 7.4 aggregates of the Alzheimer's amyloid peptide Abeta. J Mol Biol 256:870-877.

Zagorski MG, Yang J, Shao H, Ma K, Zeng H, Hong A (1999) Methodological and chemical factors affecting amyloid beta peptide amyloidogenicity. Methods Enzymol 309:189-204.

3 STUDY OF MONOCYTE MATURATION

3.1 Introduction

AD is characterized by severe neuronal degeneration that is manifested through a loss of memory in sufferers. The process has been linked to two types of brain lesions, NFTs and Aβ plaques. Although NFTs have been shown to play an important role in the overall AD pathology, Aβ is likely more heavily involved in the degeneration process.

Aβ plaques in AD brains have been found surrounded by activated microglial cells (McGeer et al., 1987; Heneka and O'Banion, 2007). Activation of the microglia likely represent an immune response mounted by the CNS as microglia serve as the macrophages of the brain (Davoust et al., 2008). Their primary responsibilities in the immune pathway are to phagocytose invading pathogens (Bauer et al., 1994) and to recruit further assistance through the production of proinflammatory cytokines (Banati et al., 1993).

It is known that a population of microglia reside in the brain and help maintain homeostatic activity in the absence of a threat to the CNS. However, recent *in vitro* (Fiala et al., 1998) and *in vivo* (Eglitis and Mezey, 1997; Asheuer et al., 2004; Simard and Rivest, 2004; Simard et al., 2006) studies have suggested the possibility that bone marrow derived monocytic cells can be recruited from outside of the CNS, cross the

BBB and eventually differentiate into non-resident microglial cells to aid in the defense against CNS insult. There is still considerable debate among the immunological community as to the significance of these studies (Carson et al., 2007).

Although the discussion is ongoing, Aβ has been implicated in recruiting cells of monocytic lineage to sites of the peptide accumulation (Wegiel et al., 2004; Simard et al., 2006; El Khoury et al., 2007). It has been shown to play roles in various steps of the overall recruitment process such as monocyte migration (Giri et al., 2000; Le et al., 2001), adhesion (Yan et al., 1996) and the differentiation of monocytes into macrophages (Fiala et al., 1998).

Aβ is known to cause a wide array of cellular responses that are each dependent upon the aggregation state of the peptide to induce activity. Studies of the Aβ aggregation pathway have indicated many distinct species that exist between monomer and fibril structures (Harper et al., 1997; Walsh et al., 1997; Harper et al., 1999; Walsh et al., 1999; Stine et al., 2003). Aβ plaques found *in vivo* have also been shown to exhibit some polymorphism with respect to the aggregation intermediates present (Selkoe, 2004b, 2004a). Analysis of these Aβ species reveal that they each have unique properties with respect to toxicity and other biological activities (Pike et al., 1991; Lorenzo and Yankner, 1994; Dahlgren et al., 2002; Walsh et al., 2002; Deshpande et al., 2006).

The relationship between Aβ aggregation state and its role in monocyte recruitment is unclear. Here we present evidence that Aβ can induce adherence in monocytic cells through the FPRL1 receptor. Although we have previously shown that Aβ can induce adherence in these cells very rapidly (Udan et al., 2007), in this study we provide evidence that a rapidly formed oligomeric Aβ species is responsible for this activity.

3.2 Results

3.2.1 Development of Maturation Model System

In an effort to develop a better understanding of the monocyte recruitment and differentiation process we chose to model the process using cultured THP-1 monocytes, human leukocytes derived from a leukemia patient. The cells express monocyte markers and are typically non-adherent and possess a round morphology (Tsuchiya et al., 1980). These cells are well studied and have previously been used to model the differentiation process (Auwerx, 1991) in addition to modeling the role of macrophages in various inflammatory diseases (Sakamoto et al., 2001; Kramer and Wray, 2002; Ueki et al., 2002; Hjort et al., 2003). There are several known markers of differentiation including phagocytosis (Schwende et al., 1996), upregulation of various receptors (Chomarat et al., 2000; Dzionek et al., 2000; Hayden et al., 2002; Chomarat et al., 2003), arrest of proliferation (Schwende et al., 1996) and the change from a non-adherent to an adherent phenotype (Ding et al., 2007). The easiest measure for the transformation of monocytes is the induction of adherence in the cells, so it is the primary method we used to monitor the differentiation of the cells.

To properly study the effect that Aβ treatments would have on the monocytes, we needed a control compound to use for comparison. Many studies have been performed involving THP-1 differentiation, which utilized a wide variety of differentiating compounds, so we chose to test many of them.

LPS is a component of the outer membrane of Gram-negative bacteria that is known to activate the innate immune response through its interaction with CD14 and toll-like receptor 4 (TLR4) (Boehme and Compton, 2004). It has also been shown to induce adherence in THP-1 cells (Hmama et al., 1999). We treated the THP-1 cells with 0.01, 0.1 or 10 ng/mL LPS for 6 hours, a time that we have previously shown induces pro-inflammatory cytokines through the innate immune system (Udan et al., 2007). In these experiments, we were able to elicit $4.58 \pm 2.03\%$, $16.80 \pm 5.24\%$ and $5.41 \pm 0.93\%$ from the three respective treatment concentrations (Fig. 3.1A). This result was not strong enough to allow LPS to serve as a control for further studies.

We next tested $1\alpha,25$-dihydroxycholecalciferol (Vitamin D3) as a potential control differentiating agent. Vitamin D3 has been published to induce adherence in peripheral blood monocytes (PBMC) (Remer et al., 2006) and lead to the arrest of proliferation as well as an upregulation of phagocytosis in THP-1 monocytes (Schwende et al., 1996). In our studies, we treated the THP-1 cells with 0.1 μg/ml Vitamin D3, 0.02% ethanol, or water for 6 hours and then analyzed the adherence as described in the methods. Our data showed 6.28 ± 1.14 %, $9.84 \pm 4.34\%$ and $7.95 \pm 2.03\%$ adherence for Vitamin D3 and the ethanol and water controls, respectively (Fig. 3.1B). Because we saw no significant adherence following Vitamin D3 treatment, we were unable to use it as a control.

We next tested Pam_3CSK_4 for its ability to induce adherence in the THP-1 monocytes. Pam_3CSK_4 is a synthetic triacylated lipopeptide that is known to activate the innate immune response through TLR2 (Udan et al., 2007) and lead to activation of the NF-κB pathway (Akira et al., 2001). We tested the ability of Pam_3CSK_4 to induce adherence at concentrations ranging from $0 - 100$ ng/ml. None of the concentrations tested
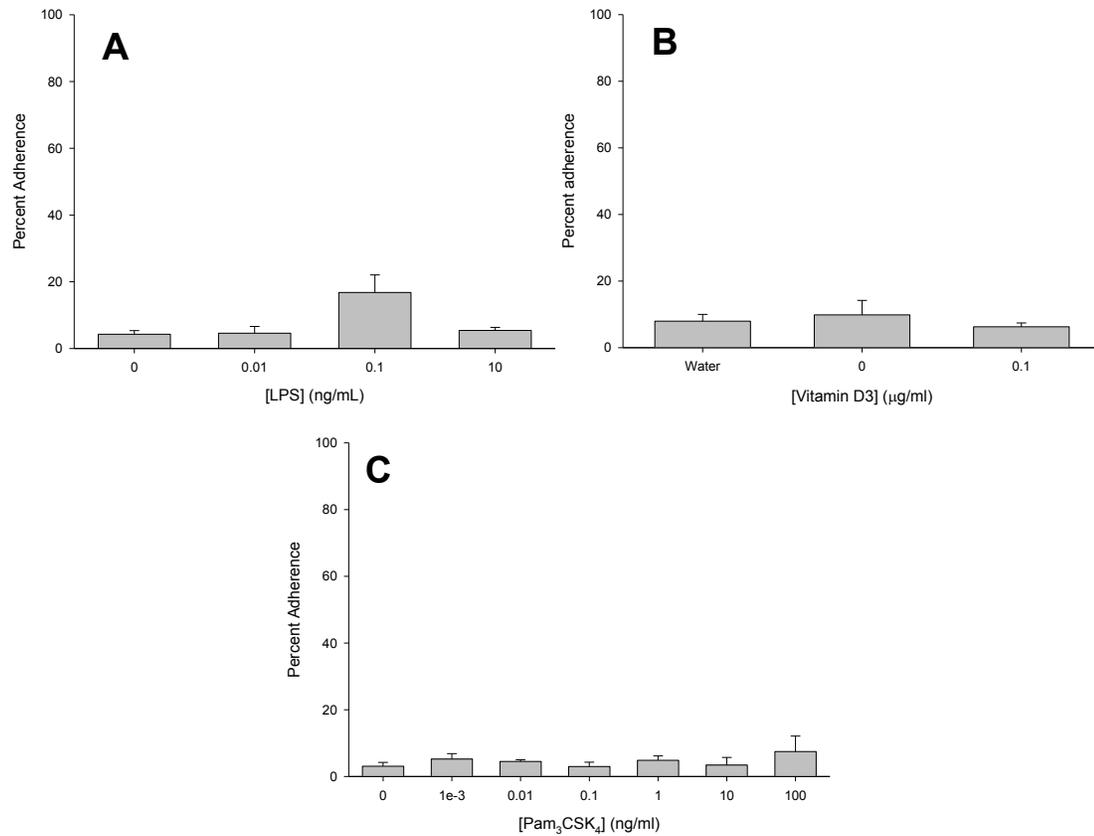
Fig. 3.1 LPS, Vitamin D3 and Pam$_3$CSK$_4$ induce no significant adherence in monocytes
THP-1 monocytes were incubated at 37°C for 6 hours with the concentrations of effectors indicated. Following the incubation time, percent adherence was determined as described in the Methods. A) LPS induced adherence where water served as the 0 ng/mL control in the experiments. Error bars are standard error for n= 7 (0 ng/mL), 2 (0.01 ng/mL), 2 (0.1 ng/mL) and 5 (10 ng/mL). B) Vitamin D3 induced adherence where 0.02% ethanol was the 0 μg/ml control and a matching water control was also performed. Error bars are standard error for n= 3 (water, ethanol) and 4 (0.1 μg/ml Vitamin D3) C) Pam$_3$CSK$_4$ induced adherence where water was the 0 ng/ml control. Error bars are standard error for n= 2 (0.001, 0.01, 0.1, 10 and 100 ng/ml Pam$_3$CSK$_4$) and 6 (0 and 1 Pam$_3$CSK$_4$).

were able to cause the THP-1 cells to adhere to the plate (Fig. 3.1C), therefore Pam_3CSK_4 was discarded as a positive control.

Our final potential control agent was PMA, which has been shown to differentiate THP-1 cells into macrophages (Tsuchiya et al., 1982; Schwende et al., 1996). It has recently been shown that using a treatment concentration of 5-10 ng/ml PMA is effective at inducing differentiation without the aberrant upregulation of genes (Park et al., 2007), therefore we chose the final treatment concentration of 10 ng/ml PMA for our experiments. In our control experiments, PMA was able to induce 55.97 ± 3.85, 87.80 ± 2.96 and $86.09 \pm 3.26\%$ adherence following 6, 24 and 48 hour incubations, respectively (Fig. 3.2). The early induction of adherence by the PMA allows it to serve as a control even at short incubation times.

With our positive control in place, we were ready to test the Aβ for its ability to affect the maturation process of the THP-1 cells. We had previously shown that a 6 hour incubation with Aβ(1-42) led to the activation of the innate immune response in THP-1 cells(Udan et al., 2007), so we chose a 6 hour incubation time for our adherence studies as well. When Aβ(1-42) was freshly reconstituted in water, it induced $41.85 \pm 4.14\%$ adherence, which was nearly identical to the $43.11 \pm 3.65\%$ induced by the PMA treated cells. Both values showed statistical significance when compared to water controls (Fig. 3.3).

3.2.2 Determination of the Active Aβ Aggregate Species

Because of the large degree of polymorphism seen in the neuritic plaques of AD
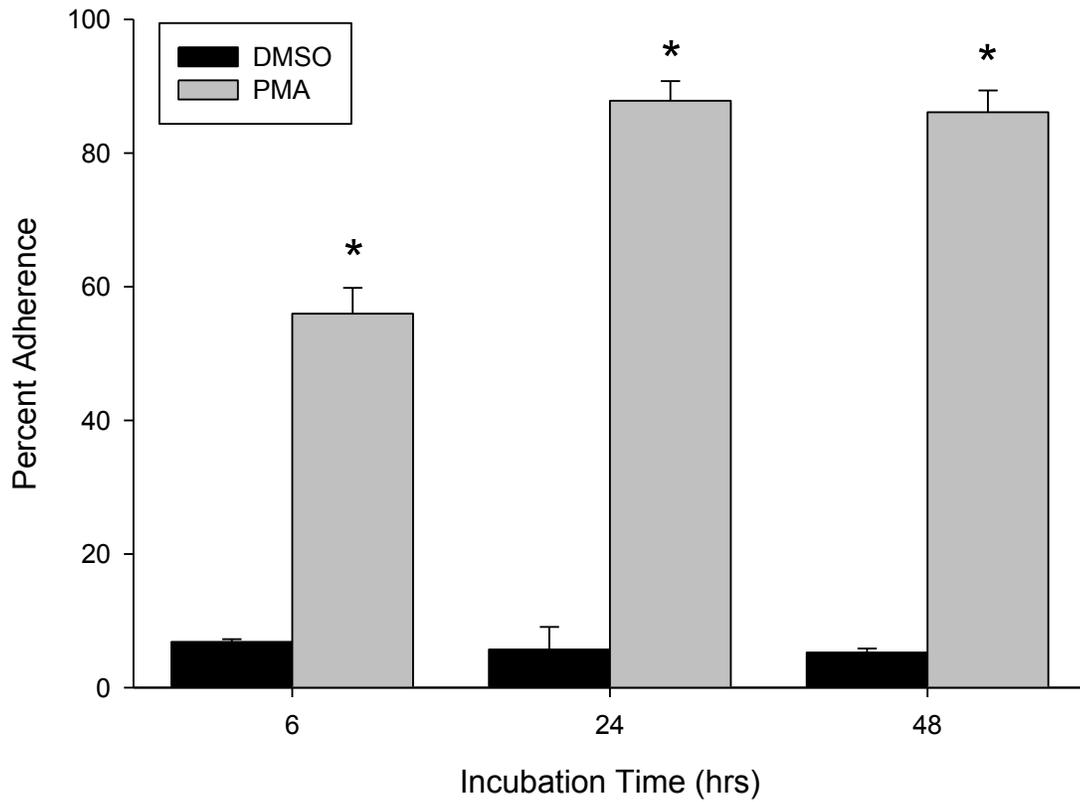
Fig. 3.2 PMA potently induces adherence following short and long incubation times
THP-1 cells were prepared in assay medium and plated into a 48-well plate. The cells were treated with either 0.005% DMSO (black bars) or 10 ng/ml PMA (grey bars) and incubated at 37°C for either 6, 24 or 48 hours. Following the incubation, the percent of cells adhering to the well was determined as described in the methods. Statistical significance of <0.0005 is denoted by * and determined for n= 3 (DMSO) or 4 (PMA).
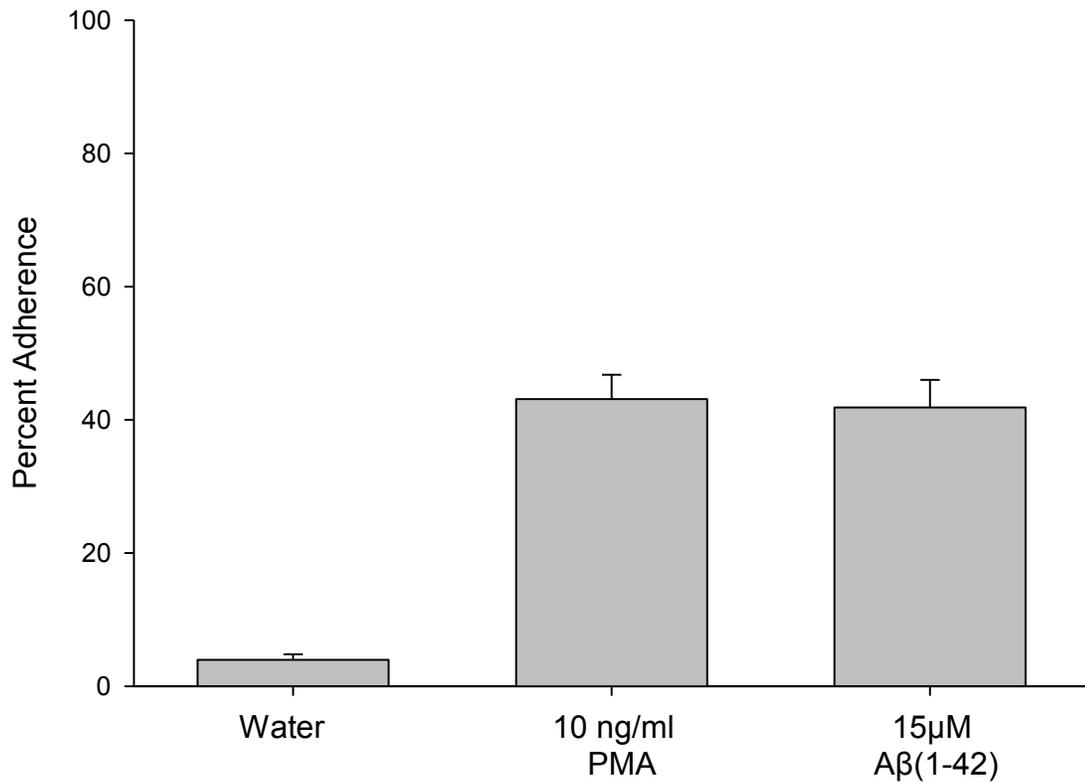
Fig. 3.3 Effect of Aβ(1-42) and PMA on THP-1 monocyte adherence.
THP-1 monocytes were treated with 10 ng/ml PMA or 15 μM Aβ(1-42) from a freshly reconstituted 100 μM water solution and incubated for 6 hours at 37°C. Percent adherence was determined by direct cell counting as described in the methods. Standard error bars were calculated from n=17 trials for PMA and n=22 trials for Aβ(1-42). Water (n=15) controls induced 5 ± 1% adherence.

brains (Selkoe, 2004a), we were interested in determining which Aβ species was responsible for inducing the adherence in the monocytes. To this end, we reconstituted Aβ(1-42) in water and either treated the cells immediately or allowed the Aβ to aggregate at 4°C before the cell treatment. We then determined the amount of adherence induced at the various stages of aggregation. Our data indicates that Aβ(1-42) is most potent at inducing adherence when it is freshly reconstituted, but as it is allowed to aggregate, the effect eventually disappears (Fig. 3.4A). AFM images taken at correlating times of Aβ(1-42) aggregation show that at 0 and 48 hours of aggregation (Fig. 3.4B and Fig. 3.4C, respectively), the predominant species are small, globular structures. By 96 hours of aggregation, Aβ(1-42) has lost nearly all ability to induce adherence, and the AFM shows the presence of long fibrilar structures (Fig. 3.4D). Because our data suggested that fibril formation was inversely correlated with Aβ(1-42) activity, we used freshly reconstituted Aβ for the remainder of our experiments unless otherwise indicated.

In order to confirm that treatment of the cells with Aβ did not induce toxicity, we applied the XTT cell viability assay. Following incubation of the cells with Aβ, the cells were treated with the XTT/PMS solution as described in the Methods. The samples were incubated for 3 hours and the amount of XTT reduced was measured by absorbance (Fig. 3.5). Although the freshly reconstituted Aβ induced the highest amount of adherence, it was not the most toxic species. The 48 and 96 hour aggregated Aβ were the most toxic species with only about 60% cell viability. Samples treated with later Aβ aggregation species showed no toxicity.

In an effort to ensure that we were using the best concentration of Aβ to achieve our results, we tested the effect of Aβ(1-42) treatment concentration on its ability to in-
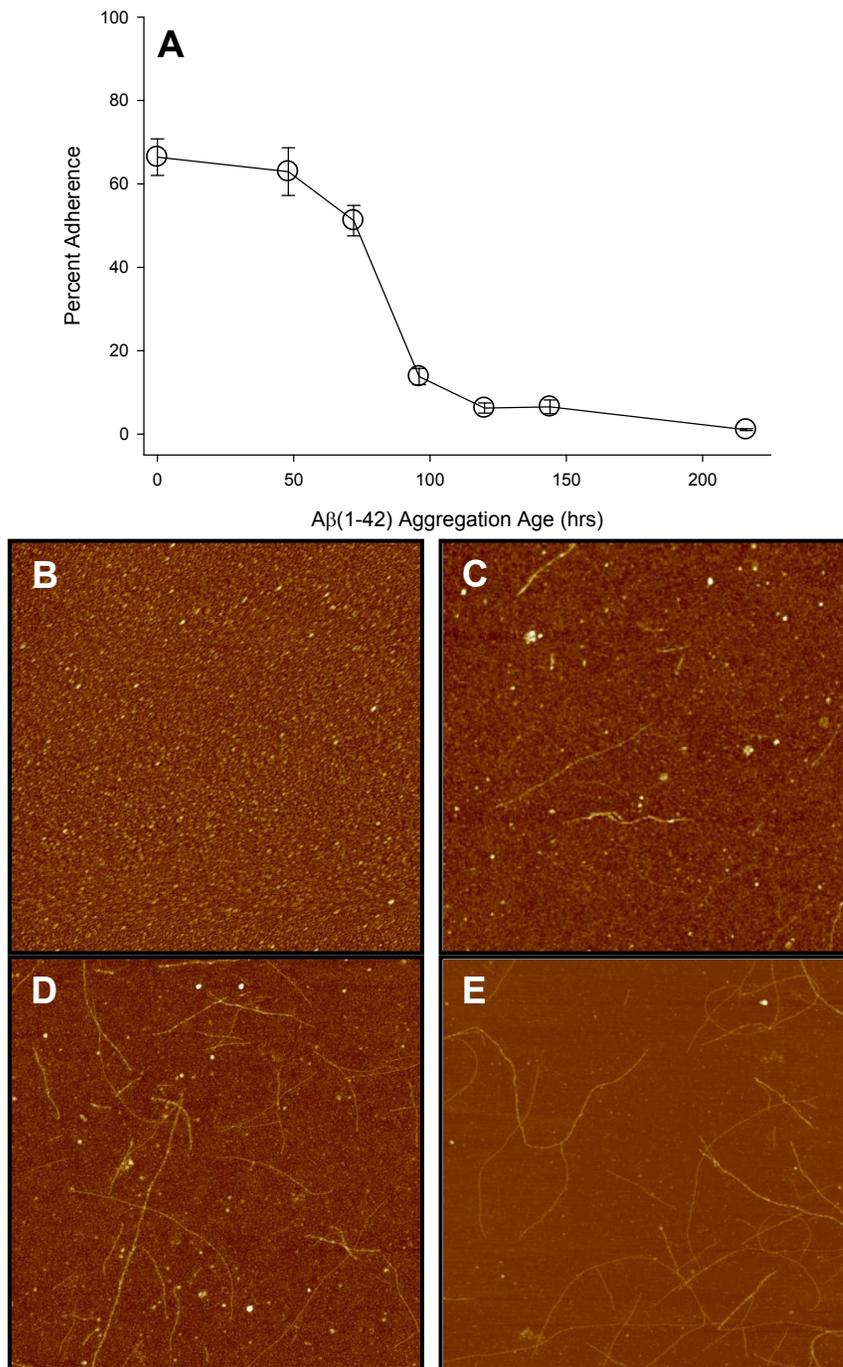
Fig. 3.4 Early Aβ(1-42) aggregates induce monocyte adherence.
Aβ(1-42) was reconstituted in sterile water to 100 μM and incubated at 4°C. A) At the given times, cells were treated with 15 μM Aβ for 6 hours and adherence was measured by direct counting as described in the Methods. Error bars represent standard error for n trials of 19 (0 h), 17 (48 h), 4 (72 h), 5 (96 h), 7 (120 h), 3 (144 h), and 7 (216 h). B-E) Representative AFM images of Aβ(1-42) aggregation at 4°C taken at 0, 48, 96 and 216 hours, respectively. Images are 5 μm x 5 μm and taken as described in Methods. Images are courtesy of Deepa Ajit.
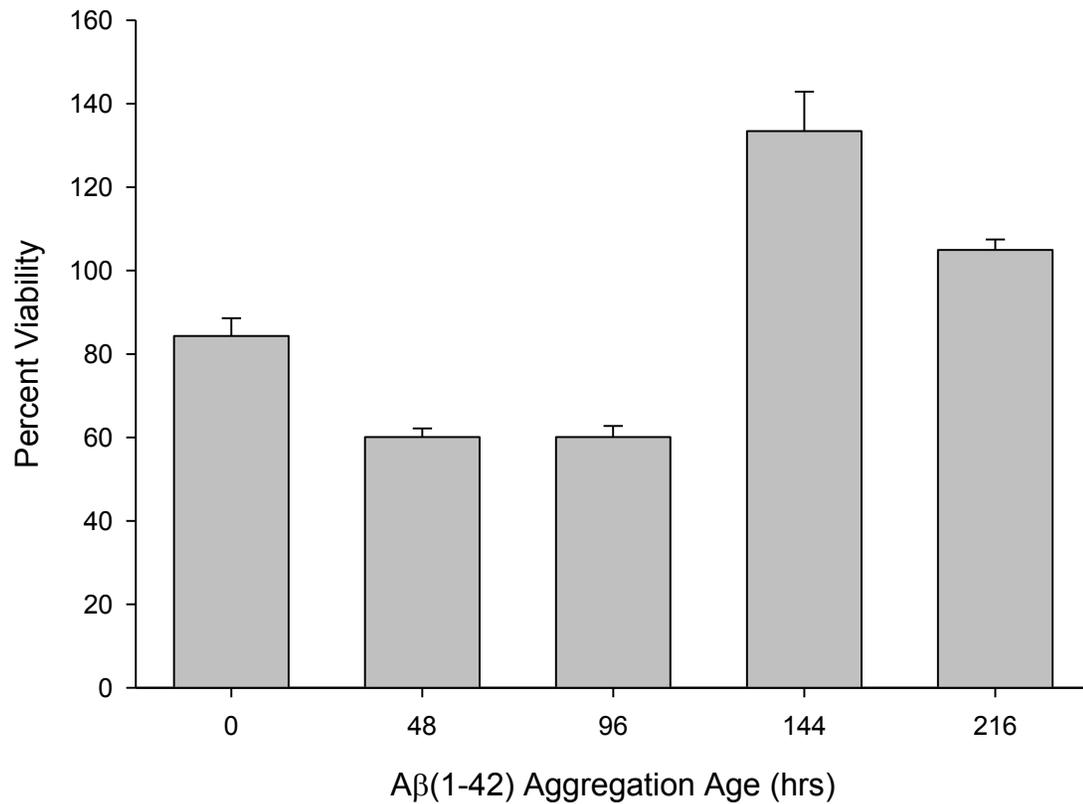
Fig. 3.5 Effect of Aβ(1-42) aggregation state on induced toxicity in THP-1 monocytes
Aβ(1-42) was reconstituted in sterile water to 100 μM and incubated at 4°C. At the given times, cells were treated with 15 μM Aβ for 6 hours and toxicity was measured by XTT of solution cells as described in the Methods. The data was corrected to percent of control survival. Error bars represent standard error for 3 trials.

duce adherence in the THP-1 monocytes. We treated the cells with 0, 5, 10 and 15 μM Aβ(1-42) that was freshly reconstituted in water (Fig. 3.6). Our data shows that 15 μM Aβ(1-42) induces the most adherence of the concentrations tested, validating it as our standard treatment concentration. We did not test higher concentrations of Aβ because the large volumes of water required could cause the cells to become distressed and mask the true effect of the treatment.

Once we confirmed our treatment concentration, we wanted to further understand which Aβ aggregation species was responsible for the activity. Because we saw the greatest amount of adherence at early time points, we hypothesized that monomeric Aβ may be the potent species. Since Aβ(1-40) is known to remain monomer for longer than Aβ(1-42) (Walsh et al., 1997), we treated the cells with Aβ(1-40) that had been aggregated at 4°C and then analyzed the adherence. We saw no significant adherence from the Aβ(1-40) treated cells throughout the time course of treatment (Fig. 3.7A), which suggested that monomer was not the active species, but led us to the idea that perhaps an early formed oligomeric species was active.

We again tested this theory with the Aβ(1-40) which we allowed to aggregate at 25° or 37°C to help speed the aggregation process. The experiment again showed no significant adherence. The Aβ(1-42) controls in the two experiments confirm the cells are responsive to stimuli (Fig. 3.7A). Because of these results, we formed two potential theories. First, monomer could still be the active species, but the recognition and activity could be dependent on the two terminal amino acids present in Aβ(1-42) but missing in Aβ(1-40). The other possibility was that because Aβ(1-40) aggregates through a different pathway than Aβ(1-42) (Bitan et al., 2003), the Aβ(1-40) may not form the active
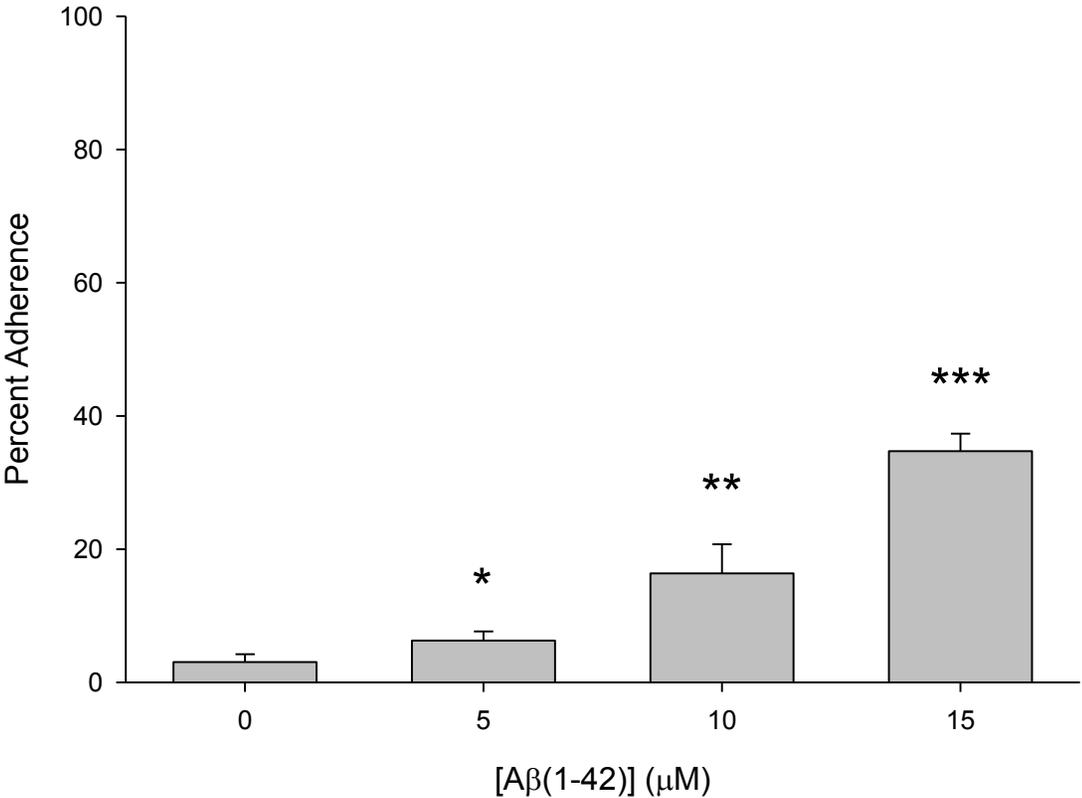
Fig. 3.6 Effect of final Aβ(1-42) treatment concentration on monocyte adherence
Freshly reconstituted 100 μM Aβ(1-42) in water was added to THP-1 monocytes in different volumes to produce different final Aβ concentrations. All treatments maintained the same cell count and volume of sterile water from well to well. The treated cells were incubated at 37°C for 6 hours and the percent of cells adhering was determined by direct counting. Statistical differences from the water control (0 μM Aβ) are as follows: * $p<0.05$, ** $p<0.01$, ***$p<0.005$.
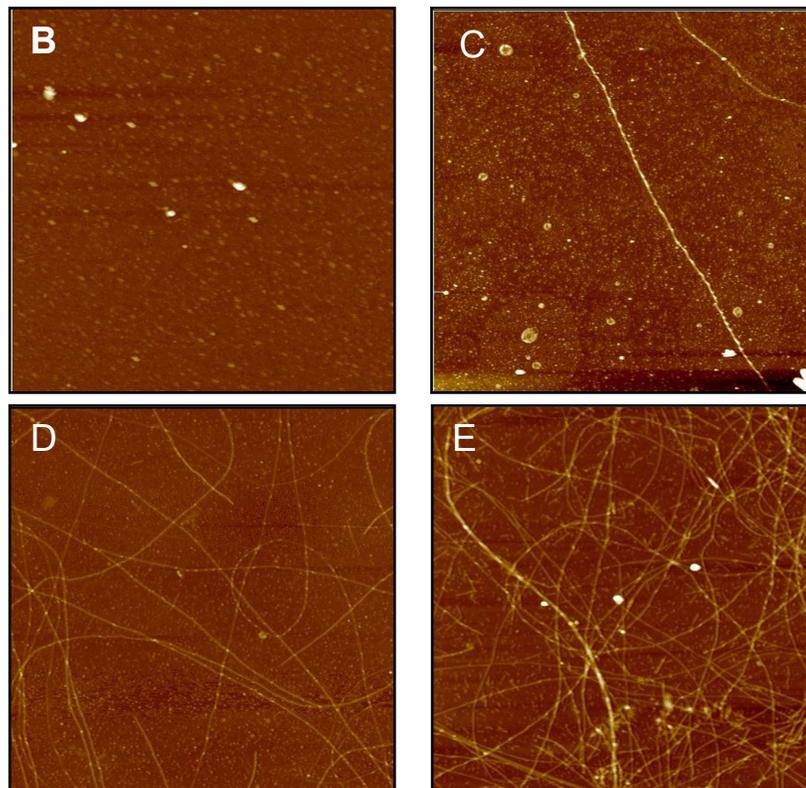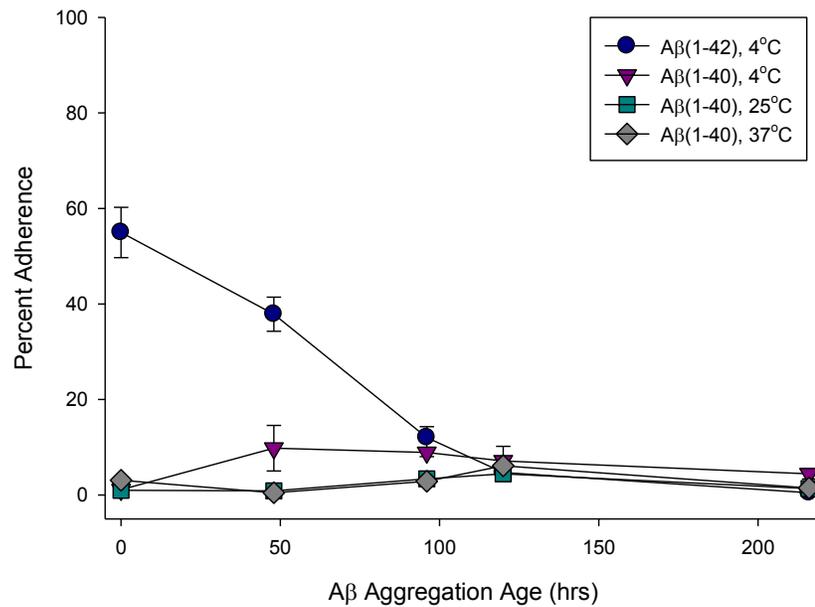
Fig. 3.7 Aβ(1-40) aggregated at different temperatures does not induce THP-1 adherence
Aβ(1-40) was reconstituted in sterile water to 100 μM and incubated at 4, 25 or 37°C. A) At the given times, cells were treated with 15 μM Aβ(1-40) or Aβ(1-42) for 6 hours and adherence was measured by direct counting as described in the Methods. Error bars represent standard error for n trials of 3. B) Representative AFM image of Aβ(1-40) aggregation taken at 0 hours. C-E) Representative AFM images of Ab(1-40) aggregation taken at 96 hours and 4, 25 or 37°C, respectively. Images are 5 μm x 5 μm. Images are courtesy of Deepa Ajit.

aggregate species.

In an effort to answer these two possibilities, we obtained Aβ(1-42) L34P, which has been shown to have restricted aggregation and instable fibrils (Williams et al., 2004). Because the mutant peptide will aggregate slowly, it provides a sample which should maintain a monomeric morphology while providing the two terminal amino acids lacking in Aβ(1-40). Treatment of the cells with Aβ(1-42) L34P aggregated at 4°C produced no significant adherence (Fig. 3.8A). Aggregating the peptide at 25°C or 37°C also produced no adherence (data not shown). AFM images confirm that the Aβ(1-40) and Aβ(1-42) L34P peptides do not aggregate to form significant fibrils even after 168 hours of aggregation at 4°C (Fig. 3.8C). Taken together, this data suggests that an early formed aggregate species that is unable to form in restricted aggregation Aβ peptides is responsible for inducing adherence in the THP-1 monocytes.

In order to confirm our hypothesis that an early formed, non-monomeric Aβ(1-42) oligomeric species was responsible for inducing adherence in the THP-1 monocytes, we chose to manipulate the aggregation conditions. It is known that Aβ aggregates in a nucleation-dependent manner during which a lag phase precedes the elongation stage (Jarrett and Lansbury, 1993). Increasing the concentration of Aβ can decrease this lag phase and lead to more rapid aggregation. We prepared two Aβ(1-42) aggregation solutions, one at 50 μM and the other at 100 μM with the belief that a lower aggregation concentration would lead to a higher monomer:oligomer ratio than in the higher concentration due to its slower aggregation process. We then proceeded to treat the THP-1 cells with different volumes of the peptides to produce a final treatment concentration of 15 μM. If the monomer is the active Aβ species, we expected to see similar amounts of ad-
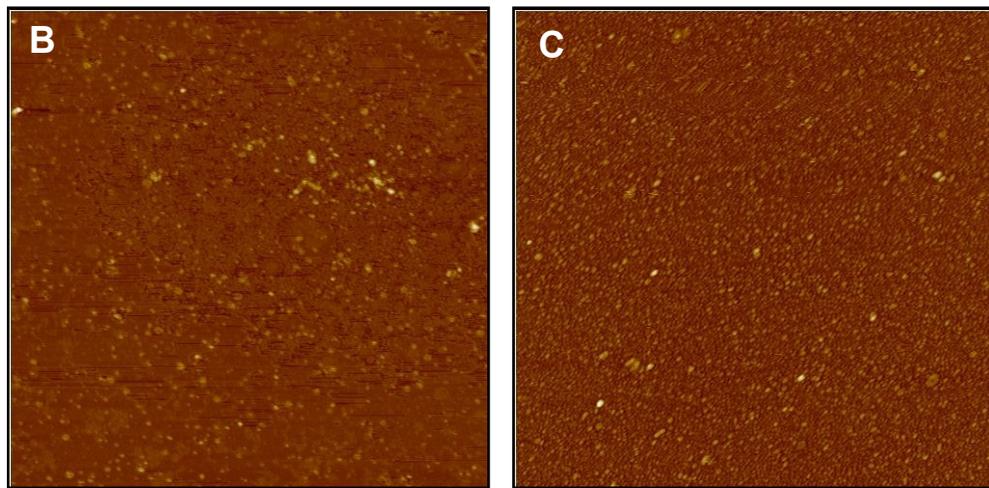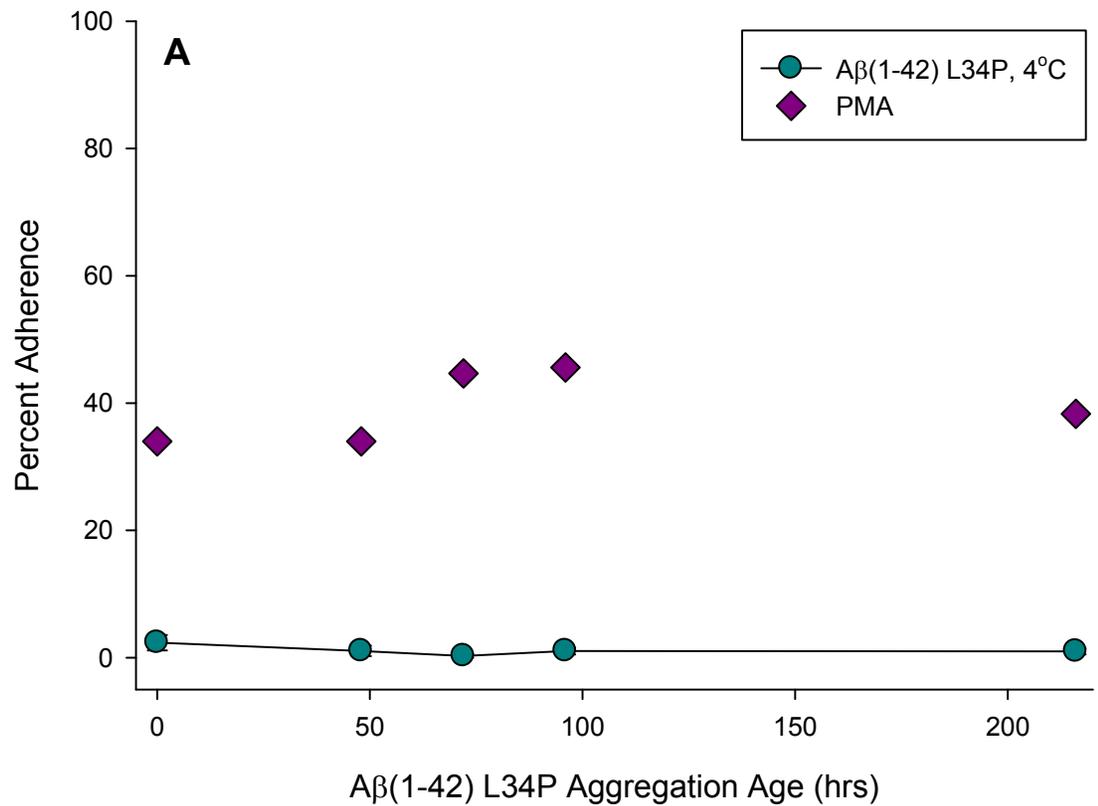
Fig. 3.8 Aβ(1-42) L34P does not induce THP-1 monocyte adherence
Aβ(1-42) L34P was reconstituted in sterile water to 100 μM and incubated at 4°C. A) At the given times, cells were treated with 15 μM Aβ L34P or 10 ng/ml PMA for 6 hours and adherence was measured by direct counting as described in the Methods. Error bars represent standard error for n trials of 5 for Aβ(1-42) L34P and 1 for PMA. B,C) Representative AFM images of Aβ(1-42) L34P aggregation at 4°C taken at 0 and 168 hours, respectively. Images are 5 μm x 5 μm and taken as described in Methods. Images are courtesy of Deepa Ajit.

herence induced following treatment of the cells with freshly reconstituted Aβ(1-42), despite the varying aggregation concentrations.

We treated the THP-1 cells with 15 μM of either 50 or 100 μM Aβ(1-42) at 0, 24 or 48 hours of Aβ aggregation. Freshly reconstituted 100 μM Aβ(1-42) induced 58.24 ± 3.63% adherence while the 50 μM Aβ(1-42) only induced 16.32 ± 4.40%. Both samples showed decreases in the amount of adherence induced as the aggregation increased (Fig. 3.9). Because the monomer:oligomer ratio was higher in the 50 μM Aβ sample yet it induced less adherence, we concluded that monomer is not the Aβ species responsible for inducing adherence in THP-1 monocytes.

Many researchers have published protocols for forming soluble intermediates on the Aβ aggregation pathway, including oligomers (Walsh et al., 1997; Lambert et al., 1998; Kayed et al., 2003; Lesne et al., 2006). In order to strengthen our conclusion that an oligomer is responsible for the transformation of cells, we tested one of these types of oligomers known as Aβ derived diffusible ligands (ADDLs). Part of the preparation protocol for the ADDLs involves a centrifugation step (see Methods), thus we tested the Aβ before and after centrifugation. The samples are termed Total and ADDLs, respectively. The Total sample induced 5.08 ± 1.93% adherence while the ADDLs induced 4.79 ± 2.53% adherence (Fig. 3.10). These results implicate a very specific Aβ(1-42) oligomer, which is not found in the ADDLs preparation, in the transformation of monocytes into adherent cells.

3.2.3 Investigation of Potential Maturation Receptor Pathways
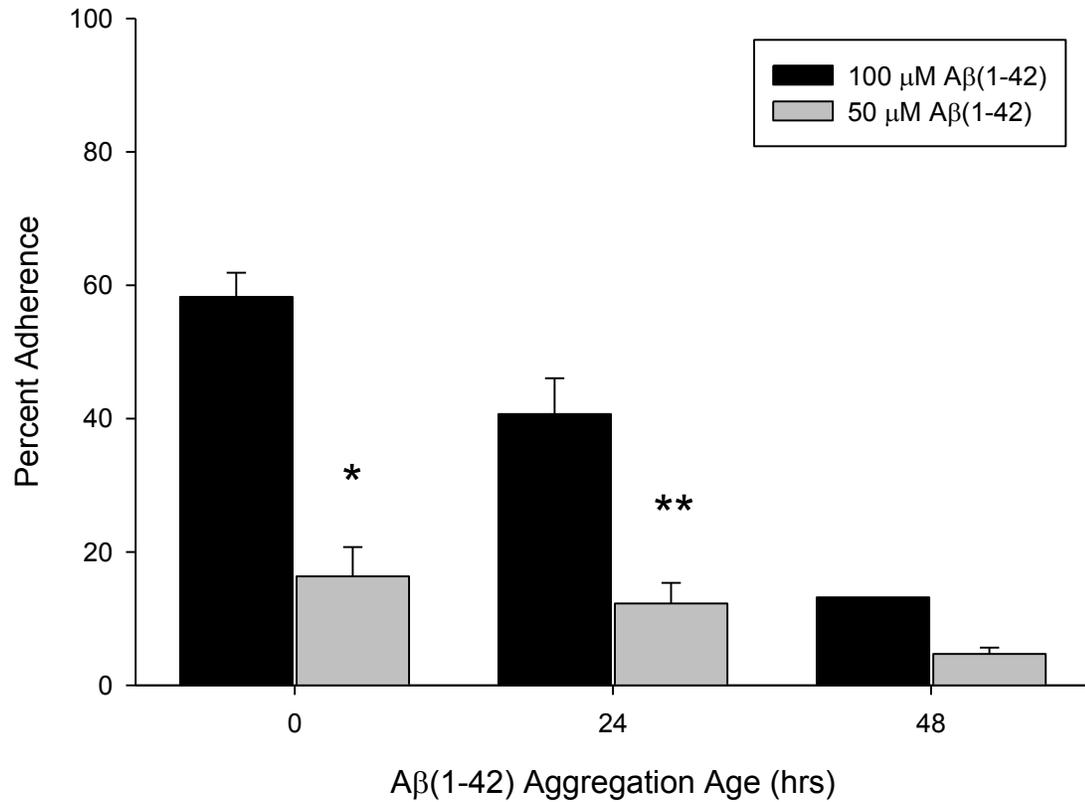
Fig. 3.9 Lowering Aβ aggregation concentration decreases monocyte adherence.
Lyophilized Aβ(1-42) was reconstituted in sterile water to either 100 μM or 50 μM and aggregated at 4°C. At the times indicated, THP-1 cells were treated with 15 μM of either solution for 6 hours at 37°C. The percent adherence was determined as described in the Methods. SE was determined for n trials of 3 (0 hours) and 2 (24 hours and 48 hours, 50 μM). Only 1 trial was done for 100 μM at 48 hours. Water-induced adherence controls (2.8 ± 0.4 %) were subtracted from final percent adherence presented. Differences between 100 μM and 50 μM treatments were significant at 0 (* $p < 0.0005$) and 24 hours (** $p < 0.005$) of aggregation.
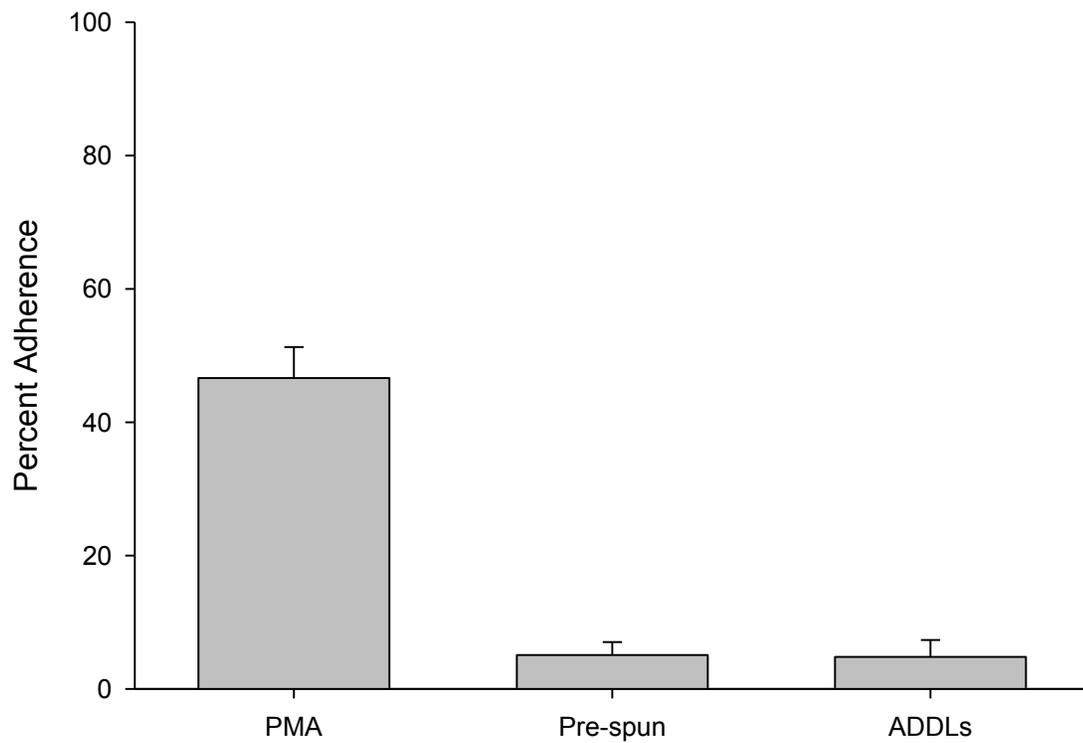
Fig. 3.10 ADDLs do not induce significant adherence in THP-1 monocytes
ADDLs were prepared as described in the Methods. Cells were treated with either the total aggregation mixture prior to centrifugation (Pre-spun) or ADDLs at a final concentration of 15 µM Aβ(1-42). A 10 ng/mL PMA control was also included. Adherence is the average ± SE for n=2 trials for PMA and n=4 trials for Total and ADDLs over two separate experiments.

Once we determined that an oligomeric Aβ(1-42) species was able to potently induce adherence in THP-1 monocytes, we were interested in exploring the receptors involved in this process. Our lab has previously shown that Aβ can use toll-like receptors 2 and -4 to induce a pro-inflammatory response in THP-1 monocytes (Udan et al., 2007). We first chose to investigate the role of these receptors in the Aβ induced adherence process of THP-1 cells.

The THP-1 cells were prepared in assay medium. The control cells were pre-treated for 1 hour with PBS, and the sample cells were pre-treated with anti-TLR2 antibodies, anti-TLR4 antibodies or an IgG isotype control. Following the pre-incubation, freshly reconstituted Aβ(1-42) was added to the cells and they were again incubated for 6 hours. After the incubation, the adherence was analyzed and the TNFα production was measured. Blocking either TLR receptor resulted in no significant change in the adherence induced by Aβ (Fig. 3.11A). However, the analysis of the TNFα production was similar to our previously reported data (Udan et al., 2007) and confirmed the efficacy of the antibody neutralization of TLR2 and TLR4 (Fig. 3.11B).

The next mechanistic pathway we investigated was the NF-κB dependent pathway known to be utilized by PMA. It has been previously shown that PMA induced differentiation in HL-60 peripheral blood leukocytes (Eck et al., 1993) and K562 monocytic/megakaryotic cells (Kang et al., 1996) is NF-κB dependent. We pre-treated the THP-1 cells with either water or 100 μM PDTC for 1 hour at 37°C (Kang et al., 1996) before adding either PMA or Aβ(1-42) for 6 hours. Following the incubation, adherent cells were counted and percent adherence calculated. PMA was only able to induce in
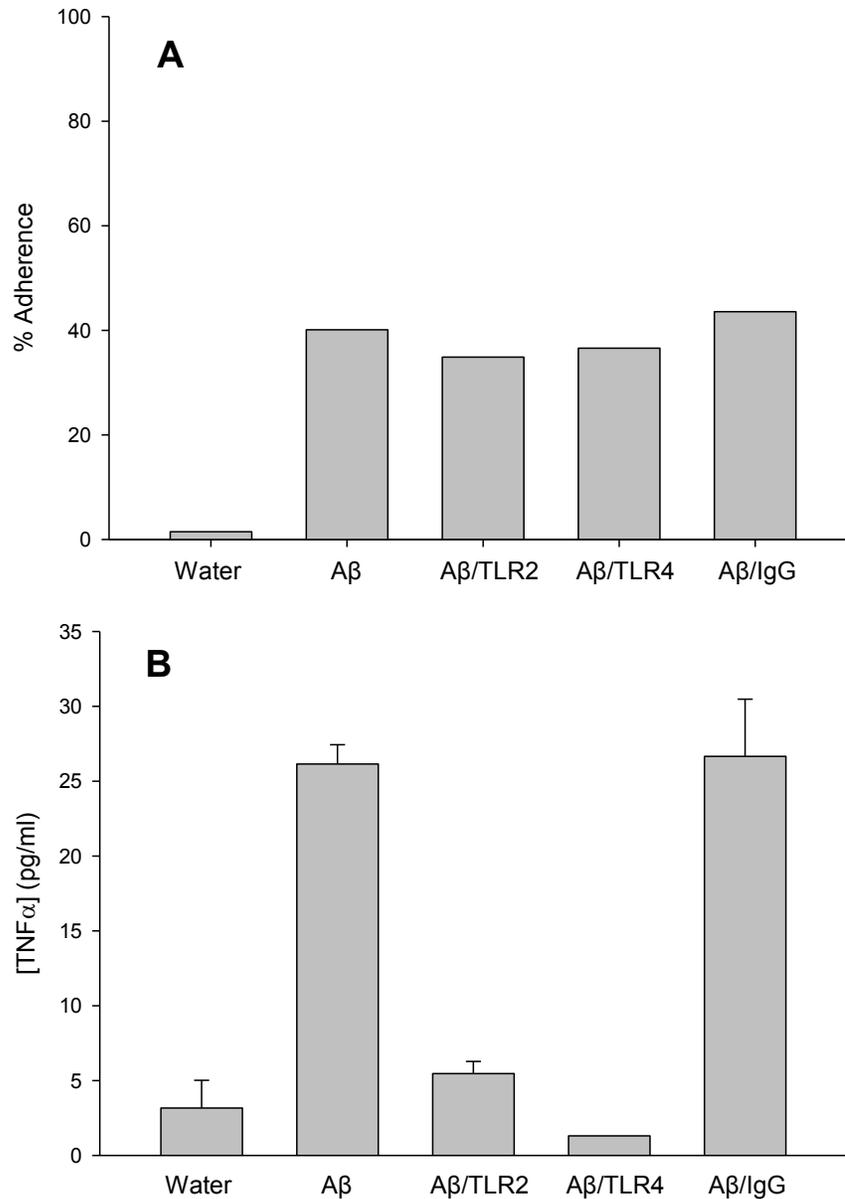
Fig. 3.11 Aβ induced adherence does not require TLR2 or TLR4
THP-1 cells were prepared in assay medium and pre-incubated for 1 hour with anti-TLR2 or anti-TLR4 antibodies, an IgG isotype control or PBS. Following incubation, the cells were incubated with Aβ(1-42) for 6 hours at 37°C. The Aβ induced adherence (A) and TNFα production (B) were determined as described in the Methods. The data is from one experiment. SE values in figure B are from three separate ELISA measurements.

the PDTC pre-treated cells $35.40 \pm 5.00\%$ of the adherence induced in water treated controls, verifying the NF-κB pathway as important in PMA induced adherence. However, when compared to the water treated control, Aβ was able to induce $101.46 \pm 5.74\%$ of the control adherence in the PDTC treated cells (Fig. 3.12). This result clearly shows that Aβ does not utilize the NF-κB dependent mechanism that PMA uses to induce adherence in the cells.

Aβ has previously been shown to utilize the G-protein coupled receptor FPRL1 for chemotaxis, with lower order Aβ aggregates being the most effect species (Le et al., 2001). Because of this, we next analyzed FPRL1 for its role in THP-1 adherence. We pre-treated the cells with either a water control or 30 μM WRW$_4$, a known antagonist to FPRL1 (Bae et al., 2004; Kam et al., 2007), for 15 minutes before treatment with PMA or Aβ(1-42). Following the 6 hour incubation, the adherent cells were counted and the percent adherence was determined. When compared with the water treated control, Aβ was only able to induce $3.30 \pm 1.91\%$ of the control adherence in the cells. The PMA induced adherence was also affected, but not as dramatically as with PDTC pre-treatment. PMA was able to induce $58.29 \pm 8.59\%$ of the control adherence in the WRW$_4$ pre-treated cells (Fig. 3.13). These data indicate that FPRL1 is the receptor that mediates Aβ(1-42) induced THP-1 adherence independent of the NF-κB pathway.

3.2.4 Indirect measurements for determining adherence

In addition to the use of the counting based adherence assay, we developed other methods to analyze the adherence induced in the THP-1 cells. Although these methods
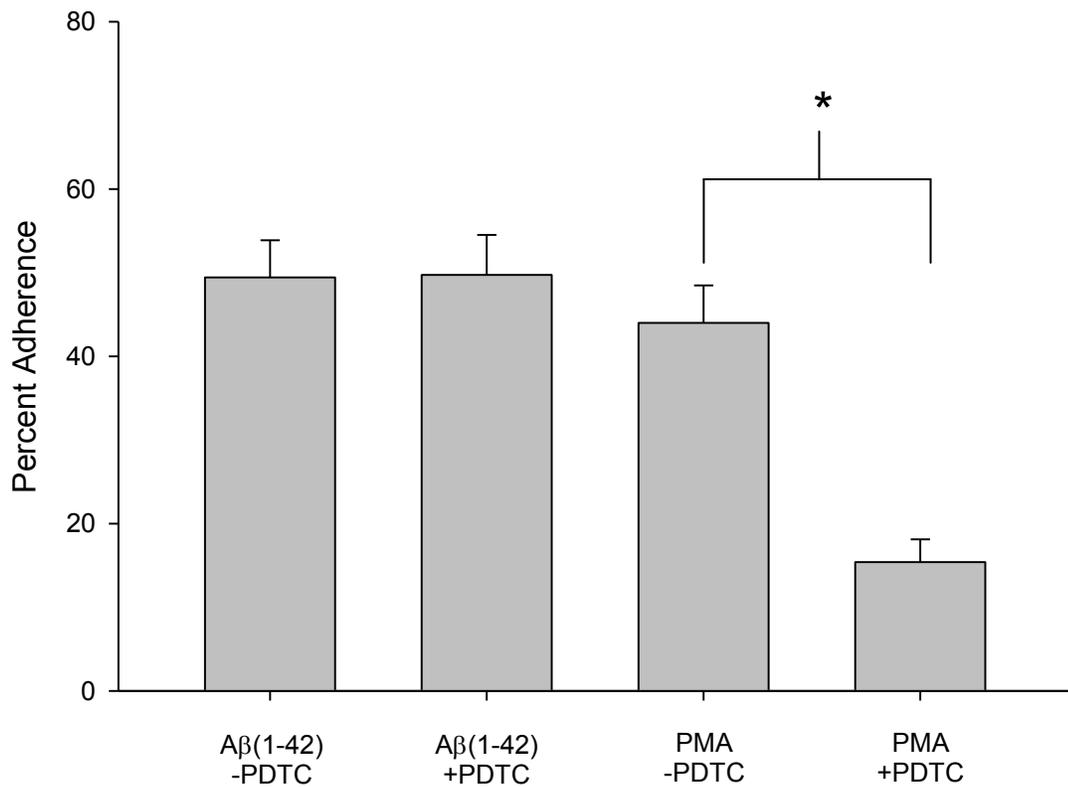
Fig. 3.12 Aβ(1-42) does not induce adherence through an NF-κB dependent pathway
THP-1 monocytes were incubated for 6 hrs with 15 µM Aβ(1-42) or 10 ng/ml PMA following a 1 hour pre-incubation with 100 µM PDTC or water control. Percent adherence was determined by direct counting of adherent cells. Data are the average of 5 and 4 separate experiments for Aβ(1-42) and PMA respectively. * p <0.0005
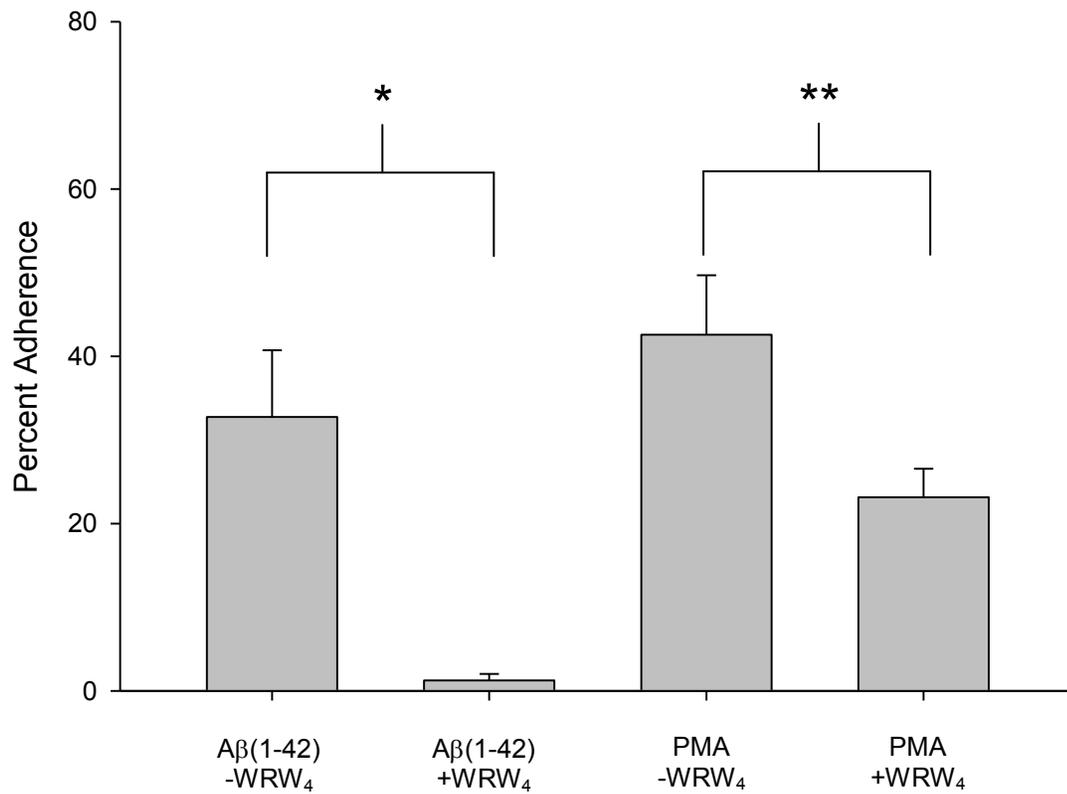
Fig. 3.13 Aβ(1-42) does induce adherence through an FPRL1 dependent pathway
THP-1 monocytes were incubated 6 hours with 15μM Aβ(1-42) or 10 ng/mL PMA following a 15 minute pre-incubation with 0.33 μg/mL WRW4. % Differentiation was determined by direct counting of adherent cells. Data are the average of 6 and 5 separate experiments for Aβ and PMA respectively. * $p < 0.005$, ** $p < 0.025$

are not as quantitative as the direct counting method, they did provide useful trending information. This section will include a brief description of the methods as well as some of the data obtained through their use.

We have previously described the use of the XTT assay for analysis of cellular metabolism and toxicity. We also applied the assay towards determining cellular adherence. To confirm that the XTT assay is capable of distinguishing cell numbers, we plated various concentrations of cells into the wells of a 48-well plate and treated them with 0.33 mg/ml XTT / 8.3 μM PMS. The cells were incubated at 37ºC for four hours. Every hour aliquots of the solution were removed and the absorbance of the reduced XTT was measured (Fig. 3.14A).

The data clearly show that as the cell count is increased, the amount of XTT reduced is increase. All samples show a linear curve as more XTT is reduced over time. When the XTT reduction values at three hours of incubation from figure 3.14A are plotted versus cell count, a linear correlation is formed with an R^2 value of 0.9997 (Fig. 3.14B). Taken together, the data suggest that the XTT assay may be a valuable qualitative tool for determining the number of cells adhering following effector treatment.

We next tested the ability of the XTT assay to measure cell adherence in PMA treated cells. We treated the THP-1 monocytes with varying concentrations of PMA and incubated them for 24 hours at 37ºC. At the end of the incubation the medium containing non-adherent cells was moved to a fresh well. Both the adherent and non-adherent cells were assayed with XTT as described in the methods (Fig. 3.15A). As amount of XTT reduced by the cells in the medium decreased, the amount reduced by the cells in the well increased. Together the data suggests that the cells at higher concentrations of

A

B

$$y = 8.317 \times 10^{-07}x + 0.0742$$
$$R^2 = 0.9997$$
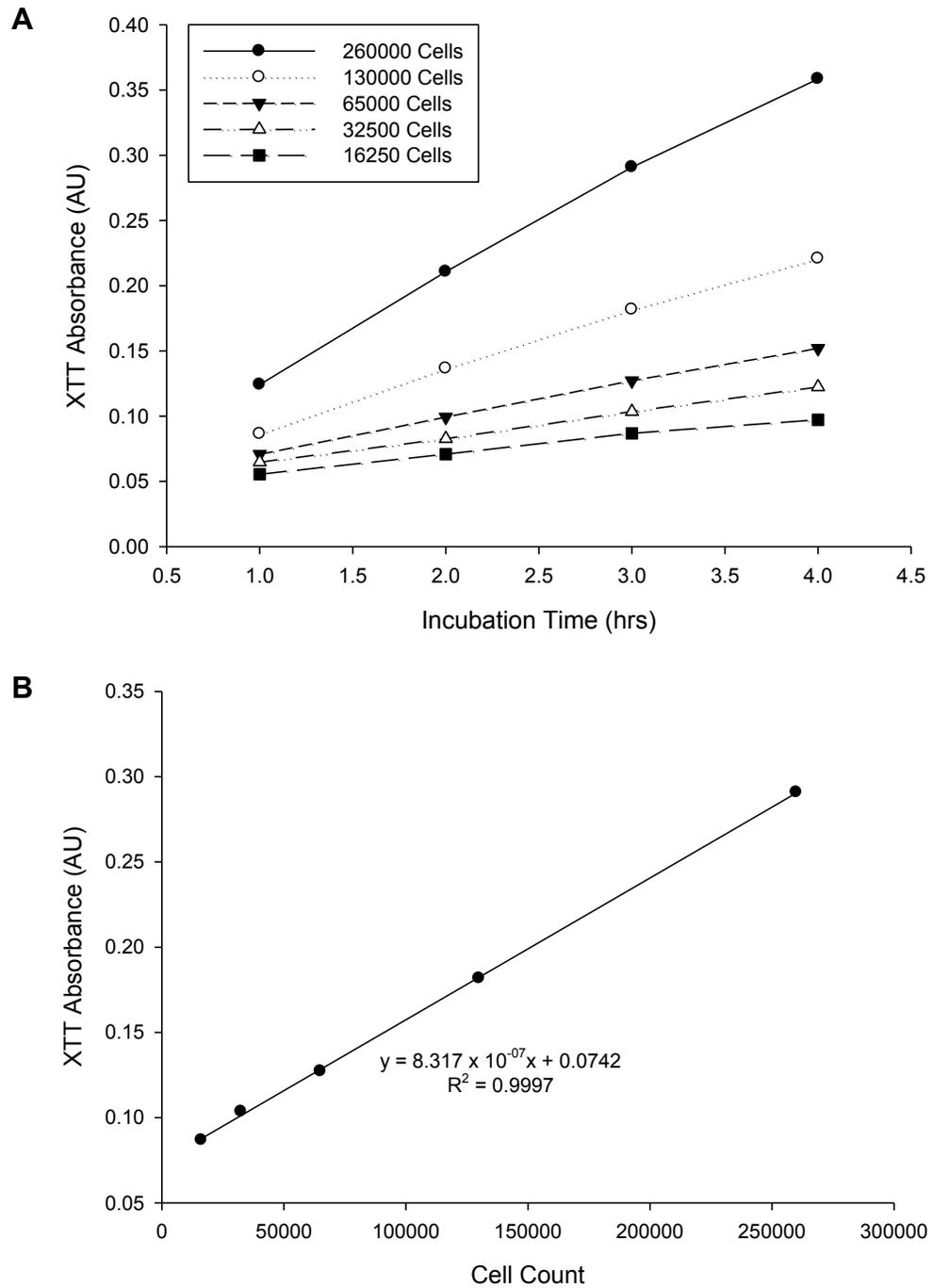
Fig. 3.14 XTT reduction correlates well with cell counts
A) Varying numbers of THP-1 cells were prepared and plated into the wells of a 48-well plate. The cells were treated with XTT and the absorbance at 467 nm was measured every hour for four hours. B) Data from the three hour absorbance reading in A was plotted versus the number of cells in the well. The equation of the line and the R^2 value were calculated in SigmaPlot.

PMA are present in the well, but not the medium. To confirm this result, we counted the number of adherent cells in each treatment and determined the percent adherence (Fig. 3.15B).

The plot of percent adherence versus PMA treatment concentration is very similar to the XTT derived results with one exception. In figure 3.15A, the 2 ng/ml PMA treatment appears to induce some adherence in the cells, but direct counting indicated that is not the case. Because there is no wash step between treatment and XTT analysis, it is possible that there are some loosely adherent cells which would have been dislodged. Despite this small inconsistency, the XTT appears to provide useful information regarding cell adherence. A decrease in XTT reduction in the medium of treated samples indicates a loss of cells from the medium and therefore an increase in adherence.

In an effort to confirm some of our earlier findings with regards to Aβ induced adherence, we repeated some experiments using the XTT analysis. To confirm our aggregation age findings, we treated the monocytes with 15 μM Aβ(1-42) at various ages of aggregation for six hours. We the moved the medium to a fresh well and treated it with XTT solution to determine the amount of reduction from the non-adherent cells. In order to combine the data from multiple experiments, the amount of XTT reduced by Aβ treated cells in each experiment was corrected to the amount reduced relative to the amount of XTT reduced by the control cells for the experiment (Fig. 3.16). The data shows that there is less reduction by the medium in samples treated with early Aβ aggregation states which suggests that more cells remain in the well while later stage treatments have more cells. The trend is consistent with the data presented in Fig. 3.5, which shows that the highest amount of adherence is induced by freshly prepared Aβ(1-42). If

A

B
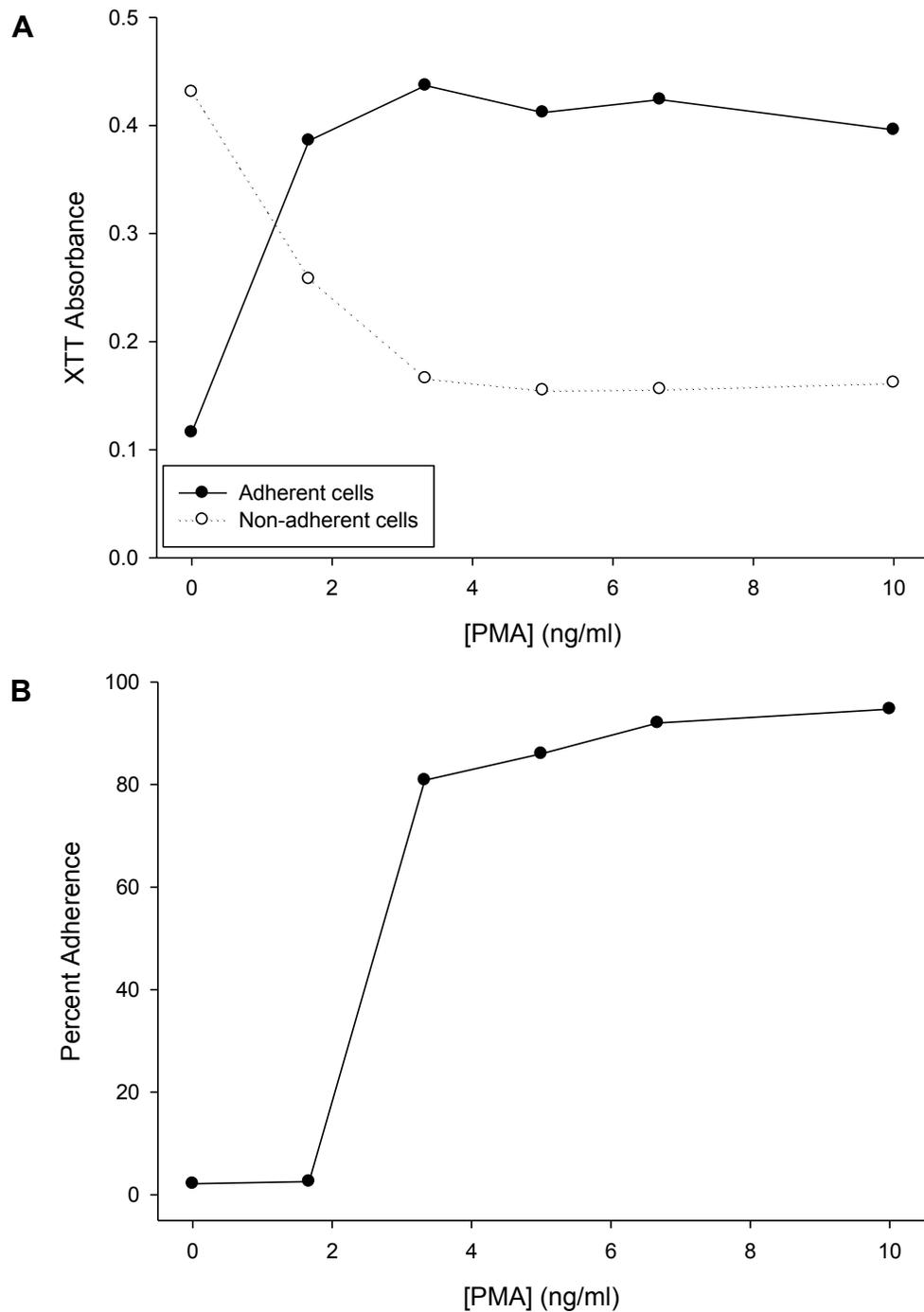
Fig. 3.15 PMA induced adherence can be studied with multiple methods
THP-1 cells were treated with 0, 1.67, 3.33, 5, 6.67 or 10 ng/ml PMA and incubated for 24 hours at 37°C. A) Non-adherent cells were moved to a new well. Adherent and non-adherent cells were treated with 0.33 mg/ml XTT/ 8.3 μM PMS for 3 hours. Absorbance of the samples was read at 467 nm. B) After XTT analysis, adherent cells were removed from the well with trypsin and counted. The adherent cells were corrected to percent adherence as described in the Methods.
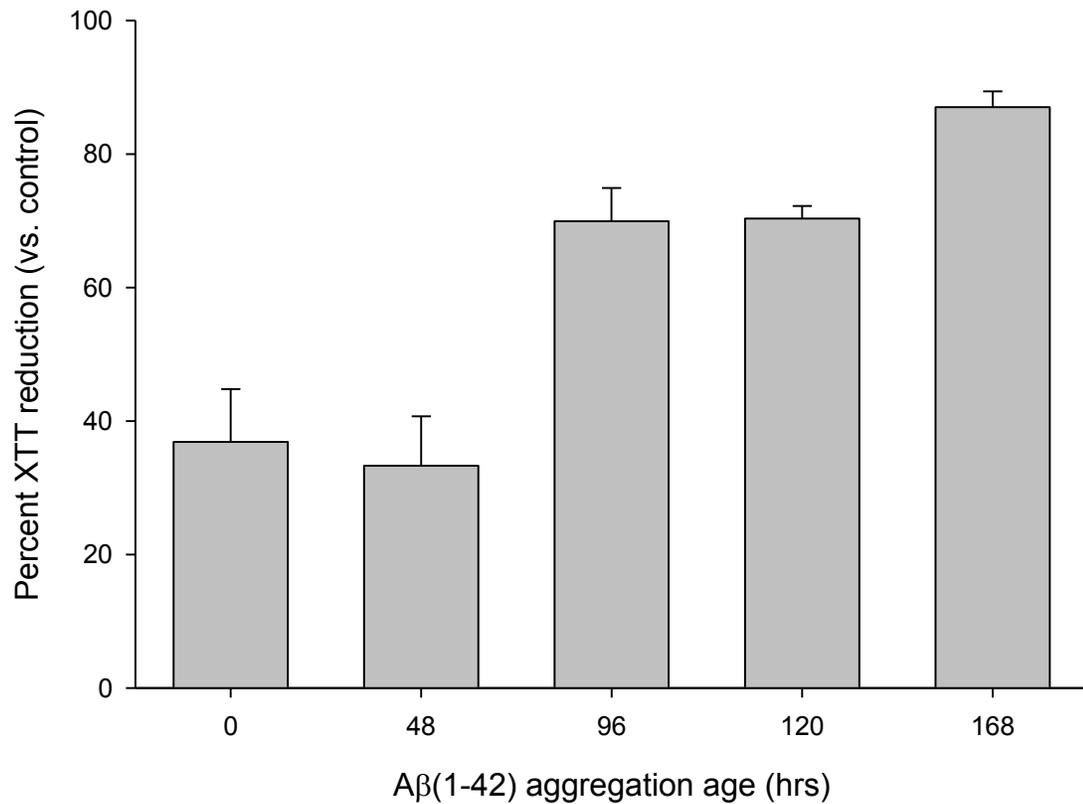
Fig. 3.16 Aβ induced adherence by XTT is similar to data from direct counting
Aβ(1-42) was reconstituted in sterile water to 100 μM and incubated at 4°C. At the given times, cells were treated with 15 μM Aβ for 6 hours. Following the treatment, non-adherent cells were moved to a new well and analyzed with XTT as described in the Methods. At each time point, the absorbance of Aβ treated cells was divided by the absorbance of water treated control cells and corrected to a percentage. Error bars represent standard error for n = 2 (0, 120 hrs), 3 (168 hrs), 4 (96 hrs) and 5 (48 hrs).

the raw percentages in figure 3.16 are considered, they suggest about 60, 65, 30, 30 and 15% adherence induced at 0, 48, 96, 120 and 168 hours of Aβ aggregation respectively. These numbers are higher than those determined by direct counting, but is likely due to the lack of a washing step before the cells were analyzed.

We also retested out Aβ(1-42) treatment concentration dependence using the XTT analysis. The cells were treated with different volumes of 100 μM Aβ(1-42) that was aggregated for 48 hours. Following a six hour incubation, the medium containing the non-adherent cells was analyzed by XTT (Fig. 3.17). As we previously found in figure 3.6, 15 μM Aβ(1-42) induced the highest amount of adherence as evidenced by a loss of non-adherent cells in the medium. The 7.5 μM Aβ treatment induced slightly less adherence, but was similar to the amount induced by the 15 μM treatment. This result is not unexpected since both 10 and 5 μM treatments induced some adherence in figure 3.6. When we performed this experiment with the direct counting assay, we did not test concentrations lower than 5 μM, but the results in 3.17 suggest that they would not induce adherence.

Our final experiment with the XTT methodology was the effect of Aβ aggregation concentration. In figure 3.9 we tested 100 μM and 1 mM Aβ(1-42) aggregation concentrations for their ability to induce adherence and analyzed the results by direct counting. Here we tested 100 μM and 1.2 mM Aβ(1-42) that was aged 48 hours and analyzed the results by XTT (Fig. 3.18). The results are in agreement with those shown in figure 3.9. Aβ that aggregates at a lower concentration maintains the ability to induce adherence while Aβ at higher concentrations does not. This result further confirms our earlier conclusion that an early-formed Aβ(1-42) oligomer is able to induce adherence in THP-
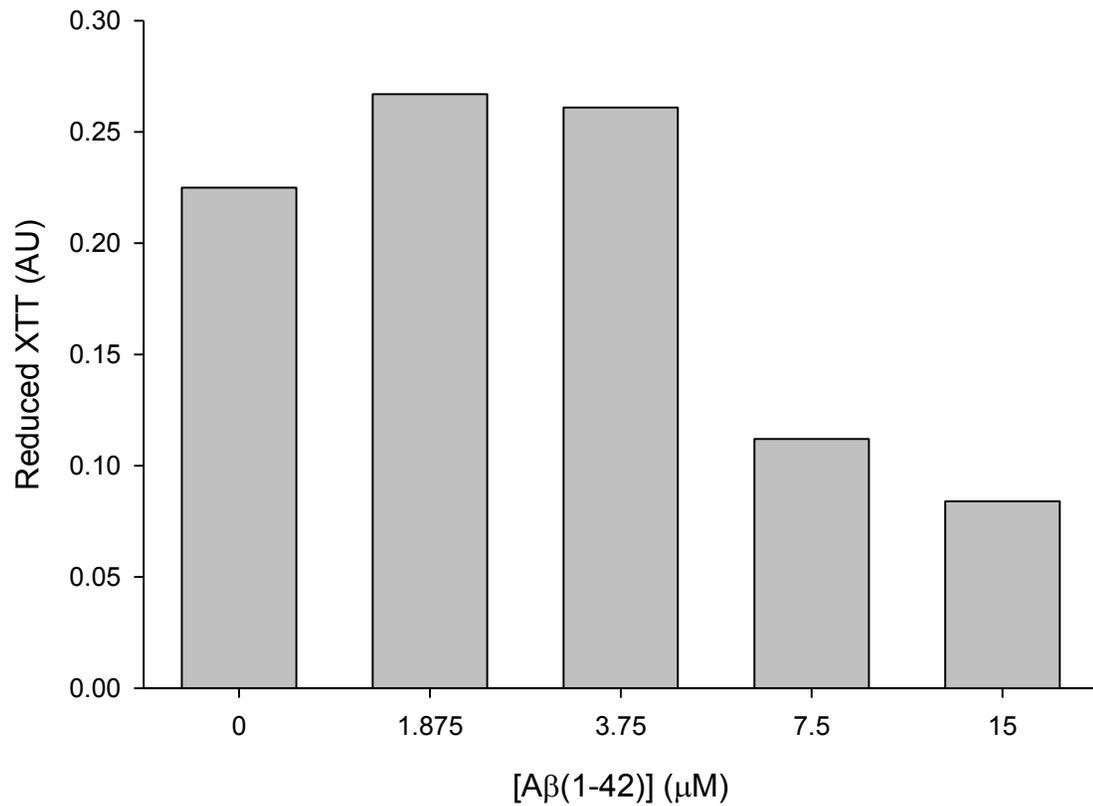
Fig. 3.17 Concentration dependence of Aβ(1-42) induced adherence measured by XTT
48 hour aggregated 100 μM Aβ(1-42) in water was added to THP-1 monocytes in different volumes to produce different final Aβ concentrations. All treatments maintained the same cell count and volume of sterile water from well to well. The treated cells were incubated at 37°C for 6 hours and the XTT reduction of the non-adherent cells was measured.
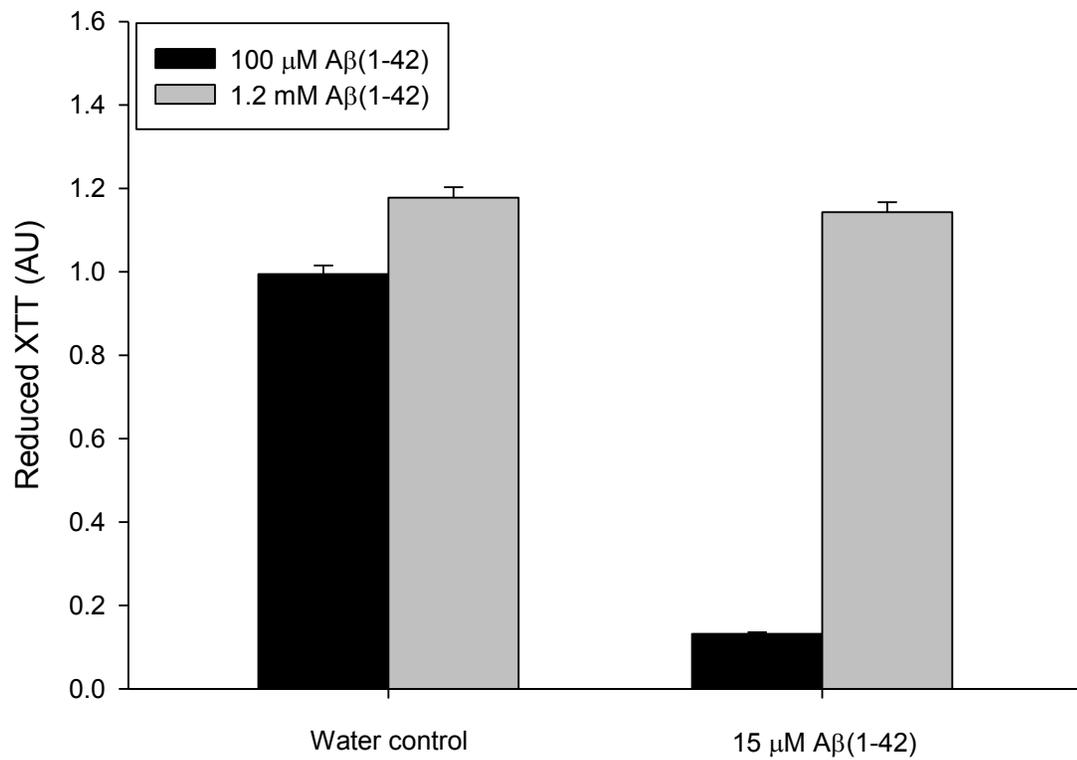
Fig. 3.18 Increasing Aβ aggregation concentration decreases monocyte adherence.
Lyophilized Aβ(1-42) was reconstituted in sterile water to either 100 μM or 1.2 mM and aggregated at 4°C for 48 hours. THP-1 cells were treated with 15 μM of either solution for 6 hours at 37°C. The XTT reduction by the non-adherent cells was measured as described in the Methods.

1 monocytes.

Aside from the absorbance based XTT assay, we have developed a fluorescence based assay to analyze adherence. Calcein AM is a non-fluorescent compound that can be taken up by living cells. Once internalized, esterase activity cleaves the ester groups from the calcein rendering the compound fluorescent (Papadopoulos et al., 1994). Although generally used to measure cell viability, we have adapted it to serve as an indicator of adherence.

We incubated THP-1 cells with 10 μM calcein AM for 30 minutes before preparing the cells in assay medium. The cells were plated and treated with 10 ng/ml PMA for 6 hours before the medium was removed and the adherent cells washed with PBS. The fluorescence of the wells was then measured before the cells were removed and counted (Fig. 3.19). A plot of calcein fluorescence versus cell count reveals a linear correlation with an R^2 value of 0.9985. This method of pre-labeling cells with calcein appears to be an effective measure of adherence following short incubations.

In order to utilize the calcein methodology for longer incubations we made a slight modification to the protocol. Instead of incubating the cells with the calcein AM before effector treatment, we induced adherence by exposing varying numbers of cells to 10 ng/ml PMA for 24 hours. We then removed the medium and washed the adherent cells with PBS before incubating the adherent cells with 10 μM calcein AM for 30 minutes. The fluorescence of each well was measured before the cells were removed from the wells and counted (Fig. 3.20).

The fluorescence of the adherent cells clearly shows the most adherent cells in the PMA treated well that had the highest plated cell count and the lowest fluorescence
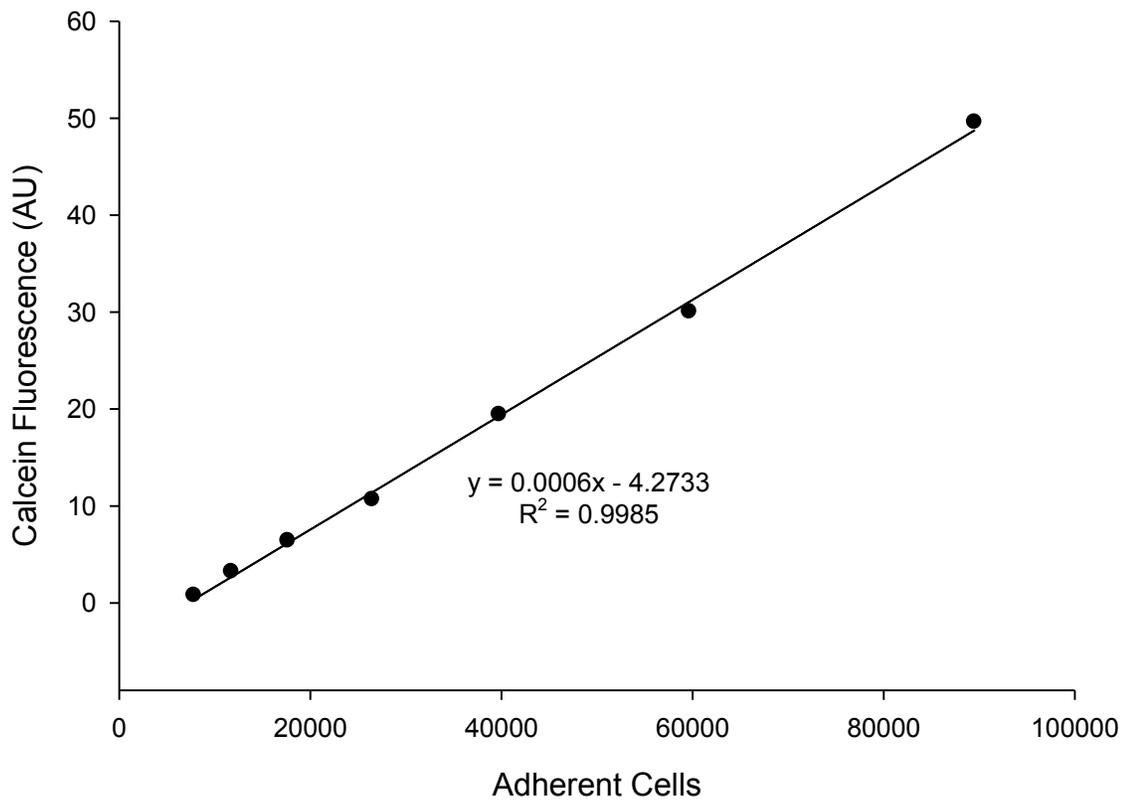
Fig. 3.19 Calcein fluorescence can be used to measure cell adherence induced by PMA
Varying numbers of THP-1 cells were pre-incubated with 10 μM calcein AM for 30 minutes at 37°C before being prepared in assay medium and treated with 10 ng/ml PMA for 6 hours. Following the treatment, the non-adherent cells were removed, the adherent cells were washed with PBS and the fluorescence of the calcein measured. The equation of the line and the R^2 value were calculated in SigmaPlot.

in the water treated well (Fig. 3.20A). The number of adherent cells counted in each well shows a similar trend (Fig. 3.20B). When the data from 3.19A,B were normalized based upon the well with the most adherence, the two sets of data are very similar (Fig. 3.20C). The number of adherent cells determined by both counts and fluorescence are in close agreement across all treatments. We have not applied the calcein assay to Aβ treatments.

<div align="center">3.3 Discussion</div>

The process of transforming monocytes into macrophages may play an important role in AD and other neurodegenerative disorders. Our work shows that Aβ(1-42) is able to induce this transformation in THP-1 monocytes based upon the change into an adherent morphology from a suspension cell type. The data presented here shows that a specific Aβ(1-42) oligomeric species is responsible for the transformation, which has specific implications in the AD model. It is well-known that Aβ(1-42) is the main component of the various plaques found in the brains of AD patients (Gravina et al., 1995; Selkoe, 2001a, 2001b). Aβ aggregates into a variety of species from monomer to large fibrillar structures, and the Aβ deposits found in the parenchyma of the brain have been shown to be a continuum of structures rather than a single, distinct aggregate species (Selkoe, 2004b).

It has been reported that Aβ accumulation in the brain can lead to the infiltration of monocyte/macrophages that are derived from the peripheral blood cells. Studies in mouse models have shown that there is a large increase in blood-derived microglia into

A

B

C
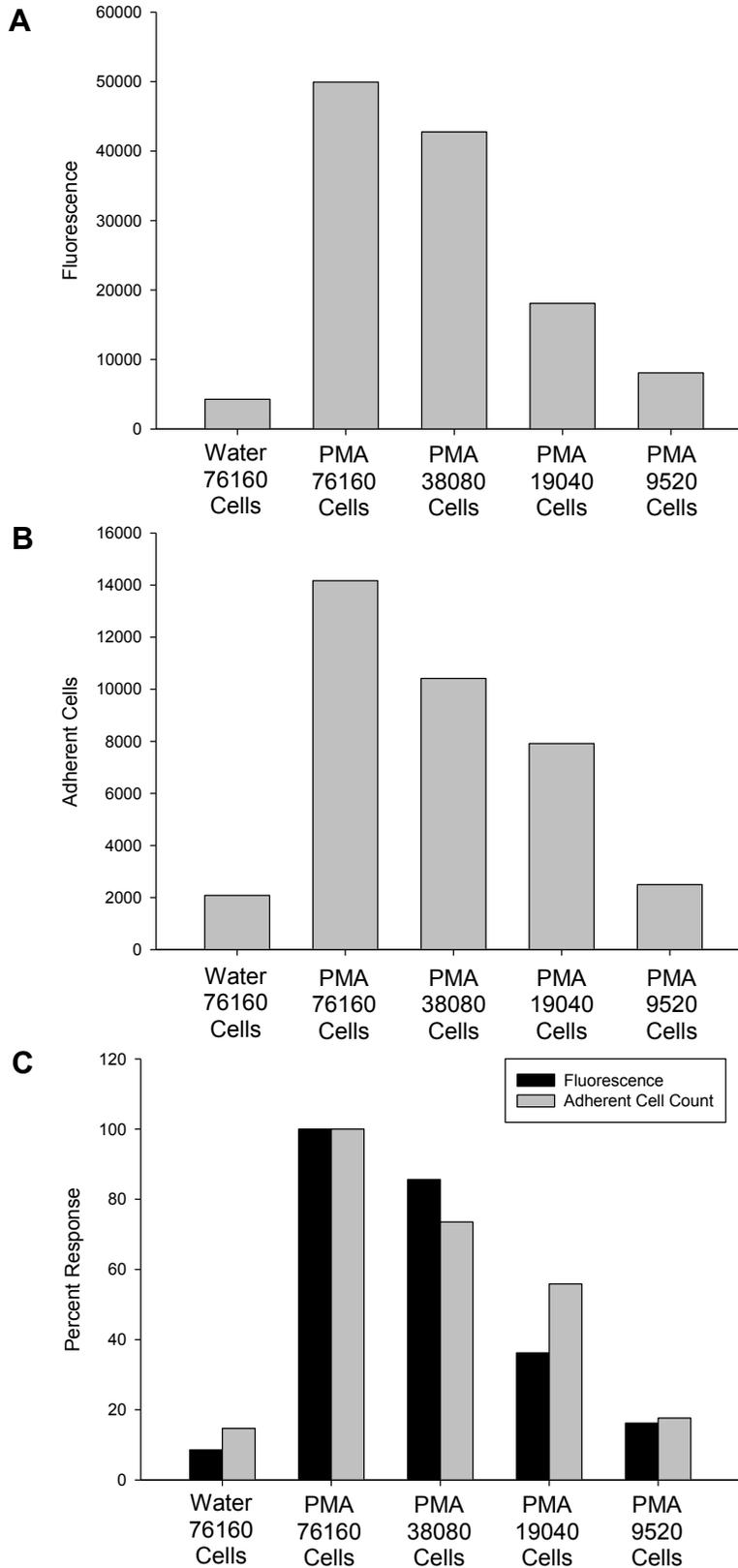
Fig. 3.20 Calcein fluorescence correlates with direct counting

THP-1 cells were prepared in assay medium and 76160, 38080, 19040 or 9520 cells were plated into the wells of a sterile 48-well plate. The cells were treated with 10 ng/ml of PMA or a water control for six hours as indicated in the legends. A) Following the incubation, the non-adherent cells were removed and the wells were washed with PBS. The adherent cells were treated with 10 μM calcein AM for 30 minutes before the fluorescence was read. B) Following fluorescent analysis, the adherent cells were trypsinized and counted as described in the Methods. C) Data from panels A and B were divided by the corresponding result for 76160 cells treated with PMA and multiplied by 100 to obtain a percentage.

the area of Aβ plaques (Simard et al., 2006). The study also showed that the infiltrating cells were more competent at phagocytosis of the Aβ than the resident microglia (Simard et al., 2006). However, as discussed at length by Carson and colleagues (Carson et al., 2007), the bone marrow chimera technique used to understand this process may itself cause the infiltration of the peripheral cells in a non-specific manner. However, the results were later confirmed by determining the unique immunoreactivity profiles of resident and recruited microglia and then analyzing the cells present in APP transgenic and normal mice. The study indicated that the mice expressing APP showed a marked increase in the recruited microglia compared to the wild type mice (El Khoury et al., 2007).

Despite the data suggesting the recruitment of non-resident cells into the CNS, it is yet unclear when the transformation from monocyte to macrophage occurs. Although it has been previously seen that Aβ can differentiate human monocytes (Fiala et al., 1998), our data suggests that an oligomeric form of Aβ(1-42) that is formed very early in the aggregation pathway can initiate the transformation process. Figure 3.3 shows that following a 6 hour incubation, freshly reconstituted Aβ(1-42) can induce a nearly identical amount of adherence as the well known differentiating agent PMA. As the Aβ(1-42) is allowed to aggregate, the dominant structure seen in the AFM images moves from a small globular species into long fibrils (Fig. 3.4 B-E). A dramatic loss in the ability to induce adherence was seen when the Aβ(1-42) was aggregated for 96 hours, which correlates with the presence of a large number of fibril structures (Fig 3.4).

We did not see any significant adherence induced by the Aβ(1-40) (Fig. 3.7 A), which was not completely unexpected since Bitan et al showed that Aβ(1-40) and Aβ(1-

42) aggregate via distinct pathways (Bitan et al., 2003). Increasing the aggregation temperature for the Aβ(1-40) did not lead to the progression to fibrils, but it also did not induce adherence, which suggests that the active oligomeric species is off-path for the Aβ (1-40). Also of interest was the Aβ(1-42) L34P mutant's inability to induce adherence in the monocytes (Fig. 3.8 B). This peptide did not aggregate well as expected (Williams et al., 2004), but it also did not form the conformation needed to induce the adherence in the cells. We had predicted that the Aβ(1-42) L34P peptide would maintain a high monomer:oligomer ratio, and thus help us determine if monomer was the active species. The lack of activity suggests that an oligomeric species that is off the aggregation pathway for Aβ(1-40) and Aβ(1-42) L34P is actually the active species in solution.

The strongest evidence for our conclusion that an Aβ(1-42) oligomer can induce adherence is found in the results from figure 3.9. Aβ aggregation rates can be manipulated through the modulation of the aggregation kinetics. By decreasing the Aβ aggregation concentration to 50 μM, the lag phase of the aggregation should be extended and lead to a higher monomer:oligomer ratio than in the 100 μM aggregation solution. Keeping the final treatment concentration constant at 15 μM, we ensure that the same total amount of Aβ is presented to the cells, and the only variable is the progression of the aggregation. Because the 50 μM Aβ(1-42) aggregation solution induced significantly less adherence than the 100 μM solution at 0 hours of aggregation, we were able to conclude that monomer is not the species responsible for inducing adherence in the cells. Rather, a very early-formed oligomeric species, which can only be formed on the unrestricted Aβ(1-42) aggregation pathway, is responsible for inducing this phenomenon.

It was somewhat unexpected that the ADDLs did not induce adherence in the

monocytes (Fig. 3.10) because of the growing number of studies detecting specific soluble Aβ intermediates, including protofibrils (Walsh et al., 1997), oligomers (Kayed et al., 2003), ADDLs (Lambert et al., 1998) and Aβ*56 (Lesne et al., 2006). However, not all of these species possess the same types of biological activities. It has been seen that ADDLs are less toxic to human cortical neurons than Aβ oligomers (Deshpande et al., 2006), but both species are more toxic than fibrillar Aβ (Lambert et al., 1998). Within the field of Aβ research it has proven very difficult to discern between the size and conformational components of the soluble aggregation species with regards to their activities. A recent report suggests that the molecular weight of ADDLs ranges from 150 – 1000 kDa (Hepler et al., 2006), which is indicative of a higher order aggregation state than previously believed. It is possible that the ADDLs are formed later in the Aβ aggregation pathway than the active oligomer species, thus explaining their inability to induce adherence in the monocytes.

Despite our previous study which showed the activation of the innate immune response by Aβ through TLR2 and TLR4 (Udan et al., 2007), blocking these receptors did not prevent the Aβ(1-42) induced adherence (Fig. 3.11). However, in combination with the ineffectiveness of blocking the NF-κB dependent pathway with PDTC (Fig. 3.12), the non-involvement of the TLRs is not terribly surprising. Activation of the innate immune system through the TLRs is an upstream activator of the NF-κB pathway (Fitzgerald and Chen, 2006). Oddly though, activation of FPRL1 with the short peptide WKYMVM has been shown to activate NF-κB in human U87 astrocytoma and Chinese hamster ovary cells (Kam et al., 2007). Despite this previous research, our studies suggest that the activation of NF-κB and the induction of adherence through FPRL1 may

involve separate pathways.

The interaction between FPRL1 and Aβ(1-42) has been previously reported to lead to mobilization of Ca^{2+} and induce chemotaxis in human PBMC (Le et al., 2001). The same study also found that if they aggregated the Aβ, it was less able to induce chemotaxis than freshly reconstituted Aβ, a result which mirrors our own. We have shown that pre-treating the THP-1 monocytes with WRW_4, an antagonist to FPRL1, significantly attenuates the adherence induced by treatment with freshly reconstituted Aβ(1-42) (Fig. 3.13). These data are also in agreement with another study which indicated that WRW_4 was able to block the phagocytosis of Aβ(1-42) in human macrophages (Bae et al., 2004).

Collectively, the findings of our work suggest that Aβ(1-42) is able to potently induce adherence in non-adherent THP-1 monocytes. If further characterization of the adherent cells indicates they have been differentiated into macrophages, these results could be vital to understanding the recruitment and transformation of non-resident monocytes into the CNS in response to AD pathology. The study by Luster and colleagues showed that this recruitment process is initiated before Aβ plaque deposits are detectable (El Khoury et al., 2007), suggesting that the presence of an early oligomeric species may be the trigger. Our results provide new insights into this process, and may lead to a greater understanding of the overall relationship between Aβ aggregation state and the response of the cells.

3.4 Bibliography

Akira S, Takeda K, Kaisho T (2001) Toll-like receptors: critical proteins linking innate and acquired immunity. Nat Immunol 2:675-680.

Asheuer M, Pflumio F, Benhamida S, Dubart-Kupperschmitt A, Fouquet F, Imai Y, Aubourg P, Cartier N (2004) Human CD34+ cells differentiate into microglia and express recombinant therapeutic protein. Proc Natl Acad Sci U S A 101:3557-3562.

Auwerx J (1991) The human leukemia cell line, THP-1: a multifacetted model for the study of monocyte-macrophage differentiation. Experientia 47:22-31.

Bae YS, Lee HY, Jo EJ, Kim JI, Kang HK, Ye RD, Kwak JY, Ryu SH (2004) Identification of peptides that antagonize formyl peptide receptor-like 1-mediated signaling. J Immunol 173:607-614.

Banati RB, Gehrmann J, Schubert P, Kreutzberg GW (1993) Cytotoxicity of microglia. Glia 7:111-118.

Bauer J, Sminia T, Wouterlood FG, Dijkstra CD (1994) Phagocytic activity of macrophages and microglial cells during the course of acute and chronic relapsing experimental autoimmune encephalomyelitis. J Neurosci Res 38:365-375.

Bitan G, Tarus B, Vollers SS, Lashuel HA, Condron MM, Straub JE, Teplow DB (2003) A molecular switch in amyloid assembly: Met35 and amyloid beta-protein oligomerization. J Am Chem Soc 125:15359-15365.

Boehme KW, Compton T (2004) Innate sensing of viruses by toll-like receptors. J Virol 78:7867-7873.

Carson MJ, Bilousova TV, Puntambekar SS, Melchior B, Doose JM, Ethell IM (2007) A rose by any other name? The potential consequences of microglial heterogeneity during CNS health and disease. Neurotherapeutics 4:571-579.

Chomarat P, Banchereau J, Davoust J, Palucka AK (2000) IL-6 switches the differentiation of monocytes from dendritic cells to macrophages. Nat Immunol 1:510-514.

Chomarat P, Dantin C, Bennett L, Banchereau J, Palucka AK (2003) TNF skews monocyte differentiation from macrophages to dendritic cells. J Immunol 171:2262-2269.

Dahlgren KN, Manelli AM, Stine WB, Jr., Baker LK, Krafft GA, LaDu MJ (2002) Oligomeric and fibrillar species of amyloid-beta peptides differentially affect neuronal viability. J Biol Chem 277:32046-32053.

Davoust N, Vuaillat C, Androdias G, Nataf S (2008) From bone marrow to microglia: barriers and avenues. Trends Immunol 29:227-234.

Deshpande A, Mina E, Glabe C, Busciglio J (2006) Different conformations of amyloid beta induce neurotoxicity by distinct mechanisms in human cortical neurons. J Neurosci 26:6011-6018.

Ding Q, Jin T, Wang Z, Chen Y (2007) Catalase potentiates retinoic acid-induced THP-1 monocyte differentiation into macrophage through inhibition of peroxisome proliferator-activated receptor gamma. J Leukoc Biol 81:1568-1576.

Dzionek A, Fuchs A, Schmidt P, Cremer S, Zysk M, Miltenyi S, Buck DW, Schmitz J (2000) BDCA-2, BDCA-3, and BDCA-4: three markers for distinct subsets of dendritic cells in human peripheral blood. J Immunol 165:6037-6046.

Eck SL, Perkins ND, Carr DP, Nabel GJ (1993) Inhibition of phorbol ester-induced cellular adhesion by competitive binding of NF-kappa B in vivo. Mol Cell Biol 13:6530-6536.

Eglitis MA, Mezey E (1997) Hematopoietic cells differentiate into both microglia and macroglia in the brains of adult mice. Proc Natl Acad Sci U S A 94:4080-4085.

El Khoury J, Toft M, Hickman SE, Means TK, Terada K, Geula C, Luster AD (2007) Ccr2 deficiency impairs microglial accumulation and accelerates progression of Alzheimer-like disease. Nat Med 13:432-438.

Fiala M, Zhang L, Gan X, Sherry B, Taub D, Graves MC, Hama S, Way D, Weinand M, Witte M, Lorton D, Kuo YM, Roher AE (1998) Amyloid-beta induces chemokine secretion and monocyte migration across a human blood--brain barrier model. Mol Med 4:480-489.

Fitzgerald KA, Chen ZJ (2006) Sorting out Toll signals. Cell 125:834-836.

Giri R, Shen Y, Stins M, Du Yan S, Schmidt AM, Stern D, Kim KS, Zlokovic B, Kalra VK (2000) beta-amyloid-induced migration of monocytes across human brain endothelial cells involves RAGE and PECAM-1. Am J Physiol Cell Physiol 279:C1772-1781.

Gravina SA, Ho L, Eckman CB, Long KE, Otvos L, Jr., Younkin LH, Suzuki N, Younkin SG (1995) Amyloid beta protein (A beta) in Alzheimer's disease brain. Biochemical and immunocytochemical analysis with antibodies specific for forms ending at A beta 40 or A beta 42(43). J Biol Chem 270:7013-7016.

Harper JD, Wong SS, Lieber CM, Lansbury PT (1997) Observation of metastable Abeta amyloid protofibrils by atomic force microscopy. Chem Biol 4:119-125.

Harper JD, Wong SS, Lieber CM, Lansbury PT, Jr. (1999) Assembly of A beta amyloid protofibrils: an in vitro model for a possible early event in Alzheimer's disease. Biochemistry 38:8972-8980.

Hayden JM, Brachova L, Higgins K, Obermiller L, Sevanian A, Khandrika S, Reaven PD (2002) Induction of monocyte differentiation and foam cell formation in vitro by 7-ketocholesterol. J Lipid Res 43:26-35.

Heneka MT, O'Banion MK (2007) Inflammatory processes in Alzheimer's disease. J Neuroimmunol 184:69-91.

Hepler RW, Grimm KM, Nahas DD, Breese R, Dodson EC, Acton P, Keller PM, Yeager M, Wang H, Shughrue P, Kinney G, Joyce JG (2006) Solution state characterization of amyloid beta-derived diffusible ligands. Biochemistry 45:15157-15167.

Hjort MR, Brenyo AJ, Finkelstein JN, Frampton MW, LoMonaco MB, Stewart JC, Johnston CJ, D'Angio CT (2003) Alveolar epithelial cell-macrophage interactions affect oxygen-stimulated interleukin-8 release. Inflammation 27:137-145.

Hmama Z, Knutson KL, Herrera-Velit P, Nandan D, Reiner NE (1999) Monocyte adherence induced by lipopolysaccharide involves CD14, LFA-1, and cytohesin-1. Regulation by Rho and phosphatidylinositol 3-kinase. J Biol Chem 274:1050-1057.

Jarrett JT, Lansbury PT, Jr. (1993) Seeding "one-dimensional crystallization" of amyloid: a pathogenic mechanism in Alzheimer's disease and scrapie? Cell 73:1055-1058.

Kam AY, Liu AM, Wong YH (2007) Formyl peptide-receptor like-1 requires lipid raft and extracellular signal-regulated protein kinase to activate inhibitor-kappa B kinase in human U87 astrocytoma cells. J Neurochem 103:1553-1566.

Kang CD, Lee BK, Kim KW, Kim CM, Kim SH, Chung BS (1996) Signaling mechanism of PMA-induced differentiation of K562 cells. Biochem Biophys Res Commun 221:95-100.

Kayed R, Head E, Thompson JL, McIntire TM, Milton SC, Cotman CW, Glabe CG (2003) Common structure of soluble amyloid oligomers implies common mechanism of pathogenesis. Science 300:486-489.

Kramer PR, Wray S (2002) 17-Beta-estradiol regulates expression of genes that function in macrophage activation and cholesterol homeostasis. J Steroid Biochem Mol Biol 81:203-216.

Lambert MP, Barlow AK, Chromy BA, Edwards C, Freed R, Liosatos M, Morgan TE, Rozovsky I, Trommer B, Viola KL, Wals P, Zhang C, Finch CE, Krafft GA, Klein WL (1998) Diffusible, nonfibrillar ligands derived from Abeta1-42 are potent central nervous system neurotoxins. Proc Natl Acad Sci U S A 95:6448-6453.

Le Y, Gong W, Tiffany HL, Tumanov A, Nedospasov S, Shen W, Dunlop NM, Gao JL, Murphy PM, Oppenheim JJ, Wang JM (2001) Amyloid (beta)42 activates a G-protein-coupled chemoattractant receptor, FPR-like-1. J Neurosci 21:RC123.

Lesne S, Koh MT, Kotilinek L, Kayed R, Glabe CG, Yang A, Gallagher M, Ashe KH (2006) A specific amyloid-beta protein assembly in the brain impairs memory. Nature 440:352-357.

Lorenzo A, Yankner BA (1994) Beta-amyloid neurotoxicity requires fibril formation and is inhibited by congo red. Proc Natl Acad Sci U S A 91:12243-12247.

McGeer PL, Itagaki S, Tago H, McGeer EG (1987) Reactive microglia in patients with senile dementia of the Alzheimer type are positive for the histocompatibility glycoprotein HLA-DR. Neurosci Lett 79:195-200.

Papadopoulos NG, Dedoussis GV, Spanakos G, Gritzapis AD, Baxevanis CN, Papamichail M (1994) An improved fluorescence assay for the determination of lymphocyte-mediated cytotoxicity using flow cytometry. J Immunol Methods 177:101-111.

Park EK, Jung HS, Yang HI, Yoo MC, Kim C, Kim KS (2007) Optimized THP-1 differentiation is required for the detection of responses to weak stimuli. Inflamm Res 56:45-50.

Pike CJ, Walencewicz AJ, Glabe CG, Cotman CW (1991) In vitro aging of beta-amyloid protein causes peptide aggregation and neurotoxicity. Brain Res 563:311-314.

Remer KA, Brcic M, Sauter KS, Jungi TW (2006) Human monocytoid cells as a model to study Toll-like receptor-mediated activation. J Immunol Methods 313:1-10.

Sakamoto H, Aikawa M, Hill CC, Weiss D, Taylor WR, Libby P, Lee RT (2001) Biomechanical strain induces class a scavenger receptor expression in human monocyte/macrophages and THP-1 cells: a potential mechanism of increased atherosclerosis in hypertension. Circulation 104:109-114.

Schwende H, Fitzke E, Ambs P, Dieter P (1996) Differences in the state of differentiation of THP-1 cells induced by phorbol ester and 1,25-dihydroxyvitamin D3. J Leukoc Biol 59:555-561.

Selkoe DJ (2001a) Alzheimer's disease results from the cerebral accumulation and cytotoxicity of amyloid beta-protein. J Alzheimers Dis 3:75-80.

Selkoe DJ (2001b) Alzheimer's disease: genes, proteins, and therapy. Physiol Rev 81:741-766.

Selkoe DJ (2004a) Cell biology of protein misfolding: the examples of Alzheimer's and Parkinson's diseases. Nat Cell Biol 6:1054-1061.

Selkoe DJ (2004b) Alzheimer disease: mechanistic understanding predicts novel therapies. Ann Intern Med 140:627-638.

Simard AR, Rivest S (2004) Bone marrow stem cells have the ability to populate the entire central nervous system into fully differentiated parenchymal microglia. Faseb J 18:998-1000.

Simard AR, Soulet D, Gowing G, Julien JP, Rivest S (2006) Bone marrow-derived microglia play a critical role in restricting senile plaque formation in Alzheimer's disease. Neuron 49:489-502.

Stine WB, Jr., Dahlgren KN, Krafft GA, LaDu MJ (2003) In vitro characterization of conditions for amyloid-beta peptide oligomerization and fibrillogenesis. J Biol Chem 278:11612-11622.

Tsuchiya S, Yamabe M, Yamaguchi Y, Kobayashi Y, Konno T, Tada K (1980) Establishment and characterization of a human acute monocytic leukemia cell line (THP-1). Int J Cancer 26:171-176.

Tsuchiya S, Kobayashi Y, Goto Y, Okumura H, Nakae S, Konno T, Tada K (1982) Induction of maturation in cultured human monocytic leukemia cells by a phorbol diester. Cancer Res 42:1530-1536.

Udan ML, Ajit D, Crouse NR, Nichols MR (2007) Toll-like receptors 2 and 4 mediate Abeta(1-42) activation of the innate immune response in a human monocytic cell line. J Neurochem.

Ueki A, Isozaki Y, Tomokuni A, Hatayama T, Ueki H, Kusaka M, Shiwa M, Arikuni H, Takeshita T, Morimoto K (2002) Intramolecular epitope spreading among anti-caspase-8 autoantibodies in patients with silicosis, systemic sclerosis and systemic lupus erythematosus, as well as in healthy individuals. Clin Exp Immunol 129:556-561.

Walsh DM, Lomakin A, Benedek GB, Condron MM, Teplow DB (1997) Amyloid beta-protein fibrillogenesis. Detection of a protofibrillar intermediate. J Biol Chem 272:22364-22372.

Walsh DM, Klyubin I, Fadeeva JV, Cullen WK, Anwyl R, Wolfe MS, Rowan MJ, Selkoe DJ (2002) Naturally secreted oligomers of amyloid beta protein potently inhibit hippocampal long-term potentiation in vivo. Nature 416:535-539.

Walsh DM, Hartley DM, Kusumoto Y, Fezoui Y, Condron MM, Lomakin A, Benedek GB, Selkoe DJ, Teplow DB (1999) Amyloid beta-protein fibrillogenesis. Structure and biological activity of protofibrillar intermediates. J Biol Chem 274:25945-25952.

Wegiel J, Imaki H, Wang KC, Wegiel J, Rubenstein R (2004) Cells of monocyte/microglial lineage are involved in both microvessel amyloidosis and fibrillar plaque formation in APPsw tg mice. Brain Res 1022:19-29.

Williams AD, Portelius E, Kheterpal I, Guo JT, Cook KD, Xu Y, Wetzel R (2004) Mapping abeta amyloid fibril secondary structure using scanning proline mutagenesis. J Mol Biol 335:833-842.

Yan SD, Chen X, Fu J, Chen M, Zhu H, Roher A, Slattery T, Zhao L, Nagashima M, Morser J, Migheli A, Nawroth P, Stern D, Schmidt AM (1996) RAGE and amyloid-beta peptide neurotoxicity in Alzheimer's disease. Nature 382:685-691.

4 CHARACTERIZATION OF ADHERENT CELLS

4.1 Introduction

The human body is a complicated system that stands ready to defend itself from a pathogenic invasion. In healthy individuals, the bone marrow produces a steady stream of monocytic cells that circulate in the bloodstream. If a pathogen invades the body, these monocytes have the potential to undergo differentiation and transform into other types of cells to protect the body (Volkman and Gowans, 1965a, 1965b; Gordon and Taylor, 2005).

In order to immediately respond to the insult associated with pathogenic invasion, the monocytes are differentiated into macrophages through the innate immune response (Van Furth et al., 1973; Reya et al., 2001). The primary function of the newly formed macrophages is to phagocytose and destroy the invader (Mackaness, 1964; Schwende et al., 1996; Benoit et al., 2008). Once the immediate threat is contained, the monocytes begin differentiation through the adaptive immune response pathway into dendricytes. These cells are antigen producing cells that aid in the formation of antibodies and the development of long-term immunity to the pathogen (Banchereau and Steinman, 1998).

In the CNS, the role of macrophages are played by the microglia. These cells

possess phagocytic abilities similar to the macrophages found in the periphery (Banati et al., 1993; Bauer et al., 1994; Davoust et al., 2008). The presence of activated microglia surrounding Aβ plaques in AD brains (McGeer et al., 1987; Heneka and O'Banion, 2007) suggests that an immune response is attempted in response to AD pathology. Because of the similarities in physiology and function, peripheral macrophages may provide a useful model system to study the activation of microglia.

When monocytes are transformed into macrophages, they undergo morphological changes including flattening and spreading and the ability to adhere (Tsuchiya et al., 1982; Schwende et al., 1996). The receptors on the surface of the cells also change upon activation and an increase is seen in the expression of CD11b, *iba*-1 and F4/80 (Davoust et al., 2008). Once in the macrophage phenotype, the cells also develop the ability to phagocytose pathogens and secrete proinflammatory cytokines (Schwende et al., 1996).

Aβ has previously been shown to induce adherence in peripheral blood monocytes (Le et al., 2001). In addition, we have shown that this process occurs in THP-1 monocytes in response to freshly reconstituted Aβ(1-42) (Crouse et al., 2009). We suggested that this transformation to an adherent phenotype is likely to be related to the differentiation of the monocytes to macrophages. Here we characterize the cells that were transformed to determine if they possess other features unique to macrophage-like cells.

<u>4.2 Results</u>

4.2.1 Integrin Receptor Expression

The family of integrins serves as receptors for cell adhesion to extracellular matrix, and mediate cell-cell adhesion. The integrins are αβ heterodimers in which 8 β subunits can associate with 18 α subunits to produce 24 known integrins (Hynes, 2002). Of these known integrins, the class of β2 integrins are known to be expressed exclusively on leukocytes and play a pivotal role in adhesion and migration of these cells. Specifically, the Mac-1 integrin made up of CD11b (αM subunit) and CD18 (β2 subunit) have been implicated in cellular migration (Mayadas and Cullere, 2005).

Fibronectin (Fn) is one of the components in the extracellular matrix that can interact with integrins (Ruoslahti and Pierschbacher, 1987). It is a known adhesion protein that has been published to stabilize the adherence of THP-1 cells treated with LPS (Kounalakis and Corbett, 2006). We wanted to explore the possibility of Fn stabilizing the adherence induced in our cells when they were treated with PMA or Aβ.

Wells of the experimental plate were pre-coated with Fn as described in the methods. The cells were treated with 10 ng/ml of PMA or 15 μM of freshly prepared Aβ (1-42) and incubated for 6 hours (Fig. 4.1A). The cells treated in wells pre-coated with Fn had increased adherence compared to cells in uncoated wells. Both effectors induced more adherence in the presence of Fn.

We have previously shown that incubation of the cells with Aβ(1-42) for 24 hours induced a similar amount of adherence as a 6 hour incubation time (Udan et al., 2007). We wanted to determine if Fn would stabilize the Aβ induced adherence during a 24 hour incubation (Fig 4.1B). Cells treated with freshly reconstituted Aβ(1-42) induced 35.32% adherence in uncoated wells and 79.17 ± 14.20% adherence in wells coated
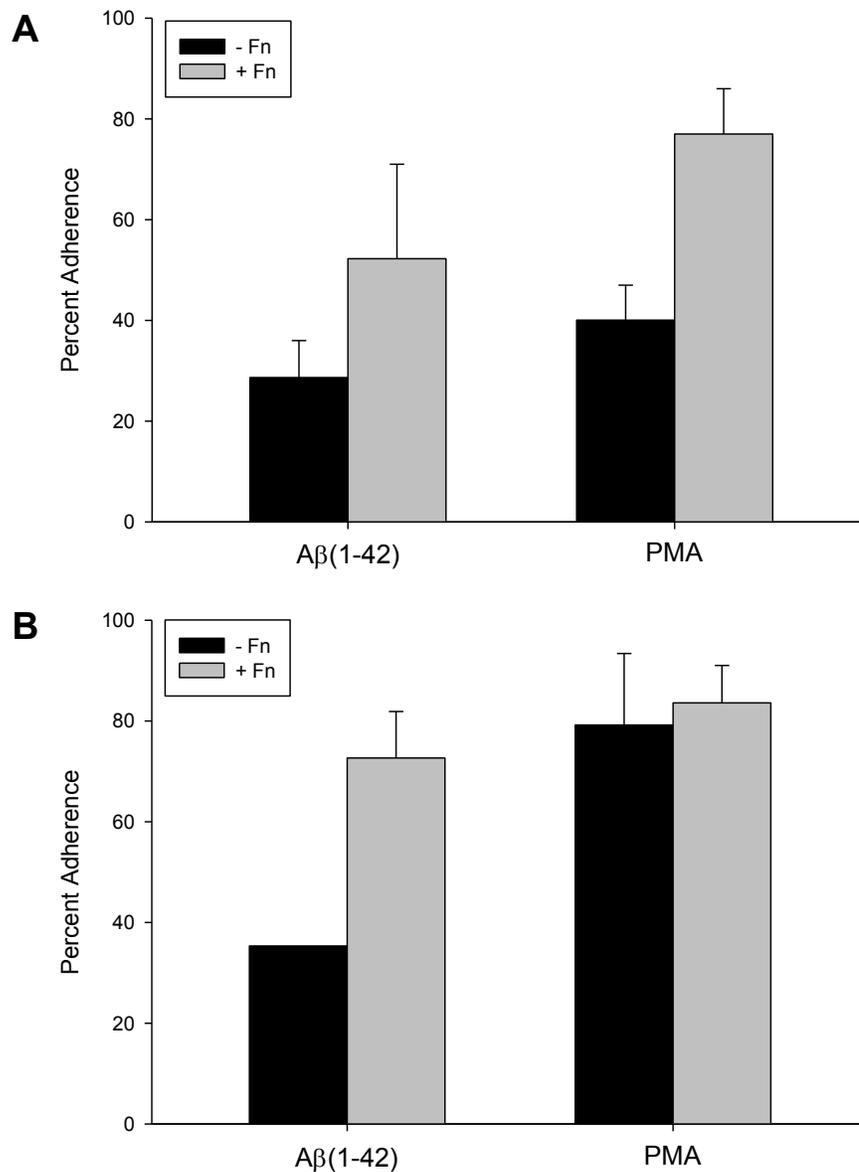
Fig. 4.1 Fn increases the adherence induced by PMA and Aβ
THP-1 monocytes were incubated at 37°C with 10 ng/ml PMA or 15 μM Aβ(1-42) in the presence or absence of Fn. Following the incubation time, percent adherence was determined as described in the Methods. A) Treated cells were incubated with the effectors for 6 hours. Error bars are standard error for n= 2 trials. B) Treated cells were incubated for 24 hours with the effectors. Error bars are standard error for n= 1 (Aβ -Fn) and 2.

with Fn. PMA induced 72.66 ± 9.23% and 83.58 ± 7.44% in uncoated and coated wells, respectively.

The results to the previous experiments suggested that Fn coating could stabilize the adherence induced by treatments that may not have induced adherence in earlier experiments. An Aβ(1-42) concentration dependence experiment revealed that concentrations of Aβ lower than our typical 15 μM treatment did not induce significant adherence in the THP-1 cells (Fig. 3.5). We retested the ability of 5 μM Aβ(1-42) to induce adherence in THP-1 cells at various incubation times (Fig. 4.2). THP-1 cells incubated with 5 μM of freshly prepared Aβ(1-42) in Fn coated plates induced 14.99 ± 4.29% adherence at 6 hours, 66.03 ± 15.21% adherence at 24 hours and 77.36% adherence at 48 hours of incubation. When the cells were treated in uncoated plates, the 6 and 24 hour adherence values dropped to 8.56 ± 3.21% and 10.97 ± 0.27%, respectively (data not shown). The ability of 5 μM Aβ(1-42) to induce adherence in uncoated plates with a 48 hour incubation was not tested.

The process of differentiation has been linked to increased expression of various cell surface markers including CD11b on the surface of the macrophages but not on the parent monocytes (Schwende et al., 1996). To determine if the increased adherence to Fn coated plates was due to an upregulation of integrin receptor expression, we analyzed the amount of CD11b expressed on the surface of adherent cells. The measurement was performed by applying an anti-CD11b to the surface of the cells followed by an anti-IgG antibody tagged with HRP, which was used to provide colormetric detection of the receptor as described in the Methods. Separate experiments were performed and the data was corrected to absorbance per 10^5 cells for averaging purposes. Cells treated with
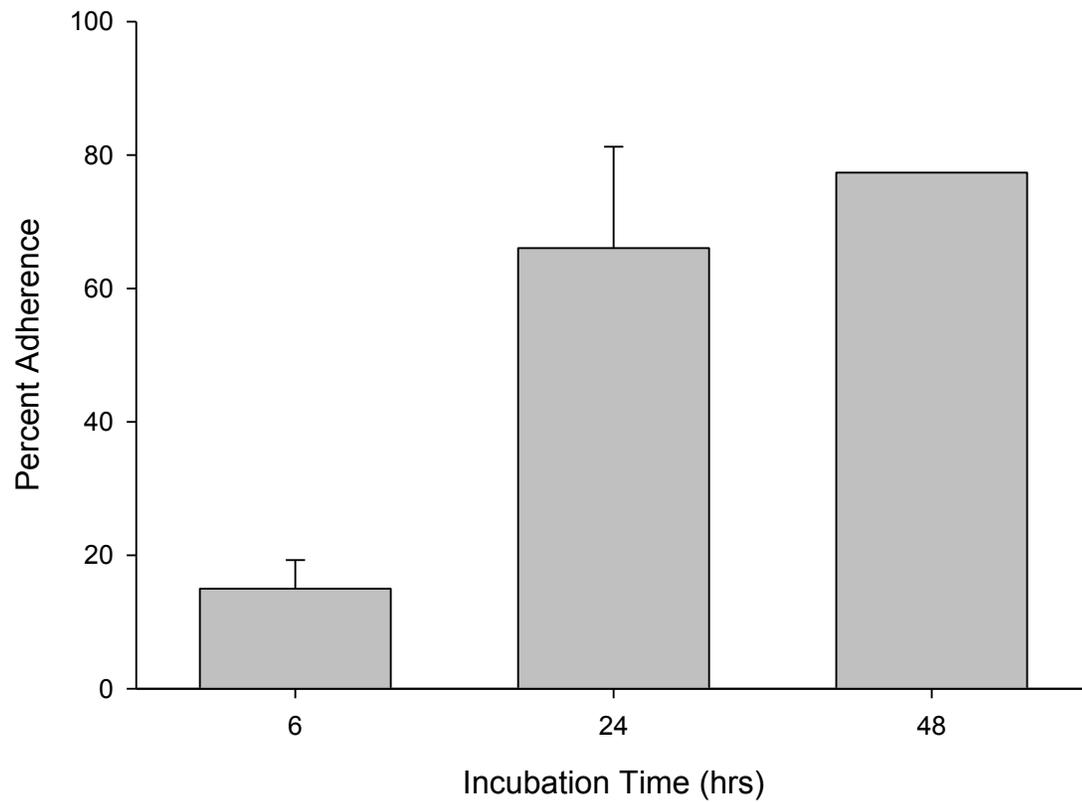
Fig. 4.2 Fn coating allows lower concentrations of Aβ to induce monocyte adherence
Wells were pre-coated with Fn as described. Cells were treated with 5 μM Aβ(1-42) and incubated at 37°C for the times indicated. Following the incubation the adherence was analyzed as described. Error bars are SE for n= 2 (6, 24) and 1 (48).

PMA induced a normalized cell surface CD11b expression of 0.16 ± 0.01 and 0.39 ± 0.03 AU/ 10^5 cells after 6 and 24 hours of exposure, respectively. Cells treated concurrently with 15 µM Aβ(1-42) expressed 0.28 ± 0.01 and 0.71 ± 0.04 AU/ 10^5 cells after 6 and 24 hour incubations, respectively (Fig. 4.3A). The lower 5 µM Aβ(1-42) treatment for 24 or 48 hours induced 0.27 ± 0.02 and 0.62 ± 0.05 AU/ 10^5 cells, respectively while concurrent PMA treatments induced 0.39 ± 0.03 and 0.54 ± 0.01 AU/ 10^5 cells with 24 and 48 hour incubations (Fig 4.3B).

4.2.2 Markers of Monocyte Differentiation

The upregulation of CD11b expression upon treatment of the THP-1 cells with Aβ compared to PMA treatment suggests that the cells are being differentiated and not simply becoming adherent. We decided to analyze the adherent cells for other markers of the differentiation process. It has been shown previously that upon differentiation, the morphology of monocytic cells will change. The cells will flatten and spread as they become adherent and they will also develop vacuoles (Tsuchiya et al., 1982).

Following treatment of the THP-1 cells with either PMA or Aβ(1-42) for 6 or 24 hours, in the presence and absence of Fn, we imaged the cells with a camera attached to an inverted microscope to study the morphological changes. The untreated monocytes have a rounded morphology with no protrusions emanating from the cell body (Fig. 4.4A). Following a 6 hour exposure to PMA or Aβ(1-42) in the absence of Fn, subtle changes became noticeable in the cells. A few of the cells were beginning to elongate and spread (Fig. 4.4 B,C). More spreading and elongation was seen in the cells treated in

A

B
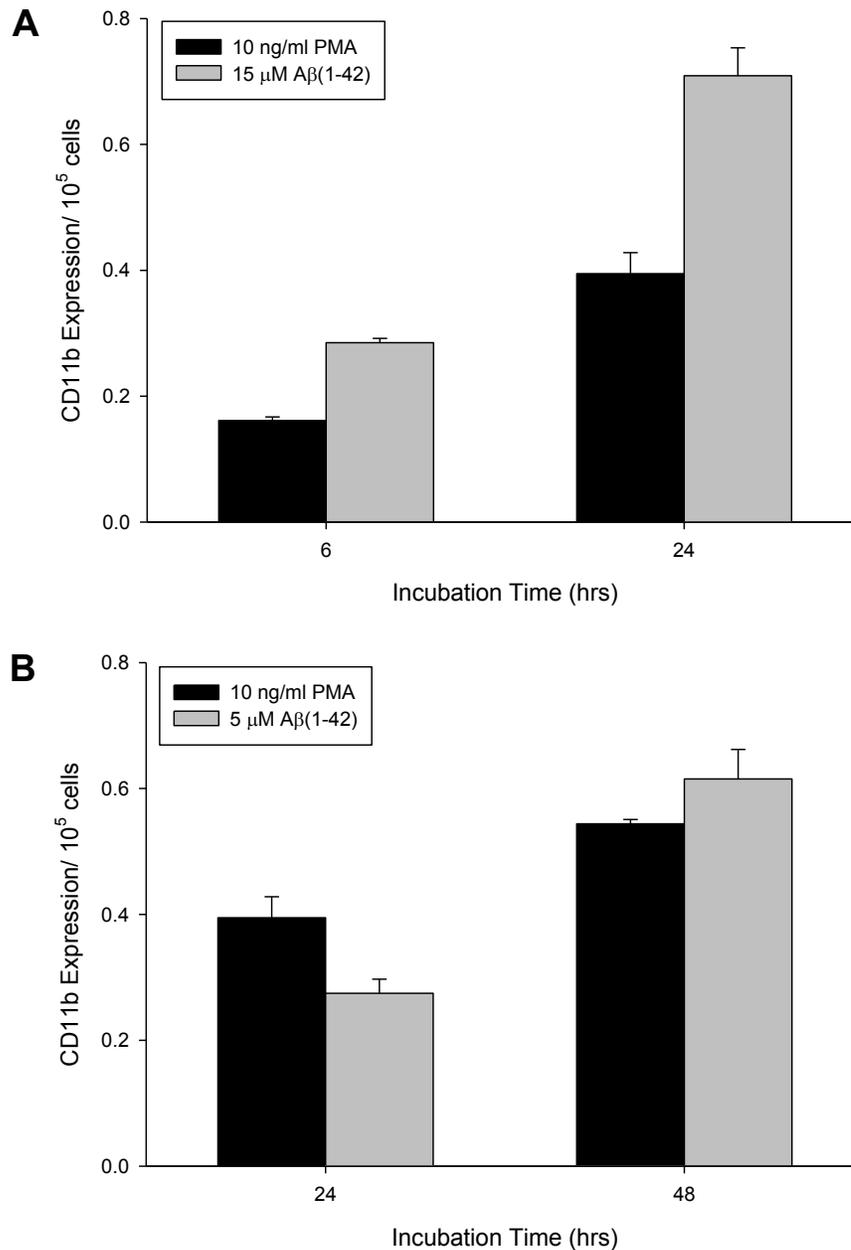
Fig. 4.3 Cell surface CD11b expression in adherent monocytes
Wells of a sterile 48-well plate were pre-coated with 5 μg of Fn to ensure cell adherence. A) THP-1 monocytes were treated with 10 ng/ml PMA or 15 μM freshly reconstituted Aβ(1-42) for 6 or 24 hours at 37°C. SE bars were calculated from n=5 trials for all data points. B) THP-1 monocytes were treated with 10 ng/ml PMA or 5 μM freshly reconstituted Aβ(1-42) for 24 or 48 hours at 37°C. SE bars were calculated from n= 5 (PMA, 24) and 2 for all other treatments. Following incubation, adhering cells were analyzed for expression of the cell surface receptor CD11b as described in the methods. The expression was normalized using the number of adhering cells.
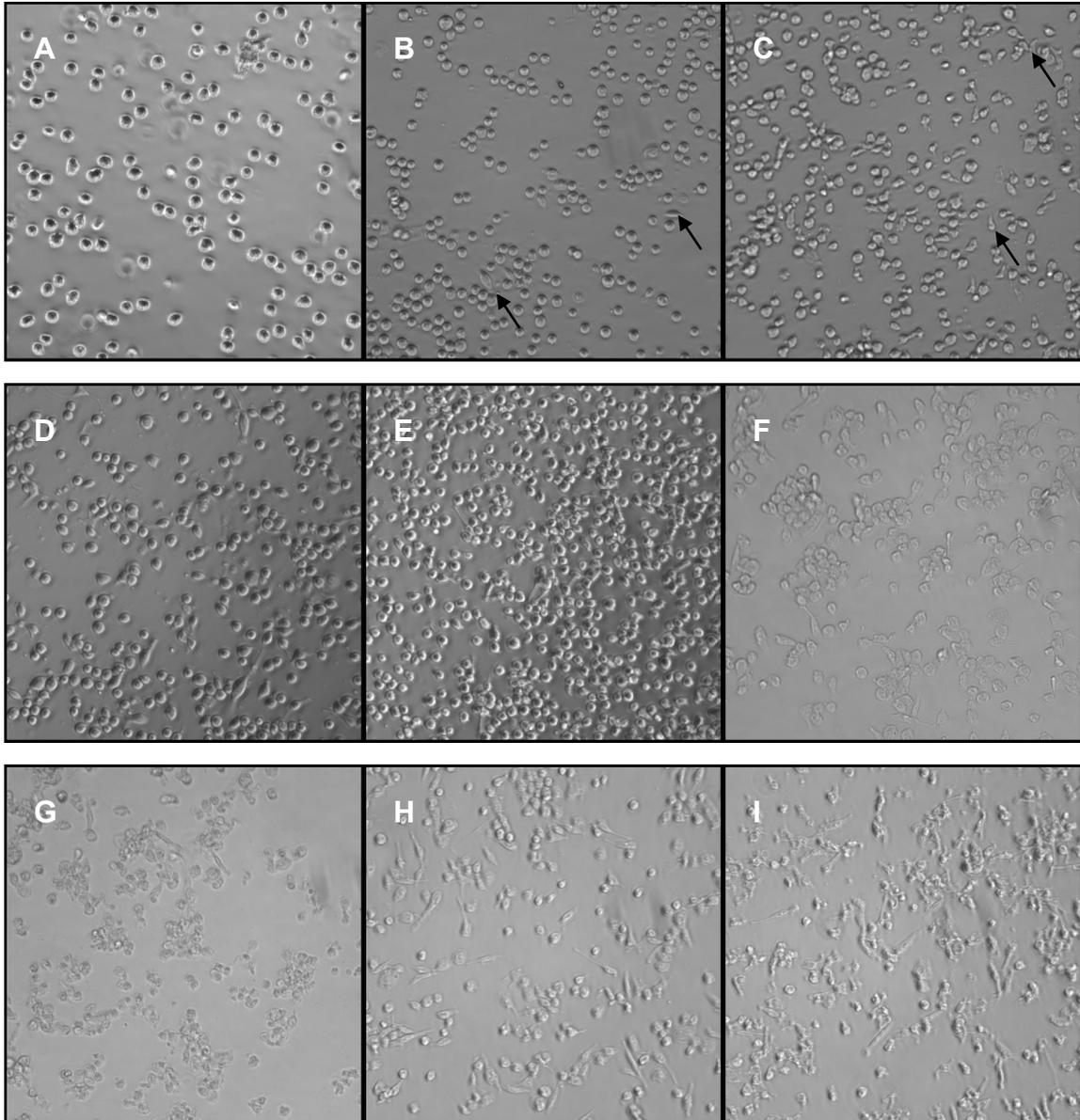
Fig. 4.4 Study of morphological changes induced in treated THP-1 monocytes
THP-1 cells were treated with 10 ng/ml PMA or 15 μM Ab(1-42) in the presence or absence of Fn. Following the incubation with effectors, the non-adherent cells were removed and pictures were taken of the adherent cells. A) Untreated THP-1 Monocytes B) 6 hour PMA treatment -Fn C) 6 hour Aβ treatment -Fn D) 6 hour PMA treatment +Fn E) 6 hour Aβ treatment +Fn F) 24 hour PMA treatment -Fn G) 24 hour Aβ treatment -Fn H) 24 hour PMA treatment +Fn I) 24 hour Aβ treatment +Fn. Arrows indicate early morphological changes.

Fn coated wells (Fig. 4.4 D,E). Many of the cells still maintained their rounded mor-

phology after a 6 hour treatment. However, following a 24 hour incubation with either

PMA or Aβ(1-42), most of the cells appeared morphologically distinct from the parent

monocytes (Fig. 4.4 F-I). Again the cells treated in the presence of Fn showed a higher

degree of spreading. It is interesting to note that in all cases the Aβ treated cells ap-

peared to transform somewhat differently than the PMA treated cells, but nevertheless

exhibited the morphological changes associated with differentiation.

We also studied the effect of PMA and Aβ(1-42) treatments on cell proliferation,

in the absence of Fn, because the transformation from monocyte to macrophage is

known to be accompanied by an arrest in the cell cycle (Schwende et al., 1996; Ding et

al., 2007). We treated THP-1 cells with 10 ng/ml PMA or 15 μM Aβ(1-42) at either 0 or

168 hours of aggregation for 6, 24 and 48 hours. At each time point all of the cells in the

wells were counted using trypan blue exclusion. None of the treatments lead to an in-

crease in total cell count (Fig. 4.5A). Even treatment with 168 hour Aβ(1-42), which

does not induce adherence in the cells (Fig. 3.4A), led to an arrest of proliferation.

There was a noticeable decrease in the cell count at 24 hours of the cells treated

with freshly reconstituted Aβ. The counts included all of the cells, living and dead, so

we quantitated the percentage of the cells that were viable based upon trypan blue exclu-

sion. At the time where we saw a decrease in cell count, we found a corresponding de-

crease in the percentage of the cells that were viable (Fig. 4.5B). The treatment with 168

hour Aβ showed no changes in viability over the course of the experiment, but the vi-

ability was decreased compared to PMA treated cells at all time points.

To clarify the results of the trypan blue exclusion assay, we used XTT to test the

A

B
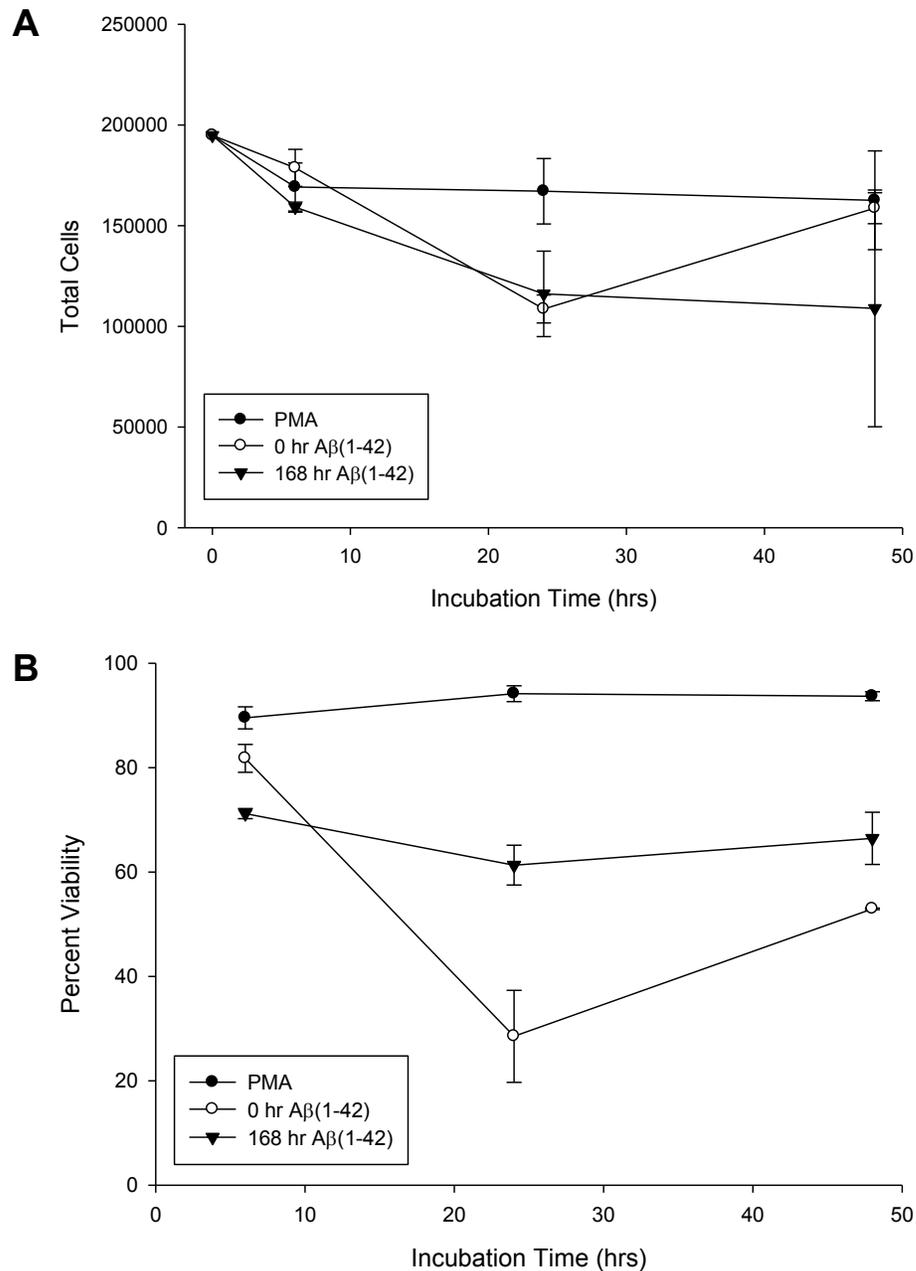
Fig 4.5 PMA and Aβ treatments decrease THP-1 cellular proliferation
THP-1 cells were treated with 10 ng/ml PMA or 15 μM Aβ(1-42) aggregated 0, or 168 hours. A) At the times indicated, the living and dead cells in each sample were counted using trypan blue exclusion and total number of cells reported. SE bars are for n= 2 (Aβ, 0 & 168 hours) or 3 (PMA). Cell counts were adjusted to the same starting count. B) At the times indicated, the living and dead cells in each sample were counted using trypan blue exclusion and percent of living cells reported. SE bars are for n= 2 (Aβ, 0 & 168 hours) or 3 (PMA).

metabolic activity of the adherent cells derived from PMA or Aβ treatment. An increase in the amount of XTT reduced indicates an increase in metabolic activity (Scudiero et al., 1988). The cells that were treated with PMA, 15 μM Aβ(1-42) or 5 μM Aβ(1-42) for 24 hours all showed an increase in XTT reduction over the background absorbance of XTT in the absence of cells (Fig. 4.6A) despite the decrease in viability seen with the trypan blue exclusion assay. Likewise, the XTT reduction from the 48 hour PMA and 5 μM Aβ(1-42) samples were both above the background (Fig. 4.6B). Although the XTT reduction by the cells treated with PMA for 48 hours is above the baseline, it is a lower amount of reduction than the cells that were only treated for 24 hours, which suggests that longer exposure to PMA may be detrimental to the cells. Both experiments indicate that Aβ treatment can increase the metabolism of the cells more than PMA treatment.

4.3 Discussion

The differentiation of monocytic cells into microglia may play an important role in AD pathogenesis. Markers of the differentiation process include upregulation of β2 integrins like CD11b, cell adherence, arrest of cellular proliferation and morphological changes (Tsuchiya et al., 1982; Schwende et al., 1996; Ding et al., 2007). We have previously shown that early-formed Aβ(1-42) aggregation intermediates can induce adherence in THP-1 monocytes as potently as PMA (Crouse et al., 2009) (Chapter 3). Although one piece of the puzzle, the adherent phenotype alone is not enough to consider the cells differentiated into macrophages, we have analyzed several of the other aspects of the differentiation process to confirm the transformation of the cells.

A

B
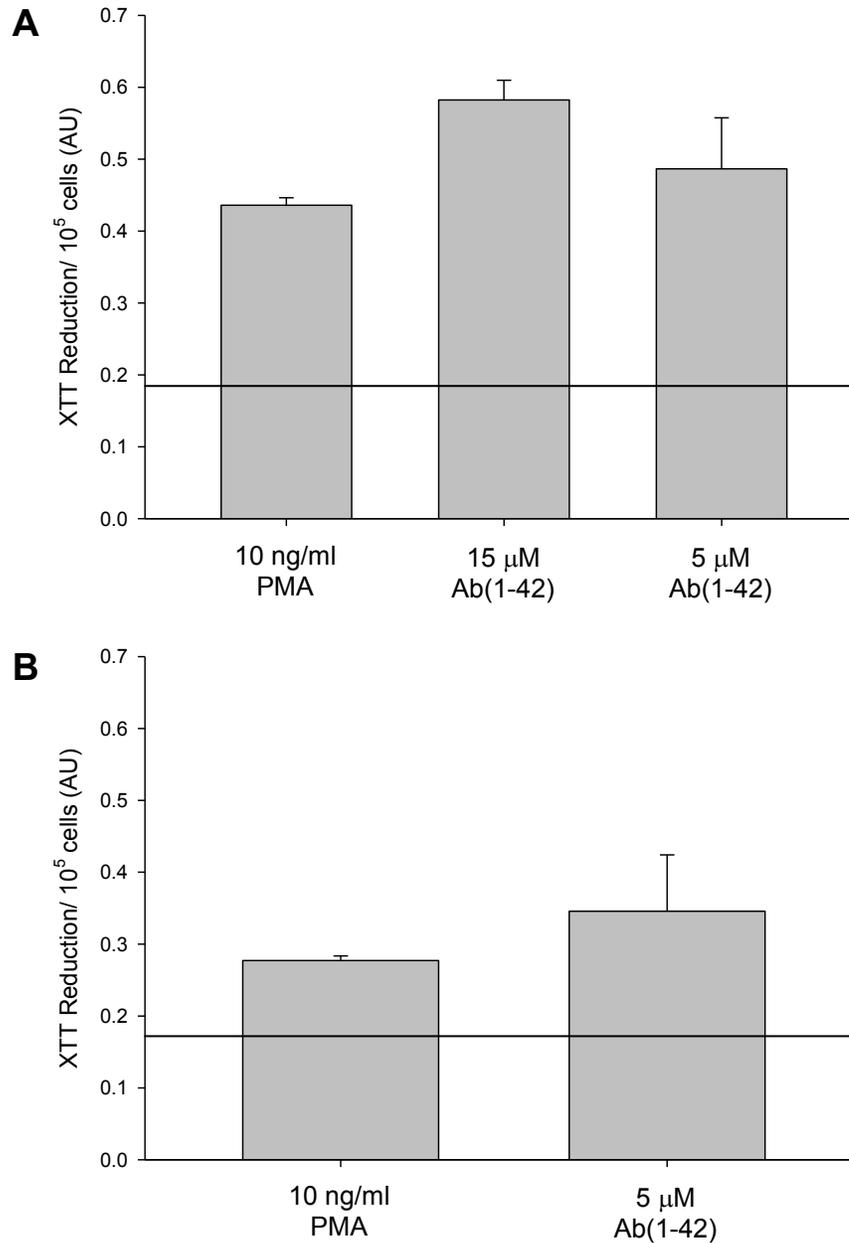
Fig. 4.6 XTT reduction from adherent THP-1 monocytes
THP-1 cells were treated for A) 24 or B) 48 hours with the concentrations of effectors listed. Following the incubation the non-adherent cells were removed and the adherent cells were treated with 0.33 mg/ml XTT/ 8.3 μM PMS for 3 hours and analyzed as described in the methods. SE bars are for n= 2 (5 μM Aβ, 24 and 48 hours, and PMA, 48 hours) and 4 (15 μM Aβ, 24 hours and PMA, 24 hours). Line indicates background absorbance of XTT in the absence of cells.

Schwende et al. have analyzed THP-1 cells treated with PMA for many of the markers of differentiation. Their results found that 87% of the cells treated with PMA expressed CD11b on their surface while only 55% of cells treated with Vitamin D3 and less than 10% of control cells expressed the marker. They also found that PMA induces an almost complete arrest of proliferation (Schwende et al., 1996).

Our results are similar to those of Schwende in that the PMA treated cells express CD11b. We were surprised to find that cells treated with 15 μM Aβ(1-42) for 6 and 24 hours expressed more CD11b on their surface (Fig. 4.3A). It is possible that because Aβ and PMA function through different pathways (Fig. 3.11), the upregulation of CD11b will also be induced differently.

The use of Fn coated plates allowed us to study the effects of a lower Aβ treatment concentration on the cells because of the added stability towards the cells. The 5 μM Aβ(1-42) treatment induced less CD11b than PMA with a 24 hour exposure, but more than PMA after a 48 hour treatment (Fig. 4.3B). Because of the lower concentration, it appears to take longer for the effects of Aβ on the cells to be seen, which is probably why without Fn pre-treatment, the cells treated with 5 μM Aβ did not adhere (Fig. 3.5). The lower Aβ treatment concentration also did not appear to have much effect on the amount of XTT reduction. The cells treated with 5 μM Aβ metabolized similar amounts of XTT as the PMA treated cells after both 24 and 48 hour exposures (Fig. 4.6).

The XTT reduction profile of the 15 μM Aβ treated cells is distinct from those of the 5 μM Aβ and PMA treated cells. Following a 24 hour exposure to the 15 μM Aβ, the cells reduced more XTT than with the other treatments (Fig. 4.6A). Many previous stud-

ies have shown that soluble Aβ species are toxic to cells (Koistinaho et al., 2001; Walsh et al., 2002), so we expected a decrease in XTT reduction. Our hypothesis is that the cells may actually be stressed and have increased their metabolism in response to the insult from Aβ.

Support for this theory can be found in the trypan blue exclusion data. Following a 24 hour exposure to 15 μM Aβ, there was a marked decrease in the percentage of living cells, which then increases after 48 hours, although the viability at 48 hours is still decreased with respect to a 6 hour treatment (Fig. 4.5B). The loss of viability correlated with a decrease in total cell count after 24 and 48 hours with the Aβ (Fig. 4.5A). We have observed that when the THP-1 cells die, they can fall apart into fragmented sections, which can make it impossible for them to be counted and thus giving a decrease in overall cell number. The stressed cells in the XTT experiment may be on the verge of death, much like those in the trypan blue assay.

Tsuchiya et al. described morphological changes that take place in THP-1 monocytes upon differentiation with phorbol esters. In general the cells become flatter and less rounded. They develop protrusions from the cell body and internal vacuoles (Tsuchiya et al., 1982).

Our cells showed significant morphological changes, both in the absence and presence of Fn, which suggest they are adopting a macrophage-like phenotype (Fig. 4.4). The PMA treated cells become elongated with smooth bodies. They develop extensions protruding from the cell body that are increased with longer exposure to the PMA or in the presence of Fn.

When compared to the Aβ treated cells, the PMA cells seem to transform into a

similar but distinct morphology. Where the PMA treated cells have smooth bodies after 24 treatments, the Aβ treated cells appear rough and irregular. A likely explanation for the difference is the previously noted potential for Aβ to be toxic. Although the cells are changing their phenotype in response to the Aβ treatment, they may not be healthy and so the transformation is not ideal.

When taken together, the data all seems to indicate that treatment with Aβ(1-42) is indeed differentiating the THP-1 cells into macrophages. The cells undergo similar changes when treated with PMA and Aβ, but in many cases the Aβ treated cells appear to be somewhat stressed or compromised, possibly due to the toxic nature of Aβ. While significant, our findings are incomplete.

A true measure of the transformation from monocytes to macrophages will include an increase in phagocytic ability by the newly differentiated cells. Schwende, Tsuchiya and others utilized phagocytosis by PMA treated THP-1 cells as a functional measure of monocyte differentiation into macrophages (Tsuchiya et al., 1982; Schwende et al., 1996; Yamaguchi et al., 2002; Shiratsuchi and Basson, 2005; Lee et al., 2007; Ustyugova et al., 2007). This type of assay, will allow us to determine if the adherent cells transformed in response to Aβ are fully functioning macrophages. In the future we intend to strengthen our current findings with the addition of a phagocytosis study.

4.4 Bibliography

Banati RB, Gehrmann J, Schubert P, Kreutzberg GW (1993) Cytotoxicity of microglia. Glia 7:111-118.

Banchereau J, Steinman RM (1998) Dendritic cells and the control of immunity. Nature 392:245-252.

Bauer J, Sminia T, Wouterlood FG, Dijkstra CD (1994) Phagocytic activity of macrophages and microglial cells during the course of acute and chronic relapsing experimental autoimmune encephalomyelitis. J Neurosci Res 38:365-375.

Benoit M, Desnues B, Mege JL (2008) Macrophage polarization in bacterial infections. J Immunol 181:3733-3739.

Crouse NR, Ajit D, Udan ML, Nichols MR (2009) Oligomeric amyloid-beta(1-42) induces THP-1 human monocyte adhesion and maturation. Brain Res 1254:109-119.

Davoust N, Vuaillat C, Androdias G, Nataf S (2008) From bone marrow to microglia: barriers and avenues. Trends Immunol 29:227-234.

Ding Q, Jin T, Wang Z, Chen Y (2007) Catalase potentiates retinoic acid-induced THP-1 monocyte differentiation into macrophage through inhibition of peroxisome proliferator-activated receptor gamma. J Leukoc Biol 81:1568-1576.

Gordon S, Taylor PR (2005) Monocyte and macrophage heterogeneity. Nat Rev Immunol 5:953-964.

Heneka MT, O'Banion MK (2007) Inflammatory processes in Alzheimer's disease. J Neuroimmunol 184:69-91.

Hynes RO (2002) Integrins: bidirectional, allosteric signaling machines. Cell 110:673-687.

Koistinaho M, Ort M, Cimadevilla JM, Vondrous R, Cordell B, Koistinaho J, Bures J, Higgins LS (2001) Specific spatial learning deficits become severe with age in beta -amyloid precursor protein transgenic mice that harbor diffuse beta -

amyloid deposits but do not form plaques. Proc Natl Acad Sci U S A 98:14675-14680.

Kounalakis NS, Corbett SA (2006) Lipopolysaccharide transiently activates THP-1 cell adhesion. J Surg Res 135:137-143.

Le Y, Gong W, Tiffany HL, Tumanov A, Nedospasov S, Shen W, Dunlop NM, Gao JL, Murphy PM, Oppenheim JJ, Wang JM (2001) Amyloid (beta)42 activates a G-protein-coupled chemoattractant receptor, FPR-like-1. J Neurosci 21:RC123.

Lee JS, Nauseef WM, Moeenrezakhanlou A, Sly LM, Noubir S, Leidal KG, Schlomann JM, Krystal G, Reiner NE (2007) Monocyte p110alpha phosphatidylinositol 3-kinase regulates phagocytosis, the phagocyte oxidase, and cytokine production. J Leukoc Biol 81:1548-1561.

Mackaness GB (1964) The Immunological Basis Of Acquired Cellular Resistance. J Exp Med 120:105-120.

Mayadas TN, Cullere X (2005) Neutrophil beta2 integrins: moderators of life or death decisions. Trends Immunol 26:388-395.

McGeer PL, Itagaki S, Tago H, McGeer EG (1987) Reactive microglia in patients with senile dementia of the Alzheimer type are positive for the histocompatibility glycoprotein HLA-DR. Neurosci Lett 79:195-200.

Reya T, Morrison SJ, Clarke MF, Weissman IL (2001) Stem cells, cancer, and cancer stem cells. Nature 414:105-111.

Ruoslahti E, Pierschbacher MD (1987) New perspectives in cell adhesion: RGD and integrins. Science 238:491-497.

Schwende H, Fitzke E, Ambs P, Dieter P (1996) Differences in the state of differentiation of THP-1 cells induced by phorbol ester and 1,25-dihydroxyvitamin D3. J Leukoc Biol 59:555-561.

Scudiero DA, Shoemaker RH, Paull KD, Monks A, Tierney S, Nofziger TH, Currens MJ, Seniff D, Boyd MR (1988) Evaluation of a soluble tetrazolium/formazan assay for cell growth and drug sensitivity in culture using human and other tumor cell lines. Cancer Res 48:4827-4833.

Shiratsuchi H, Basson MD (2005) Activation of p38 MAPKalpha by extracellular pressure mediates the stimulation of macrophage phagocytosis by pressure. Am J Physiol Cell Physiol 288:C1083-1093.

Tsuchiya S, Kobayashi Y, Goto Y, Okumura H, Nakae S, Konno T, Tada K (1982) In-

duction of maturation in cultured human monocytic leukemia cells by a phorbol diester. Cancer Res 42:1530-1536.

Udan ML, Ajit D, Crouse NR, Nichols MR (2007) Toll-like receptors 2 and 4 mediate Abeta(1-42) activation of the innate immune response in a human monocytic cell line. J Neurochem.

Ustyugova IV, Frost LL, Van Dyke K, Brundage KM, Schafer R, Barnett JB (2007) 3,4-dichloropropionaniline suppresses normal macrophage function. Toxicol Sci 97:364-374.

Van Furth R, Diesselhoff-den Dulk MC, Mattie H (1973) Quantitative study on the production and kinetics of mononuclear phagocytes during an acute inflammatory reaction. J Exp Med 138:1314-1330.

Volkman A, Gowans JL (1965a) The Origin Of Macrophages From Bone Marrow In The Rat. Br J Exp Pathol 46:62-70.

Volkman A, Gowans JL (1965b) The Production Of Macrophages In The Rat. Br J Exp Pathol 46:50-61.

Walsh DM, Klyubin I, Fadeeva JV, Cullen WK, Anwyl R, Wolfe MS, Rowan MJ, Selkoe DJ (2002) Naturally secreted oligomers of amyloid beta protein potently inhibit hippocampal long-term potentiation in vivo. Nature 416:535-539.

Yamaguchi H, Haranaga S, Widen R, Friedman H, Yamamoto Y (2002) Chlamydia pneumoniae infection induces differentiation of monocytes into macrophages. Infect Immun 70:2392-2398.

5. EFFECT OF Aβ IN A MODEL OF CAA

5.1 Introduction

AD pathology includes the deposition of Aβ plaques in the brains of afflicted patients. In addition to the brain deposition, over 80 percent of AD sufferers experience a condition known as CAA (Joachim et al., 1988; Vinters et al., 1996; Jellinger, 2002; Attems et al., 2008). Studies of AD cases involving CAA have suggested that increased vascular deposition may correlate with an increase in cognitive deficits (Pfeifer et al., 2002).

In CAA, Aβ deposits in the vasculature of the brain, which can lead to fibrinoid necrosis, microannurisms, hemorrhages and infarctions (Vinters and Gilbert, 1983; Mandybur, 1986; Vinters, 1987; Vonsattel et al., 1991; Greenberg and Vonsattel, 1997; Thal et al., 2008). Studies of cultured human SMCs show production of cytokines following Aβ treatment (Suo et al., 1998), which correlates to *in vivo* findings of increased TNFα expression in AD brain vessels (Grammas and Ovase, 2001). A separate study showed the co-localization of cAMP with vascular Aβ deposits in AD patients (Martinez et al., 2001).

Increased levels of cyclic adenosine monophosphate (cAMP) production have been shown to modulate the levels of TNFα *in vitro* (Kunkel et al., 1988; Schade and

Schudt, 1993; Sinha et al., 1995). In the presence of TNFα, human myometrium shows an increase in AC (Gogarten et al., 2003). These findings seem to substantiate the concept of cAMP serving as a gatekeeper for inflammation (Jin and Conti, 2002) and suggest a potential connection between cAMP and AD related inflammation.

In this study we investigate the effects of Aβ on HA-VSMC and THP-1 cells. We attempt to elucidate the role of cAMP in the inflammation and toxicity pathways involved in Aβ treatment of these cells.

5.2 Results

5.2.1 Development of cAMP Immunoassay

In order to be able to monitor the production of cAMP produced in the cells, we designed competition based immunoassay similar to the commercially available DELFIA kit produced by Perkin Elmer. The methodology of the assay works as described in the Methods. Briefly, cAMP from a sample competes with a Europium tagged cAMP tracer complex for the binding sites on a polyclonal anti-cAMP antibody. Following binding, an Enhancement Solution dissociates the Eu from the cAMP allowing the Eu to form a chelation complex with some components of the Enhancement Solution. The time-resolved fluorescence of the Eu complex can then be measured.

The following is an explanation of the substitutions we made to the DELFIA protocol. We were able to successfully replace the pre-coated yellow plate provided in the DELFIA kit with a white Greiner fluorescence plate in which we coated the plate

with a capture antibody. This was done by overnight incubation at room temperature with 200 μL of 10 μg/ml goat-raised anti-rabbit IgG. The wells were blocked for 1 hour at room temperature with PBS containing 1% BSA, 5% sucrose and 0.05% NaN$_3$. The Perkin Elmer wash buffer was replaced with PBS containing 0.05% Tween 20. The Perkin Elmer anti-cAMP serum was successfully replaced with anti-cAMP, which was obtained from Purdue University (Nichols and Morimoto, 1999). We were also able to substitute 20 mM Tris containing 150 mM NaCl, 0.1% BSA and 0.05% Tween 20 for the provided Perkin Elmer Assay Buffer and the Perkin Elmer cAMP Buffer for Standards. The Perkin Elmer cAMP standards were also substituted using cAMP purchased from Sigma Aldrich.

We were unable to find suitable replacements for the Eu tracer. We did prepare a cAMP-HRP conjugate (Lombardi and Schooley, 2004) to use as a competitor for the cAMP in the samples, but it did not function as well as expected. The Enhancement Solution was proprietary and the components are not available. The Perkin Elmer Victor plate reader was required for optimal sensitivity. A comparison of the results from the two methods can be seen in figure 5.1. Despite our assay development, all of the cellular samples were analyzed using the DELFIA methodology.

5.2.2 Effect of cAMP on TNFα Production in HA-VSMC

For our model system, we chose to use HA-VSMC. These cells have been shown to produce similar levels of cytokines following Aβ treatment as the cerebral vascular smooth muscle cells (Suo et al., 1998). Aβ is also capable of inducing toxicity in
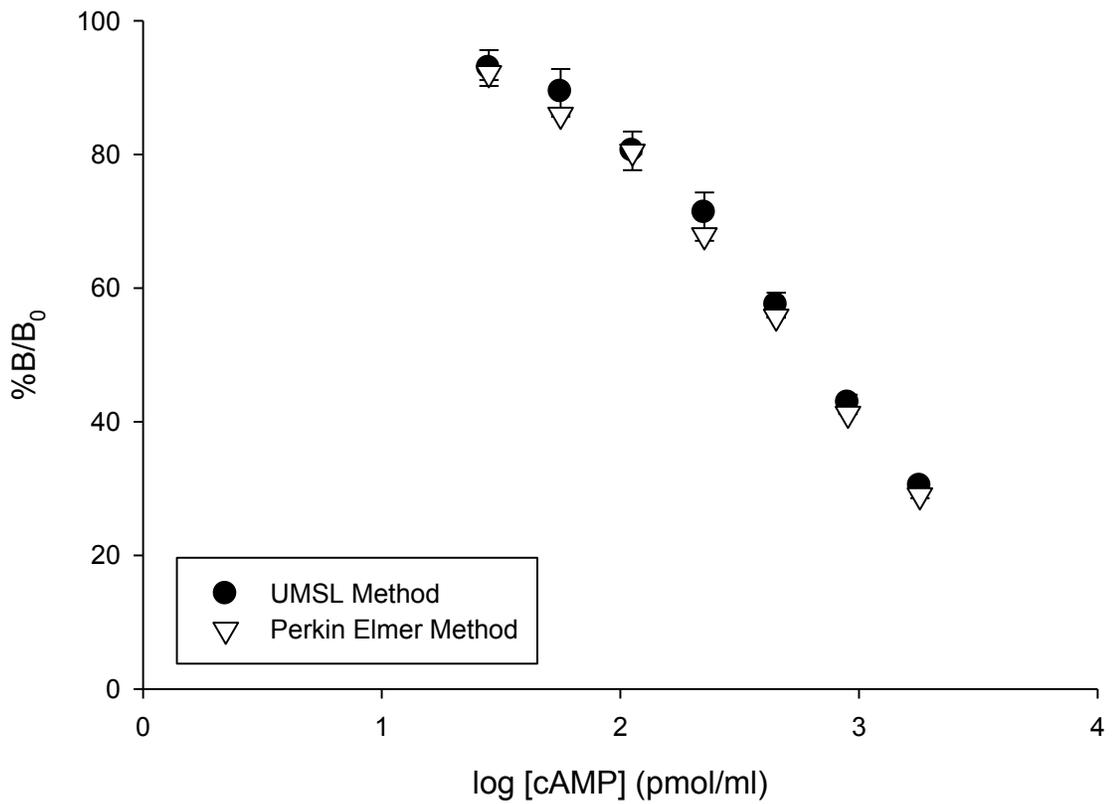
Fig. 5.1 Modifications to the DELFIA protocol are as effective as the original method
cAMP standards were prepared and analyzed using either the UMSL developed protocol (filled circles) or the Perkin Elmer DELFIA kit (open triangles). Data is presented as the % of cAMP binding in sample (B) over cAMP binding in blank (B_0) versus the log of the cAMP concentration. Error bars are standard error for n=3 trials of each method.

both cell lines in a similar manner (Wang et al., 2000).

To test the ability of cAMP to attenuate TNFα production, cells were treated with either IBMX, Fsk or a combination of both to raise the levels of cAMP in the cells. IBMX is a phosphodiesterase inhibitor, thus blocking the degradation of cAMP (Kelley et al., 2008) while Fsk is an AC activator which increases the production of cAMP (Seamon et al., 1981). THP-1 cells are faster to grow and easier to work with than HA-VSMC, making them an ideal cell line to use for some of our control experiments. We used THP-1 cells to confirm the increase of cAMP upon treatment with the cAMP elevators because they are easier and faster to grow and analyze. Treating the cells with a combination of 300 μM IBMX and 100 μM Fsk for as little as 15 minutes increases the amount of cAMP from 40.37 ± 1.34 pmol/ml to 146.09 ± 2.67 pmol/ml (Fig. 5.2). Similar increases over control treatments are seen at 60, 120, 240 and 360 minutes of treatment with the cAMP elevators.

We also tested the effect of LPS to induce cAMP production in THP-1 cells in the presence and absence of IBMX and Fsk. In our experiments, the LPS treatment did not induce an increase in cAMP (Fig. 5.3). Also, when IBMX or Fsk were used either alone or with LPS treatment, there was no significant increase in cAMP production. However, when the cells were treated with both IBMX and Fsk in the presence or absence of LPS, a dramatic increase in the levels of cAMP was noted.

5.2.3 Effect of cAMP on Aβ induced toxicity in HA-VSMC

We then moved our studies to the effect of Aβ treatments on HA-VSMC. Before
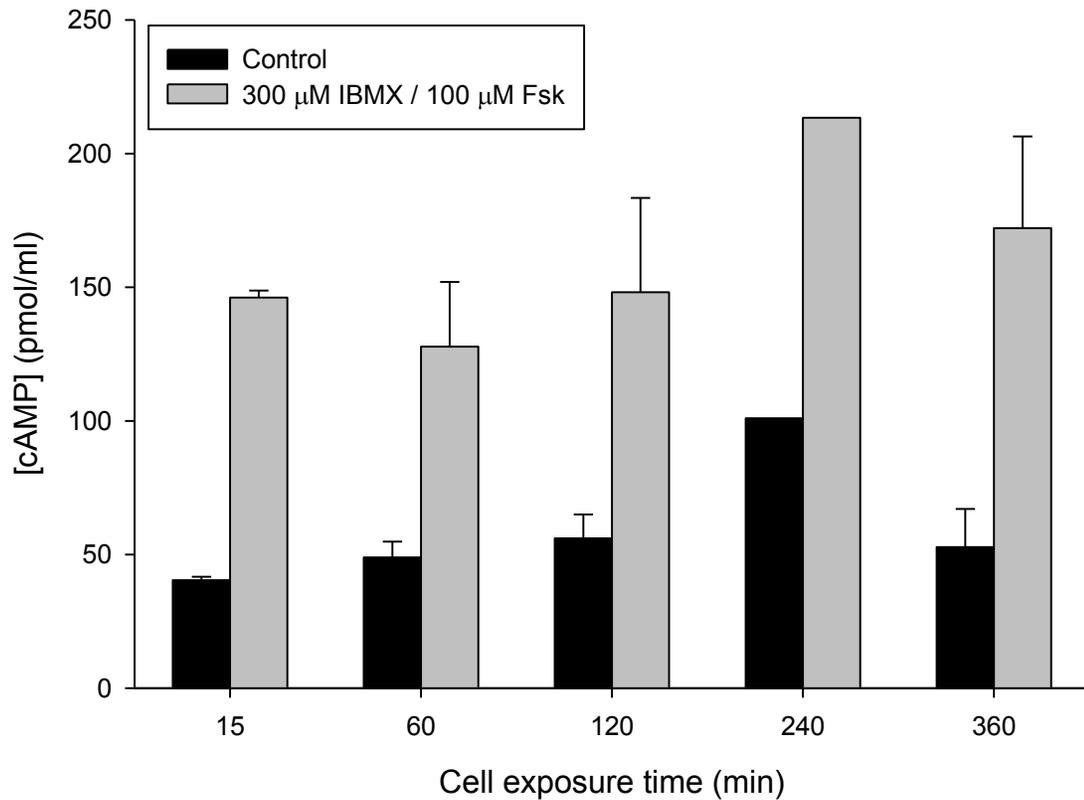
Fig. 5.2 Effect of IBMX and Fsk treatment on cAMP levels in THP-1 monocytes
THP-1 cells were prepared in assay medium and 290 mL was plated into wells of a sterile 48-well plate. The control cells were treated with 5 μL each of water and DMSO (black bars). The sample cells were treated with 5 μL of water, 2.5 μL of 36 mM IBMX and 2.5 μL of 12 mM Fsk to a final treatment concentration of 300 μM IBMX/ 100 μM Fsk. The cells were incubated for times indicated before being collected and analyzed for cAMP production as described in the methods. Data is the average ± standard error of n=6 (60, 360 minutes), 5 (15, 120 minutes) and 1 (240 minutes).
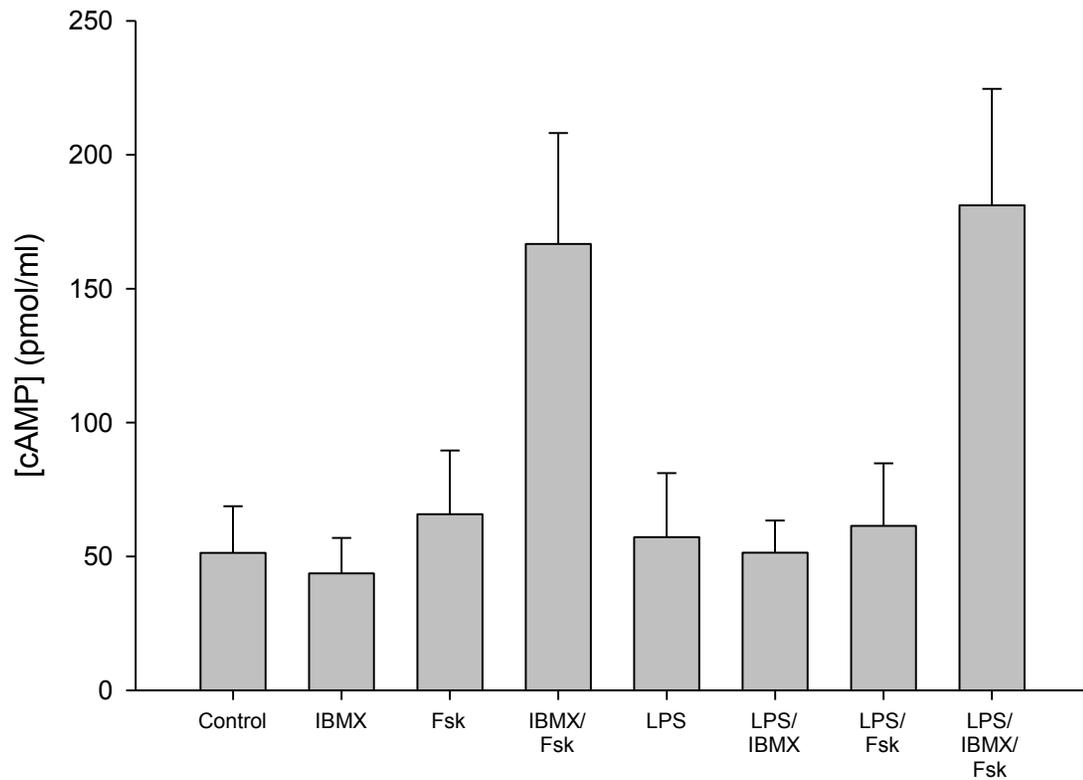
Fig. 5.3 Effect of IBMX and Fsk on LPS induced cAMP production in THP-1 cells
THP-1 cells were prepared in assay medium and 290 mL was plated into wells of a sterile 48-well plate. The control cells were treated with 5 μL each of water and DMSO. The sample cells were treated with 5 μL of 6 μg/ml LPS, 2.5 μL of 36 mM IBMX and 2.5 μL of 12 mM Fsk as indicated to achieve final treatment concentrations of 10 ng/ml LPS, 300 μM IBMX and 100 μM Fsk. The cells were incubated for 6 hours before being collected and analyzed for cAMP production as described in the methods. Data is the average ± standard error of n=5 experiments.

studying the effects of the IBMX and Fsk on Aβ treated cells, we first performed a series of control experiments to better understand how Aβ alone affects the cells. We tested the effect of Aβ(1-40) and Aβ(1-42) aggregation age as well as the effect of IBMX and Fsk concentrations on the viability of HA-VSMC.

The aggregation state of Aβ has been shown to be integral to its functions in the cells (Udan et al., 2007; Crouse et al., 2008), thus it was of interest to know if any particular aggregation species was more potent at inhibiting the cellular metabolism. We monitored the reduction of XTT by the cells following a 48 hour treatment with Aβ at different aggregation states. Freshly prepared Aβ(1-42) was able to inhibit 70.29 ± 4.77% of the HA-VSMC metabolism (Fig. 5.4). Although incubation of the peptide at 4°C for up to 48 hours was less toxic to the cells than freshly prepared Aβ(1-42), it was still capable of inhibiting the metabolic activity. However, aggregation for 72 − 144 hours did not inhibit, but rather slightly enhanced, the HA-VSMC metabolism of XTT.

To determine if all early Aβ aggregation states were toxic, we compared the effects of Aβ(1-42) and the slower aggregating Aβ(1-40) in HA-VSMC. The Aβ(1-42) was again toxic at early aggregation states as we previously observed. The Aβ(1-40), however, was not toxic at any stage, but rather enhanced the metabolism of the HA-VSMC (Fig. 5.5).

Before studying the regulation of on Aβ induced toxicity by IBMX and Fsk in HA-VSMC, we tested the concentration dependence of the compounds alone using HA-VSMC metabolism of XTT as a measure. Surprisingly, all of the concentrations of IBMX tested enhanced the metabolism of the treated cells compared to control cells (Fig. 5.6A). The effect does appear to level off around an IBMX concentration of 150
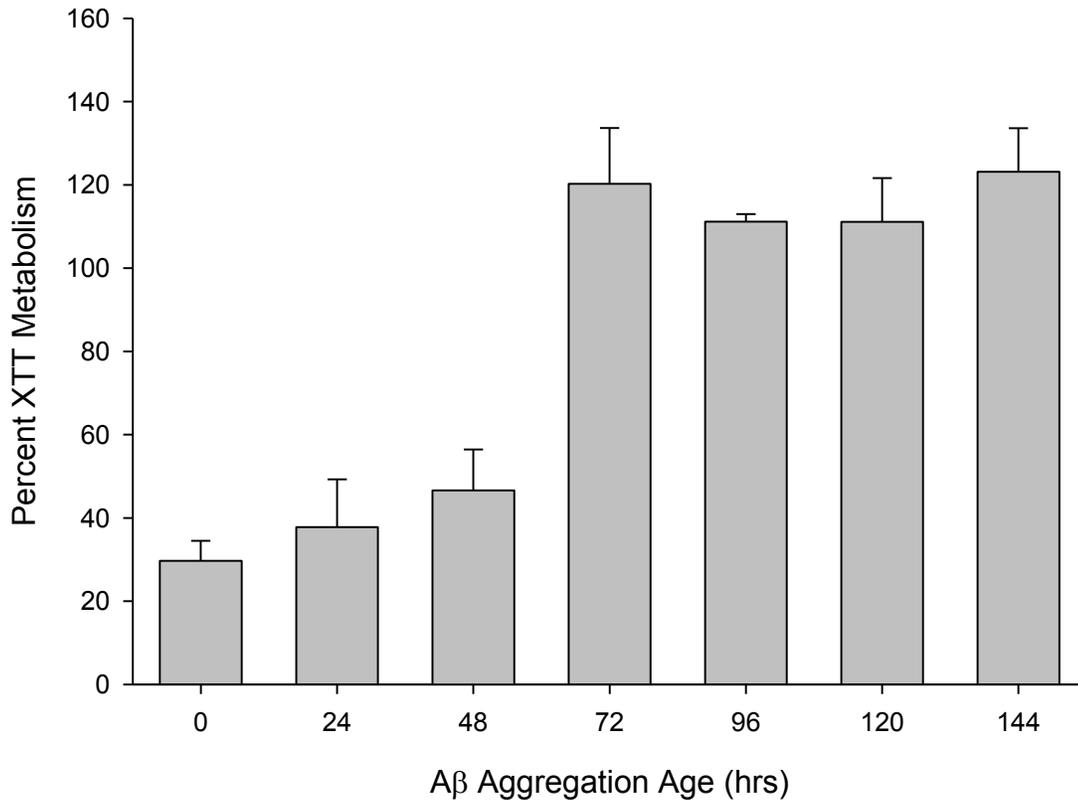
Fig. 5.4 Early formed Aβ(1-42) aggregation species are toxic to HA-VSMC

HA-VSMC were plated in 48-well plates and allowed to adhere for 24 hours. Aβ(1-42) was re-constituted in sterile water to 100 μM and incubated at 4°C. At the indicated times, cells were treated with 15 μM Aβ for 48 hours. Following the incubation, the medium was replaced with 0.33 mg/ml XTT/ 8.3 μM PMS for 3 hours. The absorbance of the XTT solution was read in a 96-well plate. The data was corrected to control cells treated only with water at each time point. Bars are average ± SE for n = 10 (0, 48 hrs), 4 (120 hrs), 3 (24, 96, 144 hrs) and 2 (72 hrs).
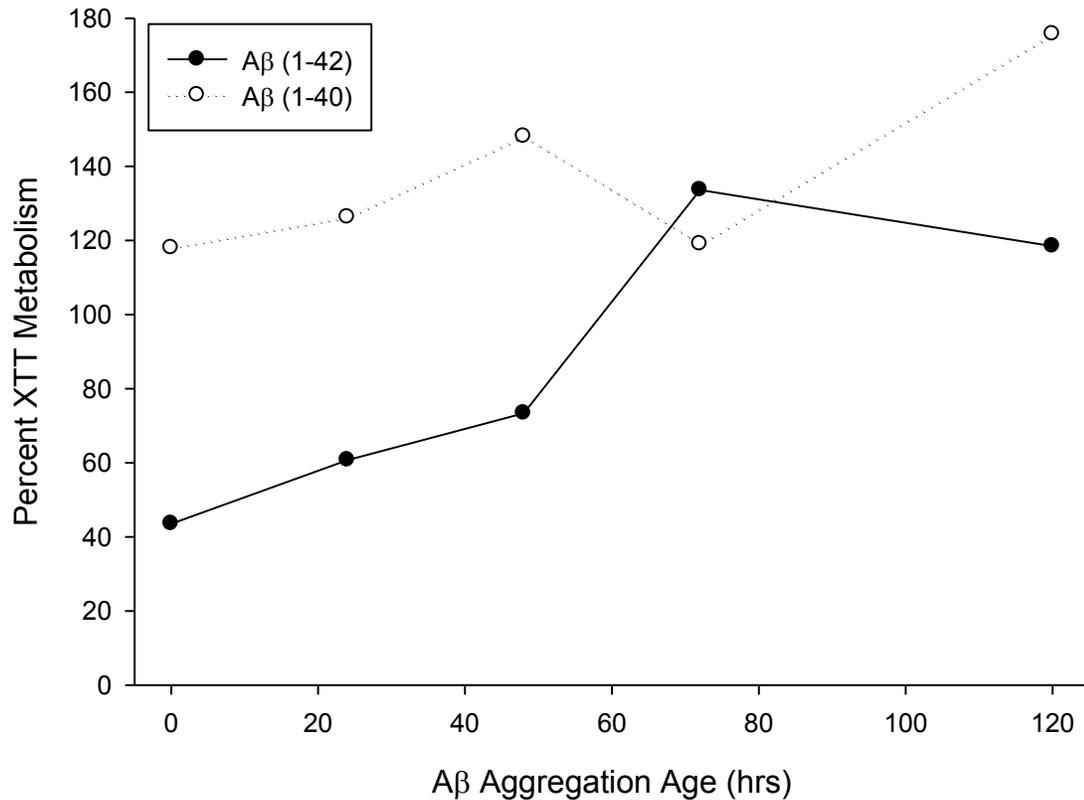
Fig. 5.5 Aβ (1-42), but not Aβ(1-40) inhibits HA-VSMC metabolism of XTT
HA-VSMC were plated in 48-well plates and allowed to adhere for 24 hours. Aβ (1-40) and Aβ(1-42) was reconstituted in sterile water to 100 μM and incubated at 4°C. At the indicated times, cells were treated with 15 μM Aβ for 48 hours. Following the incubation, the medium was replaced with 0.33 mg/ml XTT/ 8.3 μM PMS for 3 hours. The absorbance of the XTT solution was read in a 96-well plate. The data was corrected to control cells treated only with water at each time point. Data is one trial from one experiment.

Fig. 5.6 Treatment with varying concentrations of IBMX and/or Fsk increase HA-VSMC metabolism

HA-VSMC were plated in 48-well plates and allowed to adhere for 24 hours before treatment with cAMP elevating agents. A) Cells were treated with varying volumes of 1.1 or 9 mM IBMX to reach the final concentrations indicated. B) Cells were treated with varying volumes of 0.75 or 6 mM Fsk to reach the final concentrations indicated. C) Cells were treated with varying volumes of 1.1 or 9 mM IBMX and 0.75 or 6 mM Fsk to reach the concentrations indicated. All treated cells were incubated for 48 hours. Following incubation, the medium was replaced with 0.33 mg/ml XTT/ 8.3 μM PMS for 3 hours. The absorbance of the XTT solution was read in a 96-well plate. Bars are the average ± SE for n = 2 trials from 2 separate experiments.
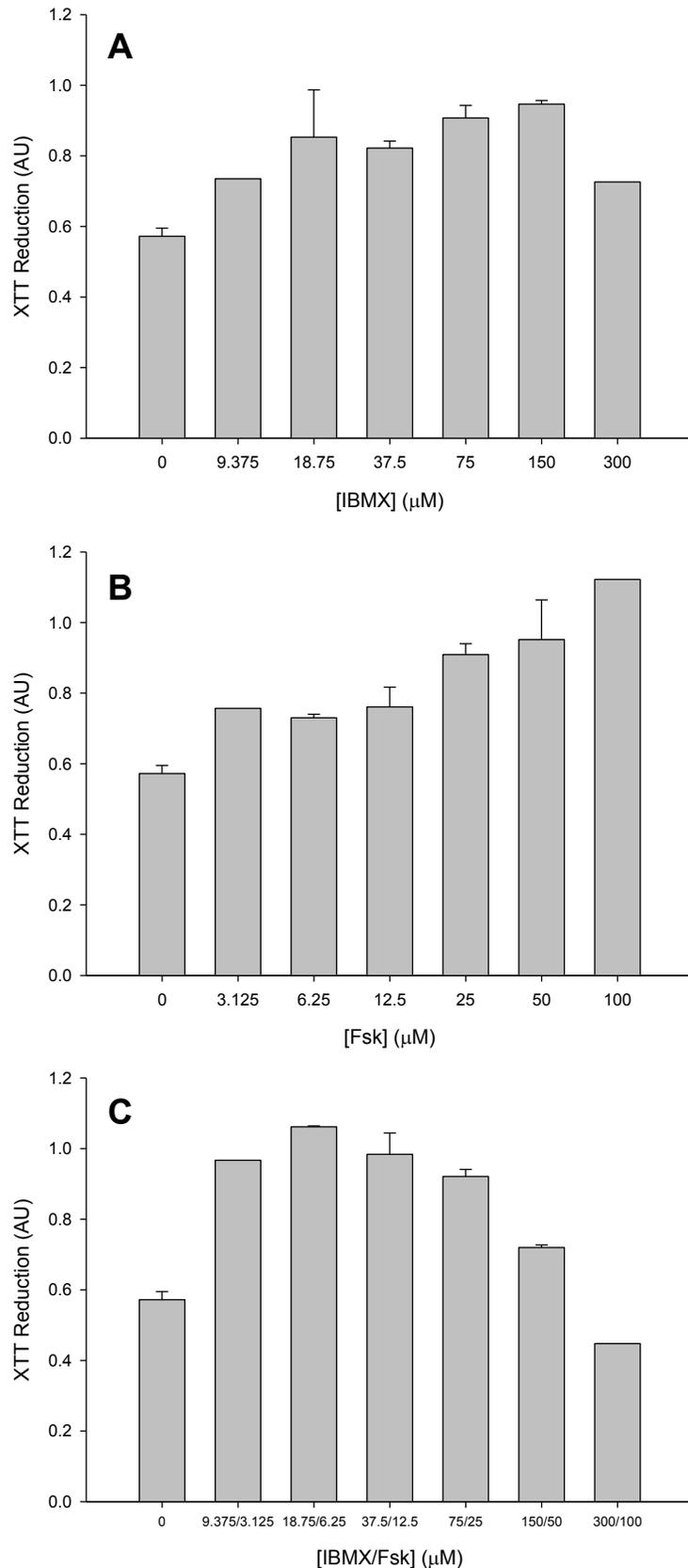
μM and drop somewhat at 300 μM. Similarly, all Fsk concentrations tested increased the reduction of XTT (Fig. 5.6B). Unlike with the IBMX treatment, the enhancement is concentration dependent across the range studied. We also tested concentrations of the combination of IBMX and Fsk together. The greatest metabolic enhancement was seen when the cells were treated with 18.75 μM IBMX and 6.25 μM Fsk (Fig. 5.6C). The other treatment combinations showed slightly lower enhancement with the exception of the 300 μM IBMX/ 100 μM Fsk combination, which appeared to be slightly toxic.

We next tested the ability of IBMX and Fsk to rescue the HA-VSMC from Aβ(1-42) induced toxicity. The cells were treated with freshly prepared Aβ(1-42) for 48 hours in the presence or absence of 75 μM IBMX, 25 μM Fsk or both 75 μM IBMX and 25 μM Fsk. Treatment with Aβ alone resulted in only 55.53 ± 5.72% cell survival while treating the cells with cAMP elevators in the absence of Aβ did not diminish cell survival (Fig. 5.7). When the IBMX, Fsk or IBMX and Fsk were combined with the Aβ treatment, no rescuing effect was seen.

Because the previous experiment showed no increase in cell survival upon upregulation of cAMP, we began adjusting the concentrations of the cAMP elevators. We repeated the previous experiment but decreased the Fsk concentration from 25 to 20 μM. Again, the Aβ treatment caused lower levels of survival (69.13 ± 4.05%) and the treatments with only cAMP elevators induced 90% or greater survival (Fig. 5.8). We did see a subtle rescuing effect in the cells treated with the cAMP elevators. Treatment of the cells with Aβ/IBMX resulted in 82.77 ± 4.27% survival, Aβ/Fsk resulted in 88.36 ± 4.07% survival and Aβ/IBMX/Fsk resulted in 91.05 ± 8.61% survival.
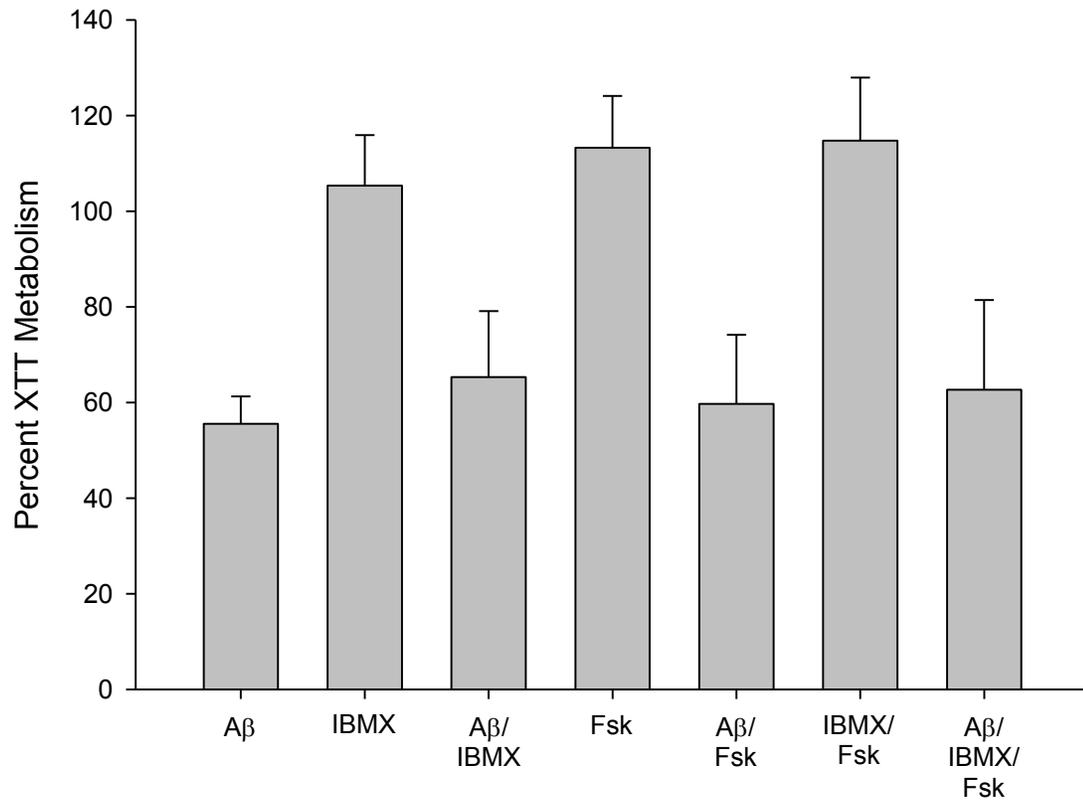
Fig. 5.7 75 μM IBMX and/or 25 μM Fsk do not rescue Aβ treated HA-VSMC
HA-VSMC were plated in a 48-well plate and allowed to adhere for 24 hours. The cells were then treated with freshly prepared 15 μM Aβ(1-42), 75 μM IBMX or 25 μM Fsk in the combinations indicated above for 48 hours. Following the incubation, the medium was re-placed with 0.33 mg/ml XTT/ 8.3 μM PMS for 3 hours. The absorbance of the XTT solution was read in a 96-well plate. The data was corrected to control cells treated only with water (0.665 ± 0.046 AU). Bars are the average ± SE for n = 8 (Aβ, IBMX, Fsk), 7 (Aβ/IBMX, Aβ/ Fsk, Aβ/IBMX/Fsk) and 5 (IBMX/Fsk) over 3 separate experiments.
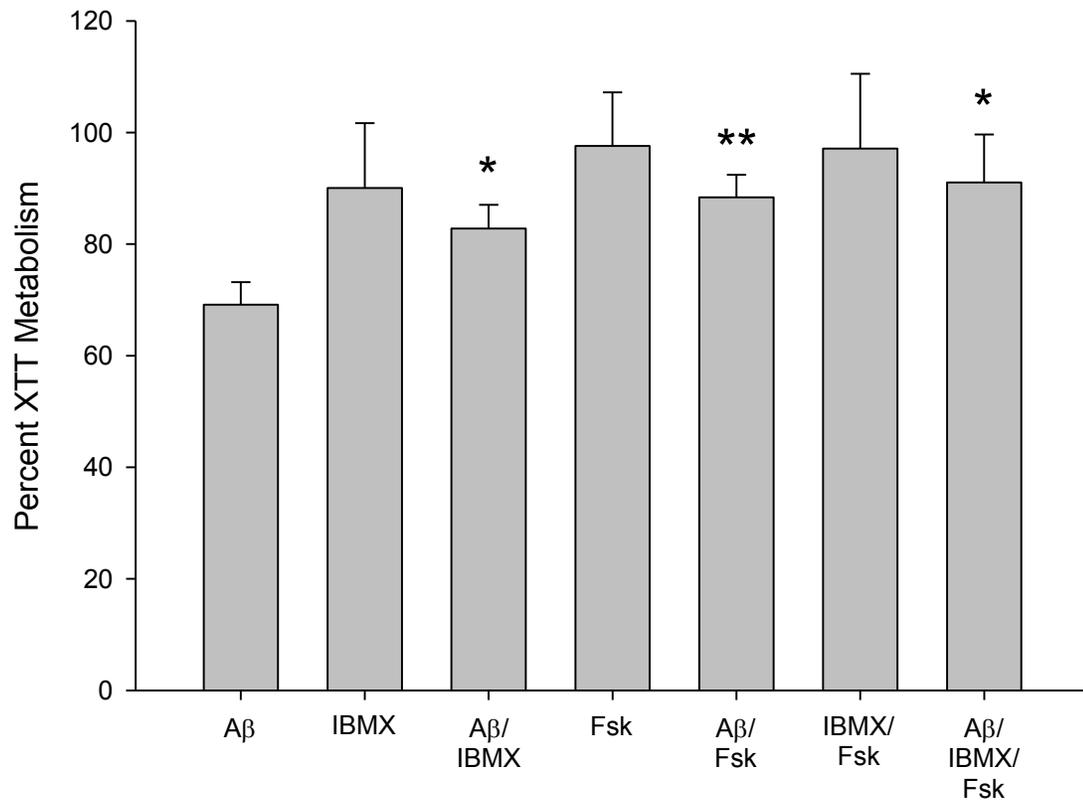
Fig. 5.8 75 μM IBMX and/or 20 μM Fsk subtly rescues Aβ treated HA-VSMC
HA-VSMC were plated in a 48-well plate and allowed to adhere for 24 hours. The cells were then treated with freshly prepared 15 μM Aβ(1-42), 75 μM IBMX or 20 μM Fsk in the combinations indicated above for 48 hours. Following the incubation, the medium was replaced with 0.33 mg/ml XTT/ 8.3 μM PMS for 3 hours. The absorbance of the XTT solution was read in a 96-well plate. The data was corrected to control cells treated only with water (0.294 ± 0.033 AU). Bars are the average ± SE for n = 12 (Aβ, Aβ/IBMX, Aβ/Fsk, Aβ/IBMX/ Fsk), 11 (IBMX, Fsk, IBMX/Fsk) over 4 separate experiments. Statistical significance of <0.025 is denoted by * and significance of <0.005 is denoted by **.

5.3 Discussion

AD is a complicated puzzle of physiological phenomena which necessitates studying the problem in small pieces with the goal of gaining a more global understanding of the situation. It is generally agreed that Aβ plays a prominent role in AD related pathology and therefore is of great importance to the overall problem. In this study, we attempted to show that Aβ(1-42) is toxic to SMCs as a model of CAA, but that the toxic effects could be modulated by the upregulation of cAMP.

We chose to perform our control experiments for this study in the THP-1 cell line due to the ease of working with these particular cells. Our selection of IBMX and Fsk as the cAMP elevating agents was made to provide the most efficient increase in cAMP levels. There are a wide variety of PDEs which degrade cAMP, and each can be regulated individually with a plethora of compounds. However, IBMX is a general PDE inhibitor which functions on the whole class of PDEs thereby ensuring the greatest possible increase in the cAMP. Fsk is a general activator of AC which catalyzes the conversion of ATP to cAMP (Kelley et al., 2008). Studies suggest that Fsk interacts with the catalytic subunit of AC and does not require the enzyme's regulatory subunit for function (Seamon and Daly, 1981; Seamon et al., 1981).

In our study we were able to confirm that incubations up to six hours of IBMX and Fsk with the THP-1 cells generated high levels of cAMP (Fig. 5.3). The incubation time of six hours was chosen for the later THP-1 experiments because in our previous studies, we found that optimal cellular response to effectors like LPS also occurs following a six hour incubation (Udan et al., 2007). We did not perform an IBMX and Fsk

concentration dependent study in the THP-1 cells because the concentrations would not necessarily transfer to the HA-VSMC cell line. We were more concerned with confirming that IBMX and Fsk do indeed increase cAMP levels in the cells.

We have previously studied the TNFα production of THP-1 cells in response to various stimuli, including LPS (Udan et al., 2007). Our results indicated that LPS is able to induce high levels of TNFα, but we wanted to see if LPS was able to induce cAMP production in response to the increase in TNFα. Gogarten and colleagues showed that in human myometrium, the presence of TNFα activates AC at the level of the AC/G-protein interaction or directly at AC itself (Gogarten et al., 2003).

As shown in figure 5.4, when we treated the THP-1 cells with LPS alone, there was very little stimulation of cAMP. There was also very little cAMP produced when IBMX or Fsk were used alone to treat the cells. However, when the two cAMP elevators were combined, the cAMP showed a dramatic increase. It is likely that if one end of the cAMP regulation pathway is affected, the other portion works harder to compensate and maintain homeostasis within the system. Therefore, if AC is stimulated by Fsk, the PDEs may increase the breakdown of the excess cAMP. Conversely, if the PDEs are inhibited and cannot breakdown cAMP, AC may decrease the amount of ATP converted to cAMP. If Fsk and IBMX are used in combination, the overall amount of cAMP produced by the activation of AC is increased, but it cannot be degraded because of the PDE inhibition leading to an overall increase in cAMP levels within the cell.

We next shifted our focus from the THP-1 cells to the HA-VSMC. Our plan was to monitor the toxicity induced by Aβ treatment of the cell using the XTT assay. Although it is a measurement of cellular metabolism, a decrease in the conversion of XTT

to formazan (see fig. 3.5) is generally interpreted as an indication of toxicity.

Although early research suggested that late stage Aβ aggregates were the most toxic species to cells (Pike et al., 1991; Roher et al., 1991; Pike et al., 1993), more recent studies have indicated that it is more likely early, soluble aggregates that are responsible for the toxic activity (Koistinaho et al., 2001; Walsh et al., 2002). We found that treatment of the HA-VSMC with Aβ(1-42) that was freshly prepared or aggregated for up to 48 hours induced a high level of toxicity in the cells. Aβ(1-42) that was aggregated for longer periods of time were not toxic to the cells. As shown in figure 3.10, Aβ (1-42) aggregated for longer than 48 hours shows the presence of long, fibrillar species.

Van Nostrand's lab has shown that in order for Aβ(1-40) to be toxic to cerebral SMCs, the peptide must assemble on the surface of the cells (Van Nostrand et al., 1998). Aβ(1-42) may also require assembly on the cellular surface to induce cellular toxicity. Since the Aβ that was aggregated for 48 hours or less contains very few fibrils (Fig. 3.10), there is still the possibility of the aggregation occurring on the cell. However, the longer aggregating solutions are high in fibril content, which suggests that they will be unable to assemble on the cell surface, which may explain their inability to induce toxicity in the HA-VSMC. Interestingly, when we compared the effects of Aβ(1-40) to Aβ(1-42), we found that Aβ(1-40) did not induce toxicity at any aggregation state. Because Aβ(1-40) does not aggregate well in our conditions, it is unlikely to assemble on the surface of the HA-VSMC, and therefore cannot induce toxicity.

It has been shown that the presence of cAMP can modulate Aβ induced toxicity in PC12 neuronal cells (Onoue et al., 2002). When we tried to rescue the HA-VSMC from Aβ(1-42) induced toxicity with 75 μM IBMX, 25 μM Fsk or a combination of

both, we did not see a change in the Aβ toxicity (Fig. 5.8). However, when we dropped the concentration of Fsk to 20 μM, we saw modest, but statistically significant, decreases in the amount of toxicity when the cells were treated with IBMX, Fsk, or both IBMX and Fsk in combination with the Aβ (Fig. 5.9). The result is promising, and further modulation of the IBMX and Fsk concentrations may lead to further rescue of the cells.

Overall, we have shown that early Aβ(1-42) aggregate species are toxic to the HA-VSMC while all species of Aβ(1-40) produced under our aggregation conditions are benign. We have also shown that treatment of the cells with IBMX and Fsk may provide a potential pathway for rescuing the cells from the toxic effects of Aβ.

5.4 Bibliography

Attems J, Lauda F, Jellinger KA (2008) Unexpectedly low prevalence of intracerebral hemorrhages in sporadic cerebral amyloid angiopathy: an autopsy study. J Neurol 255:70-76.

Crouse NR, Ajit D, Udan ML, Nichols MR (2008) Oligomeric amyloid-beta(1-42) induces THP-1 human monocyte adhesion and maturation. Brain Res.

Gogarten W, Lindeman KS, Hirshman CA, Emala CW (2003) Tumor necrosis factor alpha stimulates adenylyl cyclase activity in human myometrial cells. Biol Reprod 68:751-757.

Grammas P, Ovase R (2001) Inflammatory factors are elevated in brain microvessels in Alzheimer's disease. Neurobiol Aging 22:837-842.

Greenberg SM, Vonsattel JP (1997) Diagnosis of cerebral amyloid angiopathy. Sensitivity and specificity of cortical biopsy. Stroke 28:1418-1422.

Jellinger KA (2002) Alzheimer disease and cerebrovascular pathology: an update. J Neural Transm 109:813-836.

Jin SL, Conti M (2002) Induction of the cyclic nucleotide phosphodiesterase PDE4B is essential for LPS-activated TNF-alpha responses. Proc Natl Acad Sci U S A 99:7628-7633.

Joachim CL, Morris JH, Selkoe DJ (1988) Clinically diagnosed Alzheimer's disease: autopsy results in 150 cases. Ann Neurol 24:50-56.

Kelley DJ, Bhattacharyya A, Lahvis GP, Yin JC, Malter J, Davidson RJ (2008) The cyclic AMP phenotype of fragile X and autism. Neurosci Biobehav Rev 32:1533-1543.

Koistinaho M, Ort M, Cimadevilla JM, Vondrous R, Cordell B, Koistinaho J, Bures J, Higgins LS (2001) Specific spatial learning deficits become severe with age in beta -amyloid precursor protein transgenic mice that harbor diffuse beta -amyloid deposits but do not form plaques. Proc Natl Acad Sci U S A 98:14675-14680.

Kunkel SL, Spengler M, May MA, Spengler R, Larrick J, Remick D (1988) Prostaglandin E2 regulates macrophage-derived tumor necrosis factor gene expression. J Biol Chem 263:5380-5384.

Lombardi VC, Schooley DA (2004) A method for selective conjugation of an analyte to enzymes without unwanted enzyme-enzyme cross-linking. Anal Biochem 331:40-45.

Mandybur TI (1986) Cerebral amyloid angiopathy: the vascular pathology and complications. J Neuropathol Exp Neurol 45:79-90.

Martinez M, Hernandez AI, Hernanz A (2001) Increased cAMP immunostaining in cerebral vessels in Alzheimer's disease. Brain Res 922:148-152.

Nichols MR, Morimoto BH (1999) Tyrosine kinase-independent inhibition of cyclic-AMP phosphodiesterase by genistein and tyrphostin 51. Arch Biochem Biophys 366:224-230.

Onoue S, Endo K, Ohshima K, Yajima T, Kashimoto K (2002) The neuropeptide PACAP attenuates beta-amyloid (1-42)-induced toxicity in PC12 cells. Peptides 23:1471-1478.

Pfeifer LA, White LR, Ross GW, Petrovitch H, Launer LJ (2002) Cerebral amyloid angiopathy and cognitive function: the HAAS autopsy study. Neurology 58:1629-1634.

Pike CJ, Walencewicz AJ, Glabe CG, Cotman CW (1991) In vitro aging of beta-amyloid protein causes peptide aggregation and neurotoxicity. Brain Res 563:311-314.

Pike CJ, Burdick D, Walencewicz AJ, Glabe CG, Cotman CW (1993) Neurodegeneration induced by beta-amyloid peptides in vitro: the role of peptide assembly state. J Neurosci 13:1676-1687.

Roher AE, Ball MJ, Bhave SV, Wakade AR (1991) Beta-amyloid from Alzheimer disease brains inhibits sprouting and survival of sympathetic neurons. Biochem Biophys Res Commun 174:572-579.

Schade FU, Schudt C (1993) The specific type III and IV phosphodiesterase inhibitor zardaverine suppresses formation of tumor necrosis factor by macrophages. Eur J Pharmacol 230:9-14.

Seamon KB, Daly JW (1981) Forskolin: a unique diterpene activator of cyclic AMP-generating systems. J Cyclic Nucleotide Res 7:201-224.

Seamon KB, Padgett W, Daly JW (1981) Forskolin: unique diterpene activator of adenylate cyclase in membranes and in intact cells. Proc Natl Acad Sci U S A 78:3363-3367.

Sinha B, Semmler J, Eisenhut T, Eigler A, Endres S (1995) Enhanced tumor necrosis factor suppression and cyclic adenosine monophosphate accumulation by combination of phosphodiesterase inhibitors and prostanoids. Eur J Immunol 25:147-153.

Suo Z, Tan J, Placzek A, Crawford F, Fang C, Mullan M (1998) Alzheimer's beta-amyloid peptides induce inflammatory cascade in human vascular cells: the roles of cytokines and CD40. Brain Res 807:110-117.

Thal DR, Griffin WS, de Vos RA, Ghebremedhin E (2008) Cerebral amyloid angiopathy and its relationship to Alzheimer's disease. Acta Neuropathol 115:599-609.

Udan ML, Ajit D, Crouse NR, Nichols MR (2007) Toll-like receptors 2 and 4 mediate Abeta(1-42) activation of the innate immune response in a human monocytic cell line. J Neurochem.

Van Nostrand WE, Melchor JP, Ruffini L (1998) Pathologic amyloid beta-protein cell surface fibril assembly on cultured human cerebrovascular smooth muscle cells. J Neurochem 70:216-223.

Vinters HV (1987) Cerebral amyloid angiopathy. A critical review. Stroke 18:311-324.

Vinters HV, Gilbert JJ (1983) Cerebral amyloid angiopathy: incidence and complications in the aging brain. II. The distribution of amyloid vascular changes. Stroke 14:924-928.

Vinters HV, Wang ZZ, Secor DL (1996) Brain parenchymal and microvascular amyloid in Alzheimer's disease. Brain Pathol 6:179-195.

Vonsattel JP, Myers RH, Hedley-Whyte ET, Ropper AH, Bird ED, Richardson EP, Jr. (1991) Cerebral amyloid angiopathy without and with cerebral hemorrhages: a comparative histological study. Ann Neurol 30:637-649.

Walsh DM, Klyubin I, Fadeeva JV, Cullen WK, Anwyl R, Wolfe MS, Rowan MJ, Selkoe DJ (2002) Naturally secreted oligomers of amyloid beta protein potently inhibit hippocampal long-term potentiation in vivo. Nature 416:535-539.

Wang Z, Natte R, Berliner JA, van Duinen SG, Vinters HV (2000) Toxicity of Dutch (E22Q) and Flemish (A21G) mutant amyloid beta proteins to human cerebral microvessel and aortic smooth muscle cells. Stroke 31:534-538.

6 FUTURE WORK

6.1 Extension of Monocyte Maturation Studies

In these studies, we have presented data which indicate that Aβ(1-42) is capable of aggregating into an assembly state which possesses the ability to transform mono-cytic cells into macrophage-like cells. These data show that this ability is unique to an early-formed Aβ(1-42) aggregation intermediate which is not formed by Aβ(1-42) L34P, Aβ(1-42) ADDLs or Aβ(1-40). The Aβ transformed cells have traits which are similar to PMA-induced monocyte-derived macrophages, suggesting that the Aβ-treated cells are also transformed to macrophages.

In order to conclusively determine whether the Aβ derived adherent cells are truly macrophages, we intent to employ a cellular phagocytosis assay. Schwende et al. previously showed that THP-1 cells treated with PMA or, to a lesser degree, Vitamin D3, undergo an upregulation of latex bead phagocytosis (Schwende et al., 1996). We plan to treat the THP-1 cells with Aβ(1-42) or PMA to induce adherence followed by treatment with fluorescent latex beads. If the Aβ treated cells are indeed differentiated into macrophages, they should phagocytose the beads in a manner similar to the PMA treated cells. We believe that the addition of this assay will strengthen our results and further extend the knowledge base related to monocyte recruitment in AD.

If we are able to confirm that Aβ treated cells are differentiated into functioning macrophages through the phagocytosis assay, the next step would be to move our work into a more physiologically relevant cell system. THP-1 cells are cultured monocytes taken from a leukemia patient (Tsuchiya et al., 1980). It is possible that the presence of the leukemia in the original patient may cause the THP-1 monocytes to respond to Aβ in a manner that differs from cells of a healthy individual. Also, cultured cells often behave differently than primary cells harvested near to the experiments. Therefore, we would like to extend the studies found in Chapters 3 and 4 into PBMC.

In order to accomplish the experimental goals, we will need to harvest blood samples from volunteers and isolate the cells from the whole blood. Several protocols have been previously published for this purpose (Gyimesi et al., 2004; Ghadimi et al., 2008; Kalyan and Chow, 2008; Wang et al., 2008; Yu et al., 2008; Zhang et al., 2008). If the experiments show similar results in the primary cells as in the cultured cells, it will strengthen our position that Aβ may induce the recruitment of monocytic cells from outside the CNS and lead to the transformation into recruited microglia.

6.2 Expansion of cAMP Studies

Our studies in Chapter 5 were somewhat inconclusive. Some of the experiments indicated that the presence of cAMP could modulate toxicity induced by Aβ treatment of HA-VSMC. Due to the laborious culture and high costs of maintenance of the cells, we were forced to put this study on hold. In the future, we would like to revisit this line of experimentation because we feel we did not fully explore the possibilities.

We would also like to extend the studies from Chapter 5 into the PC12 neuronal cell line. We would like to determine if Aβ is toxic to these cells, and if so, attempt to identify the toxic species. It is also of interest whether the upregulation of cAMP can provide some protection to these cells. We already possess the PC12 cells, and have culturing protocols in place (as described in the Methods).

6.3 BIBLIOGRAPHY

Ghadimi D, Folster-Holst R, de Vrese M, Winkler P, Heller KJ, Schrezenmeir J (2008) Effects of probiotic bacteria and their genomic DNA on TH1/TH2-cytokine production by peripheral blood mononuclear cells (PBMCs) of healthy and allergic subjects. Immunobiology 213:677-692.

Gyimesi E, Bankovich AJ, Schuman TA, Goldberg JB, Lindorfer MA, Taylor RP (2004) Staphylococcus aureus bound to complement receptor 1 on human erythrocytes by bispecific monoclonal antibodies is phagocytosed by acceptor macrophages. Immunol Lett 95:185-192.

Kalyan S, Chow AW (2008) Staphylococcal toxic shock syndrome toxin-1 induces the translocation and secretion of high mobility group-1 protein from both activated T cells and monocytes. Mediators Inflamm 2008:512196.

Schwende H, Fitzke E, Ambs P, Dieter P (1996) Differences in the state of differentiation of THP-1 cells induced by phorbol ester and 1,25-dihydroxyvitamin D3. J Leukoc Biol 59:555-561.

Tsuchiya S, Yamabe M, Yamaguchi Y, Kobayashi Y, Konno T, Tada K (1980) Establishment and characterization of a human acute monocytic leukemia cell line (THP-1). Int J Cancer 26:171-176.

Wang JC, Kobie JJ, Zhang L, Cochran M, Mosmann TR, Ritchlin CT, Quataert SA (2008) An 11-color flow cytometric assay for identifying, phenotyping, and assessing endocytic ability of peripheral blood dendritic cell subsets in a single platform. J Immunol Methods.

Yu XL, Cheng YM, Shi BS, Qian FX, Wang FB, Liu XN, Yang HY, Xu QN, Qi TK, Zha LJ, Yuan ZH, Ghildyal R (2008) Measles virus infection in adults induces production of IL-10 and is associated with increased CD4+ CD25+ regulatory T cells. J Immunol 181:7356-7366.

Zhang L, Murray F, Zahno A, Kanter JR, Chou D, Suda R, Fenlon M, Rassenti L, Cottam H, Kipps TJ, Insel PA (2008) Cyclic nucleotide phosphodiesterase profiling reveals increased expression of phosphodiesterase 7B in chronic lymphocytic leukemia. Proc Natl Acad Sci U S A.

7 VITA

Nikkilina Renee (Joiner) Crouse, daughter of Dennis Joiner and Mary Ann (Johnson) Joiner was born on March 13, 1982. She graduated from Sparta High School in 2000 and went on to attend Carthage College, in Kenosha, Wisconsin. She graduated with her Bachelor of Arts in Chemistry in 2004. She entered graduated school at University of Missouri-St. Louis in the fall of 2004 where she joined the lab of Dr. Michael R. Nichols. She married Robert Crouse, son of Roger Crouse and Teresa (Knapp) Crouse on June 11, 2005.